



UNIVERSITY OF
BIRMINGHAM

**Vitamin D in pregnancy: understanding
immune effects in the decidua**

by

Jennifer Ann Tamblyn

A thesis submitted to The University of Birmingham for

the degree of

DOCTOR OF PHILOSOPHY

Institute of Metabolism and Systems Research (IMSR)

College of Medical and Dental Sciences

University of Birmingham,

2018

UNIVERSITY OF
BIRMINGHAM

University of Birmingham Research Archive

e-theses repository

This unpublished thesis/dissertation is copyright of the author and/or third parties. The intellectual property rights of the author or third parties in respect of this work are as defined by The Copyright Designs and Patents Act 1988 or as modified by any successor legislation.

Any use made of information contained in this thesis/dissertation must be in accordance with that legislation and must be properly acknowledged. Further distribution or reproduction in any format is prohibited without the permission of the copyright holder.

Abstract

Epidemiology has linked preeclampsia (PET) to vitamin D deficiency. To date, studies have focused upon serum 25-hydroxyvitamin D₃ (25(OH)D₃) alone as the marker of vitamin D status.

We provide strong evidence comprehensive analysis of vitamin D metabolites in pregnancy is highly informative, particularly within the context of PET. Uniquely, analysis of maternal urinary metabolites provides a novel insight into vitamin D and the kidney, with lower 25(OH)D₃ and 24,25(OH)₂D₃ excretion early indicators of a predisposition towards PET.

Since vitamin D is a potent regulator of immune function, and the decidua appears a key extra-renal site for vitamin D metabolism, we investigated effects of 1,25(OH)₂D₃ upon decidual uterine natural killer cells and macrophages. We show both express a functional vitamin-D system and demonstrate differential sensitivity to 1,25(OH)₂D₃ compared to their peripheral counterparts.

To understand the functional impact of vitamin D, whole transcriptomic analysis of 1,25(OH)₂D₃-mediated effects upon uNK and macrophages was performed. We show the actions of vitamin D extend far beyond simple immuno-regulation, targeting major cellular functions including migration, adhesion and apoptosis. In particular, our data support effects highly relevant to decidualisation.

We anticipate these findings to be highly relevant within the context of vitamin D deficiency, malplacentation and PET.

Acknowledgements

I would like to dedicate this thesis to my husband, Lee James, and my parents Nick and Sue Tamblin for their patience, support and belief throughout both my academic and clinical career so far. Thank you also to my sister and brother-in-law, Claire and Kevin Young, and my close friends, Laura Brown, Katie Ruck, Fran Vince and Francesca Chappell, who have all together ensured I kept smiling and believed I would actually reach this point.

I would particularly like to thank my co-supervisors, Professor Mark Kilby and Professor Martin Hewison, for their continued support throughout my fellowship. Professor Kilby has been an unfailing source of inspiration and guidance since the early clinical and academic stages of my career in obstetrics and gynaecology. Professor Hewison has been an exemplary supervisor and with his experience, enthusiasm and accessibility has greatly encouraged my development as a reproductive basic scientist.

I am particularly grateful to a number of current and past College of Medical and Dental Sciences members at University of Birmingham for their assistance and contributions to this work, in particular Louisa Jeffery, Radhika Susarla, Carl Jenkinson, and Dean Lerner. Thank you also to David Lissauer, Richard Powell, Omi Ohizua and the CHHIP research team at Birmingham Women's & Children's Foundation Hospital Trust. Without their continued support with CHHIP participant recruitment and sample collection this work simply would not have been possible.

I would also like to thank my collaborators Judith Bulmer, Gendie Lash and Barbara Innes at the University of Newcastle, Konstantin Knoblich and Anne Fletcher at the University of Birmingham, and Susan Coort, from Maastricht University. The knowledge and technical expertise they have together provided has greatly facilitated the work achieved during this fellowship, and I am extremely grateful for each of their individual contributions to this work.

Thank you finally to my principal funders Wellbeing of Women from whom I was awarded my prestigious 3-year clinical research training fellowship. Thank you also to Mason Medical Research, who specifically funded the RNA-sequence analysis component of this project. Vitabiotics Pregnacare

also generously contributed to this work through Wellbeing of Women, which independently selected the research through its AMRC accredited peer review process led by its Research Advisory Committee.

1 Contents

1	Contents	5
1.1	Figures and Table Summary	12
	Figures summary.....	12
	Tables summary	16
1.2	Abbreviations.....	20
2	General Introduction	25
2.1	Introduction.....	26
2.1.1	Vitamin D metabolism and signalling.....	26
2.1.2	DBP and vitamin D transport.....	29
2.1.3	Vitamin D epimerisation, an alternative pathway.....	30
2.1.4	Extra-renal vitamin D metabolism.....	31
2.1.5	Non-classical immune effects of vitamin D.....	33
2.1.6	Vitamin D status and assessment	34
2.1.7	Overall study aims and objectives	35
3	General Methods.....	37
3.1.1	Ethics.....	38
3.1.2	Participant recruitment.....	38
3.1.3	Sample preparation	40
3.1.4	Analysis of serum and urine vitamin D metabolites by LC MS-MS	43
3.1.5	Analysis of serum DBP	48
3.1.6	Analysis of serum albumin	48

3.1.7	Analysis of free serum 25(OH)D3	49
3.1.8	Creatinine Jaffe reaction	49
3.1.9	Positive selection immuno-magnetic isolation of immune cell subsets.....	50
3.1.10	Cell culture.....	51
3.1.11	LC MS-MS conversion assay	52
3.1.12	Flow cytometry	52
3.1.13	Cytotoxicity assay.....	55
3.1.14	RNA extraction, reverse transcription and quantitative real-time polymerase chain reaction (qRT-PCR).....	56
3.1.15	Fluorescence-activated cell sorting (FACS)	58
3.1.16	RNA extraction	60
3.1.17	cDNA library preparation	62
3.1.18	RNA sequence analysis.....	67
3.1.19	Pathway analysis.....	76
3.1.20	Statistics.....	77
4	Analysis of Vitamin D Metabolism in Pregnancy and Malplacentation.....	78
4.1	Introduction.....	79
4.1.1	Defining vitamin D status in pregnancy.....	79
4.1.2	Vitamin D supplementation in pregnancy.....	80
4.1.3	Vitamin D metabolism in human pregnancy	81
4.1.4	Vitamin D, the placenta and pregnancy	82
4.1.5	Vitamin D and pre-eclampsia (PET).....	85
4.1.6	Urinary vitamin D clearance	88

4.2	Results.....	90
4.2.1	Participant demographics – West Midlands cohort	90
4.2.2	Serum vitamin D metabolites in pregnant and non-pregnant women.....	92
4.2.3	Effect of maternal vitamin D status (serum 25(OH)D3) on other serum vitamin D metabolites in pregnant and non-pregnant women	95
4.2.4	DBP, albumin and 25(OH)D3 bioavailability in pregnant and non-pregnant women..	96
4.2.5	Placental and decidual tissue vitamin D metabolites in pregnant women across gestation	100
4.2.6	Effect of gestation upon placental vitamin D metabolite concentrations in pregnancy and PET	101
4.2.7	Effect of maternal 25(OH)D3 upon placental 25(OH)D3 in normal pregnancy and PET	103
4.2.8	SCOPE Participant demographics.....	104
4.2.9	Serum vitamin D metabolite analysis	106
4.2.10	Urinary vitamin D analysis	112
4.3	Discussion.....	115
4.3.1	Total 25(OH)D3 alone is not a reliable marker of vitamin status in pregnant women	115
4.3.2	Dysregulated vitamin D metabolism in pregnancies complicated by PET	116
4.3.3	Effects of DBP and free 25(OH)D3	118
4.3.4	Tissue concentrations of 25(OH)D and 1,25(OH) ₂ D3 are higher in decidua compared to placenta.....	119
4.3.5	Placental vitamin D metabolites across normal pregnancy.....	119
4.3.6	Dysregulation of vitamin D metabolism prior to PET onset.....	121
4.3.7	Limitations	126

5	Vitamin D and uterine natural killer cells	130
5.1	Introduction.....	131
5.1.1	Immune cell function and the decidua	131
5.1.2	Natural killer cells.....	132
5.1.3	CD56 bright NK Cells.....	133
5.1.4	Tissue resident NK cells	134
5.1.5	Uterine NK cells.....	135
5.1.6	NK cells in malplacentation.....	138
5.1.7	Vitamin D and NK Cells.....	140
5.2	Results.....	142
5.2.1	Distribution of decidua immune cells: comparative analysis with matched peripheral maternal blood – first trimester	142
5.2.2	Optimisation of NK cell activation assay.....	147
5.2.3	Analysis of the vitamin D metabolic system in NK subsets by qRT-PCR	151
5.2.4	Intracellular VDR expression in uNK and pNKs.....	154
5.2.5	uNK and pNKs convert inactive 25(OH)D3 to active 1,25(OH) ₂ D3.....	156
5.2.6	Effects of vitamin D upon uNK and pNK IFN- γ transcript expression	157
5.2.7	RNA sequence analysis purity analysis	159
5.2.8	Principal component analysis.....	161
5.2.9	Comparative analysis of CK treated uNK and pNK	162
5.2.10	Pathway analysis.....	163
5.2.11	Vitamin D effects upon CK treated pNK cells.....	166
5.2.12	Functional analysis of vitamin D-mediated uNK transcripts.....	170

5.3	Discussion.....	175
5.3.1	NK cells positively express a functional vitamin D system.....	177
5.3.2	1,25(OH) ₂ D ₃ -mediated suppression of uNK IFN- γ production	179
5.3.3	Whole transcriptome comparative analysis of CK treated uNK and pNK subsets	179
5.3.4	Complementary pathway analysis reveals distinct CK-mediated effects upon uNKs	180
5.3.5	Differential regulation of first trimester uterine and peripheral blood natural killer cells by 1,25(OH) ₂ D ₃	180
5.3.6	Study limitations	184
6	Vitamin D and monocyte - macrophages in pregnancy	187
6.1	Introduction.....	188
6.1.1	Mononuclear phagocyte system.....	188
6.1.2	Monocytes.....	188
6.1.3	Macrophages	191
6.1.4	Monocytes in pregnancy	192
6.1.5	Macrophages in pregnancy	193
6.1.6	Monocytes, macrophages and disorders of malplacentation.....	194
6.1.7	Vitamin D and monocyte and macrophage function.....	194
6.2	Results.....	197
6.2.1	Distribution of decidua immune cells: comparative analysis with matched peripheral maternal blood and fetal cord blood – third trimester.....	197
6.2.2	Comparative analysis of monocyte and macrophage subsets in decidua and maternal blood – first trimester analysis	198
6.2.3	Comparative analysis of monocyte and macrophage subsets in decidua, maternal and cord blood – third trimester analysis.....	201

6.2.4	Characterisation of first trimester monocyte and macrophage subsets in decidua and maternal blood	205
6.2.5	Characterisation of third trimester monocyte and macrophage subsets in paired decidua, maternal and cord blood	210
6.2.6	Transcript analysis of the Vitamin D metabolic system in third trimester CD14+ monocyte and macrophage subsets	211
6.2.7	Demographic summary of those participants with samples utilised for RNA-seq analysis	219
6.2.8	Purity of CD14+ FACS-sorted subsets	220
6.2.9	Principal component analysis.....	220
6.2.10	Comparative analysis of LPS treated cord, maternal and decidua monocyte/ macrophage subsets.	221
6.2.11	Pathway analysis	224
6.2.12	Vitamin D targets in maternal, cord and decidua subsets	229
6.2.13	Vitamin D effects upon maternal monocytes.....	233
6.2.14	Vitamin D effects upon cord monocytes.....	236
6.2.15	Vitamin D effects upon decidua macrophages.....	239
6.3	Discussion	243
6.3.1	A distinct immune cell population persists in third trimester decidua comparative to cord and maternal blood.....	243
6.3.2	Detailed monocyte and macrophage subset analysis reveals stark differences in third trimester decidua.....	244
6.3.3	Decidual macrophages positively express a range of recognised ‘M1’ and ‘M2’ markers	247

6.3.4	Decidual macrophages demonstrate differential transcript expression and responsivity of the vitamin D metabolic system	248
6.3.5	Whole transcriptome analysis of third trimester paired cord, maternal and decidua monocyte and macrophage subsets	252
6.3.6	Differential regulation of third trimester maternal blood, cord blood and decidua monocyte and macrophage subsets by 1,25(OH) ₂ D ₃	254
6.3.7	Study limitations	263
7	Final Discussion.....	266
8	References.....	271
9	Appendices.....	298
9.1.1	SCOPE exclusion criteria.....	298
9.1.2	Effect of maternal serum 25(OH)D ₃ and 3-epi-25(OH)D ₃ upon fetal cord concentrations at delivery	298
10	Publications arising from this thesis	299

1.1 Figures and Table Summary

Figures summary

Figure 2.0 Summary of vitamin D synthesis and metabolism

Figure 2.1 Classical and non-classical actions of active 1,25-dihydroxyvitamin D₃ (1,25(OH)₂D₃): mechanisms of action

Figure 3.0 Summary of SCOPE (Screening for Pregnancy Endpoints) Ireland study recruitment across the 6 research centres (March 2008 to January 2011)

Figure 3.1 Anatomy of human placenta.

Figure 3.2 Representative FACS analysis plots for NK cells

Figure 3.3 Representative FACS analysis plots for maternal blood, cord blood and decidua monocyte/macrophage subsets

Figure 3.4 uNK and pNK cell pre and post normalisation box plots

Figure 3.5 Quantification coverage breakdown for all NK cell RNA-seq samples

Figure 3.6 Pre and post normalisation box plots for all monocyte / macrophage samples sequenced in third trimester maternal blood, cord blood and decidua

Figure 3.7 A quantification coverage breakdown for third trimester monocyte and macrophage samples

Figure 4.0 Summary of the heterogeneous decidua cell population present at the materno-fetal interface (A).

Figure 4.1 Three stage classification of PET

Figure 4.2 Simultaneous measurement of vitamin D metabolites in pregnant and non-pregnant women reveals significant gestational and disease-dependent changes in serum metabolite concentrations.

Figure 4.3 Linear regression analysis confirms gestational age at delivery did not significantly impact serum vitamin D metabolite concentrations in NP3 and PET groups

Figure 4.4 Effect of maternal vitamin D status upon other serum vitamin D metabolites in non-pregnant and pregnant women

Figure 4.5 Comparative analysis of DBP, albumin and 25(OH)D3 bioavailability and free serum concentrations revealed no significant difference between pregnant and non-pregnant women, or within the context of PET.

Figure 4.6 Pregnancy has no significant effect upon bound, bioavailable and free 25(OH)D3

Figure 4.7 Significant differences in first trimester maternal decidua and fetal placenta tissue concentrations of active (1,25(OH)2D3) and inactive (25(OH)D3) vitamin D

Figure 4.8 Significant effect of gestation upon placental vitamin D metabolism in pregnancy and pre-eclampsia

Figure 4.9 Effect of maternal 25(OH)D3 upon placental 25(OH)D3 in normal pregnancy and pre-eclampsia

Figure 4.10 Serum vitamin D metabolites in non-pregnant women and SCOPE pregnancy cohort at 15 weeks gestation

Figure 4.11 Effect of maternal vitamin D status (serum 25(OH)D3) upon other serum vitamin D metabolites at 15 weeks gestation

Figure 4.12 Alterations in urinary vitamin D metabolite concentrations measured at 15 weeks gestation in a cohort of pregnant women, of which n=25 prospectively developed PET

Figure 4.13 Relationship between excreted urinary vitamin D metabolites

Figure 5.0 Summary of the gating strategy utilised to assess both decidua-derived and circulating maternal live CD45+ lymphocyte subsets

Figure 5.1 Characterisation of first trimester immune cells subsets

Figure 5.2 Phenotypical characterisation of paired first trimester uNK and pNK subsets

Figure 5.3 Flow cytometric analysis of the effects of 1,25(OH)₂D₃ upon isolated uNK and pNK cell CK release (IFN- γ , TNF- α) and cytotoxic potential, as characterised by CD107 expression

Figure 5.4 Summary of flow cytometry analysis of the effects of 1,25(OH)₂D₃ upon isolated pNK (blue) and uNK cell (red) CK release (IFN- γ , TNF- α) and cytotoxic potential, as characterised by CD107 expression

Figure 5.5 Transcript analysis of the vitamin D metabolic system in uNK and pNK

Figure 5.6 Summary of uNK and pNK VDR and CD69 expression

Figure 5.7 uNK and pNKs convert inactive 25(OH)D₃ to active 1,25(OH)₂D₃

Figure 5.8 Transcript and intracellular protein expression analysis of IFN- γ

Figure 5.9 Principal component analysis (PCA) analysis of cytokine (CK) stimulated uNK and pNKs in the presence and absence of 1,25(OH)₂D₃

Figure 5.10 Transcriptomic analysis of cytokine (CK)-stimulated pNK and uNKs

Figure 5.11 Summary of WikiPathways data-base analysis for CK treated uNK versus CK pNK

Figure 5.12 Summary of the Reactome data-base analysis for CK treated uNK versus CK pNK

Figure 5.13 Analysis of transcript expression of *SERPINIB1*, *LGALS9* and *RELT* in CK treated NK cells

Figure 5.14 Analysis of transcript expression of *TRIM35* and *RSAD2* in CK treated NK cells

Figure 6.0 Differentiation of monocytes to tissue macrophages

Figure 6.1 Comparative analysis of the relative proportion of CD45⁺ immune cell subsets in paired third trimester umbilical cord (vein) blood, maternal blood and decidua tissue samples

Figure 6.2 Summary of the flow cytometry gating strategy utilised to classify maternal and decidua derived whole lymphocyte subsets according to their expression of recognised mononuclear cell markers

Figure 6.3 Flow cytometry plots of first and third trimester decidua, and third trimester cord and maternal monocyte / macrophage subsets classified according to CD14 and CD16 surface expression

Figure 6.4 Summary of maternal (mat; red) classical CD14⁺⁺CD16⁻, and decidua (DC; black) classical CD14⁺⁺CD16⁻ and intermediate CD14⁺⁺CD16⁺ subset expression of monocyte and macrophage markers

Figure 6.5 Transcript analysis of the vitamin D metabolic system in cord blood, maternal blood and decidua-derived CD14⁺ cells

Figure 6.6 Transcript analysis of *cathelicidin*, *IFN- γ* , *IL-6* and *TNF- α* in cord blood, maternal blood and decidua-derived CD14⁺ cells

Figure 6.7 PCA analysis of LPS stimulated monocyte and macrophage subsets in the presence and absence of 1,25(OH)₂D₃

Figure 6.8 Comparative analysis of transcript expression in cord, maternal and decidua monocyte / macrophage subsets

Figure 6.9 Summary of WikiPathway database comparative analysis for LPS treated cord and decidua subsets

Figure 6.10 Summary of Reactome database comparative analysis for LPS treated cord and decidua subsets

Figure 6.11 Summary of WikiPathway database comparative analysis for LPS maternal and decidua subsets

Figure 6.12 Summary of Reactome database comparative analysis for LPS maternal and decidua subsets

Figure 6.13 Summary of those transcripts significantly upregulated in cord blood, maternal blood and decidua derived LPS stimulated monocyte/ macrophage subsets in response to vitamin D

Figure 6.14 Comparative analysis of cord, maternal and decidua monocyte/ macrophage transcript expression of *DIRC2*, *CA2* and *EFL1*

Figure 6.15 Hierarchical cluster dendogram analysis of maternal LPS versus maternal LPS+1,25(OH)₂D₃ subsets

Figure 6.16 Hierarchical cluster dendogram analysis of cord LPS versus cord LPS + 1,25(OH)₂D₃ subsets

Figure 6.17 Hierarchical cluster dendogram analysis of decidua LPS versus decidua LPS + 1,25(OH)₂D₃ subset

Figure 6.18 Orchestration of Metabolism by Macrophages

Tables summary

Table 3.0 Multiple-Reaction Monitoring (MRM) transitions for 4-phenyl-1,2,4-triazoline-3,5-dione (PTAD)-derivatized vitamin D metabolites.

Table 3.1 Summary of the individual cytokines (CK), the dose and mode of action assessed for NK cell stimulation.

Table 3.2 Summary of primary surface and intracellular antibodies utilised for flow cytometry.

Table 3.3 Summary of gene specific mRNAs utilised for qRT-PCR

Table 3.4 Summary of the concentration and RIN scores measured prior to cDNA library preparation for first trimester uNK and pNK subsets

Table 3.5 Summary of the concentration and RIN scores measured for paired third trimester decidua, maternal blood and cord blood monocyte/ macrophage subsets

Table 3.6 Feature distribution for each NK sample utilised for RNA-seq analysis

Table 3.7 Post alignment QA/ QC report

Table 3.8 Feature distribution for each monocyte / macrophage sample utilised for RNA-seq analysis

Table 3.9 Post alignment QA/ QC report

Table 4.0 Summary of participant demographics for non-pregnant female controls, normal pregnant women (n=20) at first (NP1, n=25) and third trimester (NP3, n=21) and women with PET (n=22) in the West Midlands cohort

Table 4.1 Summary of ethnicity for the West Midlands cohort

Table 4.2 Demographic summary and analysis of the participant sub-group assessed from the SCOPE, Ireland cohort

Table 4.3 Summary of serum vitamin D metabolites in SCOPE pregnant women at 15 weeks gestation and non-pregnant controls

Table 4.4 Urinary concentrations of 25(OH)D3 nmol/L; and 24,25(OH)₂D3 nmol/L

Table 5.0 Demographic summary of first trimester participants (n=5)

Table 5.1 Relative intracellular protein expression of perforin and granzyme B in paired uNK and pNK subsets

Table 5.2 Summary of time-point analysis of pNK cell activation

Table 5.3 IFN- γ , TNF- α and CD107 intracellular expression in isolated uNK and pNK cells

Table 5.4 Purity analysis of CD56+ subset isolation of maternal and decidua subsets

Table 5.5 Summary of donor demographic analysis

Table 5.6 uNK and pNK purity analysis

Table 5.7 Effect of 1,25(OH)₂D3 upon gene expression in CK pNK

Table 5.8 Summary of principal genes differentially regulated by 1,25(OH)₂D₃ in pNK cells

Table 5.9 Effect of 1,25(OH)₂D₃ upon gene expression in CK Unk

Table 5.10 Summary of principal genes differentially regulated by 1,25(OH)₂D₃ in uNK cells

Table 6.0 First trimester CD14⁺ cell analysis in paired decidua and maternal blood

Table 6.1 Summary of the relative frequencies of first trimester decidua and paired maternal blood subsets according to CD14 and CD16 expression

Table 6.2 Relative frequencies of third trimester CD14⁺ cells in the decidua, maternal blood and cord blood

Table 6.3 Summary of the relative frequencies of third trimester paired decidua, maternal blood and cord blood subsets according to CD14 and CD16 expression

Table 6.4 Functional summary of the surface protein markers utilised to characterise monocyte / macrophage subsets

Table 6.5 First trimester maternal and decidua subset expression of recognised monocyte and macrophage markers

Table 6.6 Paired third trimester cord blood, maternal blood and decidua analysis of recognised monocyte and macrophage markers

Table 6.7 House-keeping gene comparative analysis in third trimester paired cord blood, maternal blood and decidua

Table 6.8 Third trimester CD14⁺ purity analysis

Table 6.9 Demographic summary of third trimester maternal participant's recruited for RNA-seq analysis

Table 6.10 Purity analysis of CD14⁺ subsets from maternal blood, cord blood and decidua

Table 6.11 Summary of the shared transcripts measured in cord and maternal monocytes significantly upregulated in response to co-treatment with LPS and 1,25(OH)₂D₃

Table 6.12 Effect of 1,25(OH)₂D₃ upon gene expression in LPS maternal monocytes

Table 6.13 Effect of 1,25(OH)₂D₃ upon gene expression in LPS cord monocytes

Table 6.14 Effect of 1,25(OH)₂D₃ upon gene expression in LPS decidua macrophages

1.2 Abbreviations

Abbreviation	Definition
DMEQTAD	[2-(6,7-dimethoxy-4-methyl-3-oxo-3,4-dihydroquinoxalyl)ethyl]-1,2,4-triazoline-3,5-dione
1,24,25(OH) ₂ D ₃	1,24,25-trihydroxyvitamin D ₃
1,25(OH) ₂ D ₃	1,25-dihydroxyvitamin D ₃
24, 25(OH) ₂ D ₃	24,25 di-hydroxyvitamin D ₃
25(OH)D ₃	25-hydroxy-vitamin D ₃
1 α -hydroxylase	25-hydroxyvitamin D-1 α -hydroxylase
CYP27B1	25-hydroxyvitamin D-1 α -hydroxylase
DAPTAD	4-(4'-dimethylaminophenyl)-1,2,4-triazoline-3,5-dione
PTAD	4-phenyl-1,2,4-triazoline-3,5-dione
APCs	antigen presenting cells
B cells	B lymphocytes
BD	Becton Dickinson
BWCFT	Birmingham Women's & Children's Hospital Foundation Trust
BP	blood pressure
BMI	body mass index
epi-1,25(OH) ₂ D ₃	C3- epimer of 25-hydroxyvitamin D ₃
classical monocyte	CD14 ⁺⁺ CD16 ⁻
Intermediate	CD14 ⁺⁺ CD16 ⁺
non-classical	CD14 ⁺ CD16 ⁺⁺
ChIP	chromatin immunoprecipitation sequencing
CD	cluster of differentiation
cDNA	complementary DNA
CI	confidence interval
CYC-1	cytochrome- c-1
CK	cytokines
D	day
DCs	Dendritic cells

DNA	deoxyribonucleic acid
ELCS	elective caesarean section
EDTA	ethylenediaminetetraacetic acid
EVT	extravillous trophoblast
CD16	Fc γ -III receptor
FCS	fetal calf serum
FGF23	fibroblast-like growth factor-23
FACS	fluorescence-activated cell sorting
FSC	forward scatter
LGALS9	galectin-9
GA	gestational age
g	grams
HBSS	hanks balanced salt solution
h	hours
HGNC	HUGO Gene Nomenclature Committee
HLA	human leukocyte antigen
IFITs-5	IFN-induced protein with tetratricopeptide repeats
Th17	IL-17-secreting T cells
IVF	in vitro fertilisation
IDO	indoleamine-pyrrole 2,3-dioxygenase
ILCs	innate lymphoid cells
IOM	Institute of Medicine
IFN- γ	interferon-gamma
IL-2	interleukin-2
IQR	interquartile range
KIRs	killer immunoglobulin-like receptors
KO	knock out
KO	knockout
LXN	Latexin
SERPINB1	leukocyte elastase inhibitor

LPS	lipopolysaccharide
CD14	lipopolysaccharide receptor
LC MS-MS	liquid chromatography-mass spectrometry
LLE	liquid-liquid extraction
LNA-TSO	locked nucleic acid template switching oligo
MTA	material transfer agreement
MABP	mean arterial blood pressure
MFI	median fluorescence intensity
mRNA	messenger ribonucleic acid
Min	minutes
MPS	mononuclear phagocyte system
MRM	multiple reaction monitoring
<i>M. Tb</i>	Mycobacterium tuberculosis
NKRs	natural killer cell receptors
NKT	natural killer T cells
NO	nitrous oxide
NP1	normal first trimester
NP3	normal third trimester
PAMPs	pathogen-associated molecular pattern
PE	paired-end
PFA	Paraformaldehyde
PTH	parathyroid hormone
pNKs	peripheral natural killer cells
PPAR	peroxisome proliferator-activated receptor
PMA	phorbol 12-myristate 13-acetate
PBS	phosphate-buffered saline
PET	pre-eclampsia
PCA	principal component analysis
PI	propidium iodide
PTHrP	PTH-related peptide

FSC-W	pulse width
QA	quality assurance
QC	quality control
qRT-PCR	quantitative real-time polymerase chain reaction
RSAD2	Radical S-Adenosyl Methionine Domain-Containing Protein 2
RNS	reactive nitrogen species
ROS	reactive oxygen species
RELT	Receptor Expressed in Lymphoid Tissues
Treg	regulatory T cells
REC	Research Ethics Committee
RI	resistance index
RA	retinoic acid
RXRs	retinoid-X receptors
rpm	revolutions per minute
rRNA	ribosomal RNA
RR	Risk ratio
RIN	RNA Integration Numbers
RNA-seq	RNA sequence analysis
SACN	Scientific Advisory Committee on Nutrition
SCOPE	Screening for Pregnancy Endpoints
SSC	side scatter
SGA	small for gestational age
SPE	solid phase extraction
STAR	Spliced Transcripts Alignment to a Reference
SD	standard deviation
SEM	standard error of the mean
SLE	supportive liquid-liquid extraction
sTOP	surgical termination of pregnancy
SMART	Switching Mechanism at the 5' end of RNA Template
Th	T helper

T cells	T lymphocytes
TLR	toll-like receptor
TRIM35	tripartite motif-containing protein 35
TNF- α	tumour necrosis factor-alpha
MAVIDOS	UK Maternal Vitamin D Osteoporosis Study
UVB	ultraviolet radiation B
Iu	units
UoB	University of Birmingham
US	unstimulated
uNKs	uterine natural killer cells
Vs	versus
DBP	vitamin D binding protein
VDDR	vitamin D dependency rickets
VDR	vitamin D receptor
DRIPs	vitamin D receptor interacting proteins
VDRE	vitamin D response element
24-hydroxylase	vitamin D-24-hydroxylase
CYP24A1	vitamin D-24-hydroxylase
W	weeks
WP	WikiPathways
WT	wild-type
Y	years

2 General Introduction

Parts of this chapter have been published as:

Tamblyn JA, Lissauer DM, Powell R, Cox P, Kilby MD. The immunological basis of villitis of unknown etiology - review. *Placenta*. 2013;34(10):846-55 (1)

Tamblyn JA, Susarla R, Jenkinson C, Jeffery L, Ohizua O, Chun R, Chan S, Kilby M, Hewison M. Dysregulation of Maternal and Placental Vitamin D Metabolism in Preeclampsia. *Placenta* 50, 70-77. 2016.

2.1 Introduction

2.1.1 Vitamin D metabolism and signalling

Vitamin D is a secosteroid classically recognised for its endocrine role in bone metabolism and calcium homeostasis. In contrast to other members of the steroid family, vitamin D is produced in the skin provided there is sufficient exposure to sunlight and ultraviolet radiation B (UVB). Initially, 7-dehydrocholesterol is converted to the pre-vitamin pre-cholecalciferol, which is then converted to the activated 7-dehydrocholesterol ‘vitamin D₃’ form. As summarised in Figure 2.0, vitamin D may also be obtained naturally via ingestion from the diet either as vitamin D₂ (ergocalciferol) or D₃ (cholecalciferol), for example from milk, eggs, mushrooms and fatty fish. However, on average dietary vitamin D contributes only 10–20% of the total serum vitamin D concentrations; hence skin-derived vitamin D₃ is the primary circulating form of vitamin D for most individuals.

Regardless of source, vitamin D₂ and D₃ are subsequently rapidly metabolised to become physiologically active. Classical vitamin D metabolism involves rapid transport of both vitamin D₂ and D₃ to the liver, bound to the serum globulin vitamin D binding protein (DBP), a specific binding protein for vitamin D and its metabolites in serum. Here, hydroxylation at C-25 by one or more cytochrome P450 25-hydroxylase results in the formation of inactive 25-hydroxy-vitamin D₂ and D₃, which shall collectively be referred to as 25(OH)D₃ in relation to vitamin D ‘status’ (2, 3).

Inactive 25(OH)D₃ is the major circulating form of vitamin D, with a half-life of 25 days (d) (4, 5). Classically, this is transported from the liver, primarily via circulatory DBP, to the kidney for conversion in the proximal renal tubules to the biologically active form of vitamin D, 1,25-dihydroxyvitamin D (1,25(OH)₂D₂ and D₃; denoted as 1,25(OH)₂D₃ for the remainder of this report). The hydroxylation of 25(OH)D₃ is catalysed by 25-hydroxyvitamin D-1 α -hydroxylase (1 α -hydroxylase; CYP27B1)(6).

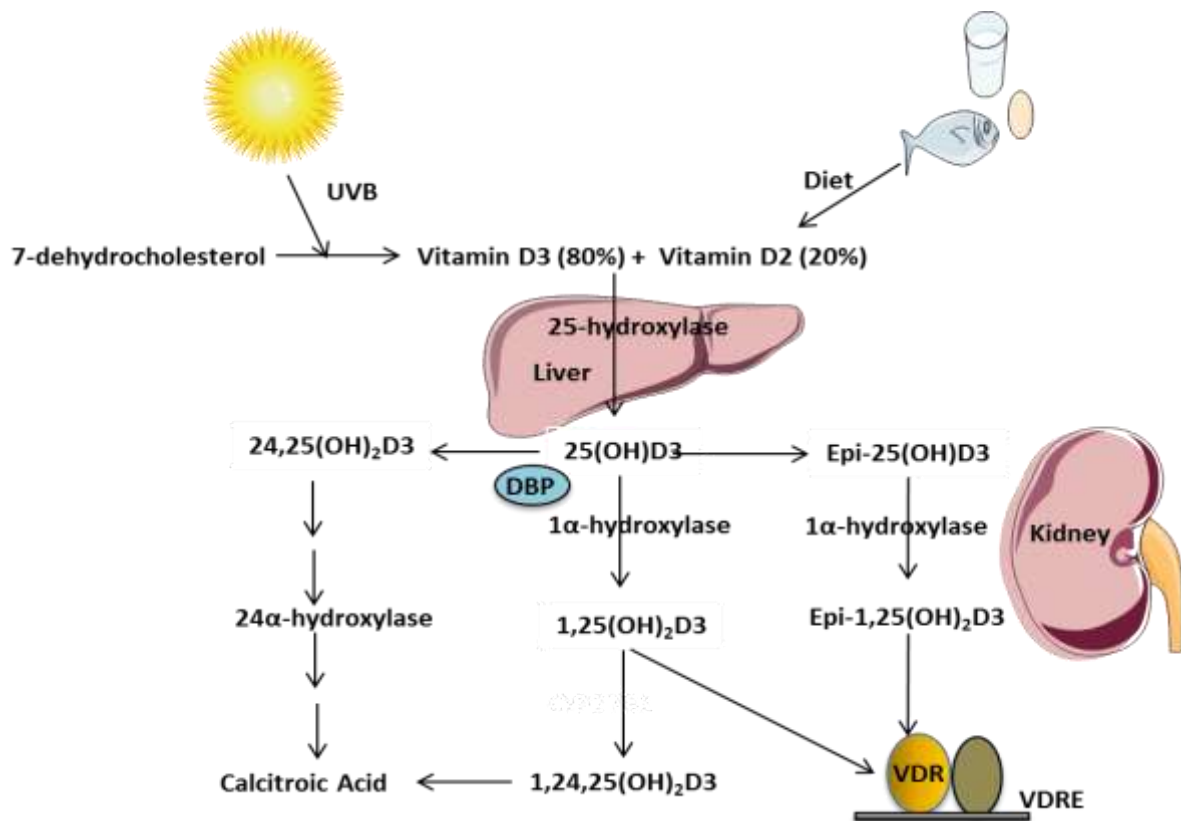


Figure 2.0 Summary of vitamin D synthesis and metabolism. UVB Solar ultraviolet B radiation, 25(OH)D₃ 25-hydroxyvitamin D₃, 1,25-dihydroxyvitamin D₃ (1,25(OH)₂D₃), 25-hydroxyvitamin D-1α-hydroxylase (1α-hydroxylase), 24,25-dihydroxyvitamin D₃ (24, 25(OH)₂D₃), 1,24,25 tri-hydroxyvitamin D (1,24,25(OH)₂D₃), vitamin D receptor (VDR), half-life (½ life), C3- epimer of 25-hydroxyvitamin D₃ (epi-25(OH)D₃) and C3- epimer of 1,25-hydroxyvitamin D₃ (epi-1,25(OH)₂D₃).

1,25(OH)₂D₃ is the principal ligand for the nuclear vitamin D receptor (VDR), which mediates both non-transcriptional and transcriptional effects of 1,25(OH)₂D₃. Unlike its precursor 25(OH)D₃, the half-life of 1,25(OH)₂D₃ is approximately 4-6 hours (h) (7, 8). Renal 1,25(OH)₂D₃ synthesis is however tightly regulated, principally via serum calcium, phosphate, parathyroid hormone (PTH) and fibroblast-like growth factor-23 (FGF23). Low serum calcium and phosphate stimulate 1,25(OH)₂D₃ production, whereas high serum levels of both inhibit active 1,25(OH)₂D₃ production. FGF23 is produced by osteocytes in response to high calcium, inhibiting 1α-hydroxylase activity (9). 1α-hydroxylase activity is also regulated by 1,25(OH)₂D₃ via a direct negative feedback signal. 1α-

hydroxylase activity appears crucial, as in mice inactivating gene mutations result in vitamin D dependency rickets (VDDR) despite normal intake of vitamin D (10).

In addition to $1,25(\text{OH})_2\text{D}_3$, the kidney also produces 24,25-dihydroxyvitamin D₃ ($24,25(\text{OH})_2\text{D}_3$) and 1,24,25-trihydroxyvitamin D₃ ($1,24,25(\text{OH})_2\text{D}_3$) from $25(\text{OH})\text{D}_3$ and $1,25(\text{OH})_2\text{D}_3$ respectively. Generally, this is considered a regulatory ‘catabolic step’, catalysed by vitamin D-24-hydroxylase (24-hydroxylase, CYP24A1) and resulting in a five-step downstream inactivation pathway to calcitroic acid (11). $1,25(\text{OH})_2\text{D}_3$ also induces *CYP24A1* to produce 24-hydroxylase, which via a negative feedback mechanism drives catabolic degradation of $1,25(\text{OH})_2\text{D}_3$ to $1,24,25(\text{OH})_2\text{D}_3$. The *Cyp24a1* knockout (KO) (*Cyp24a1*^{-/-}) mouse supports a crucial role for CYP24A1-mediated catabolic activity, with poor offspring viability (50% mortality prior to weaning) and hypercalcemia observed (7).

The intracellular vitamin D receptor (VDR) is a nuclear transcription factor belonging to the superfamily of transacting transcriptional regulatory factors; including steroid and thyroid hormone receptors, retinoid-X receptors (RXRs) and retinoic acid receptors (12). Upon binding $1,25(\text{OH})_2\text{D}_3$, VDR forms a heterodimer with RXR, which translocates to the nucleus and binds to vitamin D response element (VDRE) Deoxyribonucleic acid (DNA) sequences that are frequently found in the promoter region of target genes (20). In conjunction with several coactivators and corepressors including vitamin D receptor interacting proteins (DRIPs), this leads to both transcriptional activation and repression of genes and a successive cascade of cellular events.

As discussed throughout this paper, murine models with targeted deletion of the genes encoding the enzymes that metabolise vitamin D and its derivatives or of the genes through which vitamin D exerts its action have provided valuable insights into vitamin D biology, including the extra-skeletal effects of vitamin D function. Furthermore, these models permit investigation of the pathophysiology associated with active vitamin D deficiency and the role of treatment in the prevention and treatment of these disorders (13). In particular, murine studies have been effectively utilised to demonstrate the importance of VDR; “knock out” (KO) (*Vdr*^{-/-}) models express a phenotype analogous to vitamin D-deficient or -resistant rickets (14). Interestingly, bone pathology is normal in *Cyp24a1*^{-/-} *VDR*^{-/-}

double KO mice, which suggests that in the context of aberrantly elevated 1,25(OH)₂D₃, non VDR-mediated signal transduction may rescue bone development (14, 15). The exact mechanisms underlying this are however not yet defined. Extrapolation of the insights from these murine models to human vitamin D metabolism is often more difficult, but certainly inform future studies defining the role of vitamin D deficiency and supplementation.

2.1.2 DBP and vitamin D transport

DBP is a member of the albumin, α -fetoprotein, and α -albumin multigene family. The serum concentration is ~4–8 μ M/ L and half-life 2.5–3 days. DBP has a high-affinity binding site for 25(OH)D₃ ($5 \times 10^8 \text{ M}^{-1}$), and can also bind 1,25(OH)₂D₃ and parental vitamin D, albeit with lower affinity ($4 \times 10^7 \text{ M}^{-1}$)(16). As alluded to, the differential binding affinity of DBP is considered a crucial factor influencing availability of substrate for 1 α -hydroxylase conversion to 1,25(OH)₂D₃.

As vitamin D is lipid soluble the majority of circulating 25(OH)D₃ and 1,25(OH)₂D₃ preferentially binds DBP, with 10–15% bound to albumin, and less than 1% of circulating vitamin D in an unbound ‘free’ form. A positive correlation between 25(OH)D₃ and DBP in response to supplementation has been shown (17).As well as transporting vitamin D metabolites in the circulation, DBP facilitates the entry of 25(OH)D₃ into some cells, including proximal convoluted tubule cells of the kidney. This requires target cell expression of megalin, a large transmembrane multi-ligand receptor and so called chaperone protein. Consistent with this, megalin KO mice, which are unable to recover DBP, develop vitamin D deficiency and bone disease (18).

Studies using mice deficient in DBP have provided a valuable insight into the role of DBP in vitamin D metabolism. Albeit DBP null ($^{-/-}$) mice demonstrate markedly lower total serum levels of 25(OH)D₃ comparative to wild-type (WT) mice, calcium and PTH levels remain normal with limited impact upon the extracellular pool of biologically active 1,25(OH)₂D₃. However, following exposure to a short duration vitamin D–deficient diet, DBP $^{-/-}$ mice were more susceptible to deficiency, thereby suggesting DBP prolongs 25(OH)D₃ half-life, maintaining total 25(OH)D₃ reserves (19, 20).

However, common genetic polymorphisms in the DBP gene produce variant proteins that differ in their affinity for vitamin D. Three common polymorphisms are encoded, but with over 124 variant

alleles described worldwide, the DBP locus is clearly highly polymorphic. The prevalence of these significantly differs between racial groups (21).

Although DBP is an effective transporter of vitamin D metabolites, its role in target cell acquisition of vitamin D is much less clear. For many extra-renal tissues megalin is not ubiquitously expressed; as such it is assumed that free vitamin D metabolites as opposed to those bound to DBP are acquired intracellularly. The 'free hormone hypothesis' assumes that the most biologically active forms of steroid hormones are those that are not bound to their serum binding globulins (22, 23). Recent studies suggest that the free hormone hypothesis may play a role in mediating some of the actions of vitamin D. 'free' vitamin D is the most biologically active metabolite and can rapidly and passively diffuse across the cell membrane to target intracellular VDR. Initial association studies indicate free 25(OH)D₃ to be a more reliable correlate of bone mineral density. However, only a small fraction is in an unbound, free form, and serum concentrations are significantly lower relative to their bound counterparts, albeit strongly correlated (24).

2.1.3 Vitamin D epimerisation, an alternative pathway

When considering vitamin D metabolism, it is important to recognise an alternative parallel epimerization pathway exists (Figure 2.0). This occurs at the third carbon atom of 25(OH)D₃, which alters the hydroxyl group from an alpha to beta orientation. The structures of 25(OH)D₃ and 3-epi-25(OH)D₃ remain otherwise the same. Since the action of 1 α -hydroxylase appear unrestricted, 3-epi-25(OH)D₃ metabolites are hydroxylated to form 3-epi-1,25(OH)₂D₃. It appears all major vitamin D intermediate metabolites can be epimerized following the standard metabolic pathway.

Little is known on the source of 3-epi-25(OH)D₃, although age, season and dietary vitamin D may contribute (25). In infants, absolute concentrations appear markedly increased, with levels declining to adult concentrations in children around one year of age (26). The C-3 epimer is also detectable in adult blood samples and overall appears positively correlated with 25(OH)D₃ (27). In vitro, 3-epi-25(OH)D demonstrates reduced binding affinity to DBP (36-46%) relative to 25(OH)D₃, and 3-epi-1,25(OH)₂D₃ has reduced VDR binding affinity (2-3%) relative to 1,25(OH)₂D₃ (28, 29). Although 3-epi-1,25(OH)₂D₃ appears similar to 1,25(OH)₂D₃ in relation to PTH suppression, significantly

reduced calcaemic effects are observed comparatively (30, 31). This is important as serum 3-epi-25(OH)D may be included when vitamin D status is assessed by measuring 25(OH)D₃ by either immunoassays that display cross-reactivity, or liquid chromatography-mass spectrometry (LC MS-MS) methods that do not resolve both compounds(32).

2.1.4 Extra-renal vitamin D metabolism

Recent advances in our understanding of the ‘non-classical’ extra-renal functions of vitamin D have revealed a broad range of extra-skeletal targets beyond bone development and calcium homeostasis, including potent anti-proliferative, pro-differentiative and immunomodulatory actions (33). Broadly these may be categorised into: (1) regulation of hormone secretion, (2) regulation of immune function, and (3) regulation of cellular proliferation and differentiation, albeit a degree of functional overlap is evident(34).

A central feature of these is the autocrine/ intracrine metabolic mechanisms, which are highly distinct from the ‘classical’ endocrine renal generation of active 1,25(OH)₂D₃ characteristic of skeletal actions of vitamin D. As summarised in Figure 2.1, this involves local metabolism of precursor 25(OH)D₃, with the resulting active 1,25(OH)₂D₃ acting via endogenous VDR (35). Since most tissues in the body express VDR through which active 1,25(OH)₂D₃ subsequently acts, the scope of vitamin D function is wide-reaching. Extra-renal 1 α -hydroxylase activity is also well evidenced, with both autocrine and paracrine substrate dependent modes of action defined (36).

Whilst 1 α -hydroxylase is constitutively expressed, extra-renal expression of 24-hydroxylase appears to be part of a feedback control mechanism to attenuate 1,25(OH)₂D₃ activity.

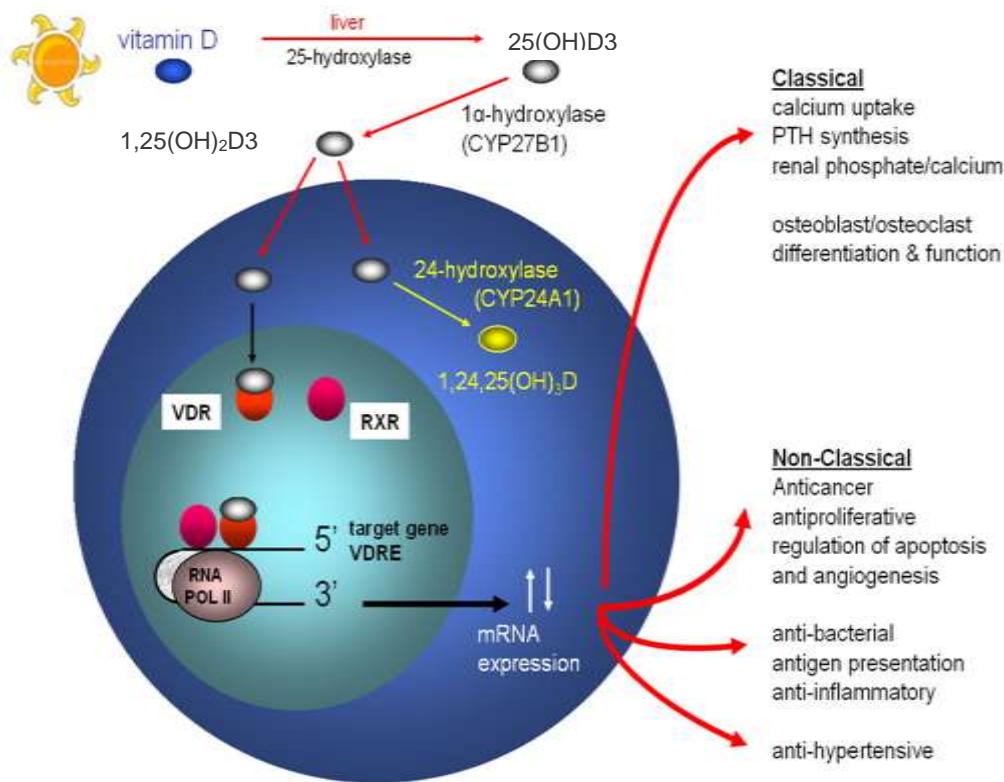


Figure 2.1 Classical and non-classical actions of active 1,25-dihydroxyvitamin D₃

(1,25(OH)₂D₃): mechanisms of action (Image courtesy of Professor Martin Hewison). Vitamin D

synthesis principally begins in the skin following direct sunlight exposure, with subsequent hydroxylation of vitamin D₃ by 25-hydroxylase to inactive 25-hydroxy-vitamin D₃ (25(OH)D₃) in the liver. Following conversion from inactive 25-hydroxyvitamin D₃ (25(OH)D₃) via 25-hydroxyvitamin D-1α-hydroxylase (1α-hydroxylase), 1,25(OH)₂D₃ may then bind the vitamin D receptor (VDR) forming a heterodimer with RXR, or undergo catabolic breakdown to less active 1,24,25 di-hydroxyvitamin D (1,24,25(OH)₂D₃). The VDR-RXR complex subsequently translocates to the nucleus and binds to vitamin D response element (VDRE) DNA sequences. These regulate target messenger ribonucleic acid (mRNA) transcript expression, with a range of classical and non-classical actions of vitamin D now recognised as summarised.

Control of 1,25(OH)₂D₃ production also differs, with PTH and FGF23 not required. For example, in peripheral human macrophages inflammatory cytokines (CK), including interferon-gamma (IFN-γ) significantly enhance the synthesis of 1,25(OH)₂D₃, whilst PTH has no observed effect (37). Instead, 1,25(OH)₂D₃ production via 1α-hydroxylase appears to be more dependent on the availability of

substrate 25(OH)D₃ (38). Whilst this provides many potential advantages for localised tissue-specific regulation of vitamin D function, it is also likely to be more sensitive to variations in the circulating concentrations of 25(OH)D₃, in other words vitamin D ‘status’. How vitamin D sufficiency or deficiency affects tissues in which there is significant metabolism of 25(OH)D₃ remains unclear. Furthermore, as evidenced by inflammatory disorders such as sarcoidosis, in which there is aberrant macrophage-mediated 1,25(OH)₂D₃ production, failure to control extra-renal 1 α -hydroxylase has serious clinical implications (39).

2.1.5 Non-classical immune effects of vitamin D

Of particular interest are the potent immune-mediated effects of vitamin D influencing both the innate and adaptive arms of the immune system. For most major immune subsets, including monocytes, macrophages, B lymphocytes (B cells), T lymphocytes (T cells) and dendritic cells (DCs), positive VDR and CYP27B1 expression is reported. As shall be outlined, these studies demonstrate the importance of localised intracrine 1,25(OH)₂D₃ production (40-42).

As discussed in detail in Chapter 5, the most well characterised extra-renal vitamin D system is within innate monocytes and macrophages. Both contain the metabolic apparatus required to synthesize and respond to active 1,25(OH)₂D₃, and this appears enhanced in response to immune challenge(43). These studies have highlighted the importance of localised production of 1,25(OH)₂D₃ as a mechanism for maintaining antibacterial activity. Initial observations arose within the context of *Mycobacterium tuberculosis* (*M. Tb*) infection, where 1,25(OH)₂D₃ treatment significantly decreased mycobacterium growth, and was enhanced in the presence of IFN- γ stimulation. Later this was found to arise via toll-like receptor (TLR)-mediated activation, with concomitant upregulation of CYP27B1, and VDR (44, 45).

Regarding vitamin D and the adaptive immune system, T cells express VDR, with increased levels measured following proliferation (46). As such, initial studies of vitamin D focused upon anti-proliferative responses (46, 47) with T helper (Th) cells the principal target. It is now clear vitamin D also influences T cell phenotype (48, 49). Specifically, 1,25(OH)₂D₃ reportedly modulates T cell pro-inflammatory CK production, limiting IFN- γ , interleukin-2 (IL-2), and tumour necrosis factor-alpha

(TNF- α) production, and inducing regulatory T cells (Treg) CK release, including IL-4, and IL-10. The effects of vitamin D on T cells in vivo may however be more complex, as in *Vdr* gene KO mice reduced levels of Th1 cells are reported (50).

Other T cell subsets, including Treg and inflammatory IL-17-secreting T cells (Th17 cells) are also now implicated. In the presence of 1,25(OH)₂D₃ a drive to Treg production is reported with their immuno-suppressive capacity also potentially increased, thereby inhibiting cytotoxic cluster of differentiation (CD)4⁺ T cell production (51). For Th17 cells, which promote immune responses to some pathogens and are linked to inflammatory tissue damage(52), exposure to 1,25(OH)₂D₃ suppresses both their development (53, 54) and IL-17 release (55).

Albeit the exact mechanisms by which vitamin D influences T-cell function remain less certain, it appears 1,25(OH)₂D₃-mediated effects can arise directly through intracrine 1,25(OH)₂D₃ synthesis, or indirectly via DCs and macrophages in a paracrine fashion (56-59).

Considering humoral responses, 1,25(OH)₂D₃ is also shown to inhibit B cell proliferation, differentiation and IgG production. Until recently this was considered an indirect T cell-mediated effect, however recent studies suggest direct effects upon B-cell homeostasis can arise in a VDR dependent manner(60). Collectively, these observations suggest that non-classical metabolism in both innate and adaptive immune subsets has a significant immuno-modulatory role involving the coordinated actions of CYP27B1 and VDR in mediating intracrine and paracrine actions of vitamin D.

2.1.6 Vitamin D status and assessment

The definition of what constitutes optimal or adequate vitamin D status remains a subject of intense debate. At present serum total 25(OH)D₃ remains the principal marker of vitamin D status with ‘deficiency’ principally defined as 25(OH)D₃ <20ng/mL (50nmol/L) and ‘insufficiency’ as 25(OH)D₃ <30ng/mL (75 nmol/L). The Institute of Medicine (IOM)(61), the UK Scientific Advisory Committee on Nutrition (SACN)(62) and the International Consensus on Prevention of Nutritional Rickets (63) identified individuals with 25(OH)D concentrations < 25–30 nmol/L. The 14th Workshop Consensus on Vitamin D advised that although an absolute minimum 25(OH)D₃ level

50nmol/L is recommended for the classic actions of vitamin D upon bone and mineral health, at least 75–100nmol/L is required when the disease data for non-classical actions of vitamin D are considered (64). Importantly, low serum levels of 25(OH)D₃ have been associated with a range of extra-renal complications, including cancers, allergic disorders, infections, autoimmune disorders and cardiovascular disease(65-71). A recent meta-analysis, which assessed the association between 25(OH)D₃ with all-cause mortality found a steep increase for participants with 25(OH)D₃ < 40nmol/L eight independent prospective European consortium studies (72). As the parameters of normal vitamin D function shift from being based solely upon parameters of skeletal integrity, defining ‘normal’ circulating levels for a healthy population presents a challenge.

With improved analytical methods, whether additional vitamin D metabolites should now be quantified to provide improved assessment of vitamin D status is of much current interest (73). LC MS-MS is now widely recognised as the gold standard technique for vitamin D analysis, reflecting its analytical flexibility, specificity and sensitivity comparative to immuno-based assays (74, 75). This permits simultaneous measurement of separate 25-hydroxylated metabolites and downstream di-hydroxylated metabolites, including 25(OH)D₃, 3-epi-25(OH)D₃, 24,25(OH)₂D₃, and 25(OH)D₂ in remarkably low total serum volumes (76). Importantly, this included measurement of active 1,25(OH)₂D₃, for which accurate quantification is particularly complex due to its 1000-fold lower concentrations (pmol/L), short half-life, and lipophilic nature (76) (77).

2.1.7 Overall study aims and objectives

This project principally aimed to investigate the potential immunomodulatory role for vitamin D in human pregnancy. In preparation, the following objectives were initially defined:

1. To perform a detailed vitamin D metabolite analysis across normal human pregnancy comparative to the non-pregnant state.
2. To understand whether vitamin D metabolism becomes dysregulated within the context of abnormal pregnancy, specifically pre-eclampsia.

3. To delineate the extra-renal immune-mediated effects of vitamin D across normal human pregnancy, in particular the effects upon decidua-derived uterine natural killer (uNK) cells and macrophages.

Together we anticipate these studies will improve our understanding of the extra-renal role of vitamin D during pregnancy, and help provide a functional mechanistic rationale for future vitamin D supplementation trials in pregnant women. A 'General Methods' for this study are first outlined in Chapter 3. In Chapter 7, the overall findings of the study are evaluated together to form the 'Final Discussion'.

3 General Methods

3.1.1 Ethics

West Midlands ethics

Ethical approval was obtained from the Local Research Ethics Committee (REC), West Midlands Health Authority. (NHS REC 06/Q2707/12 [2006]) (13/WM/0178 [2013]) (RG_14-194 [2014]). This included first trimester surgical termination of pregnancy (sTOP), and third trimester postnatal samples, including those obtained from women diagnosed with pre-eclampsia (PET) booked at Birmingham Women's & Children's Hospital Foundation Trust (BWCFT) and Walsall Manor Hospital Trust. Written informed consent was subsequently obtained from all participants recruited to the study.

SCOPE ethics

Samples were purchased from the SCOPE (Screening for Pregnancy Endpoints) Ireland study (Clinical Research Ethics Committee of the Cork Teaching Hospital: ECM5(10)05/02/08) following appropriate ethics amendment (14/WM/1146 - RG_14-194 2) and material transfer agreement (MTA) (15.04.2016 15-1386) approvals.

3.1.2 Participant recruitment

West Midlands recruitment

Women with uncomplicated pregnancies undergoing sTOP between 8-13 weeks (w) gestation (NP1; n=25), as determined by ultrasound measurement of crown rump length were recruited at Walsall Manor NHS Trust & BWCFT. Third trimester (>37 w) (NP3) and PET sera, decidua and placental samples were collected from pregnant women consented prior to delivery at BWCFT. All PET cases were diagnosed according to current International definitions (ISSHP, 2014) (78); new hypertension presenting after 20w with ≥ 1 of the following new onset conditions: 1: proteinuria (urinary protein: creatinine ratio > 30 mg/mmol or a validated 24-hour (h) urine collection > 300 mg protein); 2. other maternal organ dysfunction (renal insufficiency, liver involvement, neurological and/ or haematological complications); 3. uteroplacental dysfunction (fetal growth restriction). A healthy

non-pregnant female ‘control’ group was recruited to provide whole blood for comparative serum vitamin D analysis.

SCOPE study recruitment

Samples utilised in this study were purchased from the SCOPE Ireland study biobank (www.anzctr.org.au; ACTRN12607000551493). As summarised in Figure 3.0, SCOPE Ireland participants were recruited as part of a larger prospective international pregnancy cohort study involving six research centres, located in Auckland, Adelaide, London, Leeds, Manchester, and Cork. The study aimed to develop screening tests for PET, small for gestational age (SGA), and spontaneous preterm birth. The main inclusion criteria were a low-risk pregnancy, a singleton pregnancy <15w gestation, and no previous pregnancy >20w gestation. PET was defined as a systolic blood pressure (BP) ≥ 140 mmHg or diastolic BP ≥ 90 mmHg on ≥ 2 occasions 4h apart after 20w but before the onset of labour or postpartum with either proteinuria (24h urinary protein ≥ 300 mg or a spot urine protein: creatinine ratio ≥ 30 mg/mmol creatinine or urine dipstick protein ≥ 2) or any multisystem complication of PET. Specific exclusion criteria are outlined in Appendix 9.1.1 (79). Overall, n= 278 (5%) pregnancies were complicated by PET, n=638 (11%) SGA, n=470 (8.4%) gestational hypertension and n=236 (4%) spontaneous preterm birth.

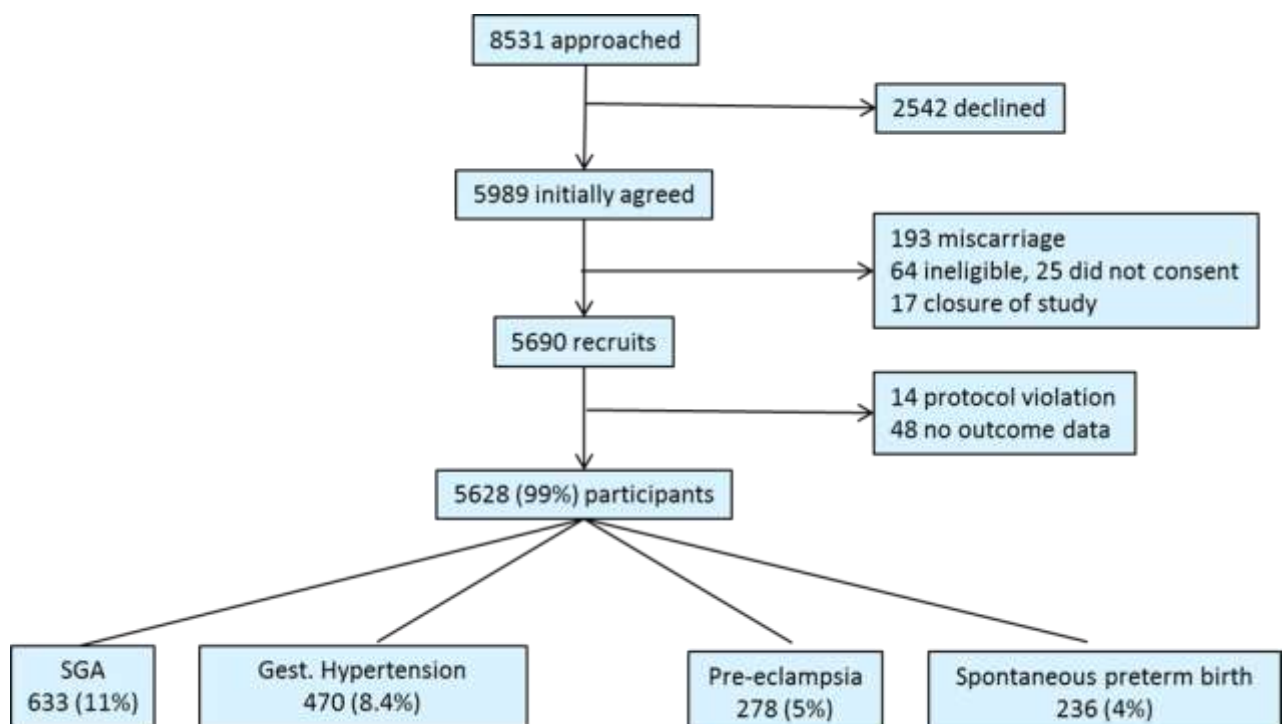


Figure 3.0 Summary of SCOPE (Screening for Pregnancy Endpoints) Ireland study recruitment across the 6 research centres (March 2008 to January 2011). Flow diagram summarising the serial stages of participant recruitment to the SCOPE study. The frequency and percentage as a proportion of those participants initially approached (%) is provided. Of the 5628 women included, 633 pregnancies were complicated by small for gestational age (SGA), 470 gestational hypertension (Gest. Hypertension), 279 pre-eclampsia and 236 spontaneous preterm birth.

Overall, a total of n=1768 participants attending for antenatal care at Cork University Maternity Hospital, Cork, Ireland (528N), were recruited to the SCOPE Ireland cohort early in their second trimester between March 2008 and January 2011. For our study, matched urine and serum samples were purchased from the biobank for n=50 low-risk nulliparous pregnant women at 15w gestation. It was pre-specified that n= 25 had prospectively developed PET, and n=25 normotensive controls matched for maternal age, ethnicity and body mass index (BMI) were provided. Samples were anonymised by the Cork SCOPE study group, with the University of Birmingham (UoB) researchers blinded to the clinical outcome at the point of analysis. A healthy non-pregnant female ‘control’ group (n=9) was also recruited at UoB (Birmingham, UK) to provide whole blood and urine for comparative vitamin D metabolite analysis.

3.1.3 Sample preparation

West Midlands

Peripheral blood & cord blood sample preparation

For all first and third trimester samples a matched peripheral maternal blood sample was obtained (~20mL) at the point of surgery / delivery. A matched cord blood sample (5-10mL total) was collected at delivery in all third trimester sample groups. Ethylenediaminetetraacetic acid (EDTA) coated sample tubes were used for all peripheral blood mononuclear cell (PBMC) extraction. Blood samples were diluted 1:1 with phosphate buffered solution (PBS) for PBMC isolation by density gradient centrifugation using Ficoll Plus (GE Healthcare Life Sciences, UK) at 1800 revolutions per minute (rpm), brake zero, for 25min. Since Ficoll is of greater density than the cell suspension, a layer

above the Ficoll with a distinct interface could subsequently be removed using a Pasteur pipette. The resultant cell fraction was washed three times with PBS at 1800, 1200 and 1500rpm prior to re-suspension in 2mL RPMI 1640 complete medium (1000 units [iu]/mL penicillin, 1mg/mL streptomycin, 2 mM L-glutamine, and 10% fetal bovine serum (Sigma, Poole, UK)], and subsequently counted using a haemocytometer.

Placenta and decidua classification

Fetal placental and decidua samples were obtained from 1st and 3rd trimester whole placental samples. In preparation for this, formal training with Dr J Bulmer's research group at the University of Newcastle (Newcastle, UK) was undertaken prior to human placental tissue sample collection at UoB. As summarised in Figure 3.1, the human placenta comprises both a fetal component formed by the chorion and a maternal portion formed by the decidua. The fetal trophoblast proliferates and form a syncytiotrophoblast and cytotrophoblast layer around the conceptus from week 2 gestation. Decidualisation arises from initial implantation, characterised by transformation of endometrial stromal cells to decidual cells by steroid hormones (progesterone) and embryonic signals into the decidua. As illustrated, this may be divided into three regions: basalis, capsularis and parietalis.

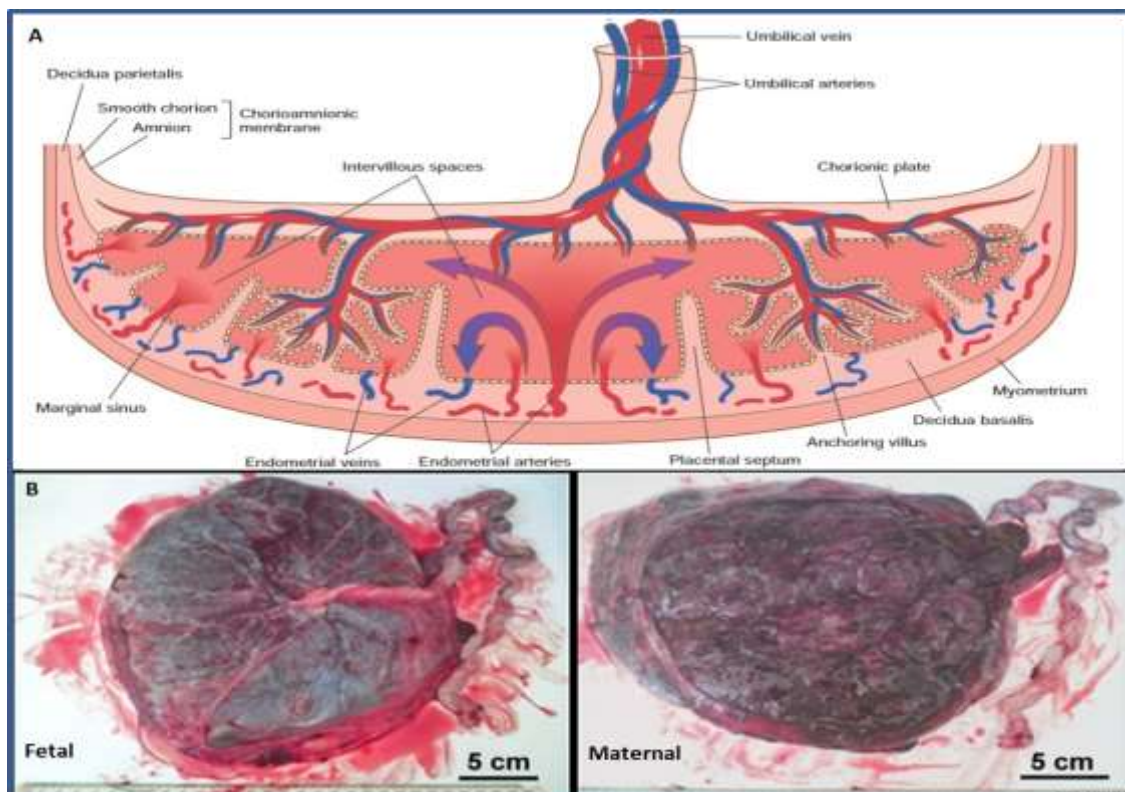


Figure 3.1 Anatomy of human placenta. A. Schematic of fetal and maternal components of human placenta. B. Image of overall placenta structure, viewed from both the fetal and maternal sides at term. 5 cm scale bar. Images revised from Anatomy Of Human Placenta Pregnancy Medicinase Body, Dec 2017 (<http://newhacks.info/anatomy-of-human-placenta/anatomy-of-human-placenta-pregnancy-medicinase-body/>).

Placental tissue biopsies

Placental samples were identified macroscopically and washed thoroughly with Hanks Balanced Salt Solution (HBSS) 10x (ThermoFisher, USA). For the first trimester cohort, decidua samples were concomitantly identified with tissue biopsies approximately ~ 1cm x 1cm x 1cm obtained under sterile conditions following thorough re-washing with HBSS 10x. They were immediately stored at -80°C until further use.

When ready for use, placental / decidual biopsies (~1g weight) were defrosted on ice and homogenised in 700µL ice-cold PBS using a gentle MACS tissue dissociator (Miltenyi Biotec, UK,) with M tubes using pre-set programs developed for total RNA or mRNA isolation from fresh or frozen samples. Homogenates were subsequently centrifuged at 10,000g for 5min and the clear homogenate was transferred to a separate eppendorf tube. Total protein content in the homogenate was immediately measured (ThermoFisher, USA).

First trimester decidua tissue preparation

Decidua was identified macroscopically at the time of collection, and washed with HBSS 10x (Thermo Fisher Scientific) thoroughly, prior to shipment on ice to UoB. Samples were immediately stored at 4°C until ready for use.

Under sterile conditions the prepared decidua tissues were finely minced and in 15mL falcon tubes enzymatically digested in incomplete RPMI 1640 medium (containing 1000iu/mL penicillin, 1mg/mL streptomycin, 2 mM L-glutamine), 1mg/mL collagenase (Sigma Aldrich, Poole, UK) and 200iu/mL DNase (Sigma Aldrich, Poole, UK) (Digest mix) at 37°C. The incubation times were 40min and 90min for the first and third trimester samples respectively. The resulting cell suspension was

centrifuged for 10min at 1800rpm, brake 3 following passage through a 40µm cell strainer. The residual first trimester decidual cell tissue was re-incubated under the same conditions using a fresh Digest mix, and similarly sieved and centrifuged prior to combination with the first digest sample.

Digested tissue was next washed and re-suspended in 20mL incomplete RPMI media. The mononuclear cells were isolated using density gradient medium as outlined for 'Peripheral blood and cord blood sample preparation', and subsequently counted using a haemocytometer.

Third trimester decidua tissue preparation

The decidua parietalis layer was isolated from the fetal chorionic membrane by carefully scraping the cell layer with a scalpel blade. The cells were then washed with HBSS 10x over a 40µm cell strainer to remove any residual maternal blood. The decidua basalis layer was obtained by sharp dissection from the underlying villous chorion. This was washed thoroughly with HBSS 10x and all remaining contaminating fetal tissue and maternal blood carefully removed.

The decidua parietalis and basalis fractions were pooled for digestion. Under sterile conditions the prepared decidua tissue was finely minced and enzymatically digested in 30mL Digest mix at 37°C for 90min. The resulting cell suspension was centrifuged for 10min at 1800rpm, brake 3 following passage through a 40µm cell strainer. As outlined for first trimester decidua, digested tissue was washed and re-suspended in incomplete RPMI media for PBMC isolation by density gradient centrifugation. The resultant cell fraction was washed and cell counted.

SCOPE

Paired serum (750µL) and urine (900µL) samples were obtained at 15w gestation from a cohort of 50 pregnant women recruited to SCOPE (80). The samples were shipped on dry ice at -20°C from University of Cork, Ireland to UoB.

3.1.4 Analysis of serum and urine vitamin D metabolites by LC MS-MS

Reference Standards

Reference standards for the following vitamin D metabolites were utilised (Sigma, UK); 25(OH)D₂, 25(OH)D₃, 24R,25(OH)₂D₃, 1,25(OH)₂D₃, 3-epi25(OH)D₃, 24,25(OH)₂D₃, 1,25(OH)₂D₂. These

were purchased as stock solutions in ethanol and diluted in methanol to prepare standard curves ranging between 5–100ng/ml and quality controls by Dr C. Jenkinson. All solutions were stored at –20°C in amber salinized vials for subsequent use. 7 α C4 Reference standard was purchased from LGC standards (Teddington, UK). External vitamin D calibrators and quality controls were purchased from Chromsystems (Am Haag, Germany).

Vitamin D metabolite analysis

Vitamin D analytes were extracted from 200 μ L patient serum and placental tissue (placenta and decidua [Section 3.1.3]). 20 μ L of internal standard was added containing 3-epi-25(OH)D3-d3 (100ng/ml), 25(OH)D3-d3 (100ng/ml) and 1 α ,25(OH)2D3-d3 (50ng/ml) in methanol/water (50/50%) (Sigma, Poole, UK), the final internal standards in solution were 16, 16 and 8ng/ml respectively.

Proteins were precipitated using 80 μ L methanol, 50 μ L isopropanol and 80 μ L of water (all LC MS-MS grade, Sigma, Poole, UK), with the solution vortexed at high speed for 30s and left for 7min, followed by centrifugation at 7516g for 5min. The supernatant was used for extraction. To extract the samples, a novel supportive liquid-liquid extraction (SLE) method, as opposed to liquid-liquid extraction (LLE) was utilised to permit faster sample preparation at a reduced cost, without compromising analyte recovery and avoid matrix affects (76). The supernatants were collected and transferred onto 96-well SLE plates (Phenomenex, Macclesfield, UK), which completely absorbed the sample into a sorbent by applying a vacuum (5Hg) for 10s. After 6min two consecutive 800 μ L volumes of MTBE/ethyl acetate (90/10%) (Sigma, Poole, UK) were added to each well. Samples were eluted under gravity initially into a 96-well collection plate, followed by applying a vacuum (5Hg) to elute final volume. The elution solvent was evaporated under nitrogen at 50°C after each 800 μ L addition. Samples were reconstituted in 125 μ L water/methanol (50/50%) (Sigma, Poole, UK) and stored at -80°C for LC MS-MS analysis.

LC MS-MS analysis was performed by C Jenkinson at the Phenome Centre University of Birmingham and the Biochemistry Clinical laboratory, University Hospital South Manchester, using an ACQUITY ultra performance liquid chromatography [uPLC] coupled to a Waters Xevo TQ-S

mass spectrometer [Waters, Manchester, UK])(76). This method has been validated previously based upon US Food and Drug Administration guidelines for analysis of these metabolites(76).

In brief, ionisation was performed in electrospray ionisation mode and the mass spectrometer was operated in positive ion mode. Multiple reaction monitoring (MRM) mode was used to monitor and quantify vitamin D analytes. The capillary voltage was 3.88kV and the desolvation temperature was 500°C. Chromatography separation was carried out using a Lux Cellulose-3 chiral column (100mm, 2mm, 3µm) (Phenomenex, Macclesfield, UK), which was maintained at 60°C in a column oven. A 0.2µm inline filter (Waters, Manchester, UK) was added before the column to prevent blocking of the column and contamination. The mobile phase was LC MS–MS grade methanol/water/0.1% formic acid (Poole, UK) at a flow rate of 330µL/min, with a total run time of 8min per sample. Vitamin D depleted charcoal stripped serum (Golden West Biologicals Inc., Temecula, US), was ran as a negative control. Known concentrations of vitamin D metabolites and internal standards were added to 200µL charcoal stripped serum to prepare calibration and QC standards. Data analysis was subsequently performed by C Jenkinson with Waters Target Lynx.

Urine method optimisation and SCOPE sample preparation

Quantitative analysis of urinary de-conjugated vitamin D metabolites was performed using a novel LC MS-MS quantification method. Optimization was performed using spot urine samples ($\leq 1000\mu\text{L}$) obtained from a cohort of healthy third trimester pregnant women at BWCFT (n=5; 28-39+2w gestation). This involved (i) evaluation of the minimum total urine volume, which ranged from 750-1000µL, (ii) optimisation of the SPE method (iii) the effect of including a derivatisation agent PTAD (Sigma-Aldrich, Poole, UK), as compared to non-derivatised samples. Therefore, all urine samples ($\leq 1000\mu\text{L}$) were prepared in duplicate to permit direct comparison.

Calibration and QC controls were prepared using steroid and vitamin D depleted urine (Sigma Aldrich). Neither 25(OH)D₃ nor 24,25(OH)₂D₃ was detected. This was used to prepare calibration curves, utilising the following standards; 25(OH)D₃, 24,25(OH)₂D₃, 1,25(OH)₂D₃ to spike the vitamin D metabolite-free urine.

Samples were vortexed gently and incubated with β -glucuronidase (1000iu /mL) (type IX-A; G7396 Sigma-Aldrich, Poole, UK), in sodium acetate–acetic acid buffer (pH 5.0, 0.1M) (3mL) at 50°C for 2h. To the reaction mixture, 1mL ice-cold LC MS-MS grade acetonitrile was added and samples were centrifuged at 1500g for 10min. The supernatants were passed through either an Oasis® HLB cartridge (60 mg; Waters Assoc., Milford, MA, USA) or Phenomenex Strate-XL cartridge (60mg; Phenomenex, Macclesfield, UK), which were first washed with ethyl acetate (2mL), methanol (2mL) and water (2mL) prior to sample loading. Sample was washed through the SPE column. The columns were subsequently washed with methanol-water (2mL)(7:3, v/v, 2mL), and hexane (1mL), and the metabolites then eluted with ethyl acetate (1mL) into a salinized glass tube. This was performed using a negative pressure vacuum collection chamber, in order to control flow rate throughout the purification procedure. The solvents were subsequently evaporated under a nitrogen gas stream prior to sample derivatisation.

Compound	Abbreviation	MRM transitions	Collision energy (eV)	Cone Voltage (V)
25-hydroxyvitamin D3	25(OH)D3	558.3> 280.5	22	26
		558.3> 298.1	14	26
24,25-dihydroxyvitamin D3	24,25(OH) ₂ D3	574.3> 175.3	20	22
		574.3> 257.3	16	26
		574.3> 298.1	20	26
25-dihydroxyvitamin D3-d3	25(OH)D3-d3	561.4> 283.1	23	24
		561.4> 301.3	15	24

Table 3.0 Multiple-Reaction Monitoring (MRM) transitions for 4-phenyl-1,2,4-triazoline-3,5-dione (PTAD)-derivatized vitamin D metabolites. The vitamin D metabolite compounds quantified, their abbreviated term, MRM transitions, collision energy (electronvolt [eV]) and cone voltage (V) are summarised.

Urine derivatisation method

To improve ionisation and enhance the sensitivity and separation of individual low concentration metabolites (pg range) an additional derivatization procedure using PTAD was utilised (81). For this, 0.5mg/mL PTAD in ethyl acetate (Sigma Aldrich) was added to samples incubated at room temperature in dark for 2h, before 20µL water was added to terminate the reaction.

The samples were assessed using a Waters Xevo-MS coupled to an AQUITY UPLC. The method utilised is as outlined in Section 3.1.4, with a Waters C18 column (2.1x50mm 1.7µm) used to separate PTAD derivatized metabolites. MRM transitions listed in the table above were optimized by running a

full scan, daughter scan and then measuring the intensity under a range of cone voltage and collision energies to determine optimal values.

3.1.5 Analysis of serum DBP

Human DBP (R&D Biosystems, UK) was measured with Dr R Susarla (UoB) using a solid phase sandwich ELISA kit (assay range 15.6 – 250ng/mL) as per manufacturer's instructions. Serum samples were diluted to 1:2000, and placenta homogenates 1:10 prior to measurement. DBP standard stock (100ng/mL) was prepared from Human DBP standard following reconstitution with calibrator diluent RD5P (1:5 dilution with distilled water). For the standard series, 200 μ L of calibrator diluent was added to each tube, with 200 μ L serial dilutions from 100ng/mL to 0ng/mL concentration prepared. First, 50 μ L of assay diluent RD1-38 (buffered protein base with preservatives) was added per well of the 96-well plate. Then, 50 μ L of DBP standard or sample was added and incubated for 2h at room temperature using a horizontal orbital microplate shaker (500rpm). Each well was aspirated and washed 4 times with 400 μ L wash buffer (wash buffer concentrate diluted 1:24 in distilled water) ensuring all solution was fully removed. Next, 200 μ L human DBP conjugate was added per well and incubated for 1h at room temperature using a horizontal shaker (500rpm). Each well was then aspirated and washed 4 times with 400 μ L wash buffer prior to adding 200 μ L of substrate solution (Colour reagents A and B; 1:1 ratio) which was covered and incubated for 30min. The reaction was terminated with 50 μ L Stop solution, and the optical density measured using a 450nm microplate reader, with wavelength correction at 570nm subtracted to improve test accuracy. For data-analysis, a standard curve with line of best fit was generated and the determined concentrations were multiplied by the dilution factor.

3.1.6 Analysis of serum albumin

Human albumin (Abcam, Cambridge, UK) was measured with Dr R Susarla (IMSR, UoB) using an ELISA. The assay was performed at room temperature, with all reagents and standards prepared in advance. The albumin standards were prepared as serial dilutions (1-8), with 240 μ L total volume, and concentration range 200ng/mL – 0ng/mL). Serum samples were diluted at 1:10,000. Placenta homogenates were diluted 1:1000 prior to measurement, with all samples performed in duplicate.

50 μ L of Albumin Standard or sample was added per well of the 96-well plate and incubated for 1h. The plate was washed 5 times with 1x wash buffer (1:20 with reagent grade water) ensuring all liquid was completely removed. Next, 50 μ L of prepared 1x biotinylated albumin antibody was added to each well and incubated for 30min, and subsequently washed 5 times with 1x wash buffer. 50 μ L of 1x streptavidin- peroxidase conjugate (1:100 with 1x diluent N [1:10 reagent grade water]) was added to each well and incubated for 30min, and re-washed as above with the wash buffer. Finally, 50 μ L of Chromogen Substrate was added per well and incubated until a visible blue colour was evident, which was at ~20min. The reaction was terminated with 50 μ L Stop solution, with the expected colour change to yellow confirmed. The absorbance was immediately read on a microplate reader at 450nm wavelength, with absorbance readings acquired at 570nm subtracted from this to improve overall assay precision.

3.1.7 Analysis of free serum 25(OH)D3

Serum concentrations of free (total minus DBP and albumin-bound) and bioavailable (total minus DBP bound) serum 25(OH)D3 were calculated by Dr R Chun (UCLA Department of Orthopaedic Surgery and Orthopaedic Hospital Research Center, Los Angeles, USA) utilising total 25(OH)D3 and DBP/albumin values (82, 83).

3.1.8 Creatinine Jaffe reaction

Urinary creatinine was quantified using a parameter assay kit (R&D systems Inc, Abingdon, UK). This utilises a colorimetric Jaffe reaction between creatinine and picrate acid to permit accurate and rapid quantification(84). For this, 10 μ L test volumes of urine (n=50) were required, which were diluted 20-fold in distilled water and prepared in duplicate. Standard controls were prepared as directed, with an 8-point 20mg/dL–0 mg/dL concentration range utilised. Either 50 μ L of sample or standard was subsequently added per well of the 96-well plate, with 100 μ L of alkaline picrate solution added for 30min at room temperature to initiate the Jaffe reaction. Alkaline picrate solution reacts with the creatinine to form an orange –red complex, the optical density of which was measured with a microplate reader at 490nm. A standard curve was plotted as a log/log curve-fit to ascertain test well concentrations, following 20-fold multiplication of the dilution factor. Urinary levels of vitamin D

metabolites were normalized to the creatinine content by dividing the concentration of the analyte of interest by the creatinine concentration obtained in the same urine sample, with the result reported as the concentration of target analyte per g of creatinine (ng/g).

3.1.9 Positive selection immuno-magnetic isolation of immune cell subsets

CD56+ cell isolation

Positive immune-magnetic bead selection was utilised to isolate CD56+ cells from decidua and maternal blood. For this, cells were washed and re-suspended in ice cold MACS buffer (80µL per 10⁷ cells) and incubated with primary anti-human CD56 (20µL per 10⁷ cells) (Miltenyi Biotec) at 4°C for 20 min. This step was also performed for matched maternal peripheral PBMCs. The cells were washed once in MACS by centrifugation for 10 min at 300g, with the resulting cell pellet re-suspended in 500µL MACS for separation using the Midi-MACS magnetic column separator with the un-bound non-CD56+cell fraction collected. Following three column washes with MACS buffer the CD56+ intra-column fraction was plunged in 1mL MACS buffer through the Midi-Macs columns in the absence of the magnet (Miltenyi Biotec). Both the unbound CD56 deplete and CD56+ fractions were collected. The resulting cell suspensions from both fractions were then counted and underwent purity analysis using flow cytometry (Section 3.1.13).

CD14+ cell isolation

Positive immune-magnetic bead selection was also utilised to isolate CD14+ cells from decidua, maternal and cord blood. This was performed as above, using primary anti-human CD14 (20µL per 10⁷ cells) (Miltenyi Biotec) for 20min at 4°C. The cells were washed once in MACS buffer by centrifugation for 10min at 300g, with the resulting cell pellet re-suspended in 500µL MACS buffer in preparation for separation using the Midi-MACS magnetic column (Miltenyi Biotec) as described. Both unbound CD14 deplete and CD14+ fractions were collected and counted, with 100,000 cells/sample similarly subjected to purity analysis.

3.1.10 Cell culture

NK Cell Culture

Matched isolated CD56⁺ cells were plated at 1.25×10^6 /mL in a 96 well round bottom cell culture plate under aseptic conditions in complete RPMI cell culture medium (penstrep 100 μ g/mL [Sigma], l-glutamine 2 mM [Sigma], RPMI 1640, fetal calf serum) at 37°C in a humidified incubator containing 5% CO₂ for 24h. A range of CK treatments were used as summarised in Table 3.1, including: IL-2, IL-12, TNF- α and IL-15 in the presence and absence of 1,25(OH)₂D3 (10nM)(Enzo Lifesciences, Exeter, UK). Stimulation with IL-2 (50iu/mL), IL-12 (10 ng/ mL), and IL-15 (10 ng/mL) CK for 24h in the presence and absence of 1,25(OH)₂D3 (10nM) was used for all subsequent assays.

Cytokine	Concentration	Functional Role
IL-2	50units/ mL	Augment NK cell cytotoxicity (85)
IL-15	10ng/ ML	Promotes proliferating NK cell accumulation and survival (86)
IL-12	10ng/ mL	Promotes NK cell IFN- γ production (86)
TNF- α	10ng/ mL	Promotes NK cell IFN- γ production (87)

Table 3.1 Summary of the individual cytokines (CK), the dose and mode of action assessed for NK cell stimulation.

Macrophage / monocyte cell culture

Matched isolated CD14⁺ cells were plated at 2.0×10^6 /mL in a 96-well round bottom cell culture plate under aseptic conditions in complete RPMI cell culture medium at 37°C in a humidified incubator containing 5% CO₂ for 24h. Lipopolysaccharide (LPS) (1 μ g/mL), a recognised stimulant of monocytes and macrophages via TLR-4 binding, was added in the presence and absence of 1,25(OH)₂D3 (10nM) to selected wells. To maximise the total cell yield, at the point of cell harvest the cell plate was cooled on ice at 4°C and the well contents re-pipetted 10 times to release highly adherent cells.

3.1.11 LC MS-MS conversion assay

In collaboration with C Jenkinson, vitamin D metabolites were measured using LC MS-MS. For this, uNK and pNK isolates were cultured in the presence and absence of CK stimulation as outlined in Section 3.1.10 in the presence and absence of inactive 25(OH)D3 (100nM) for 24h. NK culture supernatants were gently aspirated from 96 well plate and centrifuged in 500µL sterile eppendorfs at 1800rpm for 5 min to separate the culture supernatant for storage at -80°C until LC MS-MS analysis, as outlined in Section 3.1.11.

3.1.12 Flow cytometry

For all experiments detailed, a multi-channel Dako Cyan flow cytometer, with the capability of analysing up to 9 colours plus forward and side scatter was utilised. The results were analysed in the form of scatter plots, histograms and dot plots using FlowJo Software version X (Tree star, Inc., Ashland, USA). Spectral overlap refers to the wavelengths emitted by one fluorochrome, but detected by the filter designated to another fluorochrome. This was factored into the data analysis by auto-calculating compensation values derived from experimental single-stain control samples. As a result of multi-panels employed, additional manual compensation was required in certain instances.

Gating was performed sequentially, with the first step using a forward/ side scatter plot, which provides an approximate measure of cell size and individual cells 'complexity'. Pulse wave analysis was utilised to identify and exclude aggregates and damaged cells, prior to gating the viable 'live' immune cell population (88). Isotype matched controls were used to account for non-specific antibody binding. Biological experimental controls were also used to validate the success of the method. For example, for the VDR and activation assays, whole PBMC experimental controls were used.

Cell preparation for flow cytometry

All preparations were performed in 5mL round bottom polystyrene tubes (Becton Dickinson [BD] Biosciences, UK). All washes were performed in 1mL PBS unless otherwise stated, and centrifugation at 1500rpm for 5min. Wash solutions were removed by brief tube inversion to remove the excess supernatant, with the remaining pellet vortexed gently to re-suspend in 100-150µL. All

staining incubation steps were performed in the dark, to avoid direct light exposure to the fluorophores which are summarised in Table 3.2. Cells were stored in the dark until flow cytometry analysis.

Antibody	Company	Catalogue Number
CD3- FITC	BD Biosciences	345763
CD4- APC	BD Biosciences	555349
CD3-PE	BD Biosciences	555340
CD3- PerCP	BD Biosciences	345766
CD4-FITC	BD Biosciences	555346
CD4-PE	BD Biosciences	555347
CD4 -PerCP	BD Biosciences	345770
CD8-PeCF594	BD Biosciences	562282
CD56-PE	Ebioscience	12-0567-42
CD56 PE Vio770	MACS Miltenyi Biotec	130-096-831
CD10-vioblue	MACS Miltenyi Biotec	130-099-670
CD25-APC	BD Biosciences	555434
CD14-Percp	BD Biosciences	345786
CD25-PE	BD Biosciences	555432
CD20-Viogreen	MACS Miltenyi Biotec	130-096-904
CD45-RO FITC	BD Biosciences	555492
CD45-RA PE	BD Biosciences	555489
CD45-APC	Ebioscience	17-0459-41
CD45-viogreen	MACS Miltenyi Biotec	130-096-906
CD69-APC	BD Biosciences	555533
CD69-FITC	BD Biosciences	555530
NKp46 APC	MACS Miltenyi Biotec	130-092-609
NKp30-PE	Ebioscience	12-3379-41
TNF- α E450	Ebioscience	48-7349-42
TNF α FITC	Ebioscience	11-7349-81
IFN- γ e450	Ebioscience	48-7319-42
IL-10-PE	BD Biosciences	559337
CD4-e450	Ebioscience	48-0048-42
VDR-APC	Santa Cruz Biotechnology	sc-13133

Table 3.2 Summary of primary surface and intracellular antibodies utilised for flow cytometry.

The antibody, fluorescent dye, company and catalogue serial number are provided

Surface staining protocol for cell surface antigens

Live cells were first washed in PBS and then centrifuged, with the supernatant subsequently discarded. A live/ dead fixable discrimination dye, prepared as per manufacturer's instructions (Molecular Probes Life Technologies), was added to the cells and incubated for 20min on ice. The cells were re-washed and centrifuged with the supernatants discarded. Directly conjugated antibodies were then added to the appropriate samples for 30min and incubated in the dark on ice. Optimum staining concentrations were determined for each antibody by titration previously. The cells were subsequently washed and centrifuged with PBS and the supernatant discarded. Following staining, cells were either washed once with PBS and re-suspended in PBS for immediate flow cytometry analysis, or fixed with 3% paraformaldehyde (PFA). When surface staining PBMCs, non-specific antibody binding was reduced by adding 2% goat serum (Sigma-Aldrich) with the surface staining panel.

Paraformaldehyde (PFA) fixation

Cells were re-suspended in 300 μ L 3% PFA by gentle vortexing and were incubated at room temperature for 12min. Cells were pelleted and washed once with 1mL PBS, then re-suspended in 200 μ L PBS and stored at 4°C.

Intracellular staining for granzyme B, perforin and cytokines

Following PFA fixation, cells were permeabilised by first washing with 1mL 0.1% saponin in PBS for 5min. The supernatant was removed, and primary intracellular antibodies added and incubated in the dark for 30min at room temperature. Excess antibody was removed by one wash with 0.1% saponin-PBS followed by one PBS wash. Cells were re-suspended in 200 μ L PBS and collected by flow cytometry.

Intracellular staining protocols for VDR analysis assay

To optimise the VDR analysis assay different permeabilisation methods were utilised and compared. An optimised Bendix protocol was utilised for on-going VDR analysis. This protocol was initially used to measure VDR in peripheral CD8+ T cells within the context of Crohn's disease (89).

Cells were washed once with PBS prior to incubation for 20min at room temperature in 100 μ L 4% PFA. Cells were washed twice in 2mL 2% fetal calf serum (FCS) in PBS and then incubated for 30min on ice in 75 μ L 5% FCS 0.5% Triton X solution (Sigma Aldrich, Poole, UK). The primary VDR-APC antibody or concentration matched isotype control (purified mouse IgG2a) was directly added to this and incubated for a further 30min at 4°C. Cells were subsequently washed once in 1mL 2% FCS PBS solution, and then incubated with 1 μ L/ sample anti-mouse IgG2a APC-conjugated secondary antibody for a further 30min at 4°C. The cells were re-washed in 1mL 2% FCS-PBS, followed by 1mL PBS, and re-suspended in 200 μ L PBS for collection by flow cytometry.

3.1.13 Cytotoxicity assay

To assess the functional effects of 1,25(OH)₂D₃ upon NKs, the expression of a range of recognised pro-inflammatory and regulatory NK cell markers were measured. For this, isolated NK cells were cultured as described in Section 3.1.10 in the presence or absence of 1,25(OH)₂D₃ (10nM, ENZO Life Sciences). CD107a (LAMP1) is a characterised marker of NK cell degranulation. It is required for efficient delivery of perforin to lytic granules and the delivery of cytotoxic granules to target cells(90). CD107a transit to the cell surface during a 6hr culture period with the MHC-devoid k562 cell line was used as a measure of NK cell cytotoxicity(91). Expression of IFN- γ and TNF- α was measured as an indication of NK cell activity. Specifically, k562 cells were added to NK cells at 1:5 ratios along with anti-human CD107a (BD Biosciences, California, USA). After 1h, cells were treated with protein trafficking inhibitors, Brefeldin A (5 μ g/mL, Sigma-Aldrich, UK) and monensin (golgi stop BD Biosciences, USA) to prevent CD107a degradation by re-internalisation and to block cytokine export. At 6h, cells were transferred to FACs tubes, dead cell labelled, surface stained and fixed with PFA. Intracellular cytokines were stained according to the intracellular staining protocol in Section 3.1.10.

Matched PBMCs that had been cultured overnight at 37°C, 5% CO₂ in complete RPMI medium at 2x10⁶/mL (2x10⁵/well) were used as a positive control for CK expression and vitamin D response. PBMCs were stimulated with phorbol 12-myristate 13-acetate (PMA) (25ng/mL) and ionomycin (0.5 μ M) for 5-6h. After 1h, they were treated with Brefeldin A (5 μ g/mL). At 6h, cells were dead cell

stained, surface labelled, fixed and intracellularly stained for cytokines and CTLA-4, a known 1,25(OH)₂D₃ target (56).

3.1.14 RNA extraction, reverse transcription and quantitative real-time polymerase chain reaction (qRT-PCR)

RNA extraction

Total RNA was extracted using TRI-reagent (800µL) (Sigma-Aldrich, Dorset, U.K.) following NK isolation and 24h culture in the presence and absence of CK stimulation and 1,25(OH)₂D₃. Following dissociation of the nucleoprotein complexes, 0.1mL 1-bromo-3-chloropropane (Sigma-Aldrich, Poole, UK) was added and samples were centrifuged (12,000g for 15min at 4°C) to separate the cell lysate into 3 distinct layers; lower organic DNA phase, middle protein interface, and upper aqueous RNA phase. The RNA layer was subsequently obtained and precipitated with 0.5mL isopropanol (Sigma-Aldrich, Dorset). Samples were incubated at room temperature and centrifuged for 10min at 12,000g to obtain the RNA pellet. The RNA pellet was washed with 1mL 75% ethanol and centrifuged for 5min at 12,000g with the supernatant discarded. RNA was re-suspended in 20µL nuclease free water (ThermoFisher Scientific, MA, USA). The purity and quantification of RNA extraction was checked by measuring the A_{260}/A_{280} and A_{260} by Nanodrop spectrometry in preparation for complementary DNA (cDNA) synthesis. From the A_{260} value, RNA is quantified using the relationship $40\mu\text{g}/\text{mL}$ RNA = 1 unit of A_{260} in a 1cm path length. Concentration of RNA in the samples ($\mu\text{g}/\mu\text{L}$) = $A_{260} \times 40$ x dilution factor.

Preparation for qRT-PCR

cDNA synthesis was performed using 100ng-1µg of total RNA which was reverse transcribed using Applied Biosystems Taqman Reverse Transcription Reagents Kit following the manufacturer's guidelines (Roche, New Jersey). This was performed by diluting in 2.5µL of 10X RT buffer, 5.5µL of 25mM MgCl₂, 5µL of 10mM dNTP mix, 0.5µL of 20 iu/µL recombinant RNase inhibitor, 1.25µL of 50µM of random hexamer primers and 1.6µL of 50 iu/mL of multiscribe reverse transcriptase made up to a total volume of 20µL with RNase-free water. The reaction was incubated at 25°C for 10min

and at 37°C for 60 min, prior to heating to 48°C for 30min and 95°C for 5min. Samples were then cooled to 4°C prior to cycle completion and cDNA collection.

qRT-PCR

qRT-PCR was subsequently performed on either 96 well plates in 20µL reactions containing 1x Taqman Universal PCR Master Mix, 1x Taqman 6-carboxy fluorescein (FAM)-labelled Gene Expression assay mix (Applied Biosystems, CA, USA) and 1µL cDNA per sample, diluted in nuclease free water. Expression of gene specific mRNAs encoding CYP27B1, CYP24A1, and VDR were determined (Table 3.3). All reactions were multiplexed with the VIC-labelled 18S rRNA housekeeping control assay (Applied Biosystems, CA, USA). The reactions were performed on ABI 7500 qPCR machine (Applied Biosystems, CA, USA), with the progress of DNA amplification monitored continuously by measuring the release of fluorescent dyes which are conjugated to the probes. The thermal cycling conditions utilised were 50°C for 2min, 95°C for 10min followed by 40 cycles of 95°C for 15s and 60°C for 1min. Quantification of gene expression was determined using the $\Delta\Delta C_t$ method and stated relative to a fixed unstimulated immune cell population.

All reactions were performed in at least duplicate and expressed as a mean of these values. Ct values were obtained as the cycle number at which logarithmic PCR plots crossed a calculated threshold line. The $\Delta\Delta C_t$ value is the difference in the ΔC_t value of a sample, with reference to the control, and the fold change is subsequently calculated using $2^{-\Delta\Delta C_t}$.

Gene	Taqman Gene Expression Assay	Label
<i>I8S</i>	4319413E	VIC
<i>CYP27B1</i>	Hs01096154_m1	FAM
<i>CYP24A1</i>	Hs00167999_m1	FAM
<i>VDR</i>	Hs00172113_m1	FAM
<i>CYC-1</i>	Hs00357717_m1	VIC
<i>IL-6</i>	Hs00174131_m1	FAM
<i>TNF-α</i>	Hs00174128_m1	FAM
<i>Cathelicidin</i>	Hs01011707_g1	FAM
<i>IFN-γ</i>	Hs00989291_m1	FAM

Table 3.3 Summary of gene specific mRNAs utilised for qRT-PCR. The Taqman gene expression code and dye label are provided for each gene target analysed.

3.1.15 Fluorescence-activated cell sorting (FACS)

Paired decidua, maternal and cord blood (third trimester only) samples were prepared as outlined in Section 3.1.3 as per gestation, with subsequent Ficoll separation and washing.

NK cell isolation and FACS

Whole immune cell populations from decidua and maternal blood were washed in PBS prior to incubation for 30 min at 4°C with the following murine monoclonal antibodies (mAbs), anti-CD45 anti-CD56 and anti-NKp46 from MACS Miltenyi (Miltenyi Biotec, UK), and anti-CD3, and anti-CD14, from BD Biosciences (CA, USA), directly conjugated with FITC, PE, PerCP, PE-Cy7, Pe-Vio 770, VioGreen, and APC. Cells were washed with 1mL MACS and re-suspended in 500 μ L PBS for FACS. Immediately prior to sorting, 1 μ L propidium iodide (PI) was added to assess cell viability. As summarised in Figure 3.2, live CD45+ CD56+ NKp46+ cells, negative for CD14 and CD3 were selected for separation into sterile collection tubes containing 2mL complete RPMI and stored immediately at 4°C. This was performed using a BD Biosciences FACS Aria Fusion at UoB. The cells were centrifuged for 5min at 1500rpm, counted with a haemocytometer and re-suspended in complete RMPI (1.25 x 10⁶ cells/mL) for cell culture. As detailed in Section 3.1.10, uNK and pNKs

were cultured with CK stimulation (IL-2, IL-12 and IL-15) in the presence and absence of 1,25(OH)₂D₃ co-treatment.

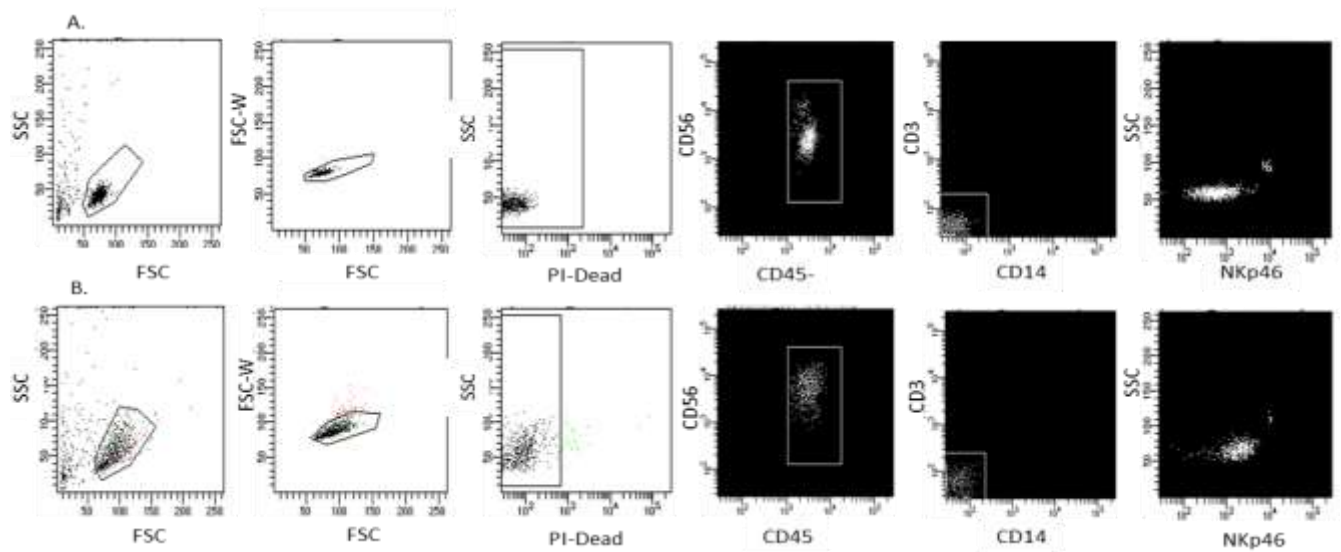


Figure 3.2 Representative FACS analysis plots for NK cells. The maternal (A) and decidua (B) FACS strategy gating is illustrated. Initially, forward scatter (FSC), side scatter (SSC), pulse width (FSC-W) were used to identify lymphocytes singlets. Propidium iodide (PI)-Dead identified live cells with CD45⁺ CD56⁺ NKp46⁺ cells, negative for CD14 and CD3 subsequently identified for FACS.

Monocyte and macrophage isolation

Following Ficoll separation, paired decidua, maternal and cord blood samples were first subjected to a CD14⁺ positive selection step (Section 3.1.9) to debulk the sample and reduce its cellular complexity allowing for faster sorting and reduced rejection rate. The cells were then washed with PBS and surface antigen stained at 4°C with the following primary mAbs, anti-HLA-DR, -CD14, -CD66, -CD56, -CD3, CD19, and CD45, directly conjugated with FITC, PerCP, PE-Cy7, Pe-Vio 770, and VioGreen. Experimental single colours were prepared alongside this to calculate compensation values. Cells were washed with 1mL MACS buffer and re-suspended in 500µL PBS for immediate FACS. Immediately prior to sorting, 1µL PI was added to assess cell viability. As summarised in Figure 3.3, The following gating strategy was applied to obtain live CD45⁺ CD14⁺ HLA-DR⁺ cells, negative for CD66, -CD56, -CD3, CD19. This was similarly performed using a BD Biosciences

FACSAria Fusion at UoB. Cells were collected under sterile conditions into FACS tubes containing 2mL complete RPMI media, washed and re-suspended at 2.0×10^6 cells/mL at 4 °C for culture.

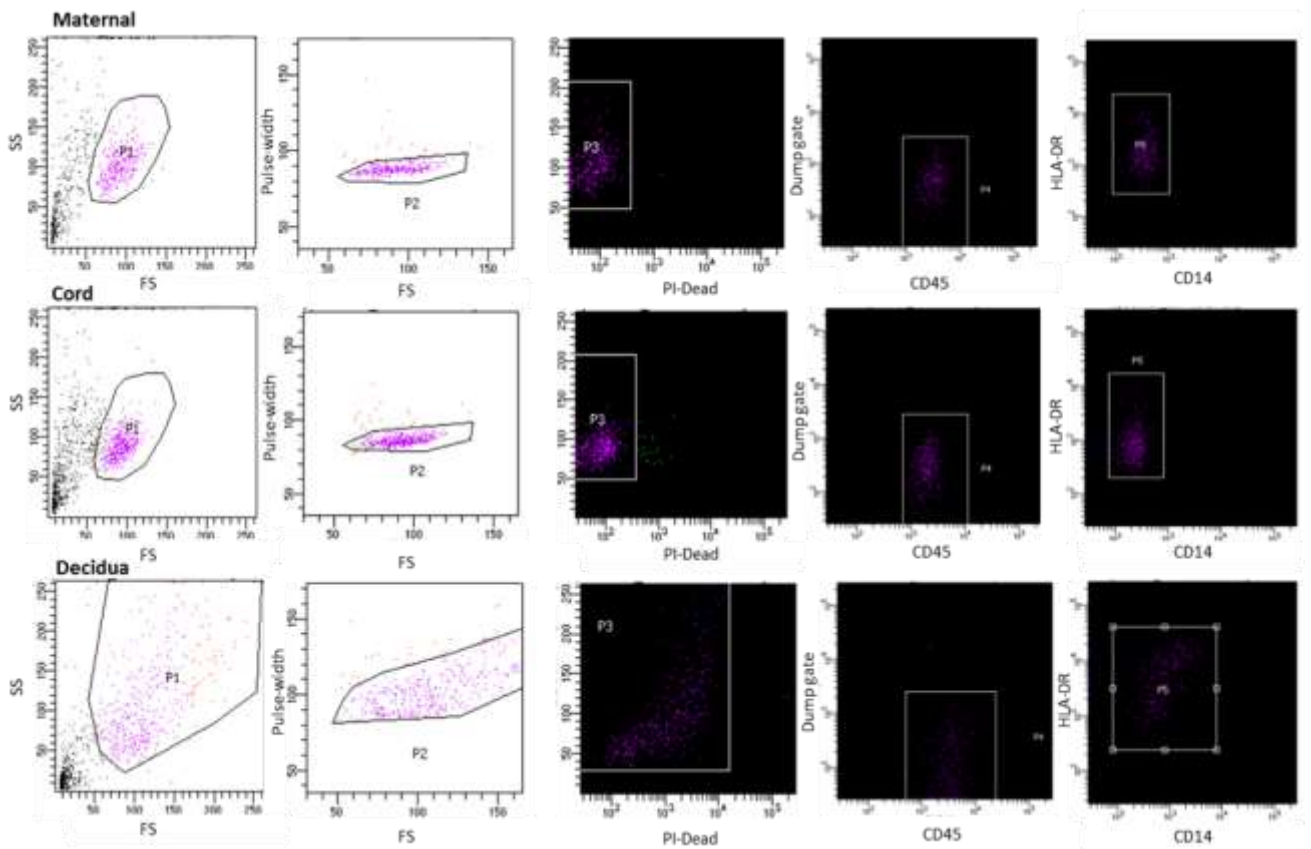


Figure 3.3 Representative FACS analysis plots for maternal blood, cord blood and decidua monocyte/ macrophage subsets. The maternal blood, cord blood and decidua (B) FACS gating is illustrated. Initially, forward scatter (FSC), side scatter (SSC), pulse width (FSC-W) were used to identify lymphocytes singlets. Propidium iodide (PI)-Dead identified live cells with CD45+ CD14+ HLA-DR+ cells, negative for CD66, CD56, CD3, CD19 subsequently identified for FACS.

3.1.16 RNA extraction

Cultured cells were harvested at 24h and immediately underwent total RNA extraction and clean-up using the RNeasy Micro Kit (QIAGEN, Germany), as per manufacturer's instructions using RNeasy MiniElute spin columns. This combines the selective binding properties of a silica-based method with the speed of microspin technology to obtain reproducible yields of total RNA from small sample numbers ($<5 \times 10^5$ cells).

Due to the high content of RNases in placental tissue, 10 μ L β -mercaptoethanol was added per 1mL Buffer RLT prior to cell lysis and homogenization. Next, 70% ethanol was added to the lysate to optimise RNA binding conditions prior to loading onto RNeasy MiniElute spin column (QIAGEN, Germany). The RNA ($\leq 45\mu$ g) binds to the silica membrane, with the column flow-through discarded. On-column digestion of genomic DNA was performed by adding 10 μ L RNase-free DNase I diluted in 70 μ L RDD buffer for 15min at room temperature. The DNase I was then fully removed with washing. Pure, concentrated RNA was eluted in 14 μ L RNase free water. 2 μ L was transferred to a fresh nuclease free tube for subsequent purity and integrity analysis. Both tubes were stored immediately at -80°C.

Prior to cDNA library preparation, evaluation of RNA quality was essential, as degraded samples can significantly influence the interpretation of expression levels of RNA-seq data. ‘Integrity’ reflects the pattern of total RNA ribosomal units 28S and 18S, and mRNA length. ‘Stability’ reflects the distribution of stable housekeeping genes across heterogeneous sample conditions. Factors such as delay time, tissue hypoxia, mode of tissue handling can all effect both properties. As such, a RNA Integrity Number (RIN) scale is recommended to assess RNA quality prior to further analysis. This digital readout ranges from 1 to 10 with 1 being the most degraded profile and 10 the most intact. In solid tissue, 6–8 RIN values are considered reliable RNA, however between 8- 10 is indicative of high quality RNA(92). Initial Integrity estimates were estimated for sample aliquots through Louise Teed (MDS Technology Hub, UoB) and samples that met RIN criteria for sequencing were shipped for cDNA library preparation and RNA seq analysis at Source Bioscience, Nottingham, UK. MTA and local ethics amendment approval (14/WM/1146 RG_14-194 (3); 2016) were obtained in advance for this. After arrival, QC checks were re-run on the samples using the Agilent BioAnalyzer 2100 (Agilent, CA, USA), with the concentration and RIN score determined.

3.1.17 cDNA library preparation

First trimester NK cell cDNA library preparation

All 16 samples of first trimester NK RNA were suitable for cDNA library preparation by Source Bioscience, Nottingham, UK, as summarised in Table 3.4 (concentration 0.67-13.0 ng/ μ L, RIN 7.5-10).

ID	Sample	Concentration (ng/ μ L)	RIN
40-3	uNK CK	4.535	9.6
40-4	uNK CK + vit D	4.144	10
40-1	pNK CK	3.285	10
40-2	pNK CK + vit D	2.832	10
41-7	uNK CK	12.076	9.4
41-8	uNK CK + vit D	13.023	9.6
41-3	pNK CK	3.753	10
41-4	pNK CK + vit D	3.007	10
42 -3	uNK CK	7.076	7.5
42- 4	uNK CK + vit D	5.302	7.7
42- 1	pNK CK	0.841	8.2
42- 2	pNK CK + vit D	0.67	8
43- 7	uNK CK	10.163	9.8
43- 8	uNK CK + vit D	9.414	9.7
43- 5	pNK CK	3.293	9.6
43- 6	pNK CK + vit D	2.332	8.5

Table 3.4 Summary of the concentration and RIN scores measured prior to cDNA library preparation for first trimester uNK and pNK subsets. Initial concentrations (ng/ μ L) and RIN scores are summarised for first trimester paired uNK and pNK following 24h culture CK +/- vitamin D (Vit D) in preparation for cDNA library preparation. Individual sample and treatment identification (ID) numbers are also shown.

Third trimester monocyte and macrophage cDNA library preparation

Initial QC checks were re-validated using the Agilent BioAnalyzer 2100 (Agilent, CA, USA) for all third trimester monocyte and macrophage samples, with the concentration and RIN score determined as summarised in Table 3.5 (concentration 0.2 - 12.8, RIN 6.5 – 9.5).

Sample ID	Site / treatment	Concentration (ng/μL)	RIN
672 -5	Decidua Mø LPS	0.234	7.5
672-6	Decidua Mø LPS + VD	0.174	7.2
672-1	Mat Mø LPS	1.833	9.4
672-2	Mat Mø LPS + VD	8.693	8.3
672-3	Cord Mø LPS	5.648	8.6
672-4	Cord Mø LPS + VD	4.93	8.7
676-5	Decidua Mø LPS	0.556	8.1
676-6	Decidua Mø LPS + VD	0.508	8.4
676-1	Mat Mø LPS	7.775	8.6
676-2	Mat Mø LPS + VD	7.882	8.5
676-3	Cord Mø LPS	4.029	8.4
676-4	Cord Mø LPS + VD	4.613	7.6
687-5	Decidua Mø LPS	0.457	7.4
687-6	Decidua Mø LPS + VD	0.607	7.7
687 -1	Mat Mø LPS	10.134	7.8

687-2	Mat Mø LPS + VD	10.228	7.7
687-3	Cord Mø LPS	12.573	6.7
687-4	Cord Mø LPS + VD	10.46	6.7
669-9	Decidua Mø LPS	0.227	6.8
669-10	Decidua Mø LPS + VD	0.318	6.5
669-3	Mat Mø LPS	2.792	8.7
669-4	Mat Mø LPS + VD	2.341	6.7
669-7	Cord Mø LPS	4.089	9.5
669-8	Cord Mø LPS + VD	5.551	9.5

Table 3.5 Summary of the concentration and RIN scores measured for paired third trimester decidua, maternal blood and cord blood monocyte/ macrophage subsets. Initial concentration (ng/ μ L) and RIN score summary for third trimester decidua, maternal and cord monocytes / macrophages (Mø) treated with LPS +/- vitamin D (VD) in preparation for cDNA library preparation are summarised. Individual sample and treatment identification (ID) numbers are also shown.

cDNA library preparation - Switching Mechanism at the 5' end of RNA Template

(SMART)er Stranded Total RNA Seq

cDNA library preparation was performed using the Switching Mechanism at the 5' end of RNA Template (SMART)er Stranded Total RNA Seq Kit – Pico (Clontech, USA) (RNA range pg). SMARTer technology is designed to account for variations in both RNA 'integrity' and 'stability' (93, 94).

For this, library sequencing preparation is performed in a different order to traditional methods to avoid initial RNA selection via the mRNA poly-A-tail which may not be intact in degraded RNA samples. Alternatively, a modifiable integrated RNA shearing 'fragmentation' step is performed to

reduce RNA fragments for sequencing. The method used was selected according to the RIN score. Unlike cDNA fragmentation, RNA fragmentation has little bias over the transcript body. However, as a potential loss of transcript ends is reported, random hexamer oligonucleotide priming and locked nucleic acid template switching oligo (LNA-TSO) technology were also utilised to maximise the pre-amplification yield and length transcriptome coverage (95). Specifically, LNA-TSO stabilises a non-templated ‘stretch’ of nucleotides to the 3’ end of the cDNA, thereby creating an extended template which ensures reverse transcription extends to the 5’ end (96). Random primers ‘hexamers’, which are oligonucleotides with random base sequences often six nucleotides long facilitate processing of poorer quality RNA samples as they are not reliant upon the presence of a poly-A-tail. Furthermore, they permit the production of shorter cDNA fragments and increase the probability that the whole 5’ ends are converted to cDNA.

Only then was the first round of PCR amplification performed, which added full-length Illumina adapters with barcodes (forward adapter AGATCGGAAGAGCACACGTCTGAACTCCAGTCAC, reverse adapter AGATCGGAAGAGCGTCGTGTAGGGAAAGAGTGTA) to both short DNA fragment ends (75 base paired-end [75bp PE] sequencing) for sequencing to generate reads typically 30–400bp in length. The Forward PCR primer binds the LNA-TSO sequence, while the reverse PCR primer binds to sequence associated with the random hexamer. The reaction utilises fluorescently labelled nucleotide analogs, which are incorporated into the oligonucleotide chain by DNA polymerases. This uses bridge amplification, a solid-phase reaction, generating clusters of identical DNA molecules on the Illumina flow cell for sequencing. By utilising this PE sequencing approach, the overall quality and quantity of sequence data identified was improved, thereby facilitating detection of genomic rearrangements, repetitive sequence elements, gene fusions and novel transcripts. Ribosomal cDNA (originating from ribosomal RNA [rRNA] – 18S and 28S) was also cleaved at this stage by ZapR in the presence of the mammalian-specific R-Probes. Non-rRNA was avoided with further PCR2 amplification and enrichment performed using universal primers. Finally, the amplified RNA-seq libraries were purified by immobilization onto AMPure beads, which were washed with 80% ethanol and the cDNA eluted in Nuclease-Free Water. All libraries were QC

validated using the Agilent BioAnalyzer 2100 (Santa Clara, USA) to confirm index samples amplified concentration and size distribution (Table 3.4 and 3.5).

3.1.18 RNA sequence analysis

Following cDNA library construction, the samples were pooled and re-validated to assess molarity and size distribution. Following this, the DNA was loaded (1.8pM concentration) onto a High Output NextSeq 500 Flow Cell pv2. (Illumina, Inc. San Diego, USA), across 4 lanes for RNA sequencing (RNA-seq). Raw data was returned by Source Bioscience (Nottingham) in the FastQ Phred+33 (Illumina 1.9) format and bioinformatics analysis subsequently performed at UoB, using Partek Flow Software (Partek, Missouri, USA) in close collaboration with Dr K Knoblich and Dr A Fletcher (Institute of Immunology and Immunotherapy, UoB), both of whom have significant expertise in transcriptomic analysis(97).

First trimester NK cell RNA-seq analysis

Overall, ~800 million total reads were generated, with an average 25 million per sample. A genome guided transcriptome approach was used to assign raw sequence reads, including those reads that cover non-continuous portions of the reference genome. Data was mapped (aligned) using Spliced Transcripts Alignment to a Reference (STAR)-2.4.1d (98). Post-alignment quality assurance (QA) /QC was performed with a coverage report generated (Table 3.6). This includes the average number of reads that align to known reference bases and the average coverage depth, which details number of aligned sequence reads, thereby increasing the confidence of detection. Reads were quantified to transcriptome hg38_RefSeq (Genome Reference Consortium GRCh38) using Cufflinks(99), and normalised using quantile normalisation (Figure 3.4) to ensure the samples were comparable by reducing sources of experimental ‘obscuring’ variability, such as differences in sample preparation or processing. This was calculated on a per sample basis, using rank-based quantile normalisation. In brief, the distribution of probe intensities is made the same for each sample, based upon the assumption that each sample has the same distribution by taking the mean quantile and substituting it as the value of the data item in the original dataset (274). The highest value in all cases becomes the mean of the highest values the second highest value becomes the mean of the second highest values,

and so on. Box-whisker expression signal plots before and after normalisation are summarised in Table 3.6, which summarises the descriptive statistics across each sample. Overall, the minimum value was 0, maximum 2.59E+06, mean 364.58, median 0, quartile (Q)1 0 and Q3 84.75.

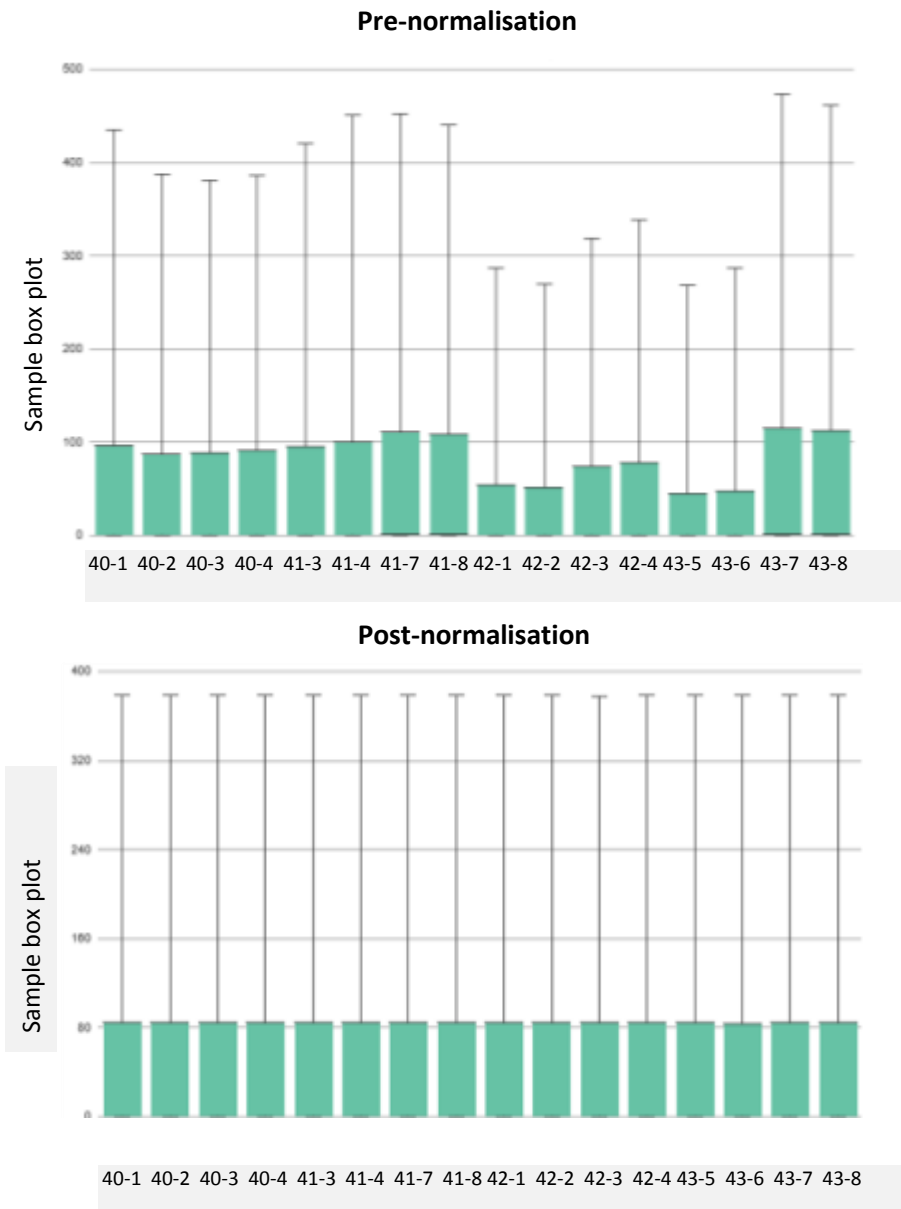


Figure 3.4 uNK and pNK cell pre and post normalisation box plots. The signal distribution for each sample, before and after normalisation, is provided for all samples sequenced. The study ID as summarised in Table 3.4 is used for NK cell site and treatment identification.

Sample	Locus	Treatment	Min	Max	Mean	Median	Q1	Q3
40-1_S3	Mat Blood	CK	0	2.59E+06	364.6	0	0	84.8
40-2_S4	Mat Blood	CK+VD	0	2.59E+06	364.6	0.00	0	84.8
40-3_S1	Decidua	CK	0	2.59E+06	364.6	0.00	0	84.6
40-4_S2	Decidua	CK+VD	0	2.59E+06	364.6	0.00	0	84.5
41-3_S7	Mat Blood	CK	0	2.59E+06	364.6	0.00	0	84.8
41-4_S8	Mat Blood	CK+VD	0	2.59E+06	364.6	0.00	0	84.8
41-7_S5	Decidua	CK	0	2.59E+06	364.6	0.19	0	84.8
41-8_S6	Decidua	CK+VD	0	2.59E+06	364.6	0.25	0	84.8
42-1_S15	Mat Blood	CK	0	2.59E+06	364.5	0.00	0	84.8
42-2_S16	Mat Blood	CK+VD	0	2.59E+06	364.5	0.00	0	84.8
42-3_S13	Decidua	CK	0	2.59E+06	364.5	0.25	0	84.3
42-4_S14	Decidua	CK+VD	0	2.59E+06	364.5	0.00	0	84.3
43-5_S11	Mat Blood	CK	0	2.59E+06	364.5	0.00	0	84.8
43-6_S12	Mat Blood	CK+VD	0	2.59E+06	364.5	0.00	0	83.9
43-7_S9	Decidua	CK	0	2.59E+06	364.6	0.19	0	84.8
43-8_S10	Decidua	CK+VD	0	2.59E+06	364.6	0.06	0	84.8

Table 3.6 Feature distribution for each NK sample utilised for RNA-seq analysis. Sample ID (sample), locus and treatment (CK +/- 1,25(OH)₂D3 [VD]), the minimum (min), maximum (max), mean, median, quartile (Q)1 and Q3 data information is provided for all NK subsets (n=16).

The median total aligned reads was 71567649 (interquartile range [IQR] 64250828–74820738), which represented 85.7% (84.5 – 87.5%) coverage (Table 3.7 and Figure 3.5). Differential gene expression analysis was performed with a cut-off fold-change of < -1.5 and > 1.5, and p-value ≤ 0.05 applied. The p-value was calculated using F-statistics, which calculates the variance within samples.

Three comparative analyses were assessed; (i) uNK CK versus (vs) pNK CK, (ii) uNK CK vs uNK CK + 1,25(OH)₂D3, and (iii) pNK CK vs pNK CK + 1,25(OH)₂D3 with expression levels represented by read counts. As summarised in Figure 3.5 and Table 3.6 overall the mean total reads was 18710400, with 58.9% fully within a coding exon, and 1.99% partly within an exon.

Sample ID	Locus	Treatment	Total reads	Total alignments	Aligned (%)	Total unaligned	Unaligned (%)	Total unique paired	Unique paired (%)	Total non-unique paired	Non-unique paired (%)	Coverage depth (x)	Avg. length	Avg. quality	%GC	
40-1_S3	Mat.Blood	CK	23197598.00	67855606.00	88.36	2700739.00	11.64	15120924.00	65.18	5379935.00	23.17	8.39	18.75	75.00	32.85	56.03
40-2_S4	Mat.Blood	CK+VD	20832387.00	59359304.00	88.50	2395285.00	11.50	13959346.00	67.01	4477756.00	21.49	8.80	15.61	75.00	32.96	55.10
40-3_S1	Decidua	CK	20975592.00	62658766.00	86.95	2736467.00	13.05	12992851.00	61.94	5246274.00	25.01	7.08	20.45	75.00	32.85	56.88
40-4_S2	Decidua	CK+VD	21596899.00	67975312.00	87.78	2639385.00	12.22	12980285.00	60.10	5977729.00	27.68	7.66	20.55	75.00	32.73	57.54
41-3_S7	Mat.Blood	CK	20759397.00	62593664.00	87.65	2563257.00	12.35	12930503.00	62.29	5265637.00	25.37	7.81	18.51	75.00	32.90	56.56
41-4_S8	Mat.Blood	CK+VD	19542063.00	64109372.00	86.22	2692549.00	13.78	10737358.00	54.94	6112156.00	31.28	4.67	31.57	75.00	32.79	58.72
41-7_S5	Decidua	CK	25488196.00	75621770.00	85.70	3646034.00	14.30	15536702.00	60.96	6305460.00	24.74	11.58	15.04	75.00	32.85	56.52
41-8_S6	Decidua	CK+VD	25823823.00	80285636.00	85.55	3731424.00	14.45	14991977.00	58.05	7100422.00	27.50	11.14	16.60	75.00	32.88	57.23
42-1_S15	Mat.Blood	CK	19274052.00	72211926.00	84.43	3001227.00	15.57	8708246.00	45.18	7564579.00	39.25	3.72	44.54	75.00	32.43	59.82
42-2_S16	Mat.Blood	CK+VD	20568967.00	72106996.00	81.42	3822366.00	18.58	9381309.00	45.61	7365292.00	35.81	4.36	37.96	75.00	32.79	59.72
42-3_S13	Decidua	CK	20103658.00	71028302.00	84.87	3040699.00	15.13	9722331.00	48.36	7340628.00	36.51	5.61	29.07	75.00	32.54	60.46
42-4_S14	Decidua	CK+VD	22546646.00	83039930.00	83.70	3674745.00	16.30	10028607.00	44.48	8843294.00	39.22	5.05	37.69	75.00	32.19	60.26
43-5_S11	Mat.Blood	CK	19695229.00	64675194.00	85.60	2833376.00	14.40	10797760.00	54.82	6062093.00	30.78	6.57	22.63	75.00	32.77	58.10
43-6_S12	Mat.Blood	CK+VD	20970828.00	72157214.00	84.36	3280133.00	15.64	10593103.00	50.51	7097592.00	33.85	5.92	27.96	75.00	32.84	58.82
43-7_S9	Decidua	CK	22972452.00	72417642.00	85.80	3262132.00	14.20	13177710.00	57.36	6532610.00	28.44	8.51	19.60	75.00	32.79	57.74
43-8_S10	Decidua	CK+VD	24038468.00	77749032.00	84.79	3656033.00	15.21	13166838.00	54.77	7215597.00	30.02	8.92	20.01	75.00	32.76	57.75

Table 3.7 Post alignment QA/QC report. Each row corresponds to a sample (n=16), permitting comparison in maternal blood pNK) and decidua uNK in the presence (CK +VD) and absence (CK) of vitamin D treatment. The total number of reads (total reads), and total number of alignments (total alignments). This includes the fraction of all the reads which were aligned to the reference assembly (Aligned). The Coverage column summarises the fraction (%) of the reference assembly sequenced, with the average (Avg.) sequencing coverage (x) of the covered regions 'Avg. coverage depth column'. Avg. length is the average read length and average read quality is given in Avg. quality. Finally, % GC is the fraction of G or C calls.

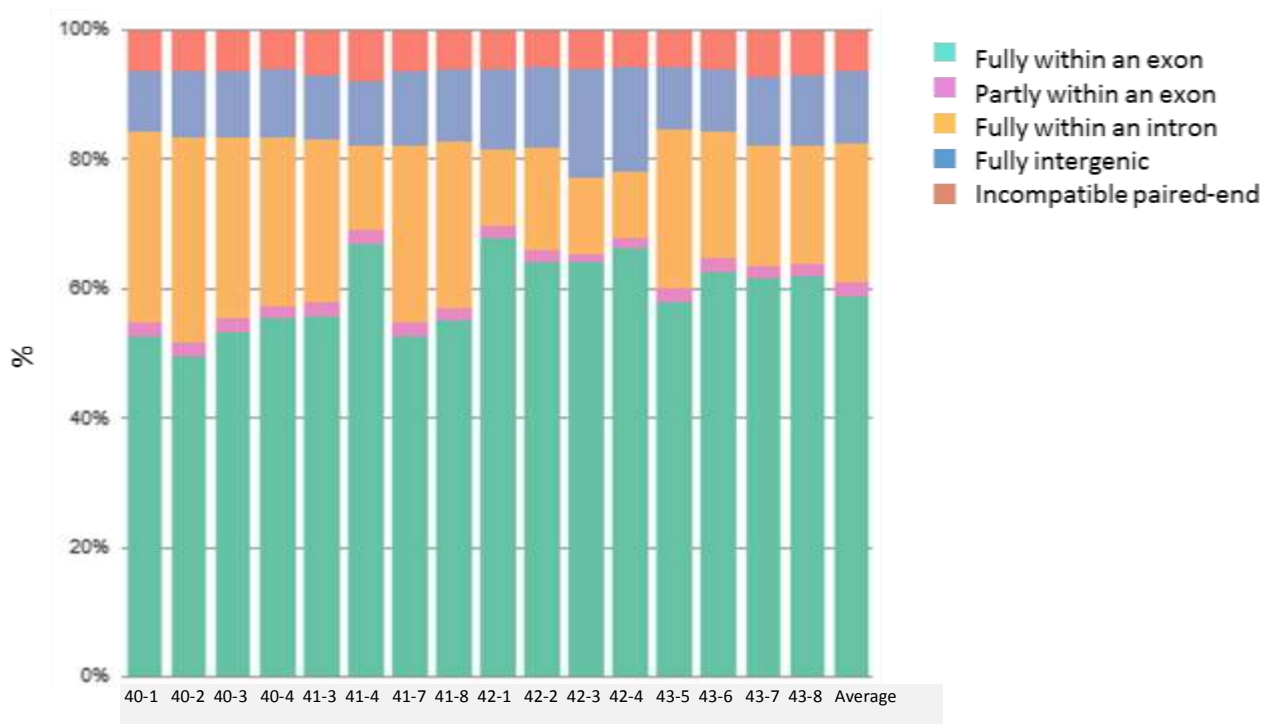


Figure 3.5 Quantification coverage breakdown for all NK cell RNA-seq samples. Each bar corresponds to an NK cell sample (n=16; Table 3.3). The fraction (%) of reads which were either fully within an exon, partly within an exon, fully within an intron, fully intergenic or incompatible paired-ends is represented as per legend.

Third trimester monocyte and macrophage RNA-seq analysis

Sequencing depth was pre-specified as 16.6 million unique clusters per sample & 33.3 million reads per sample with the total number of genes generated recorded (library size). As outlined, data was mapped using STAR-2.4.1d (98) with post-alignment QA/ QC performed as summarised in Table 3.8. The median total aligned reads was 58393797 (IQR; 50799109- 67428216), which represented 88.4% (83.1 – 88.9%) (Table 3.9).

Reads were quantified to transcriptome hg38_RefSeq, with rank-based quantile normalisation again performed on a per sample basis (Figure 3.6). Overall the minimum was 0, maximum 3.24E+06, mean 269.16, median 0.00, Q1 and Q3 19.96.

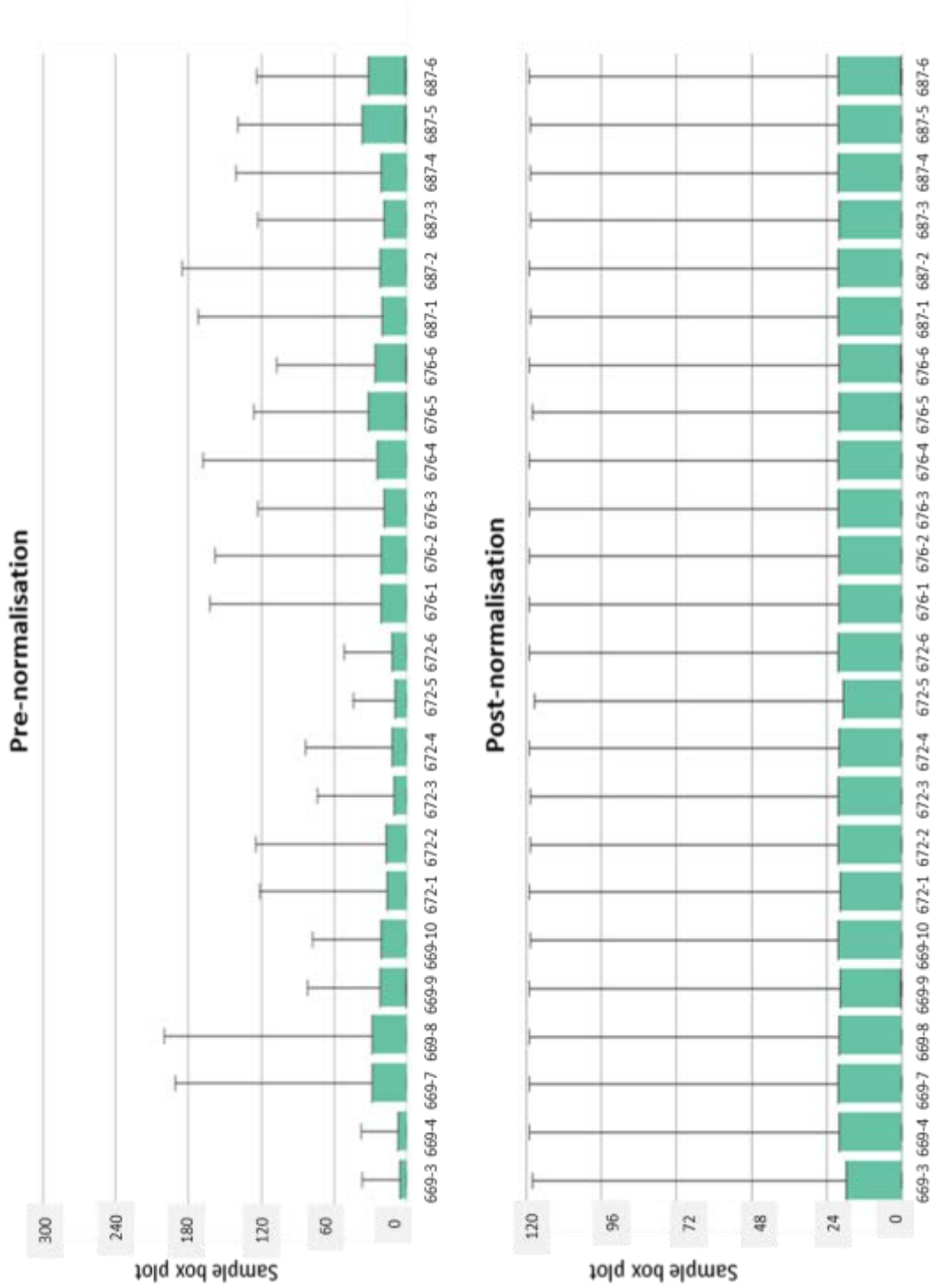


Figure 3.6 Pre and post normalisation box plots for all monocyte / macrophage samples sequenced in third trimester maternal blood, cord blood and decidua. The signal distribution for each sample, before and after normalisation, is provided.

Sample ID	Locus	Treatment	Min	Max	Mean	Median	Q1	Q3
669-10_S20	Decidua	LPS VD	0	3.24E+06	269.17	0.00	0.00	20.18
669-3_S21	Maternal	LPS	0	3.24E+06	268.89	0.00	0.00	17.57
669-4_S22	Maternal	LPS VD	0	3.24E+06	268.90	0.00	0.00	19.96
669-7_S23	Cord	LPS	0	3.24E+06	269.23	0.00	0.00	20.20
669-8_S24	Cord	LPS VD	0	3.24E+06	269.23	0.00	0.00	19.96
669-9_S19	Decidua	LPS	0	3.24E+06	269.21	0.25	0.00	19.70
672-1_S3	Maternal	LPS	0	3.24E+06	269.18	0.00	0.00	19.61
672-2_S4	Maternal	LPS VD	0	3.24E+06	269.18	0.00	0.00	20.20
672-3_S5	Cord	LPS	0	3.24E+06	269.07	0.00	0.00	20.24
672-4_S6	Cord	LPS VD	0	3.24E+06	269.12	0.00	0.00	19.96
672-5_S1	Decidua	LPS	0	3.24E+06	269.04	0.00	0.00	18.75
672-6_S2	Decidua	LPS VD	0	3.24E+06	269.09	0.00	0.00	20.29
676-1_S9	Maternal	LPS	0	3.24E+06	269.20	0.00	0.00	19.96
676-2_S10	Maternal	LPS VD	0	3.24E+06	269.21	0.00	0.00	19.98
676-3_S11	Cord	LPS	0	3.24E+06	269.20	0.00	0.00	20.30
676-4_S12	Cord	LPS VD	0	3.24E+06	269.23	0.00	0.00	20.27
676-5_S7	Decidua	LPS	0	3.24E+06	269.24	0.17	0.00	20.05
676-6_S8	Decidua	LPS VD	0	3.24E+06	269.21	0.29	0.00	19.96
687-1_S15	Maternal	LPS	0	3.24E+06	269.20	0.00	0.00	20.30
687-2_S16	Maternal	LPS VD	0	3.24E+06	269.20	0.00	0.00	20.20
687-3_S17	Cord	LPS	0	3.24E+06	269.20	0.00	0.00	19.99
687-4_S18	Cord	LPS VD	0	3.24E+06	269.21	0.00	0.00	20.18
687-5_S13	Decidua	LPS	0	3.24E+06	269.23	0.13	0.00	20.30
687-6_S14	Decidua	LPS VD	0	3.24E+06	269.25	0.25	0.00	20.30
All samples			0	3.24E+06	269.16	0.00	0.00	19.96

Table 3.8 Feature distribution for each monocyte / macrophage sample utilised for RNA-seq

analysis. Sample ID (sample), locus and treatment (LPS +/- 1,25(OH)₂D3 [VD]), the minimum (min), maximum (max), mean, median, quartile (Q)1 and Q3 data information is provided for all maternal blood, cord blood and decidua subsets (n=24).

Overall the mean total reads was 12155275, with 67.2% fully within an exon and 1.28% partly within an exon 1.28%.

Sample ID	Locus	Treatment	Total reads	Total alignments	Aligned (%)	Total unaligned	Unaligned (%)	Unique paired (%)	Total non-unique paired	Non-unique paired (%)	Coverage (%)	Avg. coverage depth (x)	Avg. length	Avg. quality	%GC
669-3_S21	Maternal	LPS	13181336	60777194	88.67	1493562	11.33	33.78	7233656	54.88	2.24	60.53	73.19	32.58	62.40
669-4_S22	Maternal	LPS+VD	12447675	5832913	88.45	1437435	11.55	35.45	6596222	52.99	2.05	61.44	73.63	32.55	61.72
669-7_S23	Cord	LPS	11240874	37040013	87.83	1368433	12.17	57.30	3430909	30.52	4.44	18.93	73.82	32.52	59.64
669-8_S24	Cord	LPS+VD	14696992	58119443	89.26	1579019	10.74	46.17	6331972	43.08	4.38	30.08	73.76	32.59	61.93
669-9_S19	Decidua	LPS	12901931	35730896	73.76	3385482	26.24	47.25	3419123	26.50	1.81	44.26	73.44	32.66	57.97
669-10_S20	Decidua	LPS+VD	12301706	35691031	73.65	3241506	26.35	44.95	3529310	28.69	1.58	50.72	73.48	32.55	59.42
672-1_S3	Maternal	LPS	14695404	5688827	88.78	1648396	11.22	48.45	5926150	40.33	4.85	26.12	73.09	32.77	60.22
672-2_S4	Maternal	LPS+VD	15380976	59542251	88.78	1725836	11.22	48.86	6138965	39.91	5.43	24.41	73.09	32.88	59.60
672-3_S5	Cord	LPS	12959287	59032579	89.11	1410815	10.89	36.00	6881388	53.10	2.70	48.50	72.99	32.79	61.82
672-4_S6	Cord	LPS+VD	15153917	73195255	89.07	1656345	10.93	31.91	8659516	57.14	3.19	50.66	72.82	32.82	61.89
672-5_S1	Decidua	LPS	10021987	24666769	58.72	4137512	41.28	33.62	2514095	25.09	1.17	45.96	72.49	32.82	58.91
672-6_S2	Decidua	LPS+VD	10597187	27519677	65.88	3615612	34.12	39.98	2744124	25.89	1.25	49.03	73.16	32.68	58.40
676-1_S9	Maternal	LPS	14089882	58668151	88.35	1641628	11.65	42.23	6497145	46.11	2.85	46.47	73.62	32.37	61.32
676-2_S10	Maternal	LPS+VD	13221974	50268053	88.23	1556866	11.77	48.46	5257272	39.76	3.89	29.17	73.60	32.48	60.88
676-3_S11	Cord	LPS	14198725	61546413	88.67	1609161	11.33	39.88	6926063	48.78	4.92	28.33	73.71	32.58	60.74
676-4_S12	Cord	LPS+VD	16576816	67276448	88.94	1832954	11.06	45.12	7263987	43.82	5.56	27.29	73.62	32.66	60.78
676-5_S7	Decidua	LPS	14685377	55093570	82.72	2536945	17.28	42.01	5978110	40.71	2.40	51.41	73.34	32.48	61.65
676-6_S8	Decidua	LPS+VD	13423980	52392276	82.99	2282920	17.01	39.52	5834807	43.47	2.13	54.99	73.38	32.58	62.45
687-1_S15	Maternal	LPS	17441937	78488593	88.87	1941011	11.13	37.36	8983743	51.51	3.32	52.85	73.27	32.71	61.19
687-2_S16	Maternal	LPS+VD	16819361	68814020	89.00	1850041	11.00	44.44	7493497	44.55	4.64	33.32	73.41	32.78	60.68
687-3_S17	Cord	LPS	17579621	77143777	88.17	2079138	11.83	37.75	8863451	50.42	5.62	31.00	73.61	32.71	61.01
687-4_S18	Cord	LPS+VD	19065792	84931538	88.83	2130077	11.17	37.43	9797638	51.39	5.35	35.69	73.47	32.76	61.47
687-5_S13	Decidua	LPS	15951826	67478805	84.04	2545281	15.96	36.34	7607986	47.69	3.38	44.10	72.86	32.75	61.79
687-6_S14	Decidua	LPS+VD	13609442	54235992	83.52	2242780	16.48	38.63	6108524	44.88	3.51	34.57	73.39	32.58	62.18

Table 3.9 Post alignment QA/ QC report. Each table row corresponds to a sample (n=24), permitting comparison in maternal blood, cord and decidua-derived monocyte / macrophage subsets in the presence (LPS+ VD) and absence (LPS) of vitamin D. Total number of reads (total reads), and total number of alignments (total alignments), including the fraction of all the reads aligned to the reference assembly (Aligned) are summarised. The Coverage column summarises the fraction (%) of the reference assembly sequenced, with average (Avg.) sequencing coverage (x) of the covered regions ‘Avg. coverage depth column’. Avg. length is the average read length and average read quality is given in Avg. quality. %GC is the fraction of G or C calls

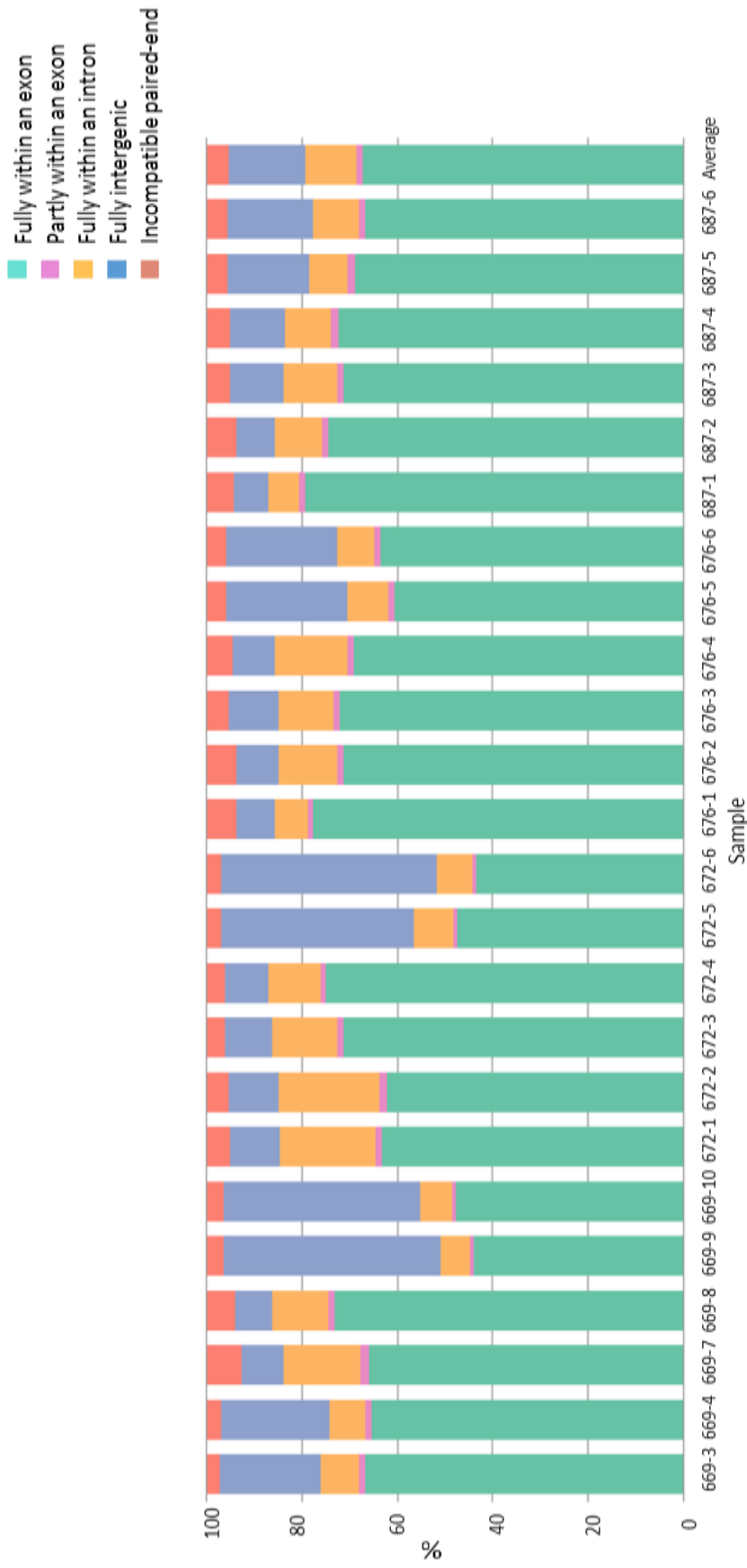


Figure 3.7 A quantification coverage breakdown for third trimester monocyte and macrophage samples. A quantitative

summary of the sample coverage for each monocyte and macrophage sample relative to hg38_RefSeq. Each bar represents a sample (n=24), with the fraction (%) of reads fully within exon, partly within exon, fully within intron, fully intergenic and incompatible paired-ends illustrated as per figure legend.

3.1.19 Pathway analysis

Pathway analysis was performed using PathVisio (Version 3.2.4), a biological data analysis software tool which enables integration, and interpretation of complex data derived from RNA-seq.

NK cell pathway analysis

Analysis was performed using the 11164 raw gene counts obtained, with corresponding ENTREZ ID (100) and symbol from the HUGO Gene Nomenclature Committee (HGNC) (101) identifiers and their corresponding log2fold change values were imported to PathVisio for pathway analysis.

Statistical analysis was performed with the total number of genes measured in the dataset (N) and the number of genes meeting the criterion (R) measured. A p-value ≤ 0.05 was applied to determine those differentially expressed genes. The Z-Score, which estimates the significance of the grouping, was also calculated for each pathway by subtracting the expected number of genes meeting the criterion from the observed number, divided by the standard deviation of the observed number of genes. All genes in N and R were present in at least one pathway. The Z-score cut-off > 1.96 was utilised, representing those genes which were differentially expressed two standard deviations above the average.

$$\text{Z-Score} = \frac{(r - n \frac{R}{N})}{\sqrt{n(\frac{R}{N})(1 - \frac{R}{N})(1 - \frac{n-1}{N-1})}}$$

The curated human pathway collection from the online-pathway repository WikiPathways (WP) (102), including the Reactome (103) collection (downloaded May 2017) were used. Data analysis was performed in collaboration with Professor S Steinbusch-Coort (BiGCaT- Maastricht University). Assistance with the data import, analysis and visualisation was obtained through attendance at a workshop training day at UoB, online tutorial material, and direct communication with BiGCaT. Biological interpretation of the pathway analysis was conducted in conjunction with RNA-seq differential gene expression analysis.

Monocyte and macrophage pathway analysis

The principal aim here was to gain an insight into the underlying biology of those differentially expressed genes identified in cord and maternal LPS treated subsets compared to those from decidua. For this, a p-value ≤ 0.05 was applied and fold-change 2.0. The Z-score cut-off > 1.96 was again utilised, representing those genes which were differentially expressed two standard deviations above the average. The curated human pathway collection from WP (102), including the Reactome (103) collection (downloaded May 2017) were again utilised, with analysis performed as outlined for the NK pathway analysis.

3.1.20 Statistics

Unless otherwise stated, in Chapter 4, data are shown as median values with IQR. Where mean values are reported, the standard error of the mean (SEM) is reported. Multifactorial data were compared using one-way ANOVA based on ranks, with Dunn's method as a post hoc multiple-comparison procedure.

Unless otherwise stated, in Chapter 5 and 6 statistical analyses for non-parametric data was performed primarily with one-way ANOVA and Friedman's post hoc test analysis. For parametric data, two-way ANOVA may have been utilised, with either Tukey's test utilised if population variances are similar, and if unequal F test. Student's T test was used when comparing only 2 parametric groups and Wilcoxon tests when the data was non-parametric. A p-value < 0.05 was set to determine statistical significance for all datasets, with Q-Q plots to help ascertain whether residuals from the mean followed a normal distribution.

All statistical analyses were carried out using GraphPad Prism (version 7.0) (California, USA).

4 Analysis of Vitamin D Metabolism in Pregnancy and Malplacentation

Parts of this chapter have been published as:

1. Tamblyn JA, Lissauer DM, Powell R, Cox P, Kilby MD. The immunological basis of villitis of unknown etiology - review. *Placenta*. 2013;34(10):846-55 (1)
2. Tamblyn JA, Hewison M, Wagner CL, Bulmer JN, Kilby MD. Immunological role of vitamin D at the maternal-fetal interface. *J Endocrinol*. 2015; 224(3):R107-21(71).
3. Tamblyn JA, Susarla R, Jenkinson C, Jeffery L, Ohizua O, Chun R, Chan S, Kilby MD, Hewison M. Dysregulation of Maternal and Placental Vitamin D Metabolism in Preeclampsia. *Placenta* 50, 70-77. 2016 (104).
4. Tamblyn J, Jenkinson C, Larner D, Hewison M, Kilby MD. Serum and urine vitamin D metabolite analysis in early preeclampsia. *Endocr Connect*. 2017 (105).

4.1 Introduction

4.1.1 Defining vitamin D status in pregnancy

A vitamin D-deficiency ($25(\text{OH})\text{D}_3 < 50 \text{ nmol/L}$) epidemic exists, with those living at high latitude with reduced sunlight exposure, dark skin pigmentation, a high BMI, and poor dietary intake at greatest risk (18, 19). One group at particular risk of vitamin D deficiency are pregnant women (106), with those with reduced sunlight exposure, poor dietary intake and with high BMI at greatest risk (107, 108). At present, no separate consensus regarding optimum vitamin D levels has been reached and general IOM standard cut-off values remain in use (109). In the UK, serum $25(\text{OH})\text{D}_3$ concentrations $< 50 \text{ nmol/L}$ were found in 49.5% of pregnant women in a prospective cohort study (110).

Black women appear at particular risk of vitamin D-deficiency during pregnancy; with recent reports that 29% and 54% of black women, and 45.6% and 46.8% black neonates at delivery were vitamin D deficient ($25(\text{OH})\text{D}_3 < 37.5 \text{ nmol/L}$) or insufficient (37.5-80 nmol/L) respectively. For the white women in this study cohort, 5% and 42% of mothers and 9.7% and 56.4% of neonates were vitamin D deficient or insufficient, respectively (111).

Adequate levels of vitamin D are important for the health of the fetus and the newborn. Classically, severe vitamin D deficiency is recognised for its negative effect on bone mineralisation, as manifested by rickets in children and osteomalacia in adults (112, 113). This is manifested in the newborn as congenital rickets, osteopenia or craniotabes (114). Since breastmilk is a relatively poor source of vitamin D, maternal vitamin D status during pregnancy is also important for vitamin D status during early infancy.

Utilising this definition, vitamin D deficiency has also been linked to a range of non-classical adverse pregnancy outcomes. Accumulating evidence from animal studies, with some supportive human evidence, indicates reproductive function and fertility may be impaired in women with low vitamin D, with links to subfertility, in vitro fertilisation (IVF) outcome, endometriosis and polycystic ovary syndrome (115).

Vitamin D deficiency is also linked to a range of pregnancy complications, including preeclampsia (PET), gestational diabetes, miscarriage, bacterial vaginosis and caesarean section (116-119). A large Dutch multi-ethnic cohort study of 3730 mothers also found infants born to women with serum 25(OH)D₃ < 29.9nmol/L at 12–14 w were more likely to be small-for-gestational age (SGA) (OR 2.4, 95% CI 1.9 to 3.2) than those born to mothers with 25(OH)D₃ ≥50nmol/L (120). Considering human studies, women with PET, have provided the basis of most available evidence as shall be discussed in detail in Section 3.1.5.

In utero and postnatal observation data indicates deficiency is also associated with fetal complications including fetal reprogramming, acute lower respiratory tract infections and recurrent wheeze (121).

At present the mechanisms for this remain unclear, with the appropriateness of comparing 25(OH)D₃ concentrations in pregnant women with thresholds established in non-pregnant adults disputed(104). As such, the evidence base at present remains insufficient to support definite clinical recommendations regarding vitamin D supplementation in pregnancy(122).

4.1.2 Vitamin D supplementation in pregnancy

Vitamin D supplementation was first recommended for pregnant women in World War II, with overt childhood rickets greatly reduced as a consequence (123). However, due to poor implementation of vitamin D fortification policies (intake > 100µg/day (d) [4000iu/d]) iatrogenic infantile hypercalcaemia ensued, and dietary fortification was withdrawn (11). As a result a resurgence of rickets and vitamin D deficiency arose in the 1960s, with immigrant Asian populations identified as at greatest risk because of decreased capacity for epidermal synthesis of vitamin D associated with darker skin pigmentation. Subsequently in the UK low-dose vitamin D supplementation with 10µg daily (400iu/d) was reintroduced, and continues to be recommended at this dose, which appears both safe and effective in preventing classical rickets in children and osteomalacia in adults(123).

However, there continues to be no clear consensus on what constitutes optimal or adequate vitamin D status in pregnancy. In light of evidence supporting non-classical vitamin D activity, in 2010 the

IOM recommended an increase in the minimal daily intake of vitamin D to ≥ 600 iu/d, with 25(OH)D₃ levels >30 ng/mL recommended. It is recognised ≥ 1500 – 2000 iu/d may be required, with up to 4000 iu/d considered safe for adults, including pregnant women (109, 124). This is consistent with recommendations from the Nordic Council of Ministers and European Food Safety. However, in the UK, the SACN recommends only 10 μ g/d (125, 126), which does not account for an increased metabolic demand for vitamin D in pregnancy (125).

The UK Maternal Vitamin D Osteoporosis Study (MAVIDOS) multicentre, double-blind, randomised, placebo-controlled trial assessed whether maternal vitamin D repletion with 1000 iu cholecalciferol (n=569) or placebo (n=565) from 14w improved offspring bone mass within 2w of birth. Albeit no overall significant improvement in offspring whole-body bone mineral content was measured, secondary analyses demonstrated a significant interaction between treatment and season, with a beneficial treatment effect for deliveries during winter months (127). Randomised control trials with large sample sizes are still required to assess the effect of maternal vitamin D supplementation on fetal bone development.

Recent systematic review and meta-analyses have concluded that new studies provide more evidence on the effects of supplementing pregnant women with vitamin D upon pregnancy outcomes and may reduce the risk of PET, SGA preterm birth and gestational diabetes (128, 129).

4.1.3 Vitamin D metabolism in human pregnancy

Human pregnancy is associated with major changes in vitamin D metabolism (71). From early gestation a dramatic increase in maternal circulating 1,25(OH)₂D₃ is observed (130), and by 12w appears 2-fold higher, reaching a peak in the third trimester and returning to normal during lactation (124). This phenomenon occurs in part to support increased fetal bone mineralisation requirements, with 2-3mg/d skeletal calcium accumulating from the first trimester, and doubling by the third.

It appears, enhanced vitamin D synthesis as opposed to decreased metabolic clearance and/ or altered half-life drives this process (131, 132). Increased maternal serum 1,25(OH)₂D₃ during pregnancy appears to be due to elevated maternal renal synthesis of the hormone. In a single case

report of a pregnant woman with renal failure only mildly elevated circulating concentrations of 1,25(OH)₂D₃ relative to pre-pregnancy were measured, with levels markedly lower than those for normal pregnant women(133, 134). Conversely, maternal 25(OH)D₃ levels do not appear to change significantly across pregnancy(135). Pregnant women receiving 4000iu (risk ratio [RR]=1.60, 95% CI 1.32-1.95) and 2000iu (RR=1.52, 95% CI 1.24-1.86) vitamin D daily demonstrated significantly higher 25(OH)D₃ concentrations ($\geq 80\text{nmol/L}$) within 1 month of delivery compared to those receiving 400iu daily, with maximal production in those receiving 4000iu (124).

In pregnant women higher plasma DBP concentrations have also been reported compared to non-pregnant controls, with a 2-fold increase from the first trimester. This was not however measured in the third trimester, indicating increased levels of free 1,25(OH)₂D₃ may arise with advancing gestation (132). However, the measurements of both total and free 25(OH)D₃ is relatively inconsistent, and whether total free 25(OH)D₃ is reduced as a result of increased DBP remains uncertain (136) (132).

There has also been much recent research interest in 3-epi-25(OH)D₃ since this appears increased in pregnant women. Inclusion of 3-epi-25(OH)D₃ within the measurement of vitamin D status 'serum 25(OH)D₃' may significantly influence the reported prevalence of sufficiency and deficiency in pregnant women. Further research to delineate the function and source of 3-epi-25(OH)D₃ in pregnancy is warranted.

4.1.4 Vitamin D, the placenta and pregnancy

The placenta plays a fundamental role in pregnancy by connecting the developing fetus to the maternal uterine wall to allow nutrient uptake, thermo-regulation, waste elimination, and gas exchange via the mother's blood supply. These main functions may be broadly termed as transport and metabolism, protection and endocrine(137).

Crucially, the placenta is of dual origin, with maternal- decidua and fetal-placental components. From initial implantation of the conceptus, the maternal uterine endometrium undergoes 'decidualisation' to support placental development and function. The resulting decidua is a tissue

formed from the maternal endometrium, originating from epithelial and stromal cells, and characterised by invasion from the extraembryonic fetal-derived trophoblasts and close cell–cell juxtaposition of these two distinct tissues (Figure 4.0) (71) (138).

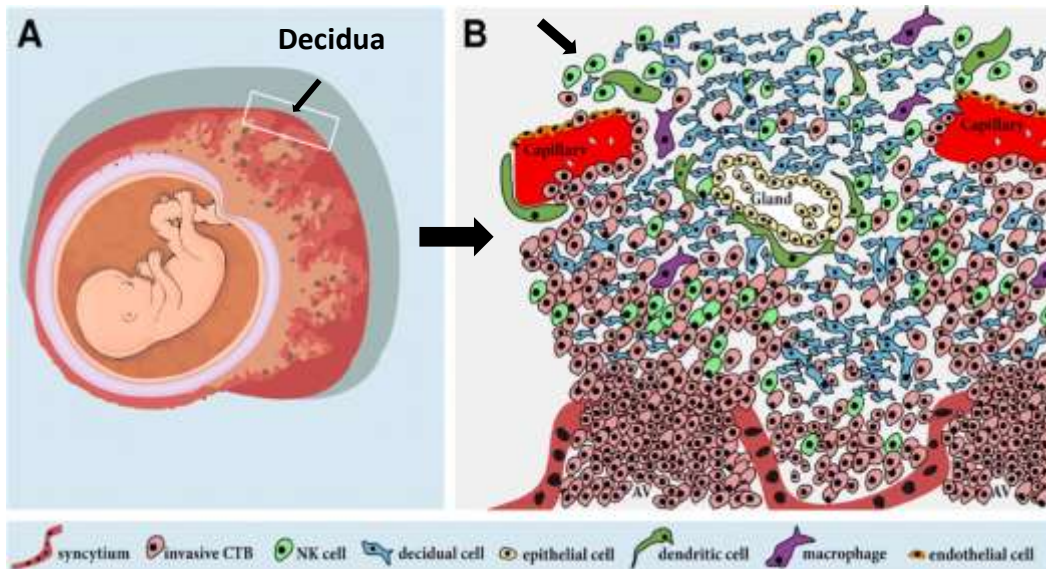


Figure 4.0 Summary of the heterogeneous decidua cell population present at the materno-fetal interface (A). As illustrated in (B), the maternal decidua tissue is highly diverse, including syncytium, invasive fetal cytotrophoblast (CTB), natural killer cells (NK cell), decidua cells, epithelial cells, dendritic cells, macrophages and endothelial cells. Image revised from Waisblum et al 2011 (139).

The principal function of the decidua is to facilitate early fetal–maternal exchange of nutrients, gases and waste, whilst also acting as a secretory source of an array of hormones, CK and growth factors. (140, 141). The decidua also plays a key role in protecting pregnancy against maternal immune surveillance, with the hallmark of this decidua during pregnancy the high proportion of resident leukocytes which display unique phenotypes and specific functions in a gestation-dependent manner.

The fundamental functional unit of the placenta, the chorionic villus, plays a major role in transfusion of oxygen from the maternal blood to the fetal blood vessels. Successful development

requires invasion of fetal trophoblast cells into the maternal decidua to facilitate maternal-fetal blood supply. Controlled early invasion of fetal cytotrophoblast and differentiated extravillous trophoblast (EVT) cells into the maternal decidua is a key process in placentation. A complex network of communications amongst trophoblast, decidual stromal, and immune cells facilitates implantation and pregnancy maintenance, with key roles in tissue remodelling, cell trafficking, and immune tolerance evident (142).

Vitamin D and placental metabolism

The observation that nephrectomised vitamin D deficient pregnant rats retain the ability to convert 25(OH)D₃ to 1,25(OH)₂D₃ first raised the possibility of extra-renal 1,25(OH)₂D₃ synthesis during pregnancy. Subsequent evidence has confirmed the potential for local 1,25(OH)₂D₃ generation in both placenta and decidua tissues (133, 143), with positive *CYP27B1* and *VDR* expression (144) from the first trimester (133, 143). By contrast, *CYP24A1* mRNA expression decreases in placental/decidual tissue across gestation (18, 19) which has the potential to enhance accumulation and 1,25(OH)₂D₃ at this site by decreasing catabolic 24-hydroxylase activity. Within the trophoblastic component of the placenta, this appears to be due to epigenetic silencing of *CYP24A1* (145).

Nevertheless, placental production of 1,25(OH)₂D₃ does not appear to make a major contribution to the elevated maternal serum 1,25(OH)₂D₃ levels associated with pregnancy. Instead it seems more likely that placental/decidual synthesised 1,25(OH)₂D₃ plays a more localised role by promoting tissue-specific effects of 1,25(OH)₂D₃. In contrast to many other extra-renal sites of 1 α -hydroxylase, placental synthesis of 1,25(OH)₂D₃ may be facilitated by the same machinery involved in renal production of 1,25(OH)₂D₃. Expression of the DBP-binding receptor megalin in placental tissue means that tissue uptake of maternal 25(OH)D₃ may occur by active receptor-mediated endocytosis of DBP and its 25(OH)D₃ cargo. The role of megalin in placental transport of vitamin D metabolites has still to be fully defined, but it is interesting to note that in megalin-KO mice, fetuses at mid-gestation appear significantly smaller compared to WT controls (146).

The function of placental VDR remains poorly defined. Using a *VDR* gene (-/-) KO model, no significant effects upon skeletal morphology or bone mineral content in fetal offspring was measured.

Serum 1,25(OH)₂D₃ levels were however significantly increased, which appeared renal 1 α -hydroxylase mediated. However maternal fertility was impaired; VDR null mice showed conception rates at 5–10% frequency with significantly fewer viable fetuses in utero. Furthermore, those born were significantly smaller and of lower birthweight. As such, VDR may not be essential for fetal mineral homeostasis, but may have significant implications for maternal fertility and reproductive outcomes (147, 148).

4.1.5 Vitamin D and pre-eclampsia (PET)

PET is a pregnancy-specific disease typically characterised by the development of hypertension and proteinuria. Complicating up to 8% of pregnancies, PET represents a leading cause of perinatal morbidity and mortality. Worldwide, the burden of PET and eclampsia is approximately 4 million births, with approximately 50,000 maternal deaths per year anticipated (149).

Certain groups of women appear at particular risk of PET, including those with chronic hypertension, diabetes, underlying renal disease, previous PET, and a raised BMI. However, despite much research interest, PET has remained a ‘morbid condition’, reflecting its insidious presentation and often complicates otherwise uncomplicated nulliparous pregnancies with potentially severe life-threatening consequences for both mother and fetus (150).

Although the pathogenesis is not fully understood, PET is considered a placental-dependent disorder, characterised by abnormal invasion of myometrium by trophoblast. The key predisposing event is aberrant utero-placental development with abnormal decidual maternal spiral artery remodelling by invading fetal EVT in the late first and second trimester. This often precedes the onset of clinical disease, which ensues in the third trimester secondary to tissue hypoxia, oxidative stress and release of anti-angiogenic and pro-inflammatory factors into the maternal circulation, which result in generalised systemic endothelial dysfunction (151). As summarised in Figure 4.1, this may be classified into 3 distinct stages (152).

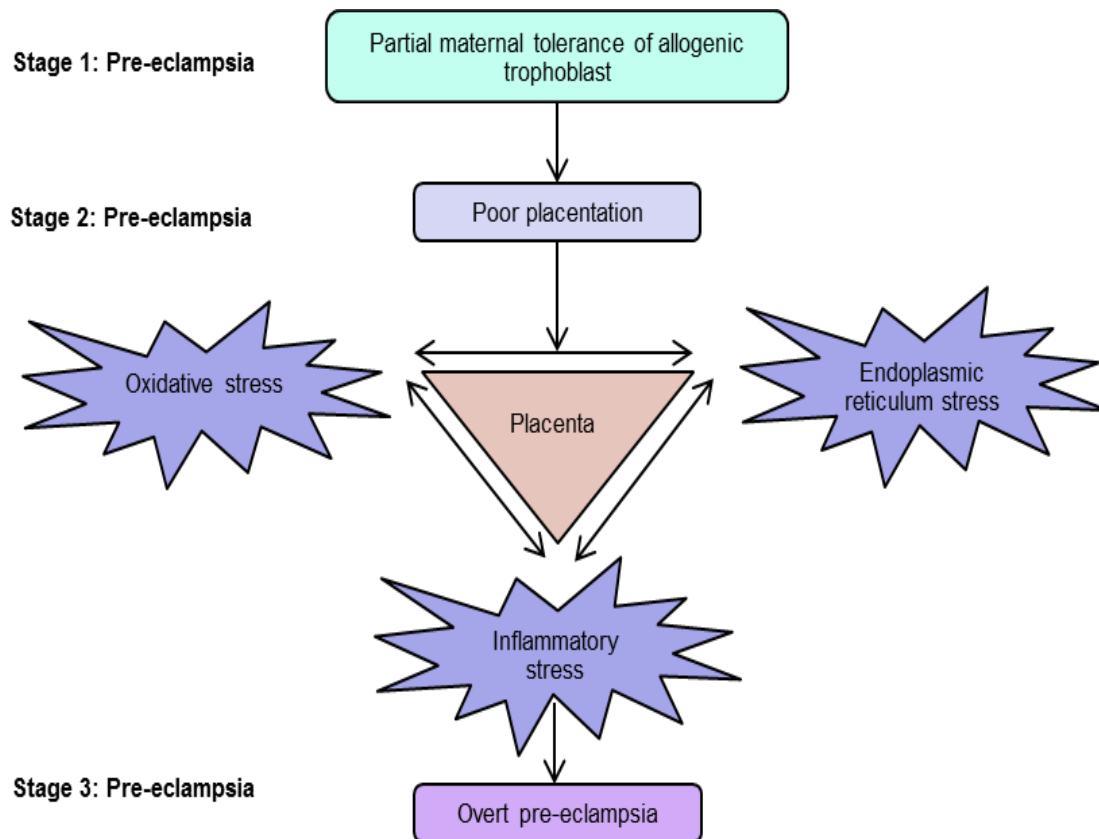


Figure 4.1 Three distinct stages of PET; (1) failure of maternal tolerance ensues from the point of implantation, (2) abnormal decidual maternal spiral artery remodelling by invading fetal EVT and (3) clinical stage of PET, generated by a maternal systemic inflammatory response. Revised from Redman *et al* 2010 (152).

Although new onset of proteinuria or hypertension has been relied upon for both the detection and diagnosis of PET, the degree of proteinuria does not correlate with the severity of PET, and may be absent in 10% of women. Furthermore, as PET ensues from the first trimester recent attention has been ascribed to potential circulating “early biomarkers” of PET (153). Since abnormal decidual maternal spiral artery remodelling and fetal EVT cell invasion underpin placental development (151), early makers of dysregulation including anti-angiogenic factors, such as placental soluble fms-like tyrosine kinase and endoglin, adhesion molecules such as placental protein 13, and vasodilators have previously been explored (154, 155).

The kidneys are among the main organs affected by PET, as inferred from the importance of proteinuria in the disease definition. In response to normal pregnancy significant renal adaptations

develop, including marked glomerular hyperfiltration and increased effective renal plasma flow. In contrast, in PET these functional changes differ with a significantly lower glomerular filtration rate secondary to altered blood flow, surface area and transfer co-efficient evident (156). Changes in basement membrane size-selectively also appear directly relevant, reflecting progressive glomerular injury and the development of proteinuria. The mechanisms by which this arises are less clearly defined with both structural alterations and renal haemodynamic mechanisms reported. Consequently, potential earlier pre-clinical markers of renal injury, such as urinary podocytes, podocyte specific proteinuria nephrin, and urinary albumin, are now being sought (157, 158).

PET and vitamin D deficiency

Maternal 25(OH)D₃-deficiency has also been linked to adverse pregnancy outcomes associated with malplacentation, including PET and SGA (116, 118, 129, 159-162). A recent systematic review and meta-analysis, which included 11 observational studies, found a significant inverse relationship between maternal 25(OH)D₃ and risk of PET in 5 of the studies. Meta-analyses similarly suggested an inverse relationship between maternal 25(OH)D₃ and PET risk, but could not infer causality (128, 163).

Considering first trimester vitamin D levels and pregnancy outcome, a systematic review, which included only two US-based studies evaluating PET risk were inconsistent. In one, which assessed the association with PET in a cohort of 49 PET women comparative to 216 normotensive controls, a five-fold increased PET risk was measured in those with levels <37.5nmol/L (116), whilst a Boston-based study reported no significant association between vitamin D levels <37.5nmol/L and PET risk (164).

A recent Cochrane review of vitamin D supplementation from early pregnancy found only one trial, including 400 women reported on PET. The data suggested that women receiving vitamin D and calcium supplementation combined were as likely to have PET as women who do not receive supplementation or placebo (relative risk 0.67; 95% CI 0.33 to 1.35). However, due to low quality, absent reporting of adverse effects and a high risk of bias in most studies, uncertainty regarding the validity of these conclusions was implied (128). Given there are at least 23 ongoing or unpublished

studies, current evidence regarding the potential value upon vitamin D supplementation in pregnancy remains indefinite (128).

However, we anticipate the significant heterogeneity observed in supplementation outcomes reflects our limited understanding of the mechanistic effects of vitamin D during pregnancy, and thus PET. Moreover, almost all studies to date have relied upon maternal serum 25(OH)D₃ as the determinant of vitamin D status and function, despite the potential importance of other vitamin D metabolites including 1,25(OH)₂D₃(165), 3-epi-25(OH)D₃(166), and 24,25(OH)₂D₃(167). Furthermore, placental expression of 1 α -hydroxylase may suggest tissue-specific concentrations of 25(OH)D₃ and other vitamin D metabolites are likely to be pivotal determinants of local vitamin D function across gestation (168). The relative impact of each of these facets of vitamin D metabolism and transport on normal and PET pregnancies remains unknown. With more than 50 vitamin D metabolites now recognised, the pathogenic role of altered metabolism in PET is gaining increased attention. Albeit epidemiology has linked PET to decreased maternal serum 25(OH)D₃, alterations in systemic and placental/ decidual transport and metabolism of 25(OH)D₃ during pregnancy suggest that other forms of vitamin D may also contribute to the pathophysiology of PET.

4.1.6 Urinary vitamin D clearance

Whilst placental vitamin D analysis offers the novel opportunity to delineate metabolism directly at the materno-fetal interface, the clinical applications of this are limited due to the inaccessibility of tissue throughout normal pregnancy. Given the prominent alterations in circulating vitamin D physiology across pregnancy, additional methods to ascertain vitamin D metabolism may be informative.

Considering vitamin D catabolism and clearance, a five-step inactivation pathway from 1,25(OH)₂D₃ to calcitroic acid is characterised, mediated via 24- α hydroxylase. An alternative 26,23-lactone pathway for converting both 25(OH)D₃ and 1,25(OH)₂D₃ to lactone products also exists, similarly catalysed by 24-hydroxylase (11). Both these metabolites have mild antagonist activity toward 1,25(OH)₂D₃ action, serving to control activity. Vitamin D is subsequently excreted, with the

primary route of via the bile into the faeces. The remainder is excreted via the kidney in urine, which occurs in the proximal renal tubules via the endocytic cubilin–megalin receptor system (169).

Studies exploring vitamin D urinary excretion have otherwise been limited to date. 23,25(OH)₂D₃ and 24,25(OH)₂D₃ appear the major metabolites in the urine samples, with equal proportions of both. Albeit modest (pg) in human health, mice unable to re-uptake vitamin D metabolites from the renal glomerular filtrate develop vitamin D deficiency and bone disease. Furthermore, partial nephrectomy of rats with reduced megalin expression results in significant upregulation of renal CYP27B1 mRNA as a compensatory mechanism (170). Entry of 25(OH)D₃ into the proximal tubule cells occurs via receptor-mediated uptake of DBP, which appears crucial for the maintenance of serum vitamin D stores (16).

In 2002, Ogawa *et al* developed an LC-MS-MS method to detect urinary 25(OH)D₃, 23,25(OH)₂D₃, 24,25(OH)₂D₃, 3-epi-24,25(OH)₂D₃ (6mL total volume). This utilised the derivatization reagent [2-(6,7-dimethoxy-4-methyl-3-oxo-3,4-dihydroquinoxalyl)ethyl]-1,2,4-triazoline-3,5-dione (DMEQTAD), which permitted detection of metabolites excreted in the pg range. A spot-urine LC MS-MS based quantification method was subsequently developed, which utilised the derivatization adduct, DAPTAD, to permit measurement of 25(OH)D₃ and 24,25(OH)₂D₃ (1mL). In contrast to serum, the concentration of 24,25(OH)₂D₃ was >2-fold higher than urinary 25(OH)D₃, indicating this is the major excreted metabolite. A significant increase in both metabolites was also measured in response to vitamin D₃ supplementation, indicating urinary 25(OH)D₃ and 24,25(OH)₂D₃ levels may be a useful indicators of vitamin D₃ status (81). Whether urinary vitamin D metabolism is altered within the context of pregnancy or disease is not known.

4.2 Results

4.2.1 Participant demographics – West Midlands cohort

All samples were obtained from cohorts of women from the West Midlands, UK (n=88). Patient demographics and baseline clinical data are summarised in Table 4.0: individually for the non-pregnant and pregnant cohorts; non-pregnant (n =20), NP1 (n=25), NP3 (n=21), PET (n=22). As anticipated, in the PET group mean arterial blood pressure (MABP) was significantly raised ($p<0.0001$) and fetal birthweight was reduced ($p<0.01$) comparative to NP3. There was also no significant difference in gestational age (GA) at delivery, which was important given the significant gestation-dependent changes in vitamin D status observed in pregnancy (171). Concerning vitamin D intake, supplementation intake was increased in the NP3 cohort (33.3%) comparative to those with PET (4.5%) ($p>0.05$). Smoking was low in both cohorts, with only 2 (9.1%) in the PET group reporting on-going use in the third trimester.

	Non- pregnant (n=20)	NP1 (n=25)	NP3 (n=21)	PET (n=22)	p value	Post-hoc analysis
Parity: nulliparous, total (%); multiparous, total (%)	-	-	3 (14.3%); 18 (85.7%)	18 (81.8%); 4 (18.2%)	-	- ^A Non-pregnant & NP1 (**); Non- pregnant & PET (*)
Maternal age, median (25th-75th interquartile range [IQR]), year	36.5 (23.0- 47.8)	27.0 (21-33)	33.0 (31.0-36.0)	30.0 (22.0-33.3)	0.003	
BMI, median (25th- 75th IQ range), unit	-	24.4 (21.3-33.8)	27.0 (24.8-31.2)	27.4 (21.8-33.1)	0.2	ns
Mean arterial blood pressure (MABP), median (25th-75th IQR), unit	-	87.7 (82.2-94.2)	85.3 (80-91.5)	112.2 (104.8- 117.4)	0.7	^A NP1 & PET (****); NP3 & PET (****)
Vitamin D supplementation (400iu daily), total (%)	0 (0%)	-	7 (33.3%)	1 (4.55%)	>0.05	ns
Positive smoking status, total (%)	0 (0%)	-	0 (0%)	2 (9.1%)	>0.05	ns
Gestational age at delivery, median (25th-75th IQR), week	-	10.6 (8.70-11.4)	39.1 (39.0-39.3)	37.4 (33.1-40.5)	0.2479	ns
Birthweight, median (25th-75th IQR), grams	-	-	3540 (3253- 3820)	2715 (1763-4210)	0.0032	^T NP3 & PET (**)

Table 4.0 Summary of participant demographics for non-pregnant female controls, normal pregnant women (n=20) at first (NP1, n=25) and third trimester (NP3, n=21) and women with PET (n=22) in the West Midlands cohort. Total frequency (n) with percentage of total group (%), and median values with 25th-75th interquartile range (IQR) values were calculated as stated. Statistically significant variations and post hoc test analyses are summarised; ^A ANOVA; ^T T-test * p<0.05, ** p<0.01, *** p<0.001, **** p< 0.0001.

As detailed in Table 4.1, most women were white (n=70; 79.5%), with only 5 (5.7%) black and 13 (14.8%) Asian women recruited. This preponderance was relatively consistent across the 4 cohorts, other than the NP1 group which was entirely white.

Ethnicity	Non-pregnant	NP1	NP3	PET
White	15	25	16	14
Black	2	0	1	2
Asian	3	0	4	6

Table 4.1 Summary of ethnicity for the West Midlands cohort; non-pregnant, normal first trimester (NP1), third trimester (NP3) and pre-eclampsia (PET) sub-groups.

4.2.2 Serum vitamin D metabolites in pregnant and non-pregnant women

Four serum vitamin D metabolites were consistently quantifiable in both pregnant and non-pregnant women; 25(OH)D₃, 1,25(OH)₂D₃, 24,25(OH)₂D₃, 3-epi-25(OH)D₃. In non-pregnant women 25(OH)D₃ concentrations (median 33.4, IQR 20.8 – 44.3 nmol/L), were similar to healthy first trimester (NP1, 28.8, 20.3 – 46.9nmol/L) and third trimester (NP3, 45.2, 32.5 – 59.2nmol/L) pregnancies, as well as women diagnosed with PET (35.3, 17.7 – 54.7 nmol/L) (Figure 4.2). No significant difference in median 25(OH) D₃ concentrations was measured. Of the 88 women included, only 19 (21.6%) had levels ≥ 50 nmol/L and 5 ≥ 75 nmol/L (5.7%), with 69 (78.4%) defined as ‘deficient’ and 83 (94.3%) ‘insufficient’(109).

By contrast, serum 1,25(OH)₂D₃ concentrations in NP women (34.2, 29.3 – 55.0 pmol/L), were significantly lower than in pregnant women, including NP1 (113.7, 82.7 – 198.3 pmol/L, p<0.0001), NP3 (254.7, 195.7 – 310.1 pmol/L, P<0.0001), and PET (171.2, 113.0 – 236.3 pmol/L, p<0.0001) groups. Consistent with previous studies(136), NP3 levels of 1,25(OH)₂D₃ were >2-fold higher than NP1 (p<0.0001), and significantly lower concentrations of 1,25(OH)₂D₃ (p<0.01) were observed in the PET cohort compared to NP3 (Figure 4.2).

Serum concentrations of 24,25(OH)₂D₃ in non-pregnant women (3.3, 1.6 – 4.7 nmol/L) were higher than NP1 (1.8, 0.8 - 3.7 nmol/L), but lower than NP3 (7.6, 5.6 - 10.0 nmol/L, p<0.05) and PET (10.9,

7.3 - 22.5 nmol/L, $p < 0.001$) (Figure 4.2). Both NP3 and PET samples showed significantly higher 24,25(OH)₂D₃ concentrations than NP1 (both $p < 0.0001$).

Concentrations of 3-epi-25(OH)D₃ were lowest in non-pregnant women (5.1, 3.9 - 6.4 nmol/L). Both NP1 (7.6, 6.0 - 9.2 nmol/L) and NP3 (7.5, 5.9 - 8.6 nmol/L) had higher levels of 3-epi-25(OH)D₃ but this was not significant. Highest 3-epi-25(OH)D₃ levels were observed with PET (8.8, 5.9 - 11.8 nmol/L), with significant differences compared to non-pregnant ($p < 0.001$), NP1 ($p < 0.05$) and NP3 groups ($p < 0.05$) (Figure 4.2).

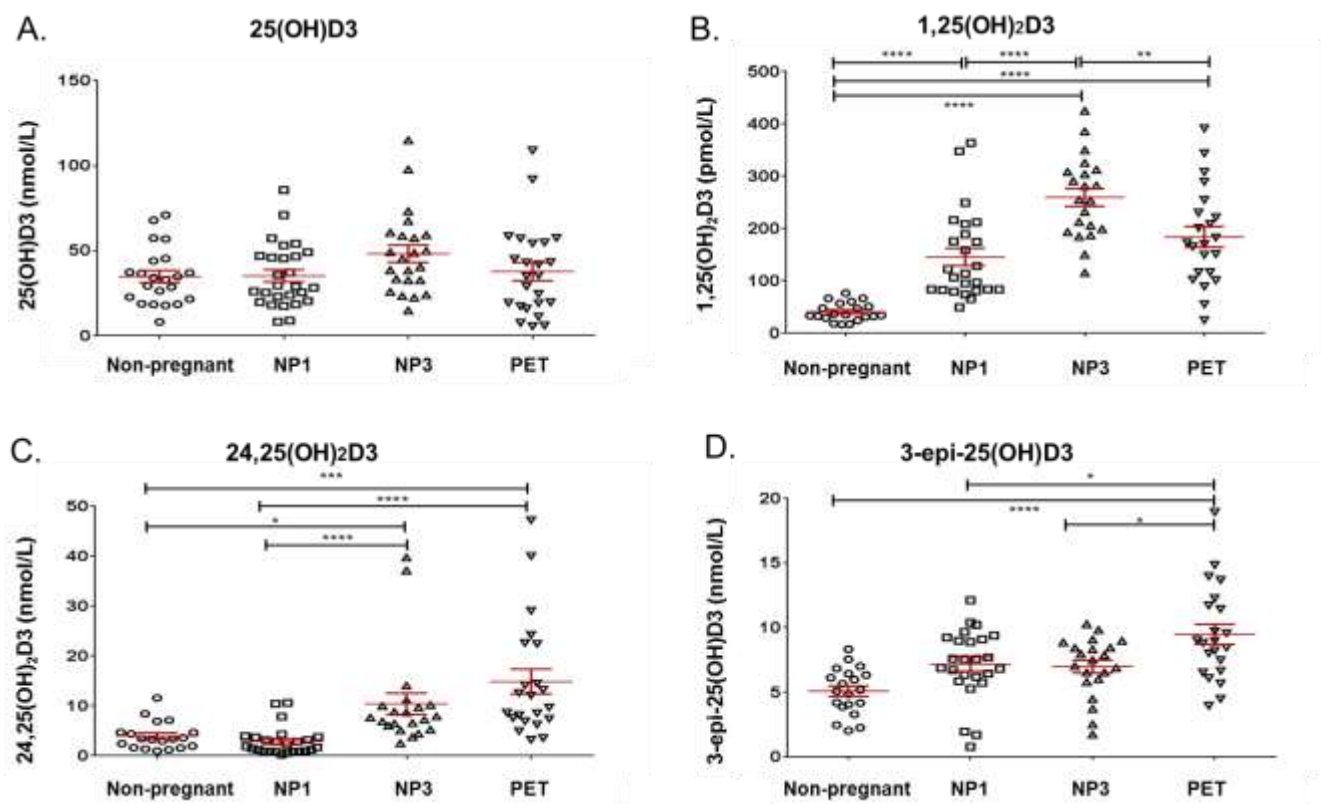


Figure 4.2 Simultaneous measurement of vitamin D metabolites in pregnant and non-pregnant women reveals significant gestational and disease-dependent changes in serum metabolite concentrations. Serum concentrations of: A) 25(OH)D₃ nmol/L; B) 1,25(OH)₂D₃ pmol/L; C) 24,25(OH)₂D₃ nmol/L; D) 3-epi-25(OH)D₃ nmol/L. Samples groups were: non-pregnant women; first trimester (NP1); third trimester (NP3); pre-eclampsia third trimester (PET). Statistically significant variations are indicated, * $p < 0.05$, ** $p < 0.01$, *** $p < 0.001$, **** $p < 0.0001$.

Simple linear regression analysis was performed to establish the impact of GA upon vitamin D metabolite serum measurements (Figure 4.3). For each metabolite, 25(OH)D3, 1,25(OH)₂D3, 24,25(OH)₂D3 and epi-25(OH)D3, gestation was shown not to significantly affect serum vitamin D metabolite concentrations in the NP3 and PET groups, for which differences in metabolite concentrations were identified.

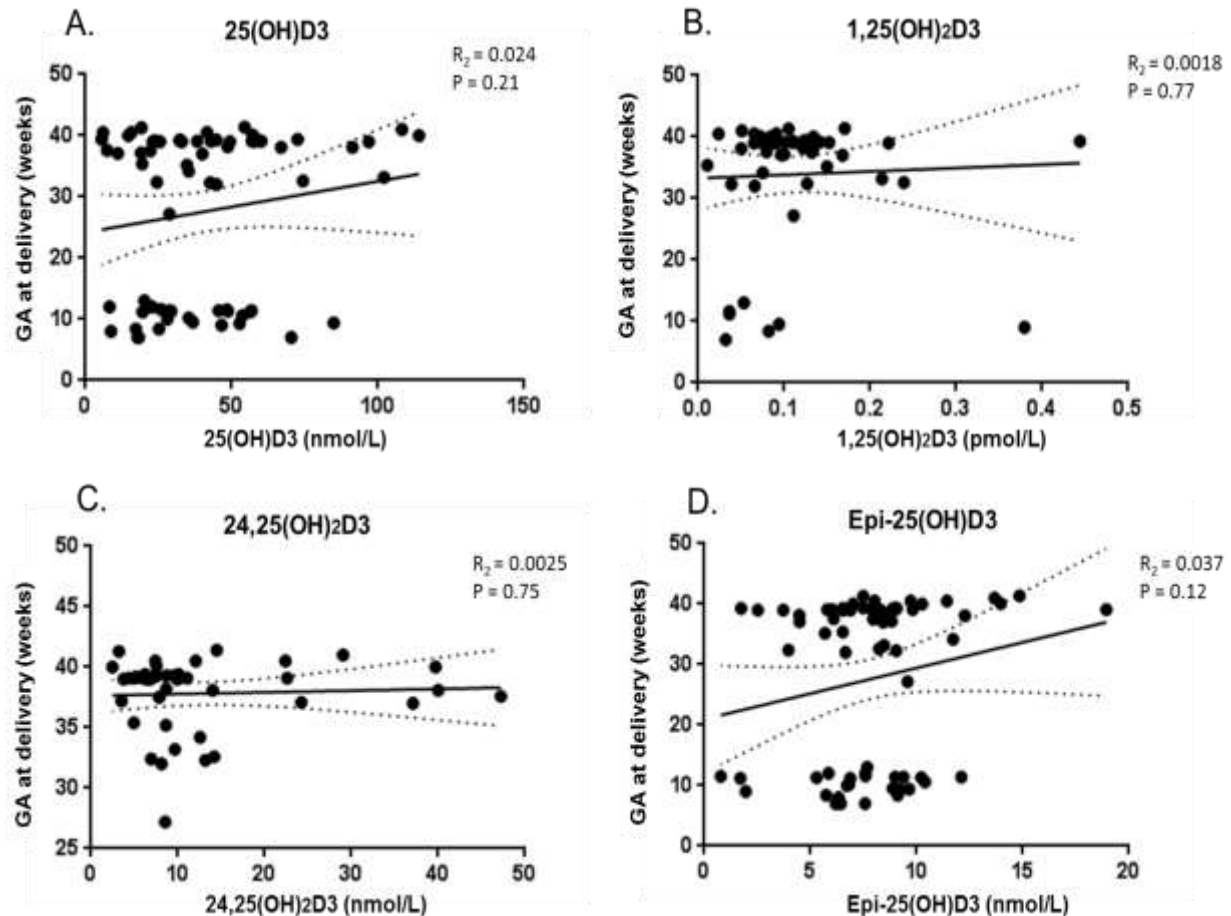


Figure 4.3 Linear regression analysis confirms gestational age at delivery did not significantly impact serum vitamin D metabolite concentrations in NP3 and PET groups. Simple linear regression analysis of serum concentrations of: A) 25(OH)D3 nmol/L; B) 1,25(OH)₂D3 pmol/L; C) 24,25(OH)₂D3 nmol/L; D) 3-epi-25(OH)D3 nmol/L and gestational age (GA) at delivery. Samples groups were compiled to include first trimester (NP1); healthy third trimester (NP3) and pre-eclampsia third trimester (PET) groups. The graphs denote the line of best fit, with R₂ and p-values calculated. No statistically significant variations were detected

4.2.3 Effect of maternal vitamin D status (serum 25(OH)D3) on other serum vitamin D metabolites in pregnant and non-pregnant women

In non-pregnant women serum 25(OH)D3 was strongly correlated with 1,25(OH)₂D3 (p=0.013), 24,25(OH)₂D3 (p<0.0001) and 3-epi-25(OH)D3 (p=0.012) (Figure 4.4). However, similar correlations were not consistently observed in pregnancy, in the NP1 group only a significant correlation with 24,25(OH)₂D3 (p<0.0001) was evident, which was lost for 1,25(OH)₂D3 (p=0.105) and 3-epi-25(OH)D3 (p=0.102). In the NP3 and PET groups, no significant correlation between 25(OH)D3 and 1,25(OH)₂D3, 24,25(OH)₂D3 or 3-epi-25(OH)D3 was measured, as summarised in Figure 4.4. Comparing the NP3 and PET groups, the correlation between 25(OH)D3 and the other serum metabolites, no clear difference was evident, particularly for 1,25(OH)₂D3, 24,25(OH)₂D3.

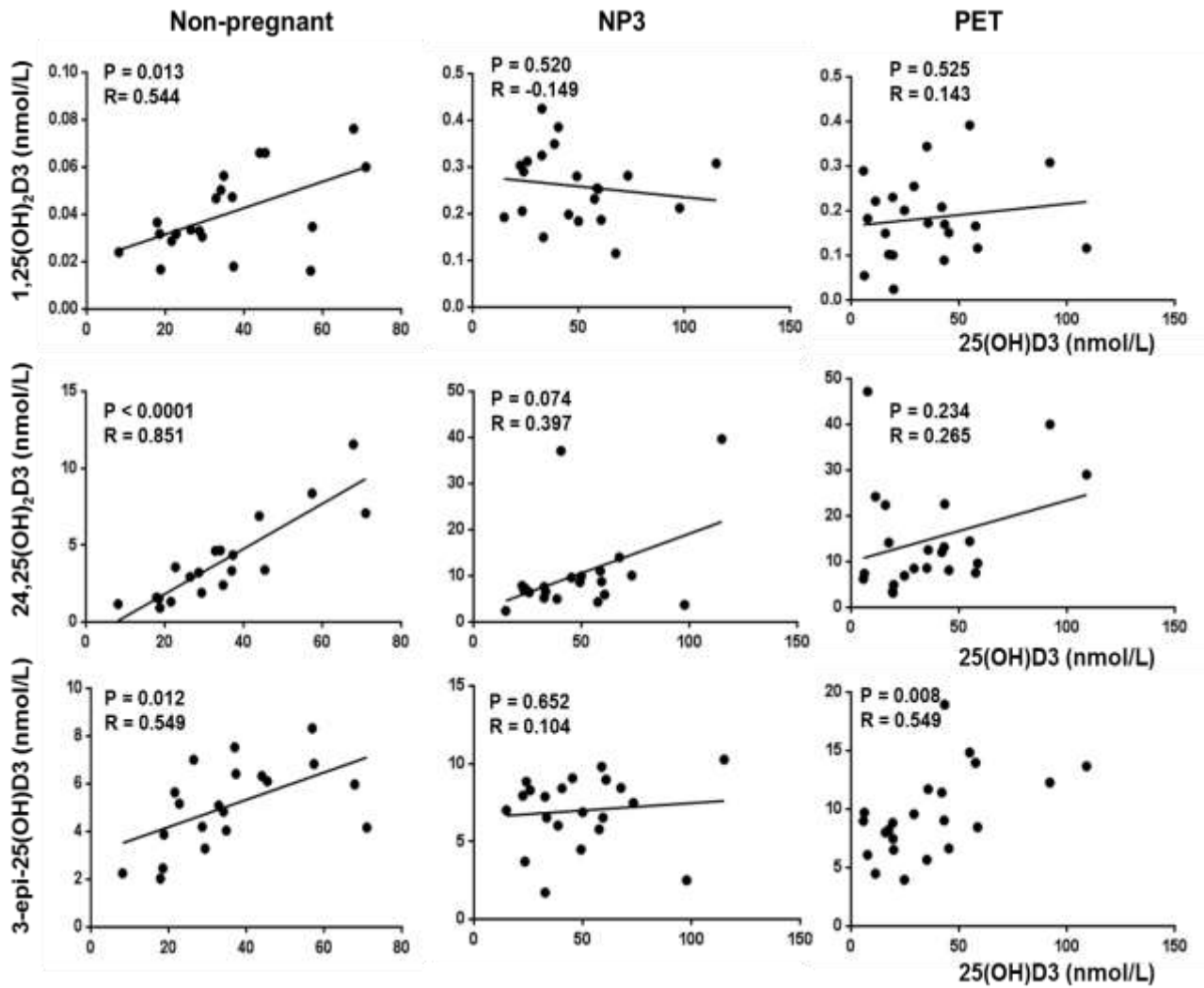


Figure 4.4 Effect of maternal vitamin D status upon other serum vitamin D metabolites in non-pregnant and pregnant women. Serum concentrations 25(OH)D₃ were correlated with 1,25(OH)₂D₃, 24,25(OH)₂D₃ and 3-epi-25(OH)D₃. All nmol/L for non-pregnant women; healthy third trimester (NP3); pre-eclampsia third trimester (PET). Statistically significant correlations are indicated as p values, with the correlation co-efficient ‘r’ value stated.

4.2.4 DBP, albumin and 25(OH)D₃ bioavailability in pregnant and non-pregnant women.

Since no difference in 25(OH)D₃ was measured between the non-pregnant and pregnant groups, we assessed free and bioavailable 25(OH)D₃ serum concentrations compared across the different groups. As summarised in Figure 4.5A, albeit a trend towards increased serum DBP in NP1 (1.93; 1.24-3.08

$\mu\text{mol/L}$) and NP3 (1.97; 1.52-3.75 $\mu\text{mol/L}$) pregnancies relative to non-pregnant women was evident, no significant difference in DBP was measured between NP3 (1.97; 1.52-3.75 $\mu\text{mol/L}$) and PET (2.212; 1.63-3.16 $\mu\text{mol/L}$), or non-pregnant controls (1.55; 1.05-2.02 $\mu\text{mol/L}$).

As anticipated, serum albumin was significantly lower in NP3 (315.4; 265.2- 400.5 $\mu\text{mol/L}$) and PET (391.9; 324.3-557 $\mu\text{mol/L}$) pregnancies relative to non-pregnant women (557.5; 458.5- 613.2 $\mu\text{mol/L}$) ($p<0.001$ and $p<0.05$ respectively) and NP1 pregnancies (538.4; 471.8-635.2 $\mu\text{mol/L}$) ($p<0.001$ and $p<0.05$ respectively) (Figure 4.5B).

The concentrations of DBP and albumin, together with total serum 25(OH)D3 levels were used to calculate bioavailable, and free serum 25(OH)D3 (Figure 4.5C and D). Consistent with total serum 25(OH)D3, no significant change across pregnancy, including those with PET, was again measured.

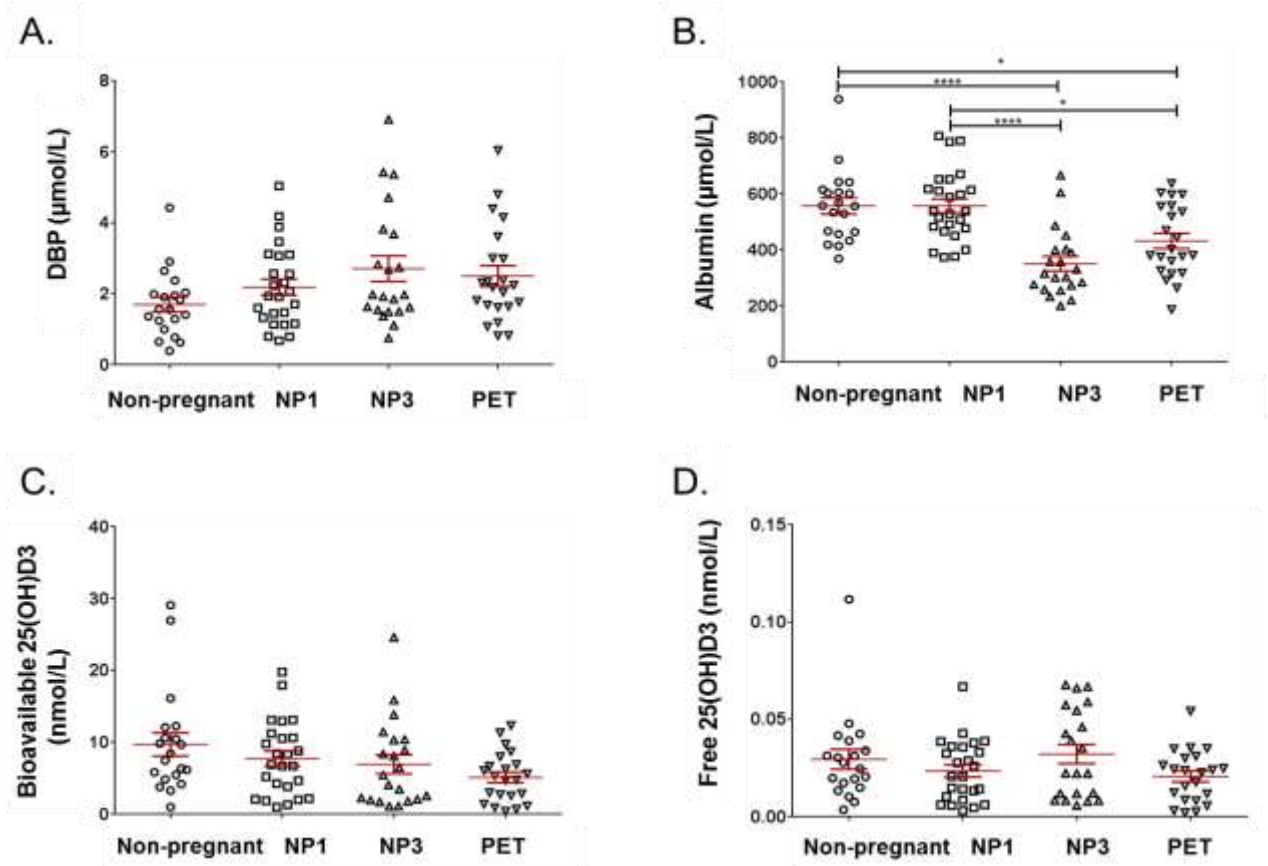


Figure 4.5 Comparative analysis of DBP, albumin and 25(OH)D3 bioavailability and free serum concentrations revealed no significant difference between pregnant and non-pregnant women, or within the context of PET. Serum concentrations of: A) DBP ($\mu\text{mol/L}$); B) albumin ($\mu\text{mol/L}$); C) bioavailable 25(OH)D3; D) free 25(OH)D3. Samples groups were: non-pregnant women; first trimester (NP1); third trimester (NP3); and pre-eclampsia (PET). Statistically significant variations are indicated, * $p < 0.05$, ** $p < 0.01$, *** $p < 0.001$, **** $p < 0.0001$.

Ratios of DBP-bound 25(OH)D3 to total 25(OH)D3 were also unaffected by pregnancy or PET as shown in Figure 4.6. However, the suppression of serum albumin with increasing GA did significantly decrease the ratio of ‘bioavailable’ 25(OH)D3 (25(OH)D3 bound to albumin but not DBP) to ‘total’ serum 25(OH)D3 consistently in the NP3 and PET groups. The modestly elevated DBP levels in pregnant women also resulted in decreased ratios of ‘free’ 25(OH)D3 to total 25(OH)D3, with this effect being more pronounced in PET pregnancies (Figure 4.6)

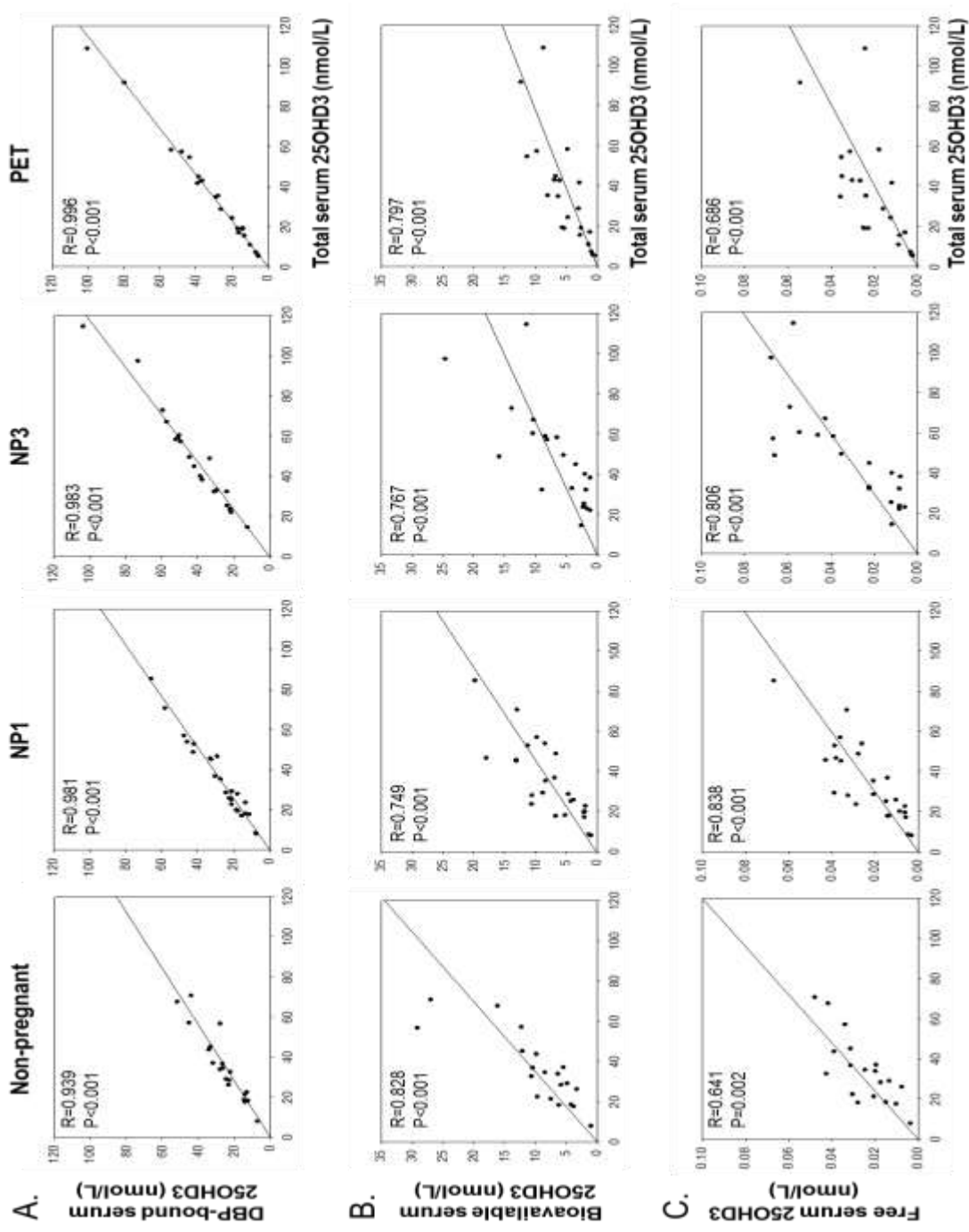


Figure 4.6 Pregnancy has no significant effect upon bound, bioavailable and free 25(OH)D3. Comparison of total serum concentrations of 25(OH)D3 (nmol/L) with (A.) DBP-bound; (B.) Bioavailable; (C.) Free 25(OH)D3 (nmol/L) for non-pregnant women, first trimester(NP1), third trimester (NP3) and preclampsia (PET) pregnancies. Statistically significant correlations are indicated as p values, with the correlation co-efficient 'r' value stated.

4.2.5 Placental and decidual tissue vitamin D metabolites in pregnant women across gestation

Utilising matched placenta and decidua samples, tissue concentrations of 24,25(OH)₂D₃, 25(OH)D₃, and 3-epi-25(OH)D₃ were quantified. 1,25(OH)₂D₃ was only quantifiable in decidual tissue (17.6, 11.0 – 23.4 pmol/mg protein), and this paralleled increased decidual concentrations of 25(OH)D₃ (21.0, 9.3 – 60.5 nmol/mg protein) relative to paired NP1 placentae (1.2, 0.7 - 2.2 nmol/mg protein, p<0.001) (Figure 4.7).

This paralleled increased decidual concentrations of 25(OH)D₃ (21.0, 9.3 – 60.5 nmol/mg protein) relative to paired NP1 placentae (1.2, 0.7 - 2.2 nmol/mg protein, p<0.001), which were markedly lower (Figure 4.7). By contrast no difference in tissue levels of 24,25(OH)₂D₃ were observed between decidua (0.3, 0.2 – 0.4 nmol/mg) and placenta (0.2, 0.1 – 0.3 nmol/mg). Similarly, decidual concentrations of 3-epi-25(OH)D₃ (0.1, 0.1 – 0.3 nmol/mg) were not significantly different to NP1 placental concentrations (0.2, 0.1 – 0.3 nmol/mg) (Figure 4.7). Furthermore, decidual 25(OH)D₃, 3-epi-25(OH)D₃ and 24,25(OH)₂D₃ showed no correlation with serum or placenta concentrations.

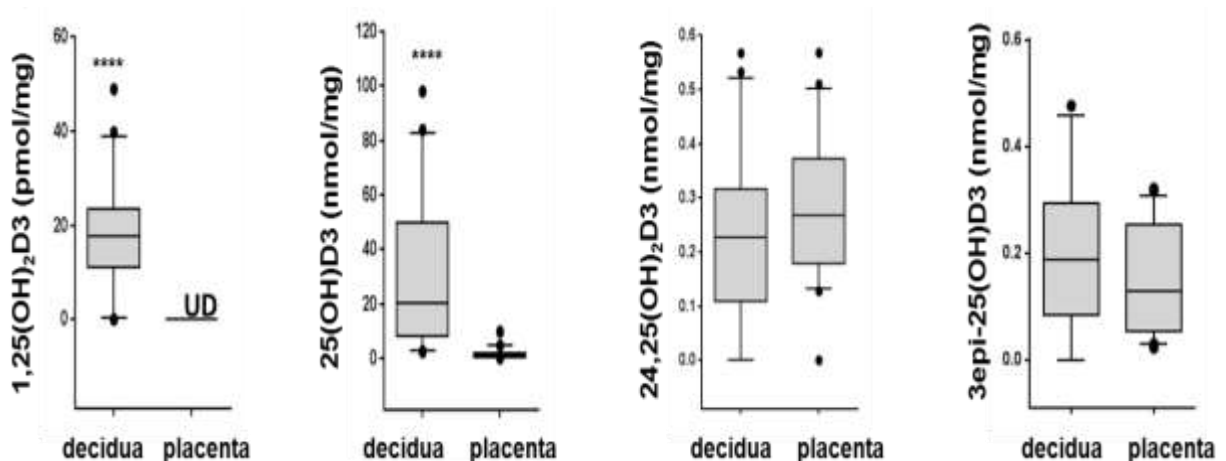


Figure 4.7 Significant differences in first trimester maternal decidua and fetal placenta tissue concentrations of active (1,25(OH)₂D₃) and inactive (25(OH)D₃) vitamin D. Comparison of decidual and placental concentrations of 1,25(OH)₂D₃, 25(OH)D₃, 24,25(OH)₂D₃, and 3-epi-25(OH)D₃ in first trimester pregnancies. All nmol/mg decidual protein.

4.2.6 Effect of gestation upon placental vitamin D metabolite concentrations in pregnancy and PET

Unlike serum concentrations of 25(OH)D3 a significant increase from NP1 (1.2; 0.7-2.2 nmol/mg) to NP3 (5.0; 4.0-6.6 nmol/mg) was measured ($P < 0.0001$) (Figure 4.8). Furthermore, within the context of PET (2.5 nmol/mg) this was significantly lower comparative to NP3 ($p < 0.01$). Interestingly, although placental 24,25(OH)₂D3 concentrations increased marginally with advancing GA from NP1 (0.2; 0.1-0.4 nmol/mg) to NP3 (0.3; 0.2-0.5 nmol/mg), this appeared more pronounced in the PET cohort (0.4; 0.3-0.6 nmol/mg ($p < 0.01$ comparative to NP1)). Placental 3-epi-25(OH)D3 also increased from NP1 (0.2; 0.1-0.3 nmol/mg) to NP3 (0.3; 0.2-0.4 nmol/mg), and similarly was significantly increased in those women with PET (0.4; 0.3-0.7 nmol/mg) comparative to both the NP1 ($p < 0.001$) and NP3 ($p < 0.05$) cohorts (Figure 4.8).

Placental 25(OH)D3 positively correlated with 24,25(OH)₂D3 in NP1 ($p = 0.009$, $r = 0.55$) and NP3 ($p = 0.008$, $r = 0.6$). This was not observed in the PET group ($p = 0.4$; $r = -0.2$). Interestingly, placental 25(OH)D3 did not correlate with 3-epi-25(OH)D3 in any of the cohorts.

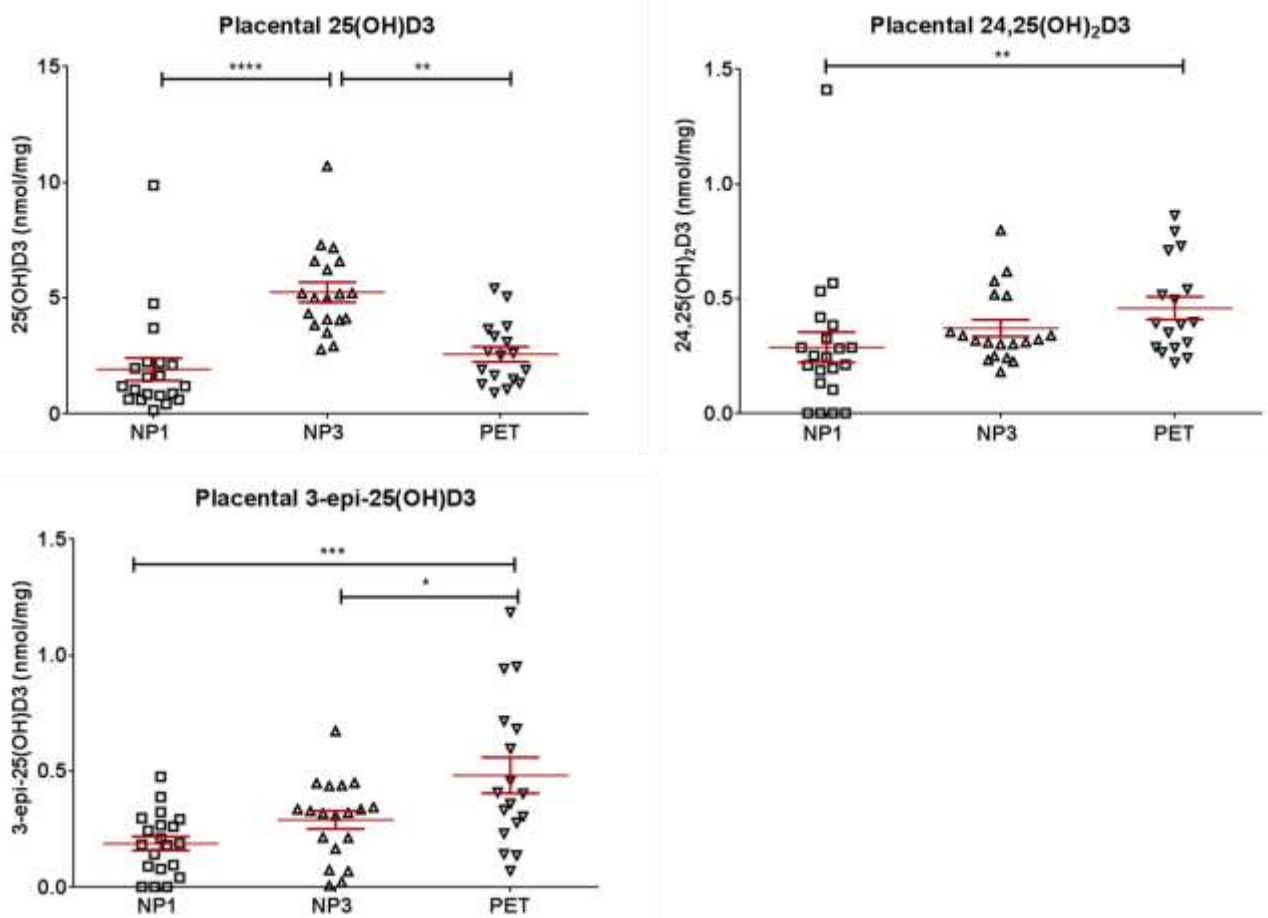


Figure 4.8 Significant effect of gestation upon placental vitamin D metabolism in pregnancy and pre-eclampsia. Comparison of placental concentrations of 25(OH)D₃, 24,25(OH)₂D₃, and 3-epi-25(OH)D₃ in first trimester (NP1), third trimester (NP3) and pre-eclampsia (PET) pregnancies. All nmol/mg decidual protein, with mean and standard error of the mean (SEM). Statistically significant variations are indicated, * p<0.05, ** p<0.01, *** p<0.001, **** p< 0.0001.

4.2.7 Effect of maternal 25(OH)D3 upon placental 25(OH)D3 in normal pregnancy

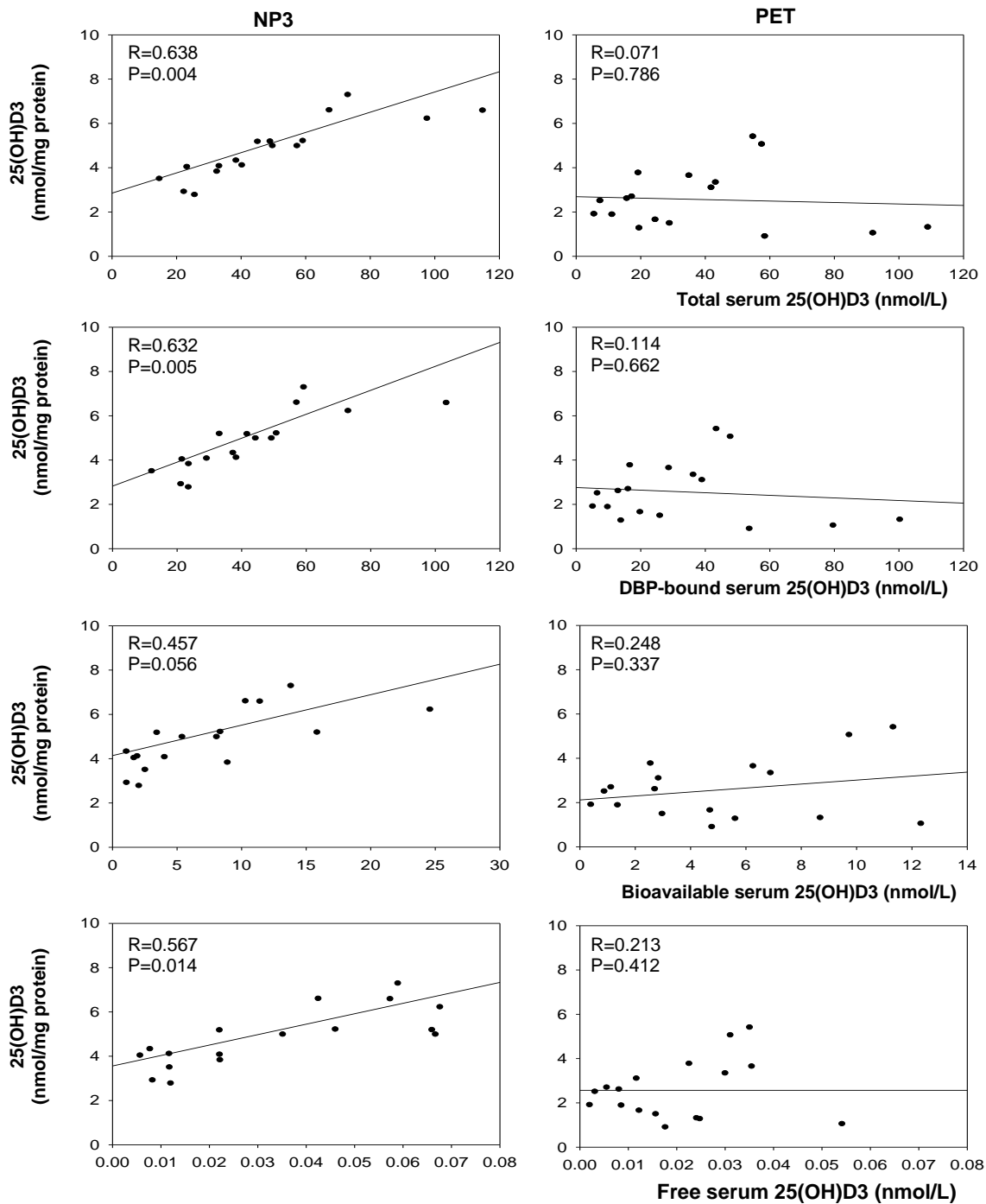


Figure 4.9 Effect of maternal 25(OH)D3 upon placental 25(OH)D3 in normal pregnancy and pre-eclampsia. Comparison of total placental 25(OH)D3 (nmol/mg protein) with serum total, DBP-bound, bioavailable and free 25(OH)D3 (nmol/L) for third trimester (NP3) and pre-eclampsia (PET) pregnancies. Statistically significant correlations are indicated as p values, with correlation coefficient 'r' value stated.

In third trimester pregnancies placental concentrations of 25(OH)D3 correlated with maternal serum concentrations of total, DBP-bound, bioavailable and free 25(OH)D3. By contrast, placental concentrations of 25(OH)D3 in PET pregnancies showed no association with any form of maternal serum 25(OH)D3 (Figure 4.9).

4.2.8 SCOPE Participant demographics

Comparative analysis of the two sub-groups of the SCOPE cohort is presented in Table 4.2. All participants were white Caucasian with a mean age of 30.5years (y) (22-38y), and were matched for age, ethnicity and BMI. Pregnant women were recruited across the calendar year, 21 in summer (June through October) and 29 in winter (November through May). Median GA at recruitment was 16w (15.0 -16w) and 15 w (15.0 -16.0w) for the pregnant normotensive and PET groups respectively. The time of urine specimen collection was not uniform, with median 10.00am (range 9.00 -14.00) and 12.00pm (range 9.00 – 15.00) collection in normotensive and PET pregnant groups respectively. Concerning dietary intake of vitamin D, 15 (10 normotensive and 5 PET women) reported intake of the recommended daily dose of vitamin D (400iu/d) as a multi-vitamin pre-pregnancy. In the first trimester ($\leq 12w$), 12 participants (9 normotensive and 3 PET) took daily low-dose (400iu) vitamin D supplementation, of which 9 (7 normotensive and 2 PET) had continued from pre-conception. Dietary intake of oily fish pre-pregnancy was modestly higher in the PET group, with 12 reporting ‘moderate – often intake’, compared to 8 in the normotensive pregnant group (data not shown).

Of the 25 women who developed PET, the mean GA at diagnosis was 37w (range 31–41); with 14 (56.0%) developing the disease at term ($GA \geq 37w$), 11 (44.0 %) pre-term ($GA < 37w$) and only 1 patient (4.0%) early-onset PET ($GA < 34w$). In total, 7 (28.0%) women were diagnosed with severe PET and 6 (24.0%) developed multi-system disease. The MABP was 117.3mmHg (IQR 113.8-124.8) in the PET group compared to 92.7mmHg (89.0-96.7) in normotensive women ($p < 0.0001$). The mean GA at delivery was 39.0w (37.0-40w) in the PET group, compared to 41w (40-41w) in those with normotensive pregnancies ($p < 0.0001$). Median fetal birthweight at 3030grams (g) (2580- 3525g) in the PET group was significantly lower than the uncomplicated cohort (3650g; 3275– 4040g)($p < 0.05$). There were 3 (12.0 %) pregnancies with a SGA fetus in the PET cohort, with none (0%) in the

uncomplicated pregnancy group. In the PET group there was one stillbirth at 41w (intrauterine death > 20w) (4.0%). A healthy non-pregnant female group (n= 9) was also recruited for comparison.

	Control n=25	PET n=25
Maternal age , years (range)	30.5 (24.0 – 38.0)	31 (22.0 – 36.0)
Body mass index , median (25th-75th IQR), unit	26.2 (22.9-29.2)	25.5 (22.9- 29.7)
Ethnicity , white Caucasian, frequency (%)	25 (100)	25 (100)
Mean arterial blood pressure , median (25th-75th IQR), unit	92.7 (89.3 – 96.7)	117.3**** (113.8 – 124.8)
Vitamin D supplementation (400iu daily) ; pre-pregnancy total (%), 1 st trimester total (%)	10 (40.0) 9 (36.0)	5 (20.0) 3 (12.0)
Season at recruitment (15 weeks) : summer, total (%); winter, total (%)	10 (40.0) 15 (60.0)	11 (44.0) 14 (56.0)
Positive smoking status at 15w , total (%)	2 (8.0)	4 (16.0%)
Gestation at PET diagnosis , mean (range), week	-	37 (31-41)
Term PET (gestation ≥ 37w) , frequency (%)	-	14 (56.0 %)
Preterm PET (gestation < 37w) , frequency (%)	-	11 (44.0)
Severe preterm PET (gestation < 34w) , frequency (%)	-	1 (4.0)
Gestation at delivery , mean (25 th -75 th IQR), weeks	41.0 (40.0-41.0)	39.0 **** (37.0-40.0)
Fetal birthweight , median (25th-75th IQR), grams:	3650 (3275 – 4040)	3030 ** (2580 – 3535)
Fetal small for gestational age , frequency (%)	0 (0)	3 (12.0)
Stillbirth , frequency (%)	0 (0)	1 (4.0)

Table 4.2 Demographic summary and analysis of the participant sub-group assessed from the SCOPE, Ireland cohort. Comparison of baseline clinical demographics in healthy pregnant ‘controls’ (n=25) and those cases who prospectively developed pre-eclampsia (PET; n=25). Cases were matched for age, ethnicity and body mass index (BMI). Statistically significant variations are summarised; * p<0.05, ** p<0.01, *** p<0.001, **** p< 0.0001.

4.2.9 Serum vitamin D metabolite analysis

In serum, five serum vitamin D metabolites were consistently quantifiable in both the pregnant (normotensive and PET women) and non-pregnant groups; 25(OH)D₃, 25(OH)D₂, 1,25(OH)₂D₃, 24,25(OH)₂D₃, 3-epi-25(OH)D₃, as summarised in Figure 4.10 and Table 4.3.

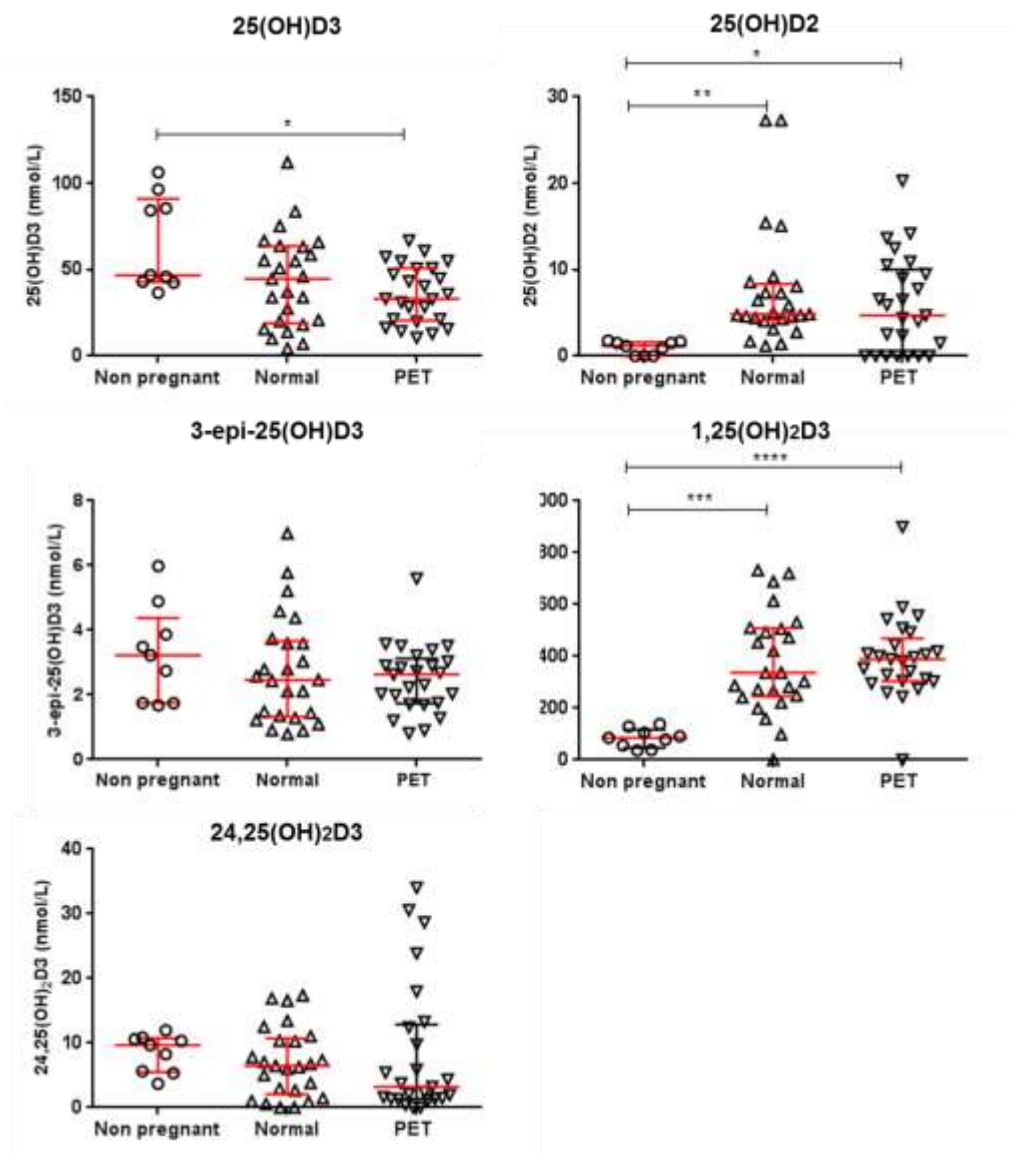


Figure 4.10 Serum vitamin D metabolite in non-pregnant women and the SCOPE pregnancy cohort at 15 weeks gestation. Serum concentrations of: 25(OH)D3 nmol/L; (25(OH)D2 nmol/L; 3-epi-25(OH)D3 nmol/L; 1,25(OH)₂D3 pmol/L; 24,25(OH)₂D3 nmol/L. Samples groups were: non-pregnant (n=9), matched normotensive pregnancies (n=25) and prospective ‘PET’ cases (n=25). Median with interquartile range is shown, with statistically significant variations indicated, * p<0.05, ** p<0.01, *** p<0.001, **** p<0.0001.

	Non-pregnant (n=9)	Control (n=25)	PET (n=25)
	(median; IQR)	(median; IQR)	median (IQR)
25(OH)D3 (nmol/L)	46.8 (42.8-91)	44.7 (19.1- 63.5)	33.1 (20.5-50.8)
25(OH)D2 (nmol/L)	1.17 (0-1.6)	4.8 (4.2- 8.3)	4.7 (0- 10.0)
1,25(OH)₂D3 (pmol/L)	85.6 (47.3-117.4)	336.3 (245.5- 508.4)	388.8 (304.2 – 468.4)
3-epi-25(OH)D3 (nmol/L)	3.2 (1.7-4.4)	2.5 (1.3- 3.7)	2.6 (1.7- 3.1)
24,25(OH)₂D3 (nmol/L)	9.7 (5.5 –10.7)	6.5 (2.07- 10.7)	3.2 (1.37- 12.9)

Table 4.3 Summary of serum vitamin D metabolites in SCOPE pregnant women at 15 weeks gestation and non-pregnant controls. Comparison of serum concentrations of 25-hydroxyvitamin D3 (25(OH)D3) nmol/L, 25-hydroxyvitamin D2 (25(OH)D2) nmol/L, 1,25-dihydroxyvitamin D3 (1,25(OH)₂D3) pmol/L, 3-epi-25(OH)D3 nmol/L, 24,25-dihydroxyvitamin D3 (24,25(OH)₂D3) nmol/L in non-pregnant (n=9), healthy normotensive pregnancies (n=25) and prospective pre-eclampsia cases (PET; n=25), with median and IQR shown.

Considering maternal ‘vitamin D status’, the IOM definition of vitamin D ‘deficiency’ is 25(OH)D3 <20ng/ml (50nM/L) and ‘insufficiency’ as 25(OH)D3>20ng/ml but <30ng/ml (75nM/L)(109). Based on these parameters, in the normotensive pregnancy group, 14 (56.0%) women were defined as vitamin D-deficient, and 8 (32.0%) insufficient. In the PET group, 18 (72.0%) women were defined as vitamin D-deficient, and 6 (24.0%) insufficient. In both pregnant groups the range of serum 25(OH)D3 levels showed wide variation; 4.4 to 112.1 nmol/L in normotensive pregnancies and 10.6 to 66.8 nmol/L in those who developed PET. At 15w gestation, although median 25(OH)D3 concentrations were lower in the PET group (median 33.1, IQR 20.5 – 50.8 nmol/L) compared to the normotensive pregnancy group (44.7, 19.1 – 63.5 nmol/L), this was not significant (p = 0.240). Conversely, in the non-pregnant group all women were classified as sufficient (46.8; 42.8-91.0 nmol/L), with 25(OH)D3 levels significantly higher than those with PET (p= 0.04).

Consistent with previous studies (79), a significant seasonal difference in serum levels of 25(OH)D3 was observed, with higher concentrations of 25(OH)D3 in summer (median 50.8; IQR 39.3-59.7 nmol/L) than winter (21.3; 14.1-41.7 nmol/L)($p=0.0004$). Sub-group analysis revealed that in the PET group, the women pregnant during winter (24.8; 15.4-37.0 nmol/L) had significantly lower 25(OH)D3 levels than those pregnant in summer (50.7; 33.1-57.3 nmol/L)($p=0.002$). For those who did not develop PET, 25(OH)D3 levels also differed in winter (20.8; 9.9- 63.2 nmol/L) and summer (55.2; 42.0 – 64.6 nmol/L), almost reaching significance ($p=0.05$).

Serum concentrations of 25(OH)D2 were similar in the normotensive (4.8; 4.2–8.3 nmol/L) and PET (4.7; 0-10.0 nmol/L) groups ($p=0.352$), and were, as anticipated, much lower than circulating 25(OH)D3. There was no significant correlation between serum 25(OH)D2 and 25(OH)D3 in either the normotensive ($r=-0.15$, $p=0.48$) or PET ($r=0.00$, $p>0.10$) groups. 25(OH)D2 levels were significantly lower in the non-pregnant group comparative to both the PET ($p=0.02$) and normotensive women ($p=0.001$). There was no significant difference in serum concentrations of 3-epi-25(OH)D3 between the normotensive pregnant (2.5; 1.3-3.7 nmol/L), PET (2.6; 1.7–3.1 nmol/L) and non-pregnant (3.2; 1.7-4.4 nmol/L) cohorts. There was a significant positive correlation between 25(OH)D3 and 3-epi-25(OH)D3 in the normotensive pregnancy group ($r=0.645$, $p=0.0005$), but this was not evident in women who developed PET ($r =0.195$, $p =0.349$) (Figure 4.11).

Distinct from previous publications from the SCOPE study (80), 1,25(OH)₂D3 and 24,25(OH)₂D3 concentrations were both quantifiable in serum samples. No significant difference in 1,25(OH)₂D3 concentrations was measured in the PET group (388.8; 304.2–468.4 pmol/L) comparative to the normotensive pregnant group (336.3; 245.5–508.4 pmol /L). Consistent with previous reports(104), 1,25(OH)₂D3 levels were significantly higher in both the PET ($p <0.0001$) and normotensive ($p=0.0005$) women compared to the non-pregnant group (85.6; 47.3-117.4 pmol/L).

No significant difference in serum 24,25(OH)₂D3 concentrations was observed across the 3 groups. Similar to 1,25(OH)₂D3, no difference in 24,25(OH)₂D3 circulating concentrations in the PET (3.2; 1.4-12.9) and normotensive (6.5; 2.1–10.7) groups was measured. However, as summarised in Figure 4.11, serum 25(OH)D3 levels significantly correlated with 24,25(OH)₂D3 ($r =0.43$, $p=0.03$) in the

normotensive women, whilst in those who developed PET no similar correlation ($r = 0.25$, $p = 0.23$) was observed. The significant negative relationship between $24,25(\text{OH})_2\text{D}_3$ and $1,25(\text{OH})_2\text{D}_3$ measured in the normotensive group ($r = -0.48$, $p = 0.02$) was lost in those who developed PET ($r = -0.15$, $p = 0.484$). No correlation between serum $25(\text{OH})\text{D}_3$ and $1,25(\text{OH})_2\text{D}_3$ was observed for any of the groups.

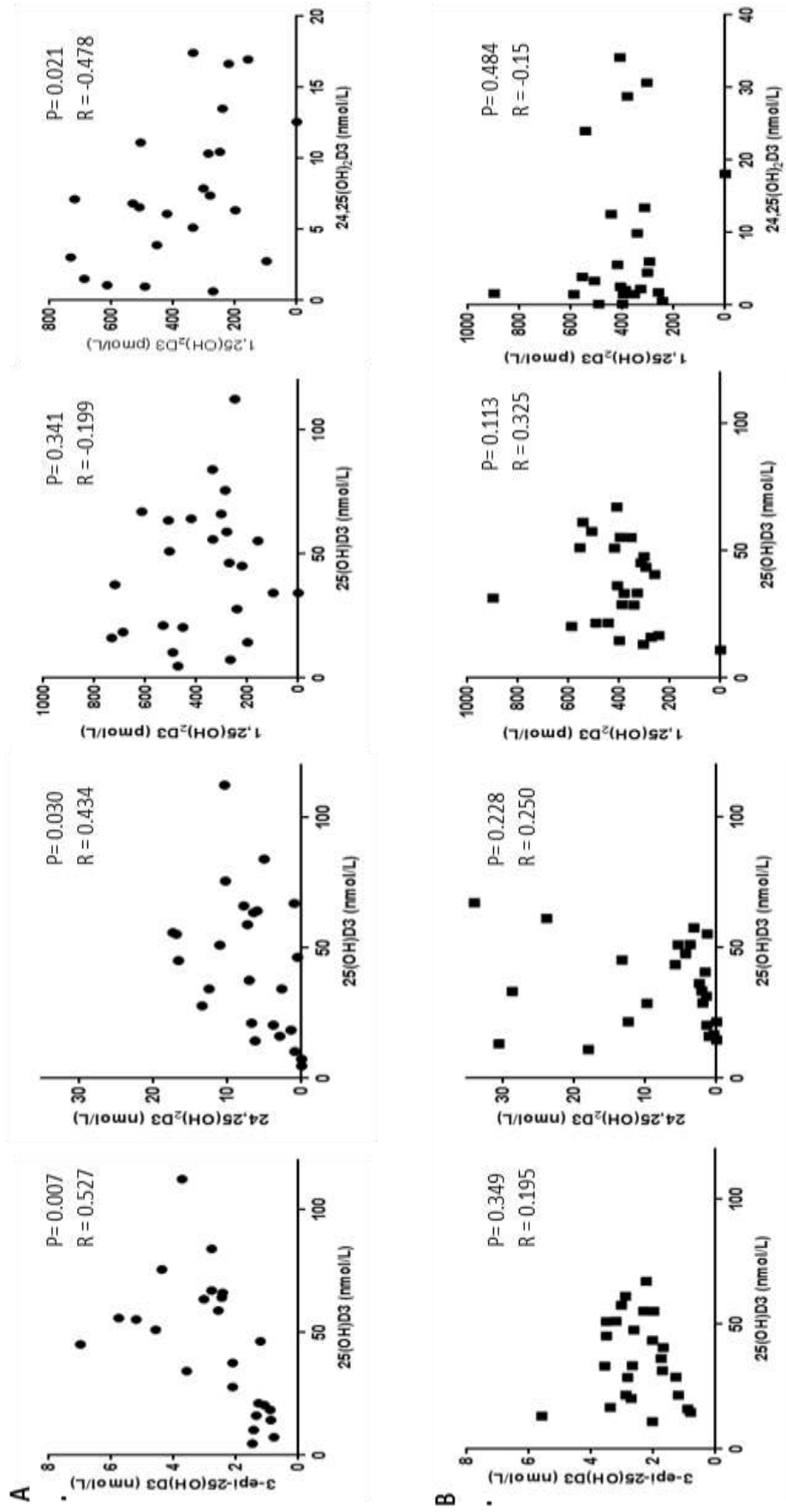


Figure 4.11 Effect of maternal vitamin D status (serum 25(OH)D3) upon other serum vitamin D metabolites at 15 weeks gestation;

comparative analysis in normotensive pregnancies and prospective PET cases. Serum concentrations 25(OH)D3 were correlated with 3-epi-25(OH)D3 (nmol/L), 1,25(OH)₂D₃(pmol/L), and 24,25(OH)₂D₃ (nmol/L) in (A) normotensive pregnancies and (B) prospective pre-eclampsia (PET) cases. Statistically significant correlations are indicated as p values, with Pearson R values shown.

4.2.10 Urinary vitamin D analysis

Urinary 25(OH)D3 and 24,25(OH)2D3 were consistently quantifiable in both pregnant and non-pregnant groups as summarised in Figure 4.12 and Table 4.4.

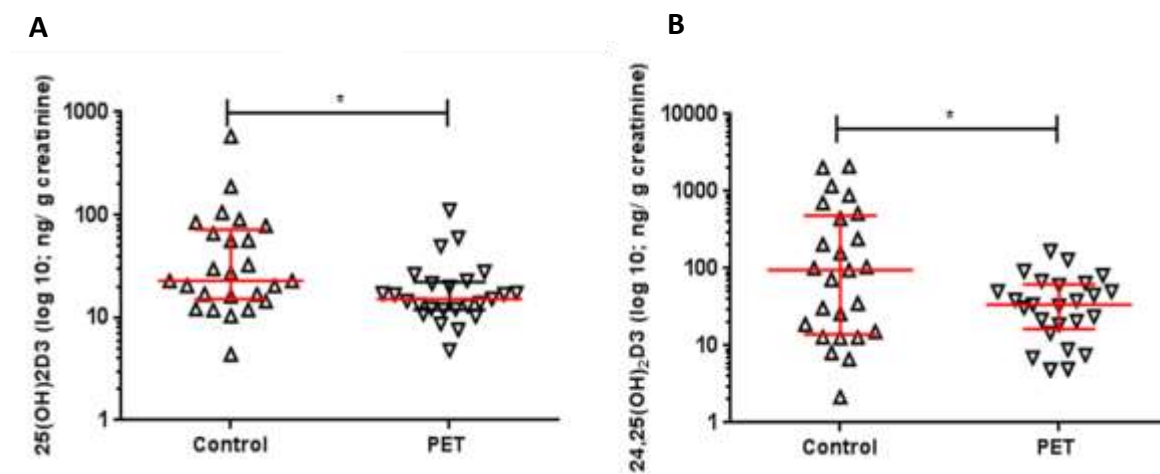


Figure 4.12 Alterations in urinary vitamin D metabolite concentrations measured at 15 weeks gestation in a cohort of pregnant women, of which n=25 prospectively developed PET. Urinary concentrations of: A) 25(OH)D3 nmol/L; and B) 24,25(OH)₂D3 nmol/L normalised for urinary creatinine (ng/ g creatinine) for matched normotensive pregnancies (control) and prospective pre-eclampsia cases (PET). Median with IQR values is illustrated. Statistically significant variations are indicated, * p<0.05.

	Non-pregnant	Control	PET
25(OH)D3	55.8(14.3-84.7)	22.9 (14.8-63.5)	14.8 (11.9-22.5)
24,25(OH)₂D3	55.4 (22.4-118.8)	84.1 (13.5-395.9)	35.6 (15.5-63.7)

Table 4.4 Urinary concentrations of 25(OH)D3 nmol/L; and 24,25(OH)₂D3 nmol/L. Urinary vitamin D metabolite concentrations were normalised for urinary creatinine (ng/g creatinine) in non-pregnant controls (n=9), normotensive pregnancies (control; n=25) and matched prospective pre-eclampsia cases (PET; n=25). Mean values with IQR are shown.

Urinary 25(OH)D₃ concentrations were significantly lower in the PET group (15.2; 12.0–22.2 ng/g creatinine) compared to normotensive pregnant women (22.9; 15.3–72.1 ng/g creatinine) (p=0.018). Concentrations of urinary 24,25(OH)₂D₃ were similarly significantly reduced in those women who developed PET (34.1; 16.6–62.8 ng/g creatinine) (p=0.018) (Table 4.4 and Figure 4.12).

A significant positive correlation between urinary 24,25(OH)₂D₃ and 25(OH)D₃ was measured across the non-pregnant (r= 0.90, p=0.002), normotensive (r=0.64, p = 0.0006) and PET groups (r=0.65, p=0.0005) (Figure 4.13).

Measurement of the metabolites 1,25(OH)₂D₃ and 23,25(OH)₂D₃ was incorporated into the method but these analytes could not be quantified as concentrations were below the lower limit of detection.

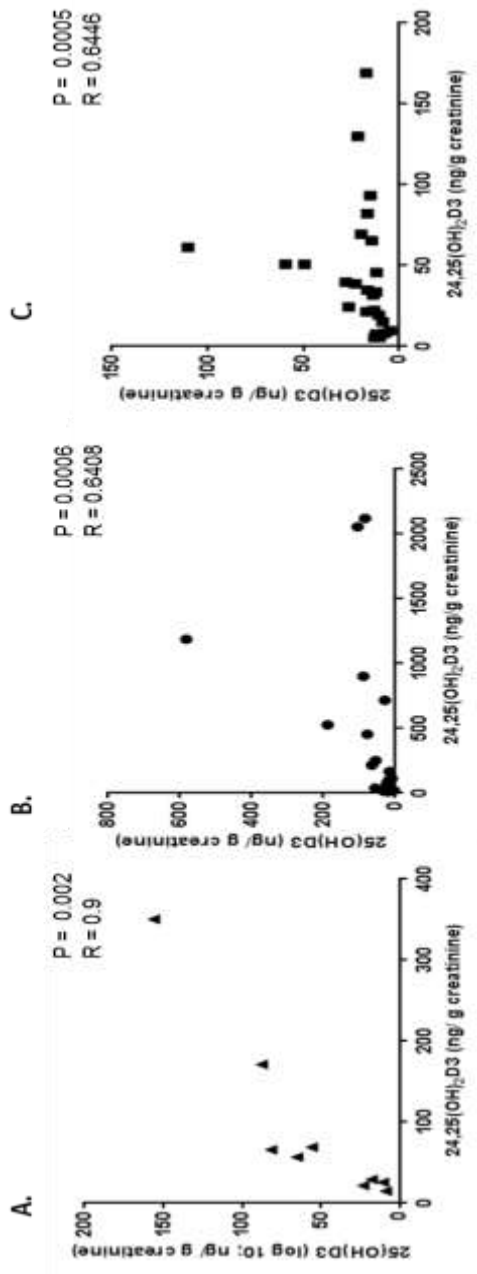


Figure 4.13 Relationship between excreted urinary vitamin D metabolites. Urine concentrations 25(OH)D3 were correlated with 24,25(OH)₂D3 (nmol/L) in (A) non-pregnant, (B) normotensive pregnancies and (C) prospective pre-eclampsia (PET) cases. All nmol/L. Statistically significant correlations are indicated as p values, with Pearson R values shown.

4.3 Discussion

To date most studies assessing vitamin D status and pregnant outcome have relied upon maternal serum concentrations of 25(OH)D₃ as the principal determinant of vitamin D status and function, despite the potential importance of other vitamin D metabolites such as 1,25(OH)₂D₃ (165), 3-epi-25(OH)D₃ (166), and 24,25(OH)₂D₃ (172).

Here we performed a detailed cross sectional analysis of normal pregnant women at first (NP1, n=25) and third trimester (NP3, n=21) and pregnant women with PET (n=22), as well as non-pregnant female controls (n=20). For this a novel LC MS-MS protocol was used to quantify the vitamin D metabolome in paired maternal serum, placental, and decidual tissue, with 25(OH)D₃, 1,25(OH)₂D₃, 24,25(OH)₂D₃, 3-epi-25(OH)D₃ successfully quantified. Parallel analysis of DBP and albumin was used to calculate bound, bioavailable and free fractions of vitamin D. Importantly, simple linear regression analysis confirmed gestational age alone did not significantly alter serum vitamin D metabolite concentrations in the PET and NP3 groups.

4.3.1 Total 25(OH)D₃ alone is not a reliable marker of vitamin status in pregnant women

Data presented here suggest that total 25(OH)D₃ may not be sufficient to accurately evaluate vitamin D status in pregnant women. According to current recommendations (64), vitamin D-deficiency (serum 25(OH)D <50 nmol/L) was highly prevalent in most of the pregnant and non-pregnant women analysed in the current study despite this being a predominantly white Caucasian cohort. Furthermore, no difference in 25(OH)D₃ concentrations was measured across gestation, i.e. first and third trimester normal pregnancy groups. This is consistent with previous cross-sectional analysis of vitamin D status, in which a high prevalence of hypovitaminosis D was observed in pregnancy, lactation and infancy with no significant inter-trimester differences in serum 25(OH)D₃ level measured across gestation in 541 healthy Indian women (173). Albeit not assessed, we anticipate this may have a direct negative impact upon fetal concentrations of vitamin D, with even lower 25(OH)D₃ concentrations than those measured in maternal serum.

In contrast to previous reports (159, 174, 175), PET was not associated with serum 25(OH)D₃. This may reflect the smaller sample size and non-matched cohort used relative to previous studies (159), or the fact that some previous studies quantified serum 25(OH)D₃ using ELISA technology which cannot distinguish between 25(OH)D₃ and 3-epi-25(OH)D₃ and as such may over-estimate serum vitamin D 'status' (174, 175). Nevertheless, the over-arching conclusion from data presented here is that simple measurement of serum 25(OH)D₃ provides only a limited perspective on vitamin D in pregnancy.

4.3.2 Dysregulated vitamin D metabolism in pregnancies complicated by PET

Increased maternal serum 1,25(OH)₂D₃ is a well-established feature of normal pregnancy (130, 176), and in the current study NP3 values were significantly higher than for NP1 and PET. This marked upregulation in NP3 compared to NP1 has previously been demonstrated, with concentrations returning to normal during lactation (124). In part this reflects the increased fetal demand for calcium to support their increasing fetal bone mineralisation requirements. The stimulus for this rise is not however clear, since PTH concentrations are unchanged throughout pregnancy. One potent stimulus may be PTH-related peptide (PTHrP), which is produced in the fetal parathyroid and placental tissues and increases with gestation (177). PTHrP can enter the maternal circulation to act via PTH/PTHrP receptors in the kidney and bone to increase 1,25(OH)₂D₃, thereby regulating calcium and PTH levels. Other factors shown to positively regulate active calcium homeostasis and vitamin D synthesis during pregnancy include prolactin, placental lactogen, both of which stimulate PTHrP and 1,25(OH)₂D₃ production(178). It appears, enhanced vitamin D synthesis as opposed to decreased metabolic clearance and/ or altered half-life drives this process (131, 132), with maternal renal synthesis appearing a key mediator(133). Elevation of 1,25(OH)₂D₃ may be expected to increase 25(OH)D₃ usage directly and potentially result in a decrease in the 25(OH)D₃ total stores and increase in 24,25(OH)₂D₃ production as observed between the NP1 and NP3 cohorts here.

Previous studies with similar sized NP3 and PET cohorts reported PET-associated declines in serum 1,25(OH)₂D₃ of 30% (174) and 14% (179) respectively. Suppressed serum 1,25(OH)₂D₃ in PET may

be due to decreased serum levels of insulin-like growth factor 1, a stimulator of renal 1α -hydroxylase, or lower expression of 1α -hydroxylase in the placenta (180), but other PET studies have reported increased whole human placental tissue 1α -hydroxylase expression(181). Data from the current study suggest that metabolism of $25(\text{OH})\text{D}_3$ to $24,25(\text{OH})_2\text{D}_3$ may indirectly contribute to the lower levels of $1,25(\text{OH})_2\text{D}_3$ in PET, with concentrations significantly elevated compared to non-pregnant and NP1 observed.

Alternative metabolism of vitamin D can also occur via epimerisation of $25(\text{OH})\text{D}_3$. Studies have shown that 3-epi- $25(\text{OH})\text{D}_3$ can undergo 1α -hydroxylation to 3-epi- $1,25(\text{OH})_2\text{D}_3$, and then bind to VDR to activate target gene transcription(182). However, as 3-epi- $1,25(\text{OH})_2\text{D}_3$ is a less potent VDR agonist than $1,25(\text{OH})_2\text{D}_3$, epimerisation of $25(\text{OH})\text{D}_3$ may act to control VDR activity by generating a less effective ligand for the receptor(183). Here we find that in the context of PET, 3-epi- $25(\text{OH})\text{D}_3$ concentrations were significantly higher, so that as with 24-hydroxylase, epimerisation may play a role in the dysregulation of vitamin D function in PET.

Considering the physiological role of 3-epi- $1,25(\text{OH})_2\text{D}$ this is not yet elucidated in pregnancy. There has been more recent interest in fetal cord 3-epi- $25(\text{OH})\text{D}_3$ as the relative proportion of the total $25(\text{OH})\text{D}_3$ which is in the 3-epi- $25(\text{OH})\text{D}_3$ form appears significantly enriched. Postnatally, 3-epi- $25(\text{OH})\text{D}_3$ may represent up to 25% of total $25(\text{OH})\text{D}_3$, and this subsequently declines in the first year postpartum. Importantly, the prevalence of fetal vitamin D deficiency is likely under-estimated as most methods do not discriminate the less active 3-epimer form. For example, in a cohort of 92 paired maternal and cord blood samples the concentrations of $25(\text{OH})\text{D}_3$ were 82.9 and 60.1 nmol/L and 3-epi- $25(\text{OH})\text{D}_3$ were 5.3 and 5.1 nmol/L respectively. Importantly, when 3-epi- $25(\text{OH})\text{D}_3$ was excluded, 4% of maternal and 28% of cord blood had concentrations <50 nmol/L; whilst with 3-epi- $25(\text{OH})\text{D}_3$ included, the estimates were 2% and 21% (184). Albeit based upon small total repeats, we have preliminary data consistent with this (Appendix Figure 9.0). Together these findings suggest clinical measurement of the 3-epi- $25(\text{OH})\text{D}_3$ may be required to permit accurate determination of both maternal and neonatal vitamin D status. This may also account for the current disparity between observational and supplementation studies. Further studies are required to understand the in vivo roles

of epimers in human pregnancy. How this should impact upon vitamin D status interpretation and supplementation guidance is therefore unclear (185).

Our findings suggest parallel quantification of the major vitamin D metabolites offers a more comprehensive insight into vitamin D status than 25(OH)D₃ measurement alone in normal pregnancy and within the context of PET.

4.3.3 Effects of DBP and free 25(OH)D₃

There has been increasing interest in the potential role of serum DBP not only as a carrier of vitamin D metabolites, but also as a determinant of tissue access of 25(OH)D₃ either as ‘unbound’ or ‘free’ 25(OH)D₃, or through megalin-mediated uptake of DBP-bound 25(OH)D₃ (25). This is particularly important in pregnancy as megalin is expressed in the placenta (38). In the current study, changes in DBP and albumin concentrations across pregnancy resulted in subtle changes in the relative proportions of bioavailable and free 25(OH)D₃. Higher plasma DBP concentrations have been reported previously compared to non-pregnant controls, with a 2-fold increase from the first trimester (132). However, measurement of total and free 25(OH)D₃ have been inconsistent to date, and whether free 25(OH)D₃ is reduced as a result of increased DBP remains uncertain (136) (132). For our cohort, no significant difference in ‘free’ or ‘bioavailable’ 25(OH)D₃ was measured, although suppression of serum albumin with increasing GA did significantly decrease the ratio of ‘bioavailable’ 25(OH)D₃ to ‘total’ serum 25(OH)D₃ consistently in the NP3 and PET groups. The modestly elevated DBP levels in pregnant women also resulted in decrease ratios of ‘free’ 25(OH)D₃ to total 25(OH)D₃, with this effect being more pronounced in PET pregnancies.

Serum albumin decreases with pregnancy as a consequence of increased maternal blood volume. This effect may be exacerbated in PET, although the extent to which this occurs varies according to disease severity (186). Previous studies using first trimester serum samples did not demonstrate any significant variation in DBP or 25(OH)D₃ concentrations between pregnancies that went to normal term delivery, and those complicated by PET(164). To our knowledge, this is the first study to assess expression of serum DBP in NP3 and PET pregnancies, with data showing no major variations in free or bioavailable 25(OH)D₃ with PET. Whether changes in the affinity of DBP for vitamin D

metabolites in normal and/ or complicated pregnancies alter free vitamin D metabolites is not clear however and requires future study.

4.3.4 Tissue concentrations of 25(OH)D and 1,25(OH)₂D₃ are higher in decidua compared to placenta

This is the first study to use paired placental/ decidual and serum samples to assess the relationship between circulating and tissue-specific levels of vitamin D metabolites. Distinctly, the relatively high levels of 25(OH)D₃ in decidua enabled quantification of 1,25(OH)₂D₃, whilst in the placenta concentrations of 1,25(OH)₂D₃ were undetectable. These findings are consistent with our primary hypothesis that the maternal decidua represents a key site for extra-renal metabolism, with intracrine conversion of inactive to active vitamin D a pivotal process from early pregnancy(71). What remains less clear is the determinants of decidual 25(OH)D₃ and 1,25(OH)₂D₃. The most likely driver of decidual 1,25(OH)₂D₃ is local tissue expression of 1 α -hydroxylase. In unpublished studies we have shown 1 α -hydroxylase mRNA correlates with mRNA for inflammatory CK such as IL-6 and IFN- γ , suggesting immune activity to be key for initiating decidual 1,25(OH)₂D₃ production. Consistent with this, immune cell infiltration is a key feature within decidua with leukocytes comprising at least 40% of the total decidual cell population from the first trimester(187).

What is less clear is what determines decidual levels of the substrate for 1 α -hydroxylase, 25(OH)D₃. Here, neither maternal serum nor placental 25(OH)D₃ showed any correlation with decidual 25(OH)D₃, despite the proximity of these tissues. This suggests the decidua has an autonomously regulated vitamin D system. This is distinct from extra-renal adipose tissue, where 25(OH)D₃ positively correlates with serum vitamin D status (188). Closer comparisons may be drawn to the human colon, where 1,25(OH)₂D₃ is detected and although partly determined by serum concentrations, demonstrates significant in vivo synthesis (189).

4.3.5 Placental vitamin D metabolites across normal pregnancy

Considering placental vitamin D metabolism, 25(OH)D₃ concentrations significantly increased with advancing gestational age. Alongside this, a non-significant modest rise in 24,25(OH)₂D₃ and 3-epi-

25(OH)D₃ was measured, thereby indicating local 25(OH)D₃ metabolism. Consistent with this, positive expression of CYP27B1, VDR and CYP24A1 from the first trimester have been reported, with catabolic CYP24A1 expression decreasing with advanced GA (133, 143, 144) (145). This indicates 25(OH)D₃ exerts VDR-mediated effects within the fetal placenta. Within the placental trophoblast both 24,25(OH)₂D₃ and 23,25(OH)₂D₃ have previously been measured following culture with 25(OH)D₃. Consistent with placental 1,25(OH)₂D₃ being undetectable in our placental cohorts, only in the presence of ‘supra-physiological’ doses of 25(OH)D₃ was a concomitant increase in placental 1,25(OH)₂D₃ detected (190).

Consistent with recent reports (191), in the NP3 group a significant positive correlation between maternal serum and placental 25(OH)D₃ concentrations was measured. This was consistently observed for DBP-bound, bioavailable and free serum 25(OH)D₃. We anticipate this may reflect the increased demands of the fetus for calcium and/or phosphate transport across the placenta to support fetal skeletal development. There is strong evidence that adequate maternal vitamin D levels are crucial for the prevention of fetal and neonatal rickets (192). Cord concentrations of 25(OH)D₃, and 24,25(OH)₂D₃ correlate significantly with those found in the maternal circulation at the point of delivery, thus suggesting both metabolites readily diffuse across the placenta. This is less certain for 1,25(OH)₂D₃, with conflicting evidence reported (193-195). Future detailed analysis of paired cord and placental vitamin D metabolites may help delineate the relationship between materno-placental vitamin D status and perinatal metabolism in utero.

In the PET cohort, stark changes in placental vitamin D metabolite concentrations were observed for 25(OH)D₃, 24,25(OH)₂D₃ and 3-epi-25(OH)D₃. Notably, placental 25(OH)D₃ was significantly lower compared to the NP3 group, with concentrations equivalent to those measured for NP1. It is possible that placental uptake of 25(OH)D₃ is influenced by its serum carrier protein, DBP (23). For both NP1 and NP3, serum and placental DBP were positively correlated with tissue 25(OH)D₃ whilst this was not observed in PET placentas. Thus it is possible that PET is associated with dysregulated endocytic uptake of DBP via megalin, which is expressed by the placenta (196).

Enhanced placental metabolism of 25(OH)D₃ to 24,25(OH)₂D₃ may also contribute to lower total placental concentrations of 25(OH)D₃ in PET. Consistent with the serum analysis, increased 24,25(OH)₂D₃ and epi-25(OH)D₃ were measured. Enhanced ‘catabolism’ has previously been reported in PET, with upregulated placental (trophoblast) expression of CYP24A1 identified (181). Increased expression of CYP27B1 and decreased VDR in placentas from PET pregnancies has been reported previously (181), underlining the potential importance of vitamin D metabolism for this pregnancy disorder.

In mice, vitamin D-deficiency is shown to be associated with dysregulated placental vascularisation and elevated maternal blood pressure(197). Chan *et al*, who investigated the effect of vitamin D upon human EVT provided early evidence that vitamin D deficiency may impair invasion in the first trimester (198). Specifically, isolated EVT, which positively express CYP27B1 and VDR, demonstrated increased cell invasion in response to both 1,25(OH)₂D₃. Alongside this, increased secretion of pro-metalloproteinase -2 and 9, which degrade collagen networks in extracellular matrices, were measured. Whether enhanced placental catabolism of vitamin D arises in PET as a compensatory mechanism to promote EVT invasion is unclear (198). Further studies to ascertain whether decreased placental 25(OH)D₃ is a cause or consequence of PET are first required.

4.3.6 Dysregulation of vitamin D metabolism prior to PET onset

Whilst placental vitamin D analysis offers the novel opportunity to delineate metabolism at the materno-fetal interface, the clinical applications of this are limited due to the inaccessibility of this tissue throughout normal pregnancy. Given the prominent alterations in circulating vitamin D physiology across pregnancy, additional methods to ascertain vitamin D metabolism across gestation may be informative.

To advance these observations we performed detailed comparative analysis of serum vitamin D metabolites in a cohort of nulliparous ‘low-risk’ pregnancies at 15w gestation of which half prospectively developed PET. To further enhance this approach, a novel urinary vitamin D metabolite quantification method was incorporated. Given the anticipated low concentrations of steroid metabolites present in urine, the analytical method employed utilised a derivatization procedure using

PTAD to enhance both the sensitivity and separation of individual metabolites. To our knowledge, this is the first time circulating and urinary vitamin D has been measured for clinical analysis, describing changes in both circulating and excreted levels on pregnancy outcome. This optimised method presents a reference range for urinary vitamin D during pregnancy, along with comparison to circulating levels. This method combined with serum analysis will provide a comprehensive assessment in vitamin D metabolism in clinical conditions related to vitamin D deficiency.

Importantly, pregnant women were matched for age, BMI, ethnicity. Albeit not significant, consistent with previous larger studies we found first trimester MABP readings were higher in women who subsequently developed PET compared to those pregnant women who remained normotensive (164). Unlike the larger SCOPE series (79), we were not significantly powered to evaluate vitamin D metabolism within the context of SGA (n=3).

Consistent with our West Midlands data-set, vitamin D deficiency was highly prevalent in the Irish SCOPE cohort, particularly in winter months, with 64% (n=32) of pregnant women having 25(OH)D3 levels < 50 nmol/L at 15w gestation. We anticipate this would be higher still if the cohort included pregnant women with darker skin pigmentation; as demonstrated in large epidemiological studies (111). Despite current clinical recommendations for pregnant women to take daily vitamin D supplementation (199) (200), in this cohort only 20% of women reported taking preconception vitamin D supplementation, and by the first trimester adherence to supplementation advice dropped to 18%.

Considering the potential predictive value of vitamin D status assessment, a nested case-control study was undertaken following a cohort of nulliparous singleton pregnant women from < 16w gestation to delivery and correlated maternal Vitamin D status with the risk of developing PET. Of the 55 women who developed PET, serum 25(OH)D3 levels were significantly lower comparative to normotensive pregnant controls (n=219) (116). The potential predictive role of vitamin D within the context of PET was similarly suggested in a 2-phase discovery/validation metabolic profiling study performed by Kenny *et al*, which identified potential metabolomic markers of PET. In the discovery phase, a nested case-control study was performed which assessed serum samples obtained at 15±1w

gestation from 60 women who subsequently developed PET and 60 matched controls. A multivariate predictive model combining 14 metabolites was developed, with an odds ratio for developing PET of 36 (95% CI: 12 to 108), and area under the receiver operator characteristic curve of 0.94. In the validation phase, these findings were re-assessed in a different country using an independent case-control study design, with n= 39 women at 15w who prospectively developed PET and n=40 matched controls. All 14 metabolites were re-identified as significant; odds ratio 23 (95% CI 7-73), amongst which vitamin D3 derivatives were included (p=0.002)(201). However in other previous published work this has not been similarly observed (80).

In the SCOPE whole dataset (n=1768) circulating 25(OH)D3, 3-epi-25(OH)D3, and 25(OH)D2 were measured with LC MS-MS, with 25(OH)D3 alone not able to predict PET at 15 w. It was concluded that in women with 25(OH)D3 levels >75nM a protective effect (adjusted odds ratio 0.64; 95% CI: 0.43, 0.96) upon PET plus SGA outcome was evident following adjustment for potential confounding factors (80). In our smaller subset only 3 (12.0%) of the total pregnant cohort (n=50), none of which were in the PET group had 25(OH)D3 levels > 75nmol/L (maximum 25(OH)D3 =60.9 nmol/L), this could not be assessed. Circulating 25(OH)D3 concentrations in those who developed PET were statistically lower than the non-pregnant group, but not those who remained normotensive through pregnancy. This may simply reflect a small cohort size resulting in a type 1 error and the heterogeneity of the PET cohort with respect to both timing of disease onset and progression. It is possible our cohort was not representative of the whole SCPOPE cohort. Our findings are however consistent with others (202), who similarly found no significant difference in 25(OH)D3 in pregnant women who subsequently developed PET compared to normotensive pregnant controls (27.4±1.9 versus [vs] 28.8±0.80; p= 0.435). DBP and free 25(OH)D levels were also assessed with no difference measured (164). As 25(OH)D3 reflects total body stores, we anticipate this may be preserved during early PET, and as such alone is unlikely to be informative within the context of ascertaining potential risk of PET.

Although we did not observe any significant difference in serum vitamin D metabolites between the two pregnancy groups, the associations between these metabolites differed significantly. In women

who developed PET, no positive correlation between serum 25(OH)D₃ and the vitamin D catabolites 3-epi-25(OH)D₃ and 24,25(OH)₂D₃ was measured. Albeit not clearly understood, alternative metabolism of vitamin D via epimerisation to 3-epi-25(OH)D₃ results in the formation of 3-epi-1,25(OH)₂D₃ which binds to VDR to activate target gene transcription. Importantly, 3-epi-1,25(OH)₂D₃ appears a less potent VDR agonist than 1,25(OH)₂D₃, which may have physiological consequences (182). In normal pregnancy, 3-epi-25(OH)₂D₃ appears directly linked to 25(OH)D₃ concentrations (80), however this relationship was dysregulated only in those women who developed PET.

A trend towards elevated serum 1,25(OH)₂D₃ was also observed in the PET samples. Healthy pregnancy is characterised by a drive towards 1,25(OH)₂D₃ production (104). In women with PET increased upregulation of placental CYP27B1 and CYP24A1 is reported(181). Increased metabolism of 25(OH)D₃ to 1,25(OH)₂D₃ may also be secondary to decreased total serum calcium concentrations, which arise during normal human pregnancy but is more pronounced in PET (203).

Intriguingly, serum levels of 25(OH)D₂ were significantly higher in both pregnancy groups relative to non-pregnant controls. The explanation for this is unclear as vitamin D₂ is principally obtained from plants and mushrooms. One possibility is that enhanced circulating 25(OH)D₂ is due to dietary modifications undertaken by women when they are pregnant. Furthermore, when considering 25(OH)D₃ and 25(OH)D₂ together, no significant difference in total vitamin D status was measured. Therefore, despite significantly lower 25(OH)D₃ concentrations in those pregnant women who developed PET compared to the non-pregnant group, overall vitamin D status was not altered. This is consistent with previous data from the Osteoporotic Fractures in Men Study which found higher 25(OH)D₂ levels not to correlate with higher total 25(OH)D concentrations, and that increased 25(OH)D₂ concentrations were associated with lower 25(OH)D₃ ($p < 0.01$)(204). Recent supplementation data similarly indicates 25(OH)D₂ supplementation decreases serum 25(OH)D₃ levels (205). In serum, 25(OH)D₂ binds serum DBP with lower affinity, which may account for the increased serum clearance of 25(OH)D₂ relative to 25(OH)D₃ (206). However, in the current study 25(OH)D₂ was not quantifiable in urine, suggesting that renal handling of 25(OH)D₂ bound to DBP

is efficient enough to limit urinary excretion of 25(OH)D₂ with concentrations below the level of detection. Reabsorption of 25(OH)D₂ from glomerular filtrates into the proximal tubules may lead to increased synthesis of 24,25(OH)₂D₂ and 1,25(OH)₂D₂, but as neither of these metabolites were measured this is to be confirmed.

The method utilised was adapted from that reported by Ogawa *et al*, who quantified 25(OH)D₃ and 24,25(OH)₂D₃ in spot urine samples (1mL) from healthy male subjects (n=20) pre- and post- vitamin D supplementation (81). In pregnancy, urinary 24,25(OH)₂D₃ concentrations were approximately 3-fold higher than 25(OH)D₃, representing the predominant excreted vitamin D metabolite. This was not evident in the non-pregnant group, for which urinary 25(OH)D₃ and 24,25(OH)₂D₃ concentrations were comparable. Furthermore, in the healthy non-pregnant females, median urinary 25(OH)D₃ concentrations were at least 2-fold higher than both pregnant groups, in particular those who subsequently developed PET. Together these findings are consistent with an increased role for 25(OH)D₃ in pregnancy, with significantly enhanced classical and non-classical placental 1,25(OH)₂D₃ production and turnover from the first trimester (104, 207). Reduced 25(OH)D₃ excretion may also reflect increased neonatal vitamin D metabolism, as 25(OH)D₃ readily diffuses across the placenta principally to permit later fetal bone development and growth(208). In rat models VDR expression is demonstrated from a very early stage in fetal development(209).

Urinary 25(OH)D₃ and 24,25(OH)₂D₃ were significantly correlated in both the normotensive and PET groups. This is consistent with serum 25(OH)D₃ and 24,25(OH)₂D₃ in normal pregnancy, as evidenced in the West Midlands data-set (104). Uniquely we assessed the relationship between circulating and urinary metabolites. Here we find in normal pregnancy serum concentrations of 25(OH)D₃ and 24,25(OH)₂D₃ do not correlate with their respective urinary concentrations. Given the number of known extra-renal sites of vitamin D storage and metabolism, including the placenta, this may be anticipated. Furthermore, the kidney has the capacity to actively reabsorb vitamin D metabolites via DBP- megalin (18), which may contribute to the lack of correlation between serum and urinary vitamin D metabolites.

In the current study urinary vitamin D metabolite analysis suggests dysregulation of vitamin D metabolism occurs at an early stage in women who later develop PET as both urinary 25(OH)D3 and 24,25(OH)₂D3 concentrations were significantly decreased compared to those who remained normotensive throughout pregnancy. Alongside this increased serum concentrations of 1,25(OH)₂D3 were measured in those with PET. Increased vitamin D metabolism in PET may arise secondary to decreased serum calcium concentrations (210, 211). There are also several reports that hypocalciuria is associated with PET and could be considered a risk factor for development of PET in pregnancy (179, 212). A prospective study measuring the calcium/ creatinine clearance ratio found women with PET excrete significantly less calcium (n=60) compared to normotensive controls (213). This may account for enhanced renal 25(OH)D3 re-uptake, thereby limiting metabolite excretion. Evidence from Cochrane review found daily calcium supplementation to significantly reduce the risk of PET (n=16490 women, risk ratio 0.48; CI 0.34- 0.67; 15 trials), and improved maternal -infant outcomes from 20w. Although women's responses to calcium were heterogeneous, a consistent protective overall effect was observed (214, 215).

Together our preliminary data indicate dysregulation of vitamin D metabolism may precede clinical onset of PET. Spot urinary analyses may offer novel insights into the underlying pathogenesis of vitamin D dysregulation in PET. From the data presented we demonstrate that routine measurement of serum 25(OH)D3 alone provides only a limited perspective on the requirement for vitamin D in pregnancy. Detailed analysis of vitamin D metabolism, including renal catabolism and excretion is required.

4.3.7 Limitations

For the West Midlands cohort, most women recruited were white (79.5%), with only 5.7% black and 14.8% Asian women. Albeit consistent across all 4 cohorts, due to the sample size there were insufficient numbers to ascertain whether ethnicity had a significant impact upon vitamin D metabolite concentrations. Certainly within the context of 25(OH)D3 black women appear at particular risk of deficiency. A recent report of pregnant women reported that at delivery, 29.2% and 54.1% of black women, and 45.6% and 46.8% black neonates were vitamin D deficient (<37.5

nmol/L) and insufficient (37.5-80 nmol/L) respectively. Conversely, in the white cohort, 5% and 42.1% of mothers and 9.7% and 56.4% of white neonates were vitamin D deficient and insufficient, respectively (111). This is particularly concerning, given the high-prevalence of vitamin D deficiency within our cohort, despite over-representation of white pregnant women.

The validity of the monoclonal DBP assay utilised here has been subject to recent debate, specifically its differential immunoreactivity against variant DBP targets(24). Whether test accuracy is contributory to our differential findings in sera and placental tissue is unclear, however this is particularly relevant for black populations due to their Gc1F variant expression predominance, whereas our cohort was predominantly white Caucasian. A direct measurement method for 'free' 25(OH)D₃ and bioavailable 25(OH)D₃ would however resolve this.

In response to the upsurge of studies investigating the prevalence and clinical implications of vitamin D deficiency, the demand for more accurate and efficient measurement modalities has risen. Consequently, the accuracy of earlier measurement assays has been investigated, with clear differences in the sensitivities and specificities evident. An understanding of these methods is important to interpret the current evidence base on vitamin D metabolite analysis, and conflicting outcomes reported (216). Despite significant improvements in assay standardisation procedures by the international vitamin D external quality assurance scheme(217), the precision and accuracy of different vitamin D metabolite methods remains contentious with significant inter-assay variability and deviation of analyte concentrations reported (218). LC MS-MS is however widely recognised as the gold standard technique for vitamin D analysis, reflecting its greater analytical flexibility, specificity and sensitivity comparative to immuno-based assays (74, 75). This permits simultaneous measurement of separate 25-hydroxylated metabolites and downstream di-hydroxylated metabolites using only small total serum volumes (76). This includes measurement of active 1,25(OH)₂D₃, for which accurate quantification is complex due to its 1000-fold lower concentrations, short half-life, and lipophilic nature (76) (77). Further standardisation of LC MS-MS technology is still required to improve the accuracy, precision and consistency of results generated by LC MS-MS. It is also important to recognise the high cost and technical expertise necessary to run and maintain LC MS-MS

remain a major obstacle to its routine use. Whilst increased surveillance of these methods is becoming increasingly evident, as evidenced by scientific journals now only accepting fully validated assays for the analysis of steroids and sterols including vitamin D, concerns regarding the lack of standardisation of 'in-house methods' reported still exist. (219).

In common with all studies of pregnancy, the interpretation of biochemical parameters is complex due to the effects of haemodilution, changes in renal and hepatic clearance and the influence of pregnancy specific hormones. Furthermore, from the early first trimester significant changes in renal function arise, in particular a dramatic increase in glomerular filtration (up to 50%) and renal plasma blood flow and thus urinary frequency. There is also often increased renal size and pelvic dilation (220).

Considering the measurement methods available to assess urinary compounds, 24h urinary analysis is considered the gold-standard measurement. This accounts for the susceptibility of urinary metabolite concentrations to variation by extrinsic factors including hydration status and overall renal function. However this method is both cumbersome and reliant upon strict compliance. However, spot samples and first morning void are widely deemed acceptable for analyte measures, provided the effect of sample dilution is quantified and appropriately adjusted (221, 222). At present no consensus upon which is most appropriate adjustment technique, however creatinine remains commonly applied. This simply calculates the ratio to creatinine concentrations and does not account for temporal variations in creatinine excretion rates (222).

The potential value of a urinary marker of vitamin D status has wider clinical implications outside of pregnancy, and certainly, this method will be highly transferrable. Under the current method conditions levels of $1,25(\text{OH})_2\text{D}_3$ and $23,25(\text{OH})_2\text{D}_3$ could not be measured following derivatization, as these concentration were below the limits of detection. To assess the ability to quantify these analytes in urine, method development will be required on a later generation mass spectrometer that will enable reduced detection limits.

Moving forward, serial serum and urinary analyses at a set time-point would provide a more detailed insight into the pathogenesis of vitamin D dysregulation. It would have been interesting to include more early-onset PET cases (<34w n=1) in this cohort, as this may have been associated with more severe placental pathology. Subgroup analysis of those women who developed PET preterm (≤ 37 w) (n=9) did not reveal any significant differences with regards to the 5 major serum vitamin D metabolites measured (data not shown), but numbers were too small to draw any robust conclusions from this.

Finally, a major restriction in understanding fetal physiology is imposed by the relative inaccessibility of the human fetus, with metabolite analysis only permissible at the point of delivery. Whether placental vitamin D metabolites correlate with fetal cord metabolites is an important question, which was not addressed in this study.

5 Vitamin D and uterine natural killer cells

Parts of this chapter have been published as:

1. Tamblyn JA, Lissauer DM, Powell R, Cox P, Kilby MD. The immunological basis of villitis of unknown etiology - review. *Placenta*. 2013;34(10):846-55 (1)
2. Tamblyn JA, Hewison M, Wagner CL, Bulmer JN, Kilby MD. Immunological role of vitamin D at the maternal-fetal interface. *J Endocrinol*. 2015; 224(3):R107-21(71).
3. JA Tamblyn, LE Jeffery, R Susarla, DM Lissauer, SL Coort, A Muñoz Garcia¹, K Knoblich, AL Fletcher, JN Bulmer, MD Kilby, M Hewison. Differential regulation of first trimester uterine and peripheral blood natural killer cells by 1,25-dihydroxyvitamin D₃. Submitted *Human Reproduction*. March 2018 (under peer-review).

5.1 Introduction

5.1.1 Immune cell function and the decidua

Pregnancy is a unique situation in which the mother and the hemiallogeneic fetus coexist. Despite previous suppositions the syncytiotrophoblast forms an impenetrable barrier preventing access of maternal cells to fetal antigens, this is now known not to be the case. Throughout pregnancy continual shedding of apoptotic syncytial nuclear aggregates (>100,000/d) and underlying trophoblast cells into the systemic maternal circulation occurs (223, 224). Exposure of the maternal immune system to fetal cells and their respective paternal-derived antigens is common with significant gestation-dependent immune adaptations develop throughout pregnancy to accommodate this (224).

From the first trimester maternal immune cells and endothelial cells of the spiral arteries are closely juxtapositioned along trophoblasts at the boundary between the decidua and junctional zone. Within the decidua a unique immune cell population exists which appears pivotal to this process. From early pregnancy, 30–40% of total decidua cells are leukocytes, including uterine natural killer cells (uNKs) (~60%), macrophages (20%) along with CD3+ T Cells (CD8+ > than CD4+), DCs. B cells are virtually undetectable (225). The remaining cells are primarily of stromal origin. The cellular cross-talk between decidual stroma, decidua immune cells and fetal trophoblast is orchestrated by hormones, CK, chemokine and growth factors, and this is crucial for normal placentation (138).

Originally, it was postulated successful pregnancy reflects an immune bias towards Th2 immunity with active suppression of the maternal immune response. This is however an oversimplification with multiple mechanisms encompassing both innate and adaptive arms of the immune system now recognised.

Certainly there is altered antigen presentation, as villous trophoblast and syncytiotrophoblast cells lack human leukocyte antigen (HLA)-A, -B, -DR, -DQ, and -DP expression. This non-specific downregulation of antigen presentation is assumed of benefit for fetal survival via direct immune evasion, however, EVT cells do express HLA-C and class HLA I antigens -E, -F, and -G which together permit selective fetal antigen presentation (226) (227). It appears a variable receptor/ligand

system has evolved to impact on reproduction and permit implantation and development of the semi-allogenic fetus. These antigens have diverse functions, which include modulation of T cells, NK cells, macrophages and DCs activity (228). The potential mechanisms employed via HLA-G at the materno-fetal interface have gained particular attention, including a potential role in the modulation of NK cell killing and migration; proliferation and IFN- γ production; regulation of CK production in mononuclear and T cells; suppression of T cell killing and viability (229, 230). The mechanisms by which T cells react to these antigens are also of certain relevance, in particular the role of Tregs (231-233). Our group has also recently shown that decidual T cells proliferate in response to fetal tissue, and depletion of T regulatory cells leads to an increase in fetal-specific proliferation (234). Furthermore, pregnant women exhibit many characteristics of a systemic pro-inflammatory response with increased leucocytosis, monocyte priming and phagocytic activity, and pro-inflammatory CK production (235, 236).

As shall be outlined, uNKs are the most prominent subset from early in the first trimester. These cells display a characteristic stage-dependent migration and distribution across pregnancy, with active regulatory roles during early placentation and fetal development anticipated (237, 238).

5.1.2 Natural killer cells

NK cells are members of the distinct hematopoietic lineage of innate lymphoid cells (ILCs). They represent a key component of the innate immune system and in humans are distinguished by the absence of CD3 and their density of CD56 and CD16 expression. In the circulation, most (90-95%) peripheral NK cells (pNKs) convey low CD56 (CD56dim) and high CD16, with only a small sub-population of CD56bright CD16- (~5%) evident. Distinct from other ILC subsets, CD56dim pNK cells are key drivers of the innate effector response, mediating potent cytotoxic effects, which are critical for immuno-surveillance, and anti-tumour and anti-microbial protection (239, 240).

The major mechanism that governs NK cell contact-dependent functions is the relative contribution of inhibitory and activating natural killer cell receptors (NKRrs) to cognate ligands. These permit recognition and selective targeting of MHC low/ absent cells, the so called 'missing self' hypothesis (241). NK cell activation is primarily achieved via engagement of NKRrs, including activatory

NKp46, CD16 and NKG2D. Inhibitory receptors, such as killer immunoglobulin-like receptors (KIRs) and NKG2A, counterbalance this response acting through MHC I. This is however an oversimplification of NK cell responsiveness, with the diversity and balance of activatory and inhibitory receptor expression crucial for mediating NK functions, which also include synergy, no enhancement, or additive effects (242). Furthermore, NK cells are activated via innate CKs including IL-2, IL-12, IL-15, and IFN- γ , leading to dramatically increased cytotoxic activity against target cells and abundant pro-inflammatory CK production (243). IL-12 appears particularly potent (244), however IL-2 and IL-15 also differentially activate endogenous NK cells influencing both their differentiation and cytotoxic function (245).

NK cells are critical mediators of human innate immunity. In humans a complete lack of NKs results in overwhelming fatal infection during childhood (246). Classically, NK cells target 'non-self' tumour and virally infected cells upon the basis of altered, foreign or absent MHC I expression without former priming or antigen specificity. This involves secretion of a range of CK and chemokines that influence the host's immune response, and/or kill certain infected or transformed cells via perforin/ granzyme or death receptors (247).

pNKs also have the capacity to shape adaptive immunity by regulating T cell responses. IFN- γ is considered pivotal to this process, mediating many direct and indirect cytotoxic effects, including T cell priming and pro-inflammatory Th1 differentiation from naive CD4 T cells, antigen presenting cell (APC) activation and maturation, and macrophage-mediated killing (248).

5.1.3 CD56 bright NK Cells

As outlined, in the peripheral circulation only a small sub-population of CD56bright CD16+ (~5%) is evident. The ontogeny of these subsets remains unresolved with several models proposed. Firstly, a common NK cell precursor, which differentiates to either CD56bright or CD56dim subsets, may exist. Alternatively, these subsets represent a distinct lineage that switches from one form to another as determined by their local microenvironment. A developmental model in which CD56bright CD16+ pNK subsets represent an early precursor of CD56dim cells has also gained much attention (249).

Attempts to drive CD56 bright differentiation towards a CD56dim phenotype have however been heterogenic thus the validity of this theory remains uncertain (250).

It appears CD56bright NKs represent a functionally distinct NK subset, which conveys unique and diverse roles comparative to their dim counterparts. Firstly, they are devoid of lytic granules and demonstrate significantly weakened ability to conjugate with target k562 cells, thereby rendering them poorly cytotoxic even with prolonged stimulation (250). They also demonstrate weaker CD16-mediated antibody-dependent cellular cytotoxicity. CD56bright NK cells are however superior with regards to CK secretion, including a range of pro-inflammatory and – regulatory CK such as IFN- γ , TNF- α and IL-10. Co-stimulation of CD56bright NKs with T cell–derived IL-2 and monocyte derived IL-12 significantly enhanced IFN- γ production, which via the activation of APCs may shape antigen-driven cytotoxic T-cell responses. It appears these cells differentially regulate immunological responses via CK-mediated signalling as opposed to their cytotoxic potential (251). This population also bears homing receptors such as CCR7 and CXCR3, representing the prominent NK cell subset in several major peripheral lymphoid organs (252).

5.1.4 Tissue resident NK cells

NK cells are characterised in a range of human tissues including spleen, liver, tonsil, and lymph nodes, with their relative distribution controlled by tissue chemokine receptor and adhesion molecule expression. Allocation of NK cells is however dynamic, with recirculation between different organ sites identified (253). Notably, NK cells at these sites are phenotypically distinct, reflecting their unique local micro-environments; within the spleen 85% of NK cells are CD56dim CD16+ and strongly express perforin, whereas in the lymph nodes a CD56bright CD16- phenotype is displayed (243). Consequently, tissue NK cells are functionally highly diverse, and are not restricted to classical pro-cytotoxic and anti-tumorigenic effects, influencing tissue inflammation and immune homeostasis, including immuno-regulation and -surveillance. This in part reflects how local CKs, chemokines and adjacent cells shape NK cell activity, for example within the tumour micro-environment Treg cells and monocytes suppress NK cell mediated tumour rejection whereas in lymph nodes CD4+ T cells stimulate NK cells cytotoxicity via IFN- γ release (243, 254).

Of particular interest are hepatic NK cells, which comprise 20-30% of the total resident lymphocyte population. Two major NK populations exist, CD56^{bright} and CD56^{dim}, which reside in equal proportions. The CD56^{dim} subsets express higher levels of perforin and granzyme comparative to pNKs, which likely reflects their frequent exposure to ‘foreign’ pathogenic antigens against which they induce potent cytotoxic effects. (255). The CD56^{bright} subset appears immature, hypo-responsive and pro-regulatory, acting to maintain immune balance via CK secretion and immune-cell cross talk. The hepatic microenvironment drives acquisition of this unique phenotype, as elegantly demonstrated by adoptive transfer studies of ‘cytotoxic’ splenic NK cells, which subsequently confer a similar regulatory phenotype (256, 257).

5.1.5 Uterine NK cells

Along with the human liver, the pregnant uterus is the peripheral organ containing the highest frequency of NK cells. Albeit present in the non-pregnant endometrium, NK cells are low in number and demonstrate cyclical fluctuations. In response to fertilization and implantation, a surge in uNKs is observed (258). From the early first trimester, uNKs become the predominant immune cell population within the decidua, representing between 50-60%. From the second half of pregnancy a relative reduction in uNK numbers is observed, indicating a greater role in early pregnancy (259).

Considering uNK cell origin, these appear highly disparate from their peripheral counterparts being predominantly CD56^{bright} CD16⁻ (>80%), with a unique repertoire of activatory and inhibitory receptors(238). Murine models suggest they are recruited from peripheral blood or bone marrow, with local uterine factors driving NK cell migration (260). Certainly both the fetal trophoblast and decidua stroma produce a range of pro-migratory chemokines, with pNK cell migration mediated via CXCR4- and CXCL12-dependent mechanisms (261). Local stromal cell interactions, CK and growth factors, such as IFN- γ , stromal cell-derived factor-1 and TGF- β may drive NK cell differentiation and education within the decidua microenvironment. There is however evidence to suggest some uNKs develop from early CD34⁺ hematopoietic precursors, as co-culturing uNKs with decidualised stroma causes CD34⁺ cells to differentiate into mature NK cells (262).

Historically, uNKs were considered a significant threat to the fetus (263). However, uNKs are now considered instrumental for successful pregnancy. In mice, placentae deficient of NK cells are hypotrophic and result in premature fetal death. Tg ϵ 26 females, which have <1% of normal uNK cell frequency, similarly demonstrate small placentae, absent implantation site-associated metrial glands, aberrant decidua vascular pathology and fetal loss rates >60%. Furthermore, this aberrant reproductive phenotype is reversed following bone marrow transplantation from scid/ scid (NK+ T-B-) mice (264, 265).

There is strong evidence to suggest uNKs are pro-regulatory with key roles in the two major processes required to establish successful pregnancy (266)

1. Invasion of EVT into the maternal decidua and inner myometrium (8-10w) (267)
2. Uterine spiral artery remodelling (10-12w) (268)

In brief, these processes arise from initial implantation, with successful uterine invasion crucial for blastocyst establishment within the endometrial wall. The trophoblast then invades the decidualised endometrium, migrating into the spiral arteries and here replacing maternal vascular endothelial cells. Trophoblast cells at the placental villi tips differentiate into specialised EVT which invade the decidua and inner myometrium. Extensive artery remodelling ensues (269), with the maternal decidual spiral arteries subsequently transformed to wide diameter, non-vasoactive vessels with the capacity to ensure the increasing demands of the fetus for nutrients, respiratory gases and metabolic waste removal are met.

Contradictory to previous suppositions the maternal decidua remains passive during this process, this is critical in the initiation and control of fetal trophoblast invasion. This involves complex interactions between immune cells, endothelial cells, and invading trophoblasts, with uNKs appearing key drivers of this (268). Histologically it is well recognised that uNKs aggregate around spiral arteries and glands (270). NK cell-deficient mice also display significant abnormalities in decidual artery remodelling and trophoblast invasion, which appears mediated via the secretion of an array of chemokines, growth factors and CK, including IFN- γ and TNF- α , which mediate angiogenesis, tissue

remodelling and trophoblast migration (267, 271, 272). This appears dependent upon the engagement of both NKp30 and NKp44 ligands which are expressed on stromal decidual cells and EVT (273, 274).

Local factors, including IL-15, IL-2 and IL-12, have gained particular interest with regards to mediating uNK cell function. IL-15, which is strongly expressed within the decidua from the first trimester, has gained particular interest (131) as histological examination of implantation sites from IL-15^{-/-} pregnant mice demonstrate no uNKs, no spiral-artery modification, and lack decidual integrity. Whilst indicating an important role for IL-15, it is not however critical since mice lacking IL-15 retain normal fetal viability and reproductive outcomes (272, 275). DCs appear a pivotal source of both IL-15 and IL-12, and their depletion is associated with decreased IL-15 and IL-12, and abnormal NK cell size and function. Adoptive transfer of DCs from WT mice is also shown to abrogate this effect (276).

Despite maintaining their cytotoxic machinery uNKs remain poorly cytotoxic and appear mediators of immune-tolerance at the materno-fetal interface. Albeit similar to pNK CD56dim cells in relation to their granular content, uNKs display reduced activation potential (129, 130). Recent genomic analysis by Koopman *et al* revealed that CD56bright pNK cells are more similar to CD56dim pNK cells than to their respective CD56 bright uNK counterparts. Importantly, uNKs also demonstrated enhanced immune-modulatory potential compared to both (277).

Considering the key mediators of uNK cell function, it appears that largely undefined local mechanisms including CK and hormone secretion, and cross-talk with other immune cell types are at play, which together suppresses the potential lytic effects of uNKs (121). uNKs are influenced by their differential activatory and inhibitory receptor profiles. Perhaps surprisingly, they in fact express increased levels of 'natural cytotoxicity' activatory receptors, including NKp30, NKp44, NKp46 and CD69, comparative to their peripheral counterparts. They do also however also express a unique, broad range of inhibitory receptors, including KIR2D and NKG2A (278). Cytotoxic control is likely mediated in part by the counterbalance of these two subsets, which interact with class I non-classical HLA subtypes (279).

Comparative to pNKs, uNKs demonstrate enhanced production of immunosuppressive CK including TGF- β and IL-10, and lower IFN- γ and TNF- α levels (280). They may also actively regulate fetal implantation and placentation via their local interactions with other decidual immune subsets. Some studies suggest uNKs may actively suppress Th17-mediated local inflammation via IFN- γ -dependent pathways (281). Whether uNKs initiate immune tolerance at the materno-fetal interface remains a subject of debate (237, 279). Their lack of cytotoxicity appears to favour their residence within the decidua, with a range of diverse and dichotomous functions influencing tissue inflammation, angiogenesis, and immune-regulation instead delineated.

5.1.6 NK cells in malplacentation

In humans, defective trophoblast invasion and vascular remodelling are the hallmark features of aberrant placentation. Failure of this process is associated with a range of serious ‘malplacentation disorders’, including miscarriage, PET, and SGA (282-284). Given the prominence and anticipated key roles of NK cells in healthy placentation, both pNK and uNKs have gained much research interest (285).

As outlined, murine KO models have provided important insights into NK cell biology within the context of placentation. Within the context of malplacentation, IFN- γ is considered a key mediator of uNK cell function in KO mice, as significant abnormalities in the decidual vasculature, similar to those observed in NK cell-deficient mice are observed (286). Furthermore, reconstitution of RAG-2^{-/-}/ γ C^{-/-} mice with bone marrow from IFN- γ ^{-/-} mice, restores normal uNK frequencies, but does not reverse the decidual abnormalities in the absence of IFN- γ . IFN- γ administration however reverses this decidual pathology, supporting a major role of IFN- γ in uterine vascular remodelling (286, 287). uNK cells have recently been reported as pivotal for fetal growth during early pregnancy, with adoptive transfer of induced CD49a⁺ Eomes⁺ NK subsets associated with reversal of aberrant fetal growth (288). Follow up validation studies are however clearly warranted.

Considering current human studies, which are extremely limited, pregnancies complicated by recurrent miscarriage or PET provide the basis of most available evidence. Within the context of recurrent miscarriage, attempts to predict women at risk of miscarriage based upon NK cell frequency

alone have proven highly heterogenic with NK cell function considered the more significant factor (289, 290). Considering pNKs, it is postulated the suppression of Th1 immunity towards fetal trophoblast may be lost within this context. In response to trophoblast antigens, PBMC from women with recurrent miscarriage released increased concentrations of pro-inflammatory CK, including IFN- γ and TNF- α , with a concomitant reduction in IL-10 (291).

Within the context of PET, a Th1 shift of NK cells is similarly reported, with an increased prevalence of pro-cytotoxic NK subsets comparative to normal pregnancy. This shift may account for the elevated levels of pro-inflammatory CK, including TNF- α , IL-6, IFN- γ , IL-15, IL-12 and IL-2, and lower IL-10. Correlation between these markers and PET severity may also be evident (292-294).

Within the context of PET, a major contribution was hallmark gene-linkage analysis, which revealed a significant link between fetal HLA-C and maternal KIR interaction combinations which induce potent uNK inhibition and PET. It appears appropriate NK cell activation is required to reduce the likelihood of PET. This was true even if the mother expressed a similar receptor profile, indicating that neither non-self nor missing-self discrimination was implicated in this process (295).

Progress delineating the exact aetiology of malplacentation with regards to uNK function has been hindered by the lack of accurate diagnostic tests available to identify women either pre-conception, or early in the first trimester at significant risk. Uterine artery resistance index (RI) has been utilised to some effect, with a raised RI a surrogate marker of impaired vascular remodelling. Comparative to pregnant women with a normal RI, there was no difference in uNK cell frequencies, whilst a significant reduction in uNK-mediated trophoblast motility and vascular apoptosis was measured (296, 297).

A recent systematic review and meta-analyses concluded however there remains insufficient evidence (n=12 studies) to ascertain whether high pNK or uNK percentages or activity predict subsequent miscarriage risk. Future studies are warranted to determine the role of NK cell assessment as a predictive test for screening at risk pregnant women (298).

5.1.7 Vitamin D and NK Cells

Considering the potential effects of vitamin D upon NK cell function, studies to date are relatively inconsistent and scarce. Certainly to our knowledge no studies specifically investigating the effects of 1,25(OH)₂D₃ upon uNKs have been performed.

Merino *et al* provide first the evidence that 1,25(OH)₂D₃ may modulate NK-like immune activity in the 1980's. The current belief was that serum calcium exerted important immune-regulatory effects upon both innate and adaptive immune cell subsets (299). It was subsequently found that 1,25(OH)₂D₃ inhibited CD16⁺ cytotoxic cell activity and that this related directly to hormone-mediated suppression of IL-2. Furthermore, IL-2 treatment reversed these effects. It was postulated that NK cells express a functional VDR with intrinsic immune-suppressive actions (299).

Not until 2013 was isolated pNK expression of the vitamin D metabolic system measured in a cohort of type 1 diabetics (300). pNK cells demonstrated differential expression of CYP2R1, VDR and CYP27B1, comparative to both Th1 and monocyte subsets. Unexpectedly, CYP27B1 expression was higher than monocytes but lower than Th1 cells. VDR expression was however lower than both. The reasons underlying these differences remain unclear and warrant further investigation (300).

The effects of 1,25(OH)₂D₃ upon mature and developing pNK function are highly inconsistent. Ravid *et al* found 1,25(OH)₂D₃ significantly increased pNK cytotoxic activity via upregulation of granzyme A, with no effect upon cell proliferation observed (301). Conversely, recent studies suggest an inhibitory role for 1,25(OH)₂D₃ upon pNK development, with preferential differentiation towards a monocytic cell lineage. Furthermore, a significant reduction in pNK cytotoxicity and IFN- γ release was measured (302). Similarly Ota *et al* demonstrated 1,25(OH)₂D₃ inhibited pNK cytotoxicity in a dose-dependent manner following IFN- γ and IL-2 activation (303).

As eluded to in Chapter 4, albeit the exact role of decidual 1,25(OH)₂D₃ in early pregnancy remains unclear, an important non-classical function may be anticipated (71, 304). Preliminary studies suggest certain decidual immune cells may be particularly important; following purification of non-adherent stromal cells and adherent cells (including macrophages and uNKs), adherent cells demonstrated the

greatest capacity for 1,25(OH)₂D₃ production (305). Consistent with this, Evans *et al* found decidual CD10⁻ cells (stromal cell negative) strongly express *CYP27B1*, and this closely correlates with key immune markers, including *TLR-4* and indoleamine-pyrrole 2,3-dioxygenase (*IDO*). Given their prominence within the CD10⁻ decidua cohort, uNKs may represent a major mediator of vitamin D derived immune effects, particularly in early gestation (306). Consistent with this, first trimester CD56⁺ cells treated with 1,25(OH)₂D₃ demonstrated decreased synthesis of several decidua CK including TNF- α and IL-6, and increased cathelicidin (306). We anticipate resident uNK represent a major source of 1,25(OH)₂D₃, acting in an autocrine/paracrine fashion to regulate both acquired and innate responses at the materno-fetal interface.

Considering the diverse roles undertaken by uNKs, alternative effects of vitamin D may be anticipated. 1,25(OH)₂D₃ may promote fetal-driven angiogenic effects, as EVT co-express *CYP27B1* and *VDR*, and demonstrate induction of *CYP24A1* and cathelicidin following 1,25(OH)₂D₃ treatment. Furthermore, culture with 1,25(OH)₂D₃ significantly enhanced EVT invasion, with a concomitant increase in pro-MMP2 and pro-MMP9 (304).

Outside of pregnancy, vitamin D is similarly shown to promote angiogenesis with enhanced endothelial tubule formation, pro MMP-2 activity and vascular endothelial growth factor (VEGF) reported (307). Preliminary findings by our group were not indicative of this since mRNA levels of *VEGF* and *platelet-derived growth factor (PLGF)* following culture with 1,25(OH)₂D₃ were not significantly altered (304). Conversely, within the context of cancer 1,25(OH)₂D₃ inhibits angiogenesis, with anti-proliferative and apoptotic effects mediated via *VDR* signalling reported (308). Since uNKs produce a diverse range of angiogenic factors more comprehensive studies delineating the effects of 1,25(OH)₂D₃ are warranted. Given the striking differences between uNK and pNK it is important to investigate and compare the effects of vitamin D upon both peripheral and uterine subsets.

5.2 Results

5.2.1 Distribution of decidua immune cells: comparative analysis with matched peripheral maternal blood – first trimester

Within the decidua a unique immune cell population resides in the first trimester, and notably this is highly disparate comparative to matched maternal PBMCs. Within the first trimester ‘normal’ decidua, CD45+ immune cells comprise approximately ~40% of the total live cell cohort, with the remaining tissue primarily of stromal origin (270). In preparation for these studies the relative proportion of the major innate and adaptive immune cell subsets was assessed in matched decidua and peripheral blood samples which were obtained from ‘low-risk’ pregnant women (n=5) in the first trimester (GA 6-11w), as summarised in Table 5.0.

Study ID	DOB	Ethnicity	GA (w)
DC191	23.05.73	Caribbean	6+0
DC192	01.09.79	Indian	8+3
DC193	18.01.83	Czech Republic	10+2
DC194	28.04.90	White British	11+0
DC195	17.11.82	White British	10+5

Table 5.0 Demographic summary of first trimester participants (n=5). The study identification (study ID), date of birth (DOB), ethnicity and gestational age at collection (GA) (weeks; w) is shown.

An example gating strategy is illustrated in Figure 5.0, with decidua and maternal frequencies summarised in Figure 5.1 for APCs (CD3-CD20-CD56-CD14+), NKs (CD3-CD56+NKp46+), natural killer T cells (NKT) (CD3+CD56+), CD4+ T cells (CD3+CD4+), CD8+ T cells (CD3+CD8+) and CD20+ B cells (CD3-CD56-CD14-CD20+), all of which were CD45+.

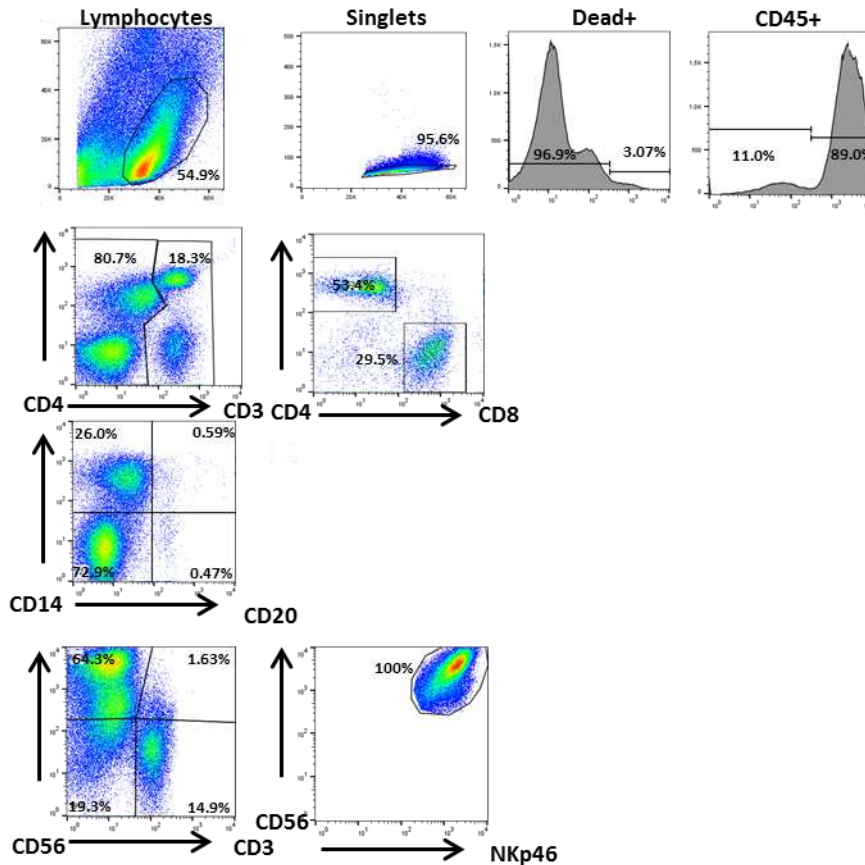


Figure 5.0 Summary of the gating strategy utilised to assess both decidua-derived and circulating maternal live CD45+ lymphocyte subsets. Example flow cytometry plots for decidua-derived whole polymononuclear blood cells, with the gating strategy for measurement of the relative frequencies of CD45+ NK cells (CD3-CD56+NKp46+), CD4+ T cells (CD3+CD4+), CD8+ T cells (CD3+CD8+) and CD20+ B cells (CD3-CD56-CD14-CD20+) subsets shown.

In the decidua, of the CD45+ immune cell cohort CD56+ NKp46+ NKs were predominant in the first trimester, representing $58.8\% \pm$ standard deviation (SD) 10.4 with APCs representing $16.2\% \pm 3.7$. In this cohort $10.0\% \pm 5.1$ were T cells, with $5.7\% \pm 2.7$ CD4+ and 3.1% CD8+ cells.

In the maternal peripheral blood conversely, only $7.5\% \pm 2.5$ of CD45+ cells were CD56+NKp46+ NKs, and $11.1\% \pm 5.8$ CD14+ APCs. Instead, CD3+ T cells were predominant representing $67.2\% \pm 10.6$ of CD45+ cells. Here CD4+ cells were highly predominant ($51.7\% \pm 11.5$), with CD8+ cells representing only $16.1\% \pm 5.6$ of the total immune cell population. Notably, a high preponderance of NKT cells ($5.6\% \pm 3.1$) is present in the maternal blood comparative to the decidua ($1.3\% \pm 3.7$). In

both decidua and maternal blood, CD20+ B cell frequencies were low representing 3.1% ±1.5 and 1.6% ±1.0 respectively.

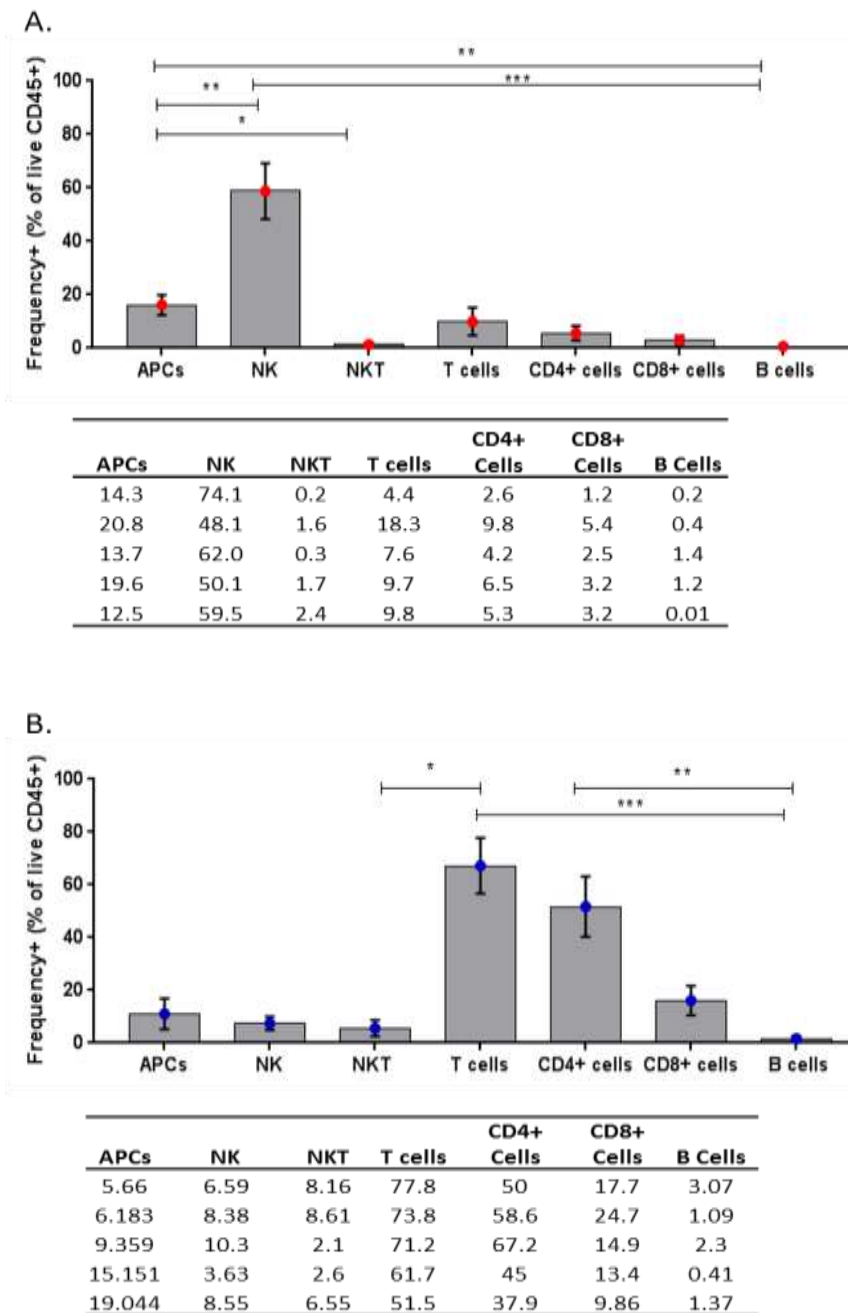


Figure 5.1 Characterisation of first trimester immune cells subsets. Comparative analysis of paired decidua (A; red) and maternal (B; blue) CD45+ immune cell subsets, using flow cytometry. Relative frequencies (%) are summarised in their respective bar chart and table (n=5), including antigen presenting cells (APCs), natural killer cells (NK), natural killer T (NKT) cells, T cells, CD4+ T cells, CD8+ T cells and B cells.

In relation to their surface activation marker expression, consistent with previous reports, NKs in the decidua were consistently CD56 NKp46 bright > 95% (n=5), as opposed to CD56 and NKp46 dim. Conversely, in the periphery, CD56+ NKs were predominantly CD56+ NKp46 dim (92.8%), with only 7.2% CD56 NKp46 bright(277). However, similar to pNKs, uNKs appear highly granular cells with clear cytotoxic potential as characterised by their positive perforin and granzyme B expression. Consistent with previous reports, uNKs exhibited similar median NK perforin and granzyme B expression to their peripheral counterparts, as summarised in Figure 5.2 and Table 5.1.

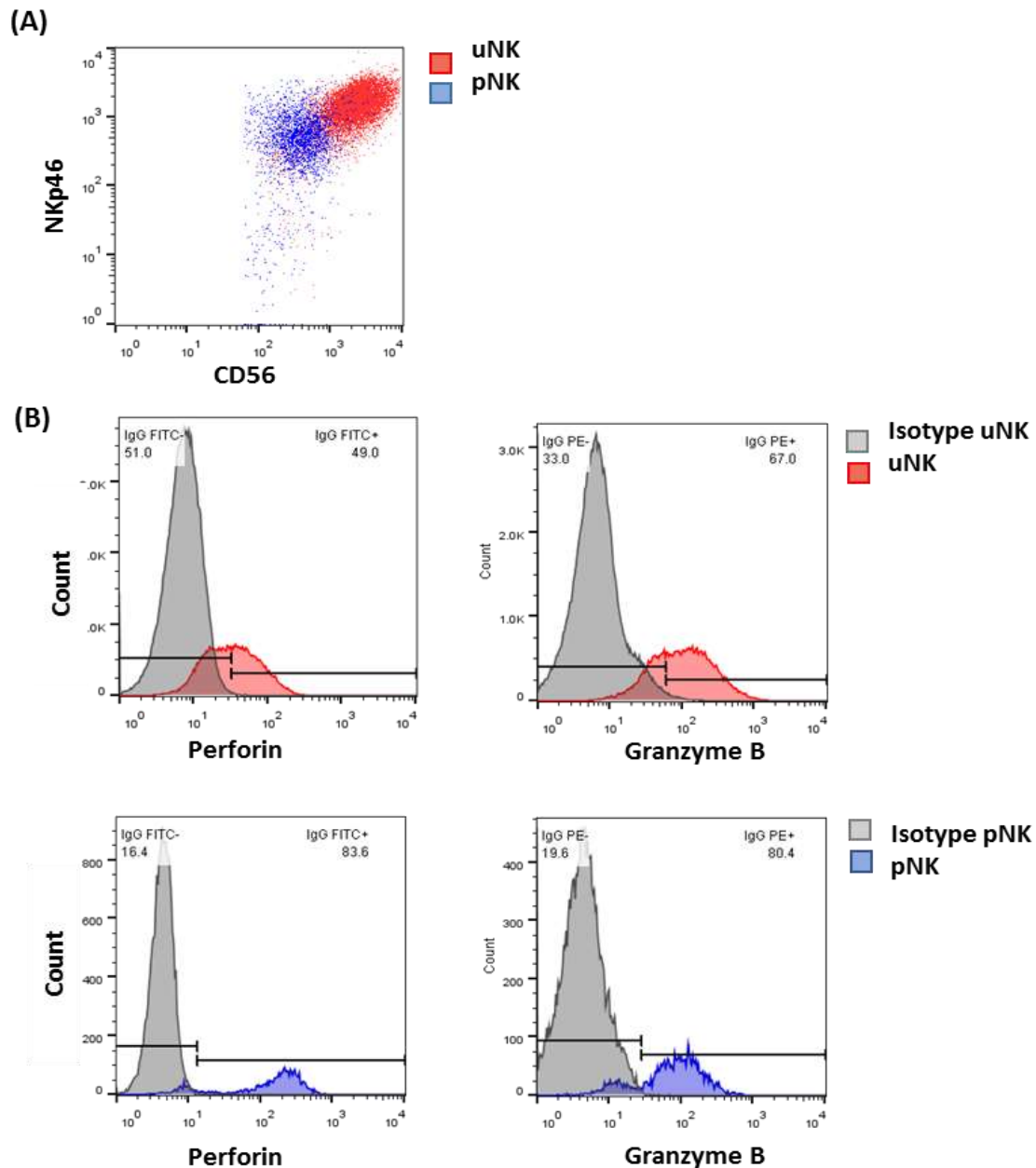


Figure 5.2 Phenotypical characterisation of paired first trimester uNK and pNK subsets. (A) Using flow cytometry, extracellular NKp46 and CD56 expression were measured in live CD45+CD3- uNK and pNK cells obtained from matched decidua and maternal peripheral blood mononuclear cells, as illustrated in the scatter plot. (B) Using FACS, relative intracellular expression of perforin and granzyme B was measured in live CD45+CD56+CD3- uNK and pNK cells. The off-set histograms illustrate perforin and granzyme B expression relative to their matched isotype control. The bars define positive and negative surface marker expression.

	uNK Freq+ (median; IQR)	pNK Freq+ (median; IQR)
Perforin	43.2; 0.7-60.6	57.7; 45.1-63.1
Granzyme B	66.0; 61.2-93.6	60.1; 44.2-77.8

Table 5.1 Relative intracellular protein expression of perforin and granzyme B in paired uNK and pNK subsets. The frequency of positive perforin and granzyme B intracellular expression for paired first trimester uNK and pNK is summarised as median and interquartile range (IQR) (n=4).

An important observation was the significant difference in uNK cell morphology and scatter comparative to their pNK counterparts. This became more marked following NK cell culture and exposure to the assays. Notably, the relative proportions of ‘dead’ uNKs also increased, as did their heterogeneity in cell structure and size.

5.2.2 Optimisation of NK cell activation assay

Prior to establishing any potential functional effects of 1,25(OH)₂D₃ upon uNK cytotoxic potential it was necessary to establish a reliable NK cell activation protocol. For this purpose, isolated CD3-CD56+ pNKs from non-pregnant healthy female controls were utilised to measure the individual and combined effects of recognised NK cell activating CK (IL-2, IL-15, IL-12 and TNF- α) (Table 5.2) in the presence or absence of a k562 cell line (309). Activation was measured according to surface expression of recognised NK activation marker CD107 and production of IFN- γ and TNF- α at a series of 24 and 48h time-points.

As summarised in Table 5.2, compared to unstimulated (US) pNKs single CK treatments (IL-12, IL-2, IL-15 or TNF- α) or co-culture with k562 cells failed to significantly activate TNF- α and IFN- γ release. Conversely, co-treatment with IL-12, IL-15 and IL-2 significantly enhanced CD107, IFN- γ , and TNF- α expression at both the 24h and 48h time-points.

Treatment	24h				48h			
	Freq + of pNKs (%)			Freq total cells (%)	Freq+ of pNK (%)			Freq total cells (%)
	CD107	IFN- γ	TNF- α	Viability	CD107	IFN- γ	TNF- α	Viability
US	9.3	5.7	1.4	88.1	1.8	0.1	0.1	70.1
IL-2	14.6	30.4	2.1	91.3	8.0	0.4	1.4	91.8
IL-12	30.1	44.8	1.8	91.5	5.8	0.8	0.5	90.0
IL-15	15.4	35.8	2.1	89.4	38.6	7.2	3.7	79.7
K562	18.4	11.4	3.3	77.9	5.4	0.3	2.0	60.7
TNF- α	30.5	4.2	7.0	86.5	8.5	0.1	2.3	89.3
PMA & ionomycin	56.8	98.1	65.9	80.5	19.3	27.7	25.7	73.4
IL-2 IL-12 IL-15	43.9	97.2	12.3	86.3	71.8	85.9	36.7	29.0
k526 IL-2 IL-12 IL-15	67.0	99.1	27.2	79.4	81.1	98.3	39.8	28.5

Table 5.2 Summary of time-point analysis of pNK cell activation. The percentage (%) frequency (freq) of CD107, IFN- γ , TNF- α expression and viability (% of live total cells) following 24 and 48 hour (h) culture with either no treatment (US) or treatment with a range of activation agent regimes (IL-2, IL-12, IL-15, k562, TNF- α , and/ or phorbol 12- myristate 13-acetate [PMA] & ionomycin) is summarised.

With increasing culture time a marked decrease in cell viability was evident with both co-treatment regimes. Although phorbol 12- myristate 13-acetate (PMA) and ionomycin, which are recognised NK cell activators(310), demonstrated high pNK activation at 24h and preserved NK viability at both time-points, CD107 and CK expression were markedly reduced by 48h. Whether this reflects earlier NK cell activation, with tailed NK responsivity by 48h is not clear. Based upon these findings, co-treatment with IL-2, IL-12, and IL-15 was selected for subsequent assays.

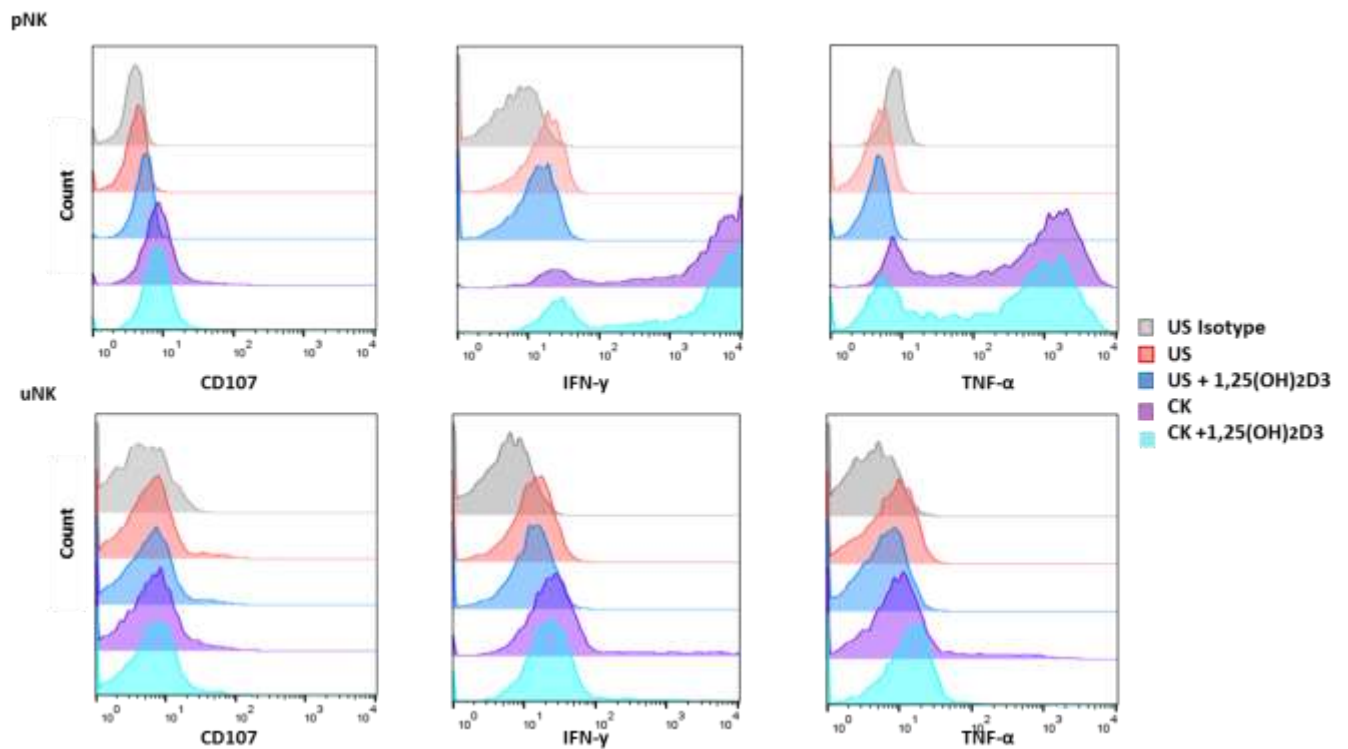


Figure 5.3 Flow cytometric analysis of the effects of 1,25(OH)₂D₃ upon isolated uNK and pNK cell CK release (IFN- γ , TNF- α) and cytotoxic potential, as characterised by CD107 expression.

Expression was measured following 24 hour (h) in one of four treatment conditions prior to analysis; (i) non-stimulated (US), (ii) non-stimulated in the presence of 1,25(OH)₂D₃ (US + 1,25(OH)₂D₃), (iii) CK stimulated (IL-2, 1L-15, IL-12), (iv) CK stimulated in the presence of vitamin D (IL-2, 1L-15, IL-12 + 1,25(OH)₂D₃). The off-set histograms illustrate CD3-CD56⁺ pNK and uNKs CD107, IFN- γ and TNF- α release.

Having optimised NK cell activation using pNK subsets alone, comparative analysis of paired uNK and pNK CK release and CD107 activation status was assessed. As summarised in Figure 5.4 and Table 5.3, in response to pNK stimulation, IFN- γ , and CD107 expression markedly increased comparative to their unstimulated counterparts. Although the proportion of IFN- γ , and CD107 positive cells increased in the uNK subsets in response to CK stimulation, this was suppressed relative to those from the periphery. Interestingly, TNF- α expression was low in both populations in response to CK stimulation.

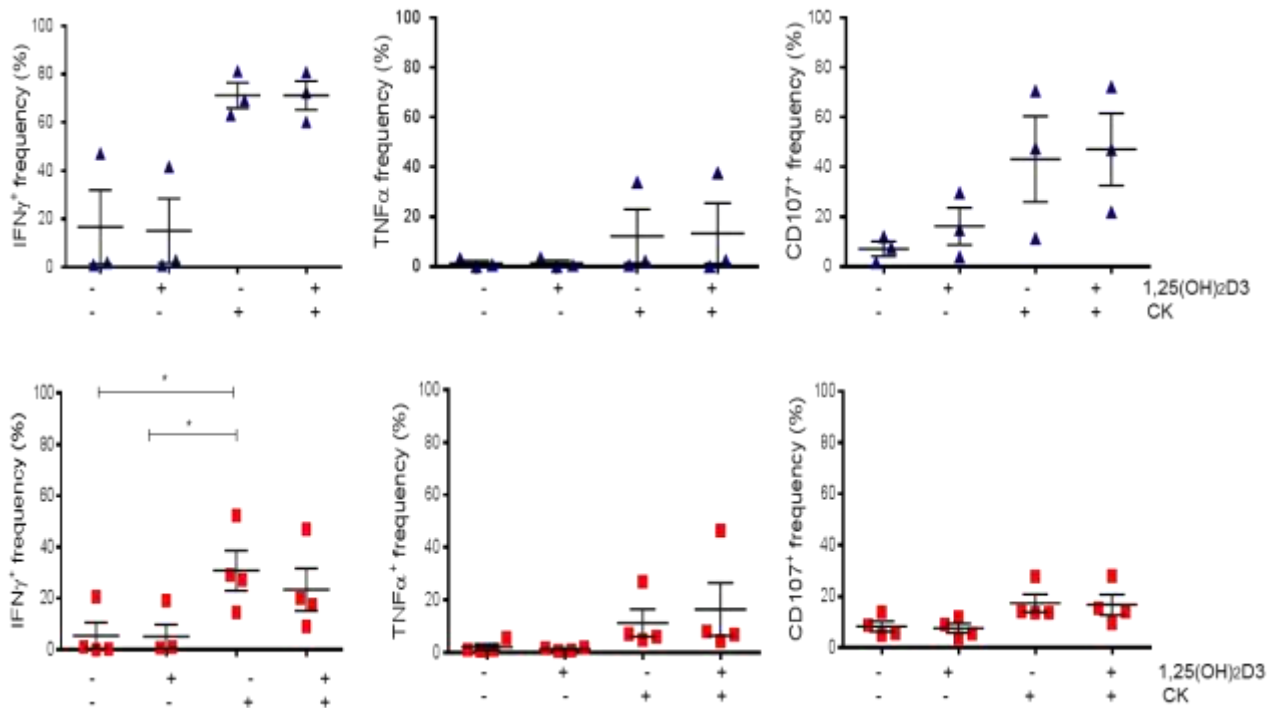


Figure 5.4 Summary of flow cytometry analysis of the effects of 1,25(OH) $_2$ D3 upon isolated pNK (blue) and uNK cell (red) CK release (IFN- γ , TNF- α) and cytotoxic potential, as characterised by CD107 expression. Expression was measured following 24 hours (h) in one of four conditions prior to analysis; (i) non-stimulated (-, -), (ii) non-stimulated in the presence of 1,25(OH) $_2$ D3 (+/-), (iii) CK stimulated (IL-2,1L-15, IL-12) (-,+), (iv) CK stimulated in the presence of vitamin D (IL-2,1L-15, IL-12 + 1,25(OH) $_2$ D3) (+,+). Mean values with standard error of the mean is illustrated, non-parametric analysis of effect of CK stimulation and 1,25(OH) $_2$ D3 were measured. Stars indicate significance level (* p<0.05).

Median Frequency positive (%) (IQR)				
	pNK US	pNK CK	uNK US	uNK CK
IFN- γ	2.0 (0.9-47.2)	69.3 (63.2-81.3)	0.76 (0.2-15.8)	28.3 (17.8-46.6)
TNF- α	0.7 (0-3.2)	2.2 (0.5-33.9)	1.0 (0.7-4.4)	6.5 (5.1-22.0)
CD107	7.6 (1.7-12.1)	47.6 (11.4-70.6)	7.2 (5.2-12.7)	14.0 (13.7-24.5)

Table 5.3 IFN- γ , TNF- α and CD107 intracellular expression in isolated uNK and pNK cells.

Median frequency of positive IFN- γ , TNF- α and CD107 in paired isolated uNK and pNK subsets following 24 h culture in the presence and absence (US) of CK (IL-2, IL-12, IL-15) stimulation (n=1). The % and IQR are illustrated.

5.2.3 Analysis of the vitamin D metabolic system in NK subsets by qRT-PCR

To ascertain whether both isolated uNK and pNKs express the metabolic apparatus required to mediate local 1,25(OH)₂D₃ production and function, qRT-PCR was performed to assess *CYP27B1*, *CYP24A1* and *VDR* transcript expression (Figure 5.5). Relative expression to US uNKs for each transcript was calculated to permit comparative analysis. The purity of the matched NK subsets was assessed, as summarised in Table 5.4, for uNKs (80.6–98.1%) and pNKs (58.2–90.3%). The lower purity obtained for the pNKs reflects both the increased relative frequencies in peripheral blood, and NKT cell preponderance. This may reflect the wide IQR bars evident in the pNK transcript data in Figure 5.6.

uNK (%)	pNK (%)
80.6	90
98.1	90.3
97.3	87.1
96.2	58.2
97.7	61
97.7	-

Table 5.4 Purity analysis of CD56+ subset isolation of maternal and decidua subsets. Percentage frequencies (%) are reported as the proportion of live CD45+ CD56+ NKp46+ (CD3- CD14-, CD19-) cells isolated.

Consistent with the surface protein data uNKs, median *VDR* transcript expression increased 4.95 fold (IQR 4.32-5.75 IQR; $p = 0.0001$) in response to CK activation. pNK *VDR* expression also increased 2.20 fold (1.20-5.2.31; $p = 0.017$) relative to US uNK subsets following CK activation, albeit this is significantly less comparative to their decidua counterparts ($p=0.02$). Importantly, 1,25(OH)₂D3 significantly suppressed *VDR* upregulation in both subsets, thereby indicating a negative feedback system exists to regulate 1,25(OH)₂D3- mediated activity via VDR (Figure 5.5).

Expression of *CYP27B1*, the principal catalyst for 1,25(OH)₂D3, concomitantly increased alongside *VDR* mRNA in response to CK stimulation in the uNKs (2.72 fold change; 2.33-3.18). A similar response was measured in the pNKs (2.93; 0.86-5.40), albeit this was non-significant, reflecting wider heterogeneity in their responsivity. No significant effect of 1,25(OH)₂D3 upon *CYP27B1* expression was measured in either NK subset, suggesting 1 α -hydroxylase activity is not driven by vitamin D status.

By contrast, 1,25(OH)₂D3 strongly induced expression of the catabolic *CYP24A1* enzyme in US uNKs (73.0; 30.7-197)($p = 0.020$). Interestingly, a greater response was evident in pNKs, with a 157.0 fold (92.9-1706) induction of *CYP24A1* in US pNKs exposed to 1,25(OH)₂D3. In the co-presence of CK this was partially suppressed in both subsets, uNKs (29.3; 12.1-72.6) and pNKs (10.1; 5.4-110.1).

Together these findings suggest that in response to CK challenge, NK cells drive 1,25(OH)₂D₃ synthesis and function via 1 α -hydroxylase, whilst restricting alternative catabolism.

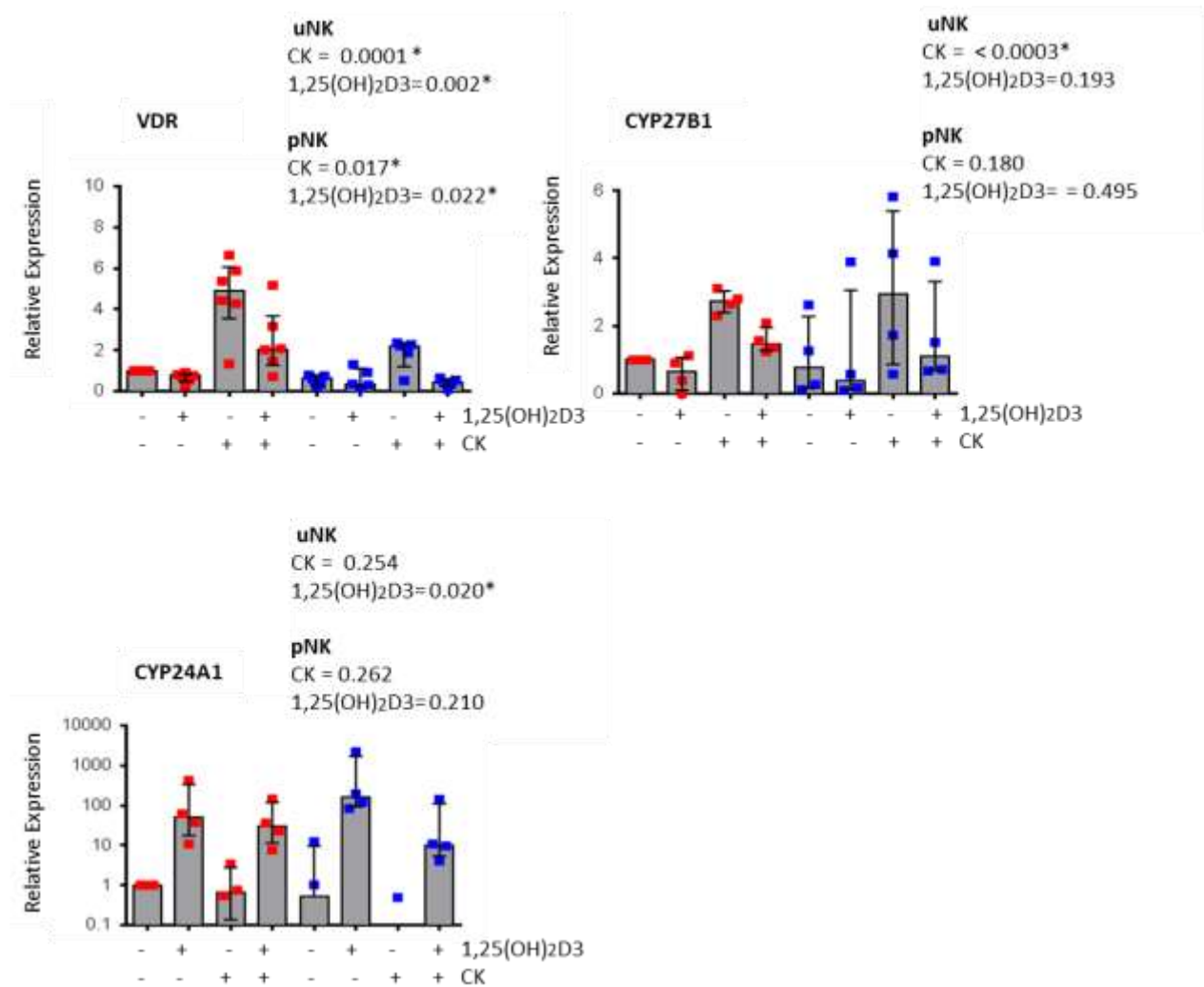


Figure 5.5 Transcript analysis of the vitamin D metabolic system in uNK and pNK. Transcript expression of *VDR*, *CYP27B1* and *CYP24A1* was measured in isolated unstimulated (-) and cytokine stimulated (CK) (+) CD3-CD56+ uNK (red) and pNK (blue) subsets in the presence (+) and absence (-) of 1,25(OH)₂D₃. Relative expression comparative to US uNK subsets is shown. Bars denote median values, with IQR intervals. Two-way ANOVA analysis was performed to assess the effect of CK stimulation and 1,25(OH)₂D₃.

5.2.4 Intracellular VDR expression in uNK and pNKs

FACS was utilised to assess intracellular VDR expression in isolated uNK and pNKs following 24h culture in the presence and absence of CK stimulation and 1,25(OH)₂D₃ (10nM). CD69 surface expression was co-assessed, as a recognised marker of NK cell activation (311). Live lymphocyte cells were selected and gated for CD3-CD56⁺ with CD69 and VDR frequency positive cells (freq⁺) measured for both NK subsets.

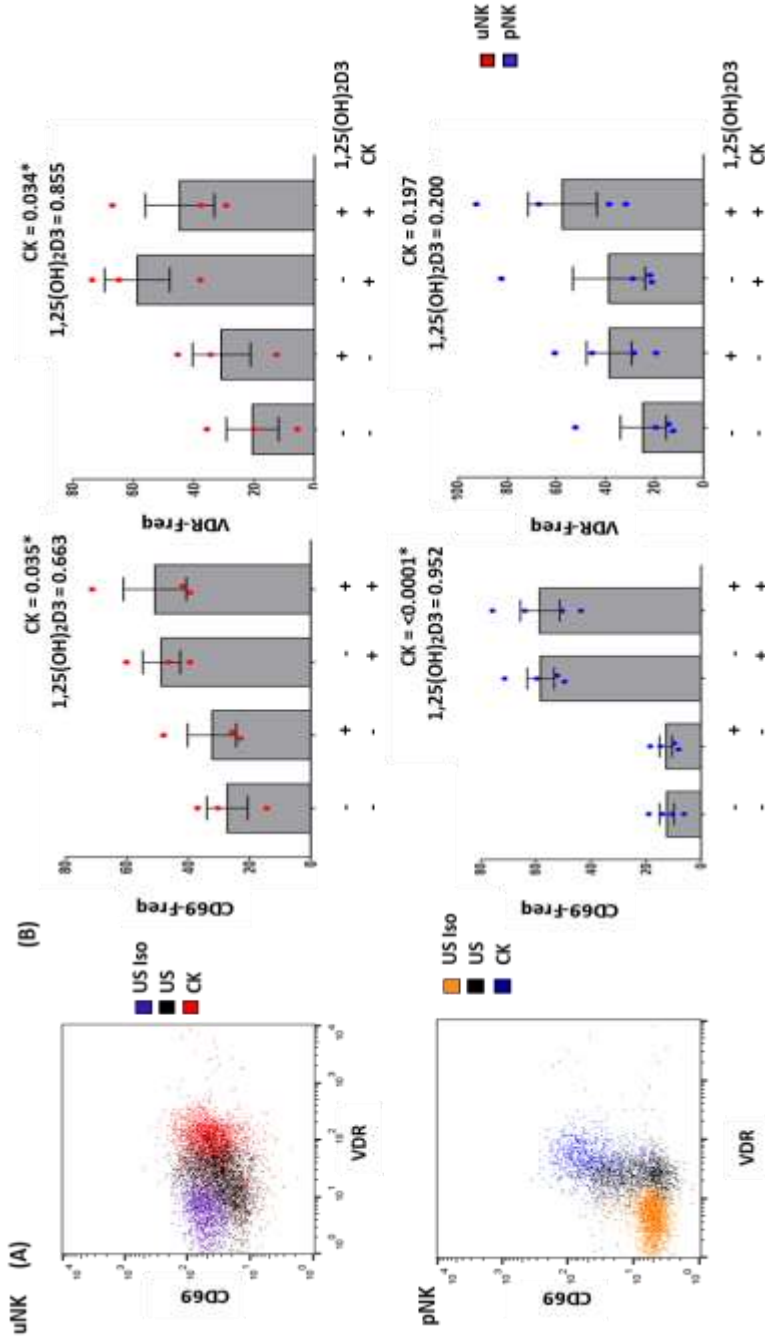


Figure 5.6 Summary of uNK and pNK VDR and CD69 expression. (A) Representative flow cytometry plots of VDR and CD69 surface expression in isolated unstimulated (US; black) and cytokine stimulated (CK) CD3-CD56+ uNK (red) and pNK (blue) subsets relative to its respective US isotype control (US Iso; blue uNK, orange pNK). (B) Summary of the frequency (%) of VDR and CD69 surface protein expression (n=3-4) in US and CK uNK (red) and pNK (blue) subsets in the presence and absence of 1,25(OH)₂D₃. The interval bars represent the mean with standard error of the mean interval.

As summarised in Figure 5.6, CD69 activation marker expression was found to be low in US uNKs (median frequency 30.5; 14.5-37.1) and matched pNKs (12.4; 7.4-17.9). The uNKs appeared less responsive to immune activation, as although both subsets significantly upregulated CD69 surface expression, this was enhanced in pNKs ($p < 0.0001$) relative to the uNKs ($p = 0.04$). Co-treatment with

1,25(OH)₂D₃ had no significant effect upon CD69 expression in either the US or CK treated uNK or pNK subsets (Figure 5.6).

Consistent with the qRT-PCR data, intracellular VDR expression was low in both US uNKs (20.2; 5.8-35.7) and pNKs (16.9; 13-44.1) at baseline. In response to CK, uNKs significantly upregulated VDR (64.8; 37.9-73.7) ($p=0.03$), whilst no similar response observed in those from the periphery despite significant *VDR* up-regulation at a transcript level. This differential CK-responsivity suggests that within the decidua NK VDR expression is more readily upregulated within the context of CK stimuli. Since 1,25(OH)₂D₃ had no significant effect on VDR protein expression in either the uNK or pNK subsets in the presence or absence of CK stimulation, it appears negative feedback occurs at a transcript level.

5.2.5 uNK and pNKs convert inactive 25(OH)D₃ to active 1,25(OH)₂D₃

Having demonstrated both uNKs and pNKs express the major components of the vitamin D metabolic system, a 25(OH)D₃ conversion assay was performed using LC MS-MS quantification. The objectives of this was to ascertain whether uNK and pNKs demonstrate the capacity to convert 25(OH)D₃ to 1,25(OH)₂D₃, and how this compares between these distinct sites. Alongside this, 24,25(OH)₂D₃ was also measured as this is the main measure of vitamin D catabolism.

As summarised in Figure 5.7, within 24h both uNK and pNKs converted 25(OH)D₃ (100 nM) to 1,25(OH)₂D₃ (pg/mL) ($n=3$). Consistent with the transcript and protein data presented, total 1,25(OH)₂D₃ activity was enhanced in response to CK challenge following co-culture with 25(OH)D₃. 24,25(OH)₂D₃ production was also measured in both NK subsets culture supernatants, and similarly increased following CK co-culture. Interestingly, 1,25(OH)₂D₃ production appeared slightly higher in matched CK + 25(OH)D₃ pNKs (0.18; 0.16-0.47 pg/mL) comparative to uNKs (0.13; 0-0.22 pg/mL). No clear difference in 24,25(OH)₂D₃ concentrations was evident in the uNK (1.7; 1.3-2.7 pg/mL) and pNKs (1.2; 1.1-2.6 pg/mL) respectively (Figure 5.7).

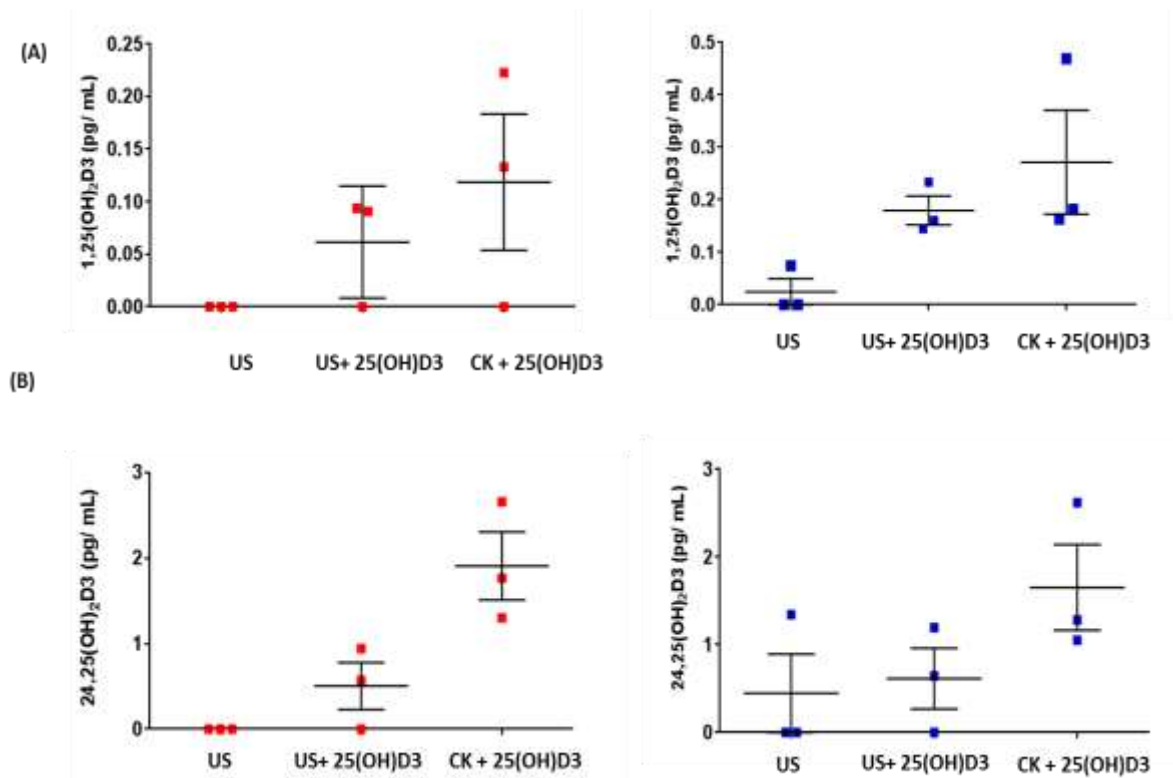


Figure 5.7 uNK and pNKs convert inactive 25(OH)D₃ to active 1,25(OH)₂D₃. Isolated matched uNK (red) and pNKs (blue) were cultured for 24h in the presence and absence (unstimulated; US) cytokine (CK) stimulation and inactive 25(OH)D₃ (100nM) and. LC MS-MS was used to measure supernatant concentrations of (A) 1,25(OH)₂D₃ (pg/mL) and (B) 24,25(OH)₂D₃ (pg/mL). The horizontal bars denote mean, with SEM interval.

5.2.6 Effects of vitamin D upon uNK and pNK IFN- γ transcript expression

Following establishment of a functional vitamin D metabolic system, the potential functional effects of 1,25(OH)₂D₃ were investigated. Since both the data here, and previous peer-reviewed data regarding immune cell function support a greater potential functional role for 1,25(OH)₂D₃ within the inflammatory setting, this was concomitantly assessed (56, 312).

Of particular interest was the effect upon IFN- γ , a key mediator by which pNKs induce cell lysis, and exhibit cytotoxic function. Within the decidua a unique role for IFN- γ is evident, with a crucial role in the initiation of uterine vascular modification and the maintenance of decidual integrity(287).

Furthermore, within the context of vitamin D, both pro-modulatory and pro-anti-microbial effects via IFN- γ are reported.

As summarised in Figure 5.8, IFN- γ production was assessed at a transcript and protein level in both uNK and pNK subsets. 1,25(OH)₂D₃ treatment alone had no significant effect upon *IFN- γ* mRNA or protein expression in either subset as illustrated. However, *IFN- γ* expression was significantly higher in CK pNKs comparative to CK uNKs at both a transcript (p=0.03) and protein (p=0.01) level. Uniquely, co-culture of uNKs with CK and 1,25(OH)₂D₃ significantly suppressed *IFN- γ* production at both an mRNA (p<0.01) and protein (p<0.001) level in the uNKs, whilst no similar responsivity was evident in matched pNKs either at a transcript (p=0.88) or protein (p=0.69) level. Together these findings suggest uNKs demonstrate differential responsivity to low-dose 1,25(OH)₂D₃, and within the decidua 1,25(OH)₂D₃ promotes IFN- γ suppression. Interestingly, no similar effect was measured.

(A)

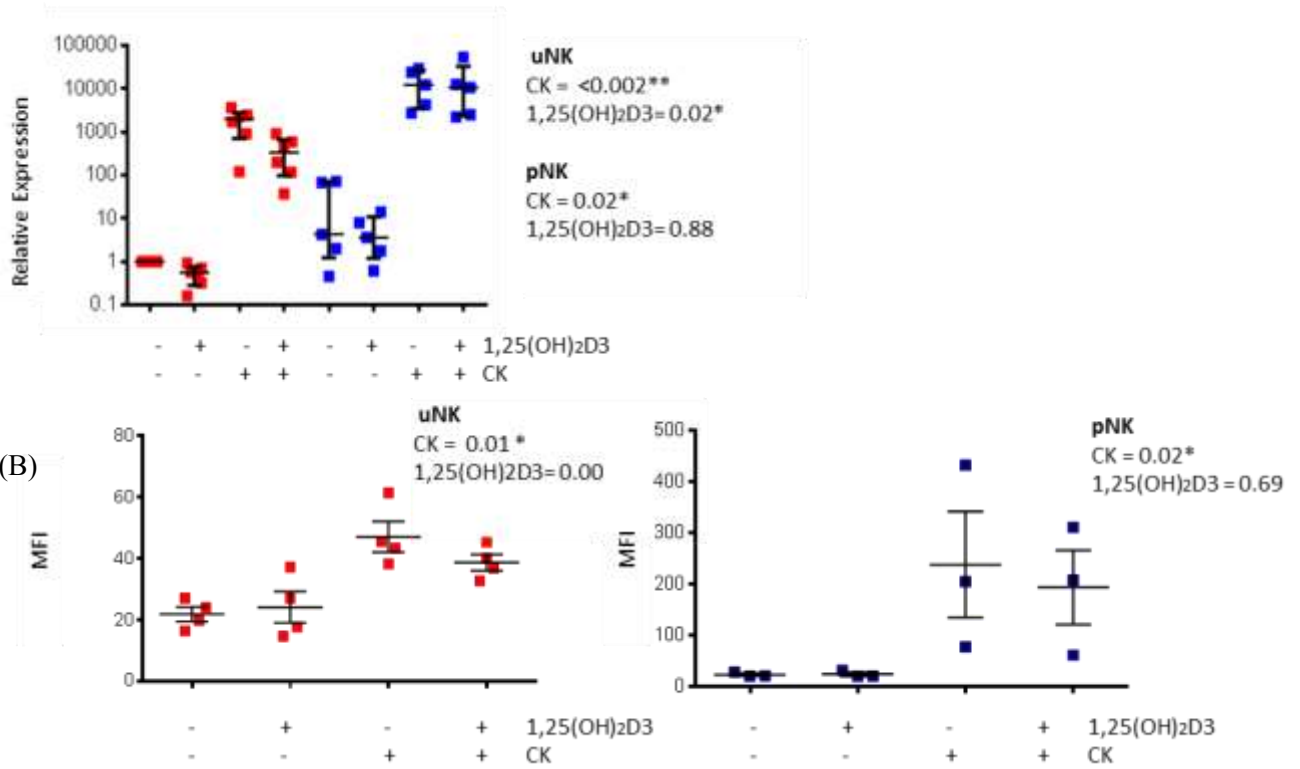


Figure 5.8 Transcript and intracellular protein expression analysis of IFN- γ

(A) IFN- γ transcript expression in isolated unstimulated (-) and cytokine stimulated (CK) (+) CD3-CD56+ uNK (red) and pNK (blue) subsets in the presence (+) and absence of 1,25(OH)₂D3 (-). Relative expression comparative to US uNK subsets; median values with bars denoting IQR, two-way ANOVA analysis of effect of CK stimulation and 1,25(OH)₂D3.

(B) Intracellular IFN- γ protein analysis using FACS in unstimulated (-) and CK (+) stimulated CD3-CD56+ uNK (red) and pNK (blue) subsets in the presence (+) and absence of 1,25(OH)₂D3 (-). The scatter plots illustrate median fluorescence intensity IFN- γ expression. Mean with SEM are shown. Two-way ANOVA analysis of effect of CK stimulation and 1,25(OH)₂D3

5.2.7 RNA sequence analysis purity analysis

To elucidate the impact of 1,25(OH)₂D3 upon NKs at a transcript level we conducted a genome-wide RNA sequence (RNA-seq) analysis of matched first trimester uNK and pNKs. Since both the data here, and previous peer-reviewed data regarding immune cell function support a greater potential

functional role for 1,25(OH)₂D₃ within the inflammatory setting, these studies were performed in the presence of CK stimulation (56, 312).

In total, n=4 participants were included, with matched FACS sorted uNK and pNKs cultured with CK in the presence and absence of 1,25(OH)₂D₃ for 24 h (total n=16 samples for RNA-seq) assessed. FACS sorting was utilised to ascertain NK cell purity, with matched live CD45+ CD3- CD14- CD56+ NKp46+ cells isolated (n=4) with ≥ 96% purity for pNK (range; 99.0-99.2%) and uNKs (96.0-98.7%) respectively (Table 5.6). Participant demographics (n=4) are summarised in Table 5.5, with all women undergoing elective sTOP at <12w gestation (range 7-11+2 w).

ID	Age	BMI	Ethnicity	Gestation	Smoking	G/P	Living	Stillbirth	Miscarriage	TOP
				(w)	status					
			White							
40	33	29.4	British	7+4	N	G5P3+1	2	0	1	0
			Black							
41	33	24.5	Caribbean	11+2	N	G1P0	0	0	0	0
			White							
43	19	22.3	British	9+4	N	G1P0	0	0	0	0
42	35	22.7	Pakistani	7	Y - 6/d	G4P3	3	0	0	0

Table 5.5 Summary of donor demographic analysis. Data show: Identification number (ID), maternal age, body mass index (BMI), ethnicity, gestational age at surgical termination of pregnancy (sTOP) (w; weeks), smoking status (yes [Y] / no [N] - total / day [d]), gravida and parity (G/P) with obstetric history; living, stillbirth, miscarriage, TOP.

ID	Maternal pNK (%)	Decidua uNK (%)
40	99.1	96.0
41	99.0	98.7
42	99.2	98.5
43	99.0	98.3

Table 5.6 uNK and pNK purity analysis. Summary of NK cell purity for n=4 matched pNK and uNKs used for RNA sequence analysis following FACS. Purity is classified as total fraction (%) of live cells which were CD45+ CD3- CD14- CD56+ NKp46+.

5.2.8 Principal component analysis

Principal components analysis (PCA) is an exploratory technique used to describe the structure of high dimensional data by reducing its dimensionality. Specifically, PCA identifies gene-expression patterns (principal components) that best explain the measured variance across a data set, as performed to the log₂ fold change on the whole dataset(313). Here, wide variance in the transcriptional patterns of purified uNK and pNKs, PC1 29.9%, PC2 11.9%, PC3 9.3%, in relation to NK cell origin was measured, i.e. peripheral blood and decidua. Intra-participant variability for pNKs was high, whereas the uNKs demonstrated low variability comparatively despite CK activation. In both subsets, co-treatment with 1,25(OH)₂D₃ was responsible for low variance in their transcript profiles (Figure 5.9)

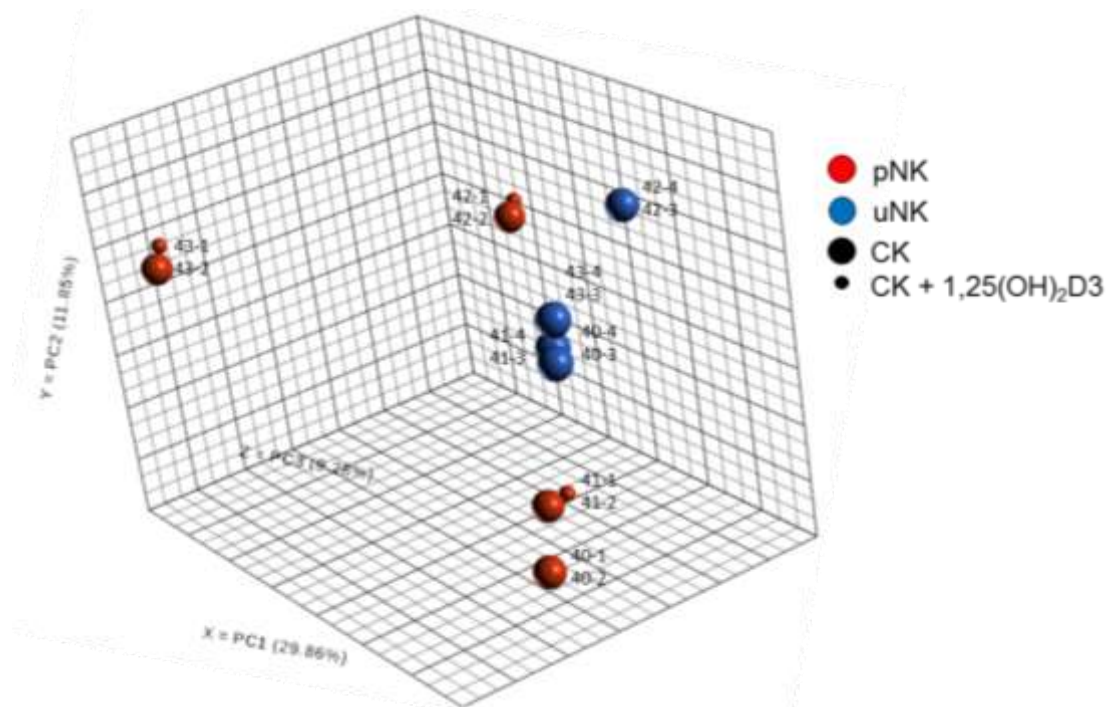


Figure 5.9 Principal component analysis (PCA) analysis of cytokine (CK) stimulated uNK and pNKs in the presence and absence of 1,25(OH)₂D₃. A 3-dimensional dot-plot to summarise the main sources of variance across the whole data set using principal components (PC) is illustrated; PC1 29.9%, PC2 11.9%, PC3 9.3% (x- y- and z-axes). This includes pNKs (red), uNK (blue) in the presence (small dot) and absence (large dot) of 1,25(OH)₂D₃ co-treatment. Numbers (i.e. 40-, 41, 42-, 43- #) denote study identification (ID) number as per Table 3.4.

5.2.9 Comparative analysis of CK treated uNK and pNK

Prior to treatment with 1,25(OH)₂D₃, 2286 transcripts were identified as differentially expressed between uNK CK and pNK CK, with 1188 transcripts downregulated, and 1098 transcripts upregulated in uNK CK (cut-off p value ≤ 0.05; fold change > 1.5) (Figure 5.10). Importantly this included significant upregulation of CD56 (NCAM1) (fold-change = 5.29, p= 0.00002) and downregulation of CD16A (FCG3RA) (fold change = -14.57, p= 0.0001) in uNK CK treated subsets, both of which are well-recognised differentially expressed CD56^{bright} NK markers comparative to CD56^{dim} pNK subsets (277, 314).

Comparatively, in the presence of 1,25(OH)₂D₃, 2373 genes were identified in uNK versus pNK; 1238 downregulated and, 1135 upregulated in uNK. The distribution of differentially expressed genes

is illustrated in Figure 5.10, indicating a similar distribution of upregulated and downregulated genes in uNKs comparative to their peripheral counterparts.

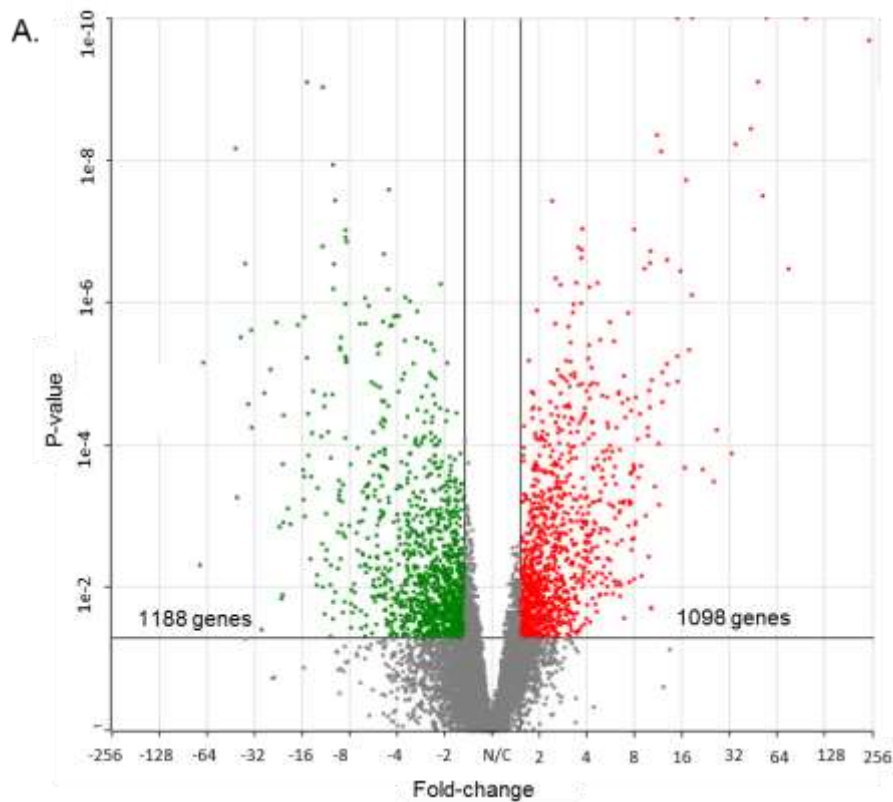


Figure 5.10 Transcriptomic analysis of cytokine (CK)-stimulated pNK and uNKs. Summary of differentially expressed genes in CK uNK relative to CK pNK; significantly upregulated genes in uNKs CK are red (n=1098), downregulated genes green (n=1188), with those not significantly different in grey (n= 11163). A cut-off of $p \leq 0.05$ and fold change ≤ -1.5 or $\geq +1.5$ was utilised.

5.2.10 Pathway analysis

To delineate the differences in transcript expression in a more informative manner, complementary pathway analysis was performed. Our principal aim was to gain a more comprehensive insight into the underlying biology of those differentially expressed genes identified in the uNK CK vs pNK CK comparison group. Across both the WikiPathways (WP) (Figure 5.11) and Reactome (Figure 5.12) databases, a broad spectrum of enriched canonical pathways were identified with those significant ($p \leq 0.05$) ranked from a high to low Z-score. Overall, 14 WikiPathways (WP) and 54 Reactome pathways were significantly enriched (Z-score > 1.96) in uNK (relative to pNK). Prominently these

included pathways related to genomic processing, immune function, cell signalling, and molecule mechanisms of cancer. For the WP database analysis, pathways included histone modification (3.29), retinoblastoma in cancer (2.18) and TGF- β receptor signalling (2.01) and nuclear receptors (1.99).

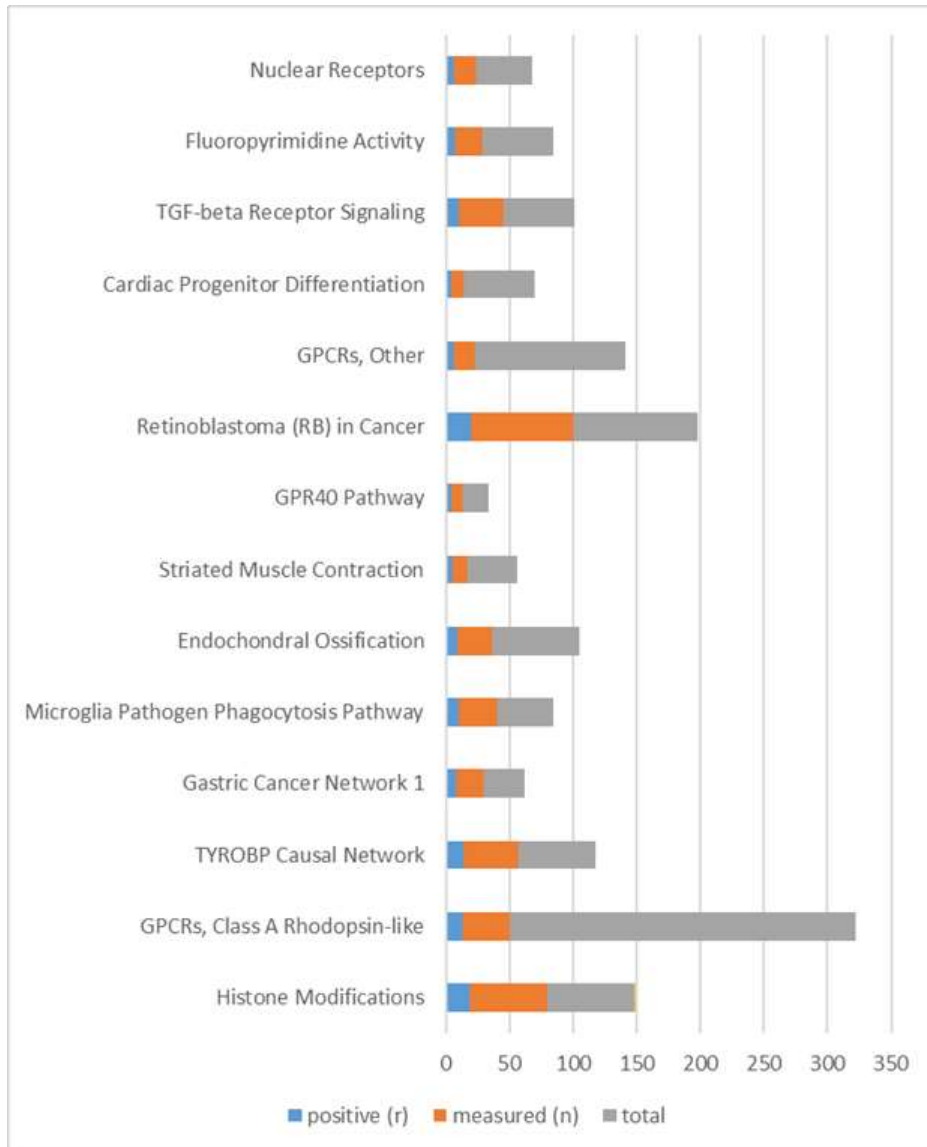


Figure 5.11 Summary of WikiPathways data-base analysis for CK treated uNK versus CK pNK. Bars represent those pathways significantly enriched (p-value <0.05, Z-Score >1.96), with the frequency of significant differentially expressed genes (blue) and total genes measured (orange) as a proportion of the total frequency of pathway genes (grey) illustrated. Bars are ranked from a high to low Z-score.

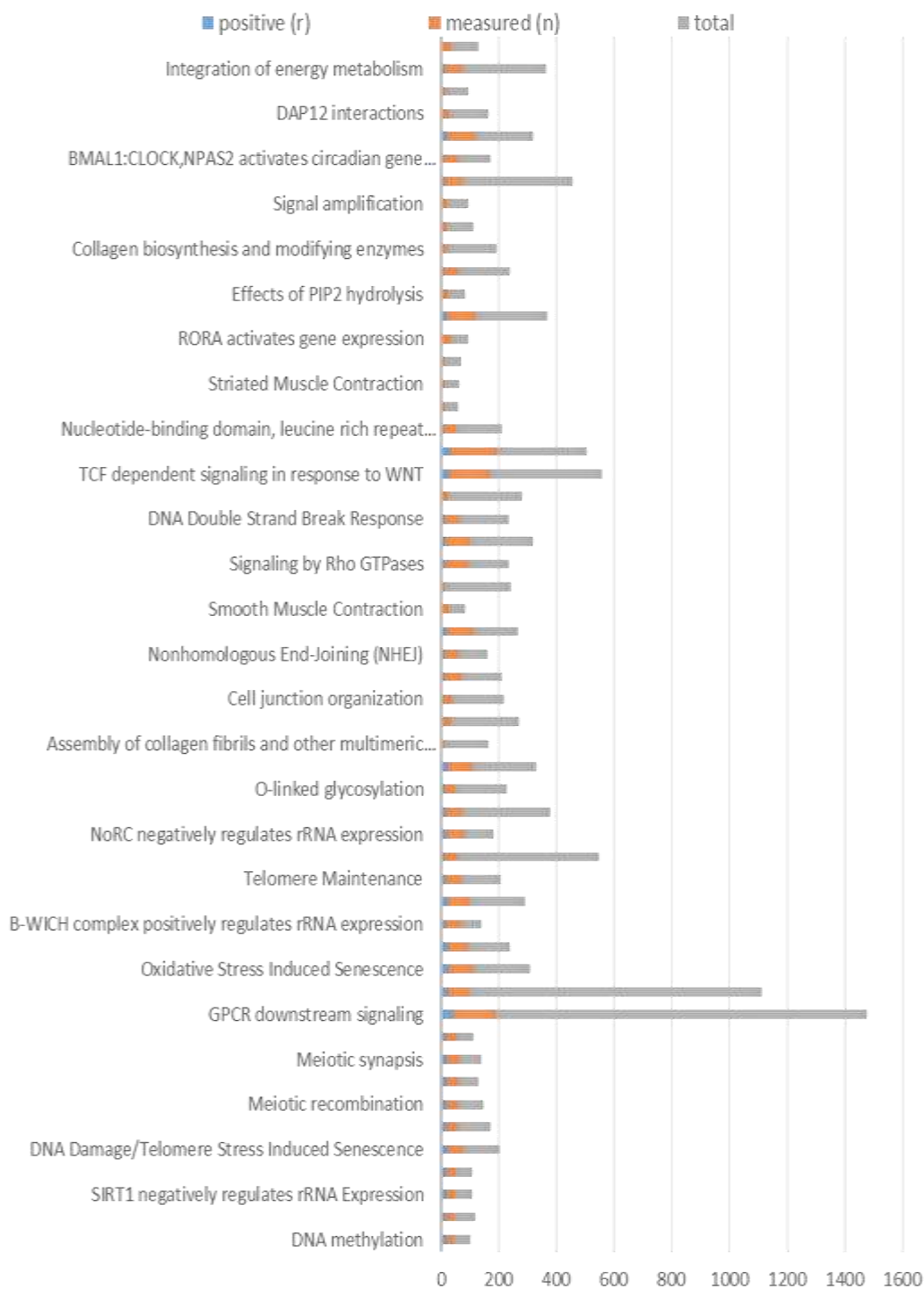


Figure 5.12 Summary of the Reactome data-base analysis for CK treated uNK versus CK pNK.

Bars represent those pathways significantly enriched ($p\text{-value} < 0.05$, $Z\text{-Score} > 1.96$), with the frequency of significant differentially expressed genes (blue) and total genes measured (orange) as a proportion of the total frequency of pathway genes (grey) illustrated. Bars are ranked from a high to low Z-score.

Similar findings were also observed utilising Reactome database analysis, with uNK enriched pathways including DNA methylation (9.69), meiotic recombination (7.43), GPCR downstream signalling (5.86), immuno-regulatory interactions between a lymphoid and a non-lymphoid cell (4.61) and integrin α IIb β 3 signalling (2.33) (Figure 5.12). Notably both databases showed differences in pathways directly related to TLR-signalling, glucose homeostasis, the electron transport chain, and MAPK signalling pathway. VDR receptor signalling also appeared enriched in uNK comparative to pNKs, but this was not significant (Z-score 1.05, $p < 0.05$).

5.2.11 Vitamin D effects upon CK treated pNK cells

Overall 71 genes were differentially expressed in the pNK CK group ($p < 0.05$; fold-change +/- 1.5). Of these, 33 genes were downregulated by 1,25(OH) $_2$ D $_3$, and 38 genes upregulated by 1,25(OH) $_2$ D $_3$.

Functional classification	Total	Up-regulation by 1,25(OH) ₂ D ₃	Down-regulation by 1,25(OH) ₂ D ₃
Cell structure	3	TLL1, FAM161A	CMYA5
Cell survival, proliferation, invasion, adhesion, angiogenesis, trafficking	15	TMEM14A, MMP14, PIK3R6, ENG, RABL2A, DEPDC1B, TRIM35, CAB39L, AP5S1	TSPAN4, SERPIN1, NRP2, RAPGEFL1, FAM195A, AP4M1
Immune function	3	LXN, MTCP1, RSAD2	
Metabolism & lipogenesis	17	ACOT1, ACSF2, CCBL1, MTHFD2L, PPP1R3F, AMPD3, GRHPR	PM20D2, TKFC, KDELC1, BDH2, GMPR, BCKDHB, NBR2, NPR2, ENPP1, NR2F6
Genetic	10	CBX8, DNAJC30, RPA3, EXOSC7, PPFIBP1	TUT1, GTPBP3, MIR600HG, TCEANC, TYRO3P
Ion transport	1	SLC35E3	
Unknown function	10	LOC101929767, TTC32, LOC100287042, PROB1,	ARMCX4, LOC441666, LOC100506804, PRRG4, CBWD6, THAP8
Anti-sense, non-coding, snoRNAs	11	BRWD1-IT2, SNORA67, SNORA17B, LOC100129083, ADNP-AS1, RPL13P5,	C22orf34, SNHG25, TRIM47, MRPL42P5, GCSHP3

Table 5.7 Effect of 1,25(OH)₂D₃ upon gene expression in CK pNK. Summary of total genes (n=71) differentially induced (green) (n=38) or suppressed (red) (n=33) by 1,25(OH)₂D₃ in CK pNK (fold change < -1.5 or > +1.5, p ≤ 0.05), with sub-classification according to transcript function.

As summarised in Table 5.7, co-treatment with 1,25(OH)₂D₃ primarily targeted genes associated with metabolism and lipogenesis (n=17), including upregulation of *ACOT1*, *ACSF2*, *MTHFDL2*, *PPP1R3F*, *AMPD3*, *GRHPR* and downregulation of *PM20D2*, *TKFC*, *KDELC1*, *BDH2*, *GMPR*, *BCKDHB*, *NBR2*, *NPR2*, *ENPP1*, *NR2F6*. A preponderance of genes related to cell processing, in particular cell signalling and cell transport (n=15) were also identified, including the upregulation of *TMEM14A*, *MMP14*, *PIK3R6*, *ENG*, *RABL2A*, *DEPDC1B*, *TRIM35*, *CAB39L*, *AP5S1*, and downregulation of *TSPAN4*, *SERPINI1*, *NRP2*, *RAPGEFL1*, *FAM195A*, *AP4M1*. Genes influencing

genomic processes (n=10) and ion transport (n=1) were also identified. Only 3 genes identified were directly implicated in immune function, with 1,25(OH)₂D₃ positively influencing *LXN* (3.94 fold change, p = 0.01), *MTCPI* (2.78 fold change, p = 0.02), and *RSAD2* (1.74 fold change, p = 0.03). A number of genes with 'unknown functions' or were classified as 'anti-sense/ non-coding' (total n=21) were detected using RNA-seq. Table 5.8 outlines the function of those significantly differentially expressed genes of particular functional interest, with scaled colour change graded according to fold-change.

FOLD-CHANGE		
Target	uNK	pNK Function
<i>TLL1</i>	5.88	Tubulin-glutamic acid ligase activity
<i>ACOT1</i>	4.28	Acyl-CoA metabolic process
<i>LXN</i>	3.94	Pro-inflammatory immune response, metalloenzyme inhibitor
<i>RABL2A</i>	3.18	GTPase mediated signal transduction; endocytosis and exocytosis regulation
<i>MTCP1</i>	2.78	Mature T cell proliferation
<i>DEPDC1B</i>	2.72	Cell signalling and cell migration
<i>ACSF2</i>	2.39,	Fatty acid metabolic processing
<i>MMP14</i>	2.37	Matrix Metalloproteinase
<i>PIK3R6</i>	2.31	Phosphoinositide-3-kinase regulatory subunit 6 - regulation of NK cytotoxicity and T cell differentiation
<i>PPF1BP1</i>	1.93	Cell division and chromosome partitioning
<i>MTHFD2L</i>	1.91	NADP+ dependent purine metabolism
<i>PPP1R3F</i>	1.93	Regulation of glycogen biosynthesis
<i>RSAD2</i>	-1.62	Anti-viral via type 1 IFN pathway, positive regulation of TLR-7 and TLR-9
<i>AMPD3</i>	1.73	Energy homeostasis
<i>GRHPR</i>	1.56	Energy homeostasis
<i>ENG</i>	1.55	Neo-angiogenesis, hypoxic response, TGF- β signalling modulation, negative regulation transcription
<i>TRIM35</i>	1.86	Positive regulation of apoptosis, inhibition of cell proliferation
<i>GMPR</i>	-2.01	Purine metabolism
<i>TSPAN4</i>	-2.05	Integrin binding, focal adhesion
<i>NPR2</i>	-2.41	Guanylyl cyclase signaling pathway
<i>SERPINI1</i>	-2.50	Regulation of cell adhesion
<i>NR2F6</i>	-2.58	Guanylyl cyclase signaling pathway
<i>TYRO3P</i>	-2.63	Negative regulation of transcription
<i>ENPP1</i>	-3.42	Energy homeostasis
<i>NRP2</i>	-3.54	Angiogenesis, regulation of endothelial cell proliferation and cell adhesion

Table 5.8 Summary of principal genes differentially regulated by 1,25(OH)₂D3 in pNK cells. Transcripts in CK pNK cells either upregulated (green) or downregulated (red) following co-treatment with CK and 1,25(OH)₂D3. The cut-off $p \leq 0.05$ and fold change ≤ -1.5 or $\geq +1.5$ was utilised to assess 1,25(OH)₂D3 effects, with scaled colour change graded according to fold-change. Transcript overlap with differential expression in uNK cells is also shown.

5.2.12 Functional analysis of vitamin D-mediated uNK transcripts

Direct comparative analysis of CK treated and CK+ 1,25(OH)₂D₃ treated uNKs revealed significantly disparate effects upon gene transcript expression. Overall, 66 genes were differentially expressed (p<0.05; fold change ± 1.5), with 20 downregulated and 46 upregulated by 1,25(OH)₂D₃ treatment.

Functional classification	Total	Up-regulation by 1,25(OH) ₂ D ₃	Down-regulation by 1,25(OH) ₂ D ₃
Cell structure	2		CAMSAP2, SOBP
Cell survival, proliferation, invasion, adhesion angiogenesis, trafficking	27	TSPAN2, ARAP3, ITGAM, RARRES3, ADGRE5, FGL2, DYSF, NINJ1, ZFP91-CNTF, DENND6B, BGLAP, DOCK3, RNF165, TAX1BP3, TRIM35, TAGLN2, RGS3	ADGRG1, TMPRSS6, CYGB, C8orf44-SGK3, LZTS3, MARCKSL1, NACAD, TCF7L2, PHOSPHO2-KLHL23, P2RY11
Immune function	4	SERPINB1, LGALS9, RELT	RSAD2
Metabolism & lipogenesis	7	TMEM56-RWDD3, SARDH, CYP1A1, GDPGP1, ACSL1, GDE1, ADA	
Genetic	9	TFEC, WWC2, ZBTB7A, HIC1, EFL1, HNRNPLL, TRAK1, CREG1	BHLHB9
Ion transport	2	SLC31A1	SLC22A1
Unknown function	8	ZSWIM5, LOC101928464, TNRC6C-AS1, POMGNT2, PLEKHO2, NARS2, INTS6L	C1QTNF3-AMACR
Anti-sense, snoRNAs	6	SNORA17A, SIGLEC17P, NPPA-AS1	CCDC102A, ALMS1-IT1, LOC100505771,

Table 5.9 Effect of 1,25(OH)₂D₃ upon gene expression in CK uNK. Summary of total genes (n=66) differentially induced (green)(n=46) or suppressed (red) (n=20) by 1,25(OH)₂D₃ in CK-uNK (fold change < -1.5 or > +1.5, p ≤ 0.05), with sub-classification according to transcript function.

As summarised in Table 5.9 co-treatment with 1,25 (OH)₂D₃ primarily targeted genes implicated in cell processing, in particular cell adhesion, apoptosis, migration and angiogenesis (n=27) . Of these,

17 were upregulated by 1,25 (OH)₂D₃, including *TSPAN2*, *ARAP3*, *ITGAM-1*, *RARRES3*, *ADGRE5*, *FGL2*, *DYSF*, *NINJI*, *ZFP91-CNTF*, *DENND6B*, *BGLAP*, *DOCK3*, *RNF165*, *TAX1BP3*, *TRIM35*, *TAGLN2*, *RGS3*, and 10 downregulated by 1,25(OH)₂D₃, including *ADGRG1*, *TMPRSS6*, *CYGB*, *C8orf44-SGK3*, *LZTS3*, *MARCKSL1*, *NACAD*, *TCF7L2*, *PHOSPHO2-KLHL23*, *P2RY11*.

Comparative to pNKs, fewer targets relating to metabolism and lipogenesis were identified (n=7); *TMEM56-RWDD3*, *SARDH*, *CYP11A1*, *GDPGP1*, *ACSL1*, *GDE1*, and *ADA*. Furthermore, as summarised in Table 5.10, these targets have distinct functional roles, which importantly appear directly related to placentation.

FOLD-CHANGE

Target	uNK	pNK	Function
TSPAN2	7.42		Pro-invasion and motility
DENND6B	6.9		Vesicle-mediated transport and membrane trafficking. Positive regulation of GTPase activity.
DOCK3	3.64		Regulates F-actin and integrin-mediated adhesion in immune cells. Promote NK cell effector function
FGL2	2.86		Promotes angiogenesis and tumour development. Recognised role in implantation
TFEC	2.82		Transcription regulator
SERPINB1	2.37		Inflammatory regulator. Restricts pro-inflammatory cytokine production, including NK cell granzyme H
TAX1BP3	2.16		Promotes cell signalling, adhesion, and migration.
RARRES3	2.13		Negative regulation of cell proliferation
ITGAM	2.01,		Integrin which promotes adhesion
TRIM35	1.86	1.5	Positive regulation of apoptosis . Inhibits cell proliferation
ARAP3	1.85		Cytoskeleton organisation, vesicle-mediated transport, cell migration negative regulation
ADGRE5	1.76		Promotes cell adhesion and cell signalling. Potential inflammatory immune response
LGALS9	1.75		NK cell tolerance induction, negative regulation of IFN- γ and TNF- α , promotes IL-4, IL-10 production.
RELT	1.72		Role in apoptotic pathway. Controls cell proliferation. Pro and regulatory immune effects
WWC2	1.72		Transcription regulator
NINJ1	1.69		Pro-adhesion
HIC1	1.69		Transcription regulator
ADA	1.58		Purine metabolism. Orchestrates cellular responses to hypoxia. Role in placental development.
TAGLN2	1.08		Promotes hypoxia-induced apoptosis via caspase-8 pathway.
ADGRG1	-1.54		Adhesion - facilitates immune cell trafficking
RSAD2	-1.62	1.74	Anti-viral properties via type 1 IFN pathway, positive regulation of TLR-7 and TLR-9
TCF7L2	-2.56		Regulator of cell growth and migration
CYGB	-2.93		Regulator of cell growth and migration
BHLHB9	-3.23		Negative regulation of neurone apoptosis
C8orf44-SGK3	-4.55		SGKs regulate cell growth, proliferation, survival and migration
LZTS3	-5.52		Potential regulator of cell growth and migration

Table 5.10 Summary of principal genes differentially regulated by 1,25(OH)₂D3 in uNK cells. Transcripts in CK-uNK cells either upregulated (green) or downregulated (red) following co-treatment with CK and 1,25(OH)₂D3. A cut-off of $p \leq 0.05$ and fold change ≤ -1.5 or $\geq +1.5$ was utilised to assess 1,25(OH)₂D3 effect, with scaled colour change graded according to fold-change. Potential overlap with regulation in uNK cells is also shown.

Importantly, only 4 genes identified are concerned with immune function; with 3 upregulated (*SERPINB1*, *LGALS9*, *RELT*) (Figure 5.13), and 1 downregulated (*RSAD2*) by 1,25(OH)₂D₃ (Figure 5.14).

Considering *RSAD2*, which encodes a cytoplasmic anti-viral protein induced by interferons, this was downregulated in uNKs (fold-change -1.62, p=0.03) and conversely upregulated in pNKs (fold-change = 1.74, p=0.03). A number of genes influencing genomic processes (n=9) and ion transport (n=2) were identified, and a number of genes with ‘unknown functions’ (n=8) or ‘anti-sense/ non-coding’ (n=6).

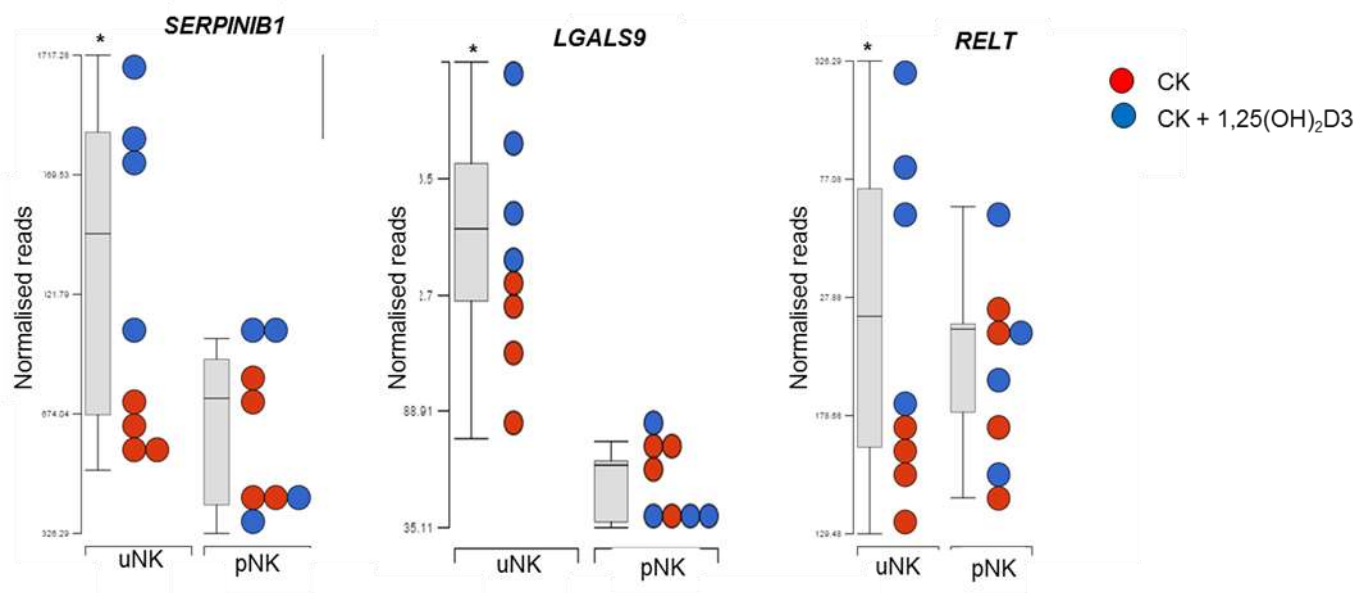


Figure 5.13 Analysis of transcript expression of *SERPINB1*, *LGALS9* and *RELT* in CK treated NK cells. Transcript expression of *SERPINB1*, *LGALS9* and *RELT* in CK treated NK cells (red) comparative to those treated with CK + 1,25(OH)₂D₃ (blue) for both uNK and pNKs (n=4). The cut-off p ≤ 0.05 and fold change ≤ -1.5 or ≥ +1.5 was utilised to assess 1,25(OH)₂D₃ effects (*).

Of the 137 genes differentially expressed in NKs treated with 1,25(OH)₂D₃, only 1 common transcript was identified for uNKs and pNKs; pro-apoptotic tripartite motif-containing protein 35 (*TRIM35*) which was upregulated in both uNK (p=0.0006, fold-change = 1.86) and pNKs (p=0.01, fold-change 1.50). Baseline expression of *TRIM35* was higher in the CK treated uNKs comparative to pNK, and a greater responsivity to 1,25(OH)₂D₃ was also evident (Figure 5.14).

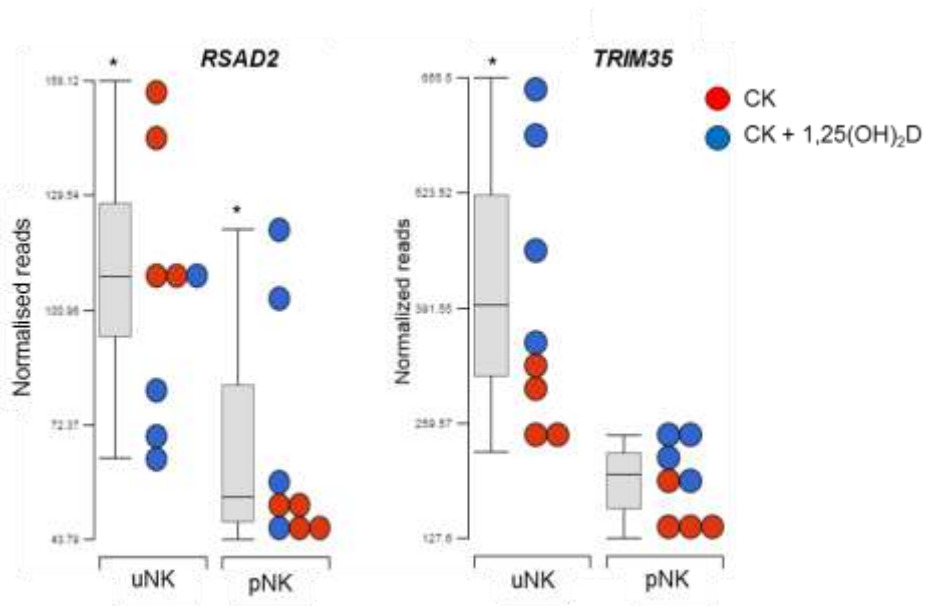


Figure 5.14 Analysis of transcript expression of *TRIM35* and *RSAD2* in CK treated NK cells.

Transcript expression of *TRIM35* and *RSAD2* was assessed in CK treated NK cells (red) comparative to those treated with CK + 1,25(OH)₂D₃ (blue) for both uNK and pNKs (n=4). A cut-off of $p \leq 0.05$ and fold change ≤ -1.5 or $\geq +1.5$ was utilised to assess 1,25(OH)₂D₃ effect (*).

5.3 Discussion

The maternal decidua represents a key extra-renal site for vitamin D metabolism (306). As demonstrated, at this interface a highly heterogenic immune cell population exists, dominated by uNKs and T cells. Of particular interest are the prominent uNKs, which are primarily recognised for their roles in EVT invasion and spiral artery remodelling (315). Moreover, these cells exert key immuno-regulatory actions (277), with aberrant NK cell function associated with adverse pregnancy outcomes and malplacentation (316). Given vitamin D exerts important immuno-regulatory effects, this has evoked many important questions regarding the potential functional effects of vitamin D upon decidua-derived uNKs (71). The exact mechanisms underlying this remain ill-defined; a potential immuno-regulatory role for vitamin D has not previously been explored. The present study provides a detailed analysis of vitamin D and its effects upon matched early pregnancy pNKs and uNKs.

Within first trimester decidua we confirm a unique immune cell population exists, dominated by uNKs (50-60%). This appears gestation dependent, as by the third trimester T cells appear more prominent with uNKs representing $\leq 25\%$ (317). Conversely, in the first trimester pNKs represent only a small fraction (3.63-10.3%) of the total immune cell population in maternal blood.

Previous studies using DNA microarrays have described marked transcriptomic variations in CD56bright pNKs and CD56dim pNKs, as well as CD56 bright uNKs (277). In the current study, we did not sub-categorise pNK or uNKs according to CD56 brightness since CD56dim pNKs predominated in peripheral blood ($\sim 95\%$ total pNKs), whilst CD56bright uNK predominated in decidua ($\sim >95\%$ total uNKs). Given the stark differences in number and frequency, some postulate uNKs represent a distinct lineage arising from a unique endometrial hematopoietic precursor (318). However, there is also strong evidence to support enhanced pNK recruitment to the decidua, with uNK phenotype and function regulated within the unique tissue micro-environment (319). Studies characterising other tissue-derived NK subsets similarly suggest this, for example, hepatic NKs which represent a high (50%) proportion of liver immune cells and reside in a constitutively active state (CD69+NKp46bright) with potent anti-viral and anti-tumour activity (320).

Here we confirm these two populations appear phenotypically highly disparate, with those from blood predominantly CD56dim NKp46dim and those from decidua almost exclusively CD56bright NKp46bright. These differences may imply that uNKs are constitutively active. In agreement with this, we find decidual cells are larger with abundant perforin and granzyme. Generally however, CD56bright NKs are considered efficient CK producers with immuno-regulatory properties, which only become cytotoxic upon appropriate activation. However, disparate to most other sites, uNKs do not express activating receptor CD16 which mediates antibody-dependent cellular cytotoxicity (314). It appears that whilst uNKs maintain an intrinsic capacity to exert cytotoxic functions when specifically challenged, this function is regulated in normal early pregnancy. Further undefined local mechanisms, such as CK or hormone secretion, or crosstalk with other immune cell types within the decidual micro-environment are also thought to suppress the potential lytic effects of uNKs (238, 321).

An increasing body of evidence now exists to suggest first trimester uNKs have the capability to transform into foes of pregnancy. NK cell frequency alone does not appear causative, as evidenced in a recent systematic review and meta-analysis of women with recurrent miscarriage(290). It appears NK cells undergo functional changes in women with spontaneous miscarriage, with a pro-inflammatory shift reported. Specifically, a decreased proportion of CD16- CD56bright NKs with increased CD16+CD56dim NKs was measured in the luteal phase endometrium (316). In pregnant mice, fetal resorption following administration of LPS was also associated with aberrant uNK cell phenotypic and function, as characterised by excessive TNF- α release at the maternal-fetal interface (322).

Consistent with previous reports, we demonstrate uNKs release low levels of inflammatory IFN- γ and TNF- α in response to CK stimulation, and appear less reactive with low CD107 expression relative to pNKs. Since CD107 is a recognised marker of degranulation, CK secretion and NK cell-mediated lysis, a correlation with IFN- γ and TNF- α was anticipated. This reflects the weak cytotoxicity of uNKs, which most likely serves to promote tolerance of the semi-allogenic fetus (309,

323). A recent report which tracked pNK cell IFN- γ production identified that in CD56dim NK cells this occurs within 2-4h, and declines beyond 16h. In contrast, CD56bright subsets released IFN- γ later, >16h post stimulation(324). Since a 24h time-point was utilised, we anticipate both uNK and pNK CD56bright and CD56dim activity was captured in the assay. It is uncertain why TNF- α expression was not clearly upregulated in pNKs in response to CK, as this is a recognised pNK cell-mediated CK outside the context of pregnancy(239).

The principal aim of the current study was to assess the NK cell responsivity to 1,25(OH) $_2$ D $_3$, in particular following immune challenge. Given the striking differences between uNK and pNK subsets it was important to investigate and compare the effects of vitamin D upon paired subsets. Pro-inflammatory IL-2, IL-12 and IL-15 were utilised for CK challenge, as these are recognised NK cell activators, with both IL-12 and IL-15 constitutively expressed within the decidua from initial implantation (325, 326). Although IL-2 concentrations appear low within normal decidua (327), significantly elevated IL-2 has been reported in the setting of malplacentaion (328), where vitamin D-deficiency is also more common (329). Furthermore, previous reports delineating the non-classical effects of vitamin D demonstrate greater functional responsivity of innate and adaptive cell subsets within the context of immune cell activation (56, 330).

5.3.1 NK cells positively express a functional vitamin D system

To our knowledge, this is the first time the vitamin D metabolic system has been characterised in purified uNKs and compared to pNKs. Our data indicate both populations express the machinery necessary to detect and control 1,25(OH) $_2$ D $_3$ in response to CK challenge via the reciprocal regulation of *CYP27B1* and *CYP24A1*. Specifically, when there is sufficient local 1,25(OH) $_2$ D $_3$, *CYP27B1* is downregulated and *CYP24A1* expression is enhanced. In response to CK conversely, a clear shift towards enhanced 1,25(OH) $_2$ D $_3$ production and maintenance is evident. Considering *CYP24A1*, in both NK populations transcript expression was upregulated in response to 1,25(OH) $_2$ D $_3$. In the decidua this may serve to regulate placental exchange of calcium to the developing fetus. However since fetal bone formation is concentrated in the third trimester, and fetal calcium supply does not

appear negatively influenced by a vitamin D status(109), alternative non-classical actions of 1,25(OH)₂D₃ may be anticipated during first trimester implantation and fetal development.

Our group has similarly shown upregulation of *CYP27B1* in decidua-derived CD10 negative cells (stromal negative) to closely correlate with several key immune markers (41). Here we find in uNKs *CYP27B1* is upregulated in response to CK challenge. Given their prominence within the CD10-decidua cohort, these findings would suggest uNKs may be a key mediator of vitamin D derived immune effects at the fetal-maternal interface. At a transcript and protein level, our data suggest both uNK and pNKs also express *VDR*, and upregulate expression in response to CK challenge. Interestingly our initial data suggests greater VDR induction by uNKs compared to pNKs in response to CK activation. Together these findings strongly support a functional role of NK cells in mediating vitamin D immune effects, with potentially a greater functional significance for vitamin D within the local decidua environment. Since uNKs display enhanced immune-regulatory properties comparative to both peripheral NK subsets (64), this may be expected.

However, genome-wide analysis of chromatin-binding of VDR, as determined by chromatin immunoprecipitation sequencing (ChIP-seq) analysis indicates VDR may employ additional non-classical mechanisms, including alternative DNA binding motifs, and indirect DNA binding, to recognise its genomic targets(331). It may be an over-simplification to state that uNKs are more responsive to vitamin D than their peripheral counterparts based upon VDR expression alone. Furthermore, although both uNK and pNKs showed a clear shift towards enhanced 1,25(OH)₂D₃ production (conversion assay) in response to pro-inflammatory CK challenge, 1,25(OH)₂D₃ production was relatively higher for pNKs, despite no significant difference in *CYP27B1* expression or 24,25(OH)₂D₃ production.

Considering the potential mechanisms by which 1,25(OH)₂D₃ may influence NK cell function, in CD4+ T cell similar VDR upregulation in response to CK stimulation is observed. Here, vitamin D exerts a range of pro-regulatory effects upon T cell development, differentiation and elicitation of effector function (110). Furthermore, T cell VDR activation is shown to be protective within the context of auto-immune disease models (111). Albeit the data regarding VDR activity in NKs is

sparse, in umbilical cord NK cell progenitors 1,25(OH)₂D₃ was shown to inhibit NK cell maturation and cytotoxic potential (112).

5.3.2 1,25(OH)₂D₃-mediated suppression of uNK IFN- γ production

We found 1,25(OH)₂D₃ significantly suppressed uNKs IFN- γ expression at both a transcript and protein level. Others have also reported a role for VDR-dependent 1,25(OH)₂D₃ in the placenta, including inhibition of pro-inflammatory CKs, IFN- γ , IL-6 and TNF- α within the trophoblast (332). Classically, NKs play an important role in immune response by producing IFN- γ to induce cell lysis, as well as exhibiting cytotoxic function. Within the decidua however a unique functional role for IFN- γ seemingly exists, with essential roles in the initiation of uterine vascular modifications and maintenance of decidual integrity. In murine models, IFN- γ is vital for normal placentation. Specifically, IFN- γ null mice exhibit aberrant NK cell frequencies, inappropriate decidualisation and spiral artery modifications, and significant fetal loss (333). Treatment with IFN- γ restores normal decidual and arterial morphology(333). In human pregnancy, uNK IFN- γ secretion also increases with gestational age (315). However, IFN- γ administration can also induce pregnancy failure, thus balancing IFN- γ expression appears important (334). Within the context of vitamin D, both pro-modulatory and pro-anti-microbial effects via IFN- γ have been reported (335, 336). This may explain why only partial suppression of uNK IFN- γ by 1,25(OH)₂D₃ was observed. A model accounting for both materno-fetal tolerance and maternal micro-organism defense is warranted.

5.3.3 Whole transcriptome comparative analysis of CK treated uNK and pNK subsets

To advance our understanding of the impact of vitamin D on early decidual function, a non-targeted whole transcriptome analysis of the effects of 1,25(OH)₂D₃ upon CK stimulated uNK and pNK was performed. Co-activation enhanced the potential for a broader transcriptomic comparison between the two different NK cell types. Previous DNA array analyses, reported >1,100 genes to be significantly differentially-expressed in US CD56dim pNK versus US CD56bright uNK (277). By contrast, in the current study >2,000 genes were differentially expressed in CK-activated uNK versus CK-activated pNKs. Furthermore, a comparable number of up and downregulated genes was detected in CK-activated uNK relative to CK-activated pNK, whereas in the absence of CK stimulation Koopman *et*

al found uNKs almost exclusively demonstrated enhanced transcription relative to pNK (277). Consistent with our preliminary data, uNK responsivity to CK challenge appears highly distinct from that observed from circulating pNKs during pregnancy.

5.3.4 Complementary pathway analysis reveals distinct CK-mediated effects upon uNKs

To facilitate interpretation further, detailed pathway analysis was performed (337). By grouping genes that function in the same pathways and identifying how expression differs between comparative groups, i.e. CK uNK and pNKs, we found this technique to offer complementary explanatory power. Specifically, we demonstrated uNK are phenotypically distinct, with cell signalling and processing, immune cell function and cancer pathways over-expressed relative to pNK. These observations are consistent with the known critical roles of uNKs for placental development and materno-fetal tolerance.

Consistent with previous microarray analysis of first trimester uNK and adult non-paired pNK (338), this study showed that uNK are strongly enriched for genes associated with the regulation of transcription, which likely serves to differentially regulate NK development and function within the decidual microenvironment. Consistent with our analysis, Koopman *et al*, identified that pro-adhesive markers, including the integrin family which influence processes such as cell adhesion, migration and interaction with target cells, were over-represented in uNKs. An enhanced immune-modulatory potential was also evident through over-expression of galectins, which are implicated in immune maturation and modulation of T cell cytotoxicity (277). Importantly, consistent with our transcript and protein analysis data VDR receptor signalling also appeared enriched in CK uNK comparative to CK pNKs.

5.3.5 Differential regulation of first trimester uterine and peripheral blood natural killer cells by 1,25(OH)₂D₃

In CK-activated uNK and pNKs the effects of 1,25(OH)₂D₃ were highly selective; with only 66 (0.59%) and 71 (0.64%) transcripts measured respectively. By contrast, in the human THP-1 spontaneously immortalized monocyte-like cell line which represents a valued tool for investigating

monocyte structure and function (339), RNA-seq analysis identified 663 stimulated genes and 541 repressed genes, with 8.9% of the expressed transcriptome (14,402 total genes) responsive to 1,25(OH)₂D₃ following 24h culture (340). This suggests monocytes may be comparatively more responsive to 1,25(OH)₂D₃ than NK, however it should be noted that a 10-fold higher treatment dose (100nM) was utilised (340) and THP-1 cell lines demonstrate important functional variances comparative to their human peripheral blood monocytic counterparts (339).

The relatively low numbers of genes influenced by 1,25(OH)₂D₃ in both pNK and uNK may be due, in part, to temporal variations in gene expression. Previous analysis of 1,25(OH)₂D₃-regulated gene expression in THP-1 cells demonstrated an exponential increase in vitamin D-mediated transcript expression over 24h. In previous studies, combined 1,25(OH)₂D₃ (100nM) and glucocorticoid treatment of PBMCs at different time points (8 and 24h) also revealed time-dependent variations in transcriptional responses to 1,25(OH)₂D₃, with enrichment of genes associated with immunomodulation and defence only occurring after 24h (341). In the current study, we assessed mRNA expression at 24 h to maximise potential for variations in gene expression, whilst ensuring high cell viability. It is possible both pNK and uNKs would have demonstrated a different pattern of gene regulation by 1,25(OH)₂D₃ at earlier or later time points. Due to both cell numbers and RNA-seq costs, a comparative time-point analysis was not feasible.

TRIM35 was the only gene significantly upregulated in both uNK and pNKs in response to 1,25(OH)₂D₃. *TRIM35* has been reported to play a role in apoptosis (342); in neoplastic Hela cells this occurs via regulation of the ‘Warburg effect’, which describes a switch in cellular metabolism from aerobic glucose metabolism and oxidative phosphorylation towards glycolysis to meet the heightened energy demands of a tumour cell (343). In macrophages and DCs, pro-inflammatory lipopolysaccharide (LPS) endotoxin challenge alone downregulates genes in the oxidative phosphorylation pathway, inducing a metabolic shift to anaerobic glycolysis and thereby driving a pro-inflammatory response (344). Recent evidence indicates that 1,25(OH)₂D₃ attenuates this response (345), suggesting that 1,25(OH)₂D₃ regulates NK cell energy metabolism and cell proliferation both within the decidua and peripherally. ‘Warburg-like glycolysis’ and local lactate

shuttle also play a critical role in early decidualisation (346, 347). We anticipate 1,25(OH)₂D₃ mediated upregulation of uNK *TRIM35* may support early decidualisation and regulate immune cell function in the first trimester. This would also be consistent with prior reports indicating 1,25(OH)₂D₃ promotes EVT invasion (304).

In uNK, treatment with 1,25(OH)₂D₃ demonstrated significant upregulation of several other key genes recognised in placentation, including *ADA* and *RARRES3*. Placental *ADA* is essential for purine metabolism, with deficiency leading to elevated adenosine with subsequent aberrant cellular responses to hypoxia, tissue damage and immune dysregulation. In mice with placental restricted *ADA* deficiency, hallmark features of ‘human malplacentation syndromes’ (i.e. PET and SGA) are evident (348). In PET, high purine levels are evident albeit their source is unknown. Uric acid, the end-product of purine metabolism, is certainly elevated which may reflect increased tissue damage or breakdown(349). *RARRES3*, an intermediate of the retinoic acid (RA) pathway, is considered a potential biomarker of endometrial receptivity (350). Importantly, within the decidua, RA suppresses endometrial stromal cell decidualisation (351). Since a direct association between VDR-RXR heterodimer-mediated gene expression and nuclear signalling by RA and 1,25(OH)₂D₃ is well established (352), future studies exploring the interaction between vitamin D and RA within the decidua are likely to be important.

Given the established effects of vitamin D on other innate immune cell subsets (353), we anticipated that 1,25(OH)₂D₃ would target multiple NK genes associated with immune regulation. However, only 4 genes directly linked to immune modulation (*SERPINB1*, *LGALS9*, *RELT* and *RSAD2*) were regulated by 1,25(OH)₂D₃ in uNKs. Galectin-9 (*LGALS9*) suppresses uNK pro-inflammatory IFN- γ release (354, 355), with decreased decidual expression of *LGALS9* in both an abortion prone mouse model, and *LGALS9* D5/10 variant in women suffering spontaneous miscarriage reported (355, 356). Since IFN- γ is reported as important for vascular changes in pregnancy (287), future studies defining uNK *LGALS9* function are merited.

NK cell cytotoxicity consists of a stepwise series of tightly regulated cellular events that requires early contact with and adherence to target cells with subsequent rapid polarization of their lytic

granules and de-granulation. This facilitates fatal secretion of perforin and lytic granzyme enzymes against the target cell and represents a major cytotoxic mechanism to induce target cell death. Intracellular leukocyte elastase inhibitor (SERPINB1) directly inhibits granzyme H, thus downregulation by $1,25(\text{OH})_2\text{D}_3$ may serve to regulate innate cytotoxicity, prevent unwanted tissue destruction and promote materno-fetal tolerance (357). Receptor Expressed in Lymphoid Tissues (RELT) is a member of the TNF receptor family, that is known to induce NF- κ B and promote apoptosis (358). Radical S-Adenosyl Methionine Domain-Containing Protein 2 (RSAD2), an early marker of conceptus development reportedly offers anti-viral protection during early implantation. Downregulation of *RSAD2* by $1,25(\text{OH})_2\text{D}_3$ may therefore serve to regulate uNK anti-viral activity, promoting immune modulation at the materno-fetal interface.

Classically pNKs are critical mediators of human innate immunity and targeting ‘non-self’ tumour and virally infected cells upon the basis of altered, foreign or absent MHC I without former priming or antigen specificity. Since many of the $1,25(\text{OH})_2\text{D}_3$ regulated transcripts were not directly related to immune function and apoptosis, the effects of $1,25(\text{OH})_2\text{D}_3$ do not appear simply concerned with innate immune function in early pregnancy.

Overall, $1,25(\text{OH})_2\text{D}_3$ induced 3 genes linked to immune function in pNKs. The first of these, *RSAD2*, which was conversely down regulated in uNK, is an antiviral interferon-inducible iron-sulphur cluster binding protein (359). Although a role for this protein in NK cells has not previously been described, enhanced expression of *RSAD2* is consistent with the established antiviral function of NK cells (360). $1,25(\text{OH})_2\text{D}_3$ also induced expression of latexin (*LXN*), a regulator of haematopoietic stem cells (361). *LXN* is the only known homolog of the retinoic acid receptor responder 1 (*RARRES1*) gene, and both *LXN* and *RARRES1* can act as tumour-suppressor genes (362), suggesting a novel role for $1,25(\text{OH})_2\text{D}_3$ in promoting tumour immune-surveillance actions of NK cells (363).

Data from the current study show for the first time that NKs are an important target for $1,25(\text{OH})_2\text{D}_3$, with effects upon uNK distinct from those observed with pNKs. For uNKs, $1,25(\text{OH})_2\text{D}_3$ primarily acts to promote NK cell recruitment and retention within the decidua, whilst

also facilitating apoptosis, angiogenesis, cell adhesion and trafficking, as well as immunomodulatory effects. All of these responses are crucial to normal healthy placentation, underlining the importance of vitamin D as a modulator of immune cell function at the fetal-maternal interface. It therefore seems likely that vitamin D-deficiency during pregnancy will have a significant impact on uNK cell function, particularly in the early stages of gestation. By contrast, in paired pNKs the predominant effects were upon expression of genes associated with metabolism and lipogenesis, indicating an entirely different function for vitamin D. Further studies are required to better understand the role of NK cells in mediating immune responses to vitamin D metabolites.

5.3.6 Study limitations

The power of RNA-seq lies in the combined aspects of high-throughput discovery and quantification. However, due to its novel and widespread applications, marked variations in RNA-seq protocols and analyses are reported, thereby making accurate interpretation and repetition of individual methodologies a challenge. The optimal method for transcript quantification, normalisation, and ultimately differentially expressed analysis remains contentious, and is dependent in part upon study design (364). With regards to experimental design, the sample preparation, library type selection, sequencing depth and total replicates requires careful advanced planning to avoid unnecessary bias.

Furthermore, whilst RNA-seq is a powerful tool for defining global changes in gene expression, it provides only a snapshot of the transcriptome, and does not routinely account for changes in gene expression over time. A time-course methodology would permit a more comprehensive insight into how vitamin D treatment targets NKs at a transcript level; however this was not feasible due to both the cost and total RNA concentrations.

Reviewing the RNA-seq methodology utilised, RNA extraction quality was confirmed prior, with only RIN values >7.5 progressed for RNA-seq. Due to the high RNase content of the human placenta, the RIN values of the uNK subsets were anticipated to be more heterogenic (7.5-10) than the pNK subsets (365). To manage this, Clontech SMARTer technology (95), which is specifically designed to

account for variations in the integrity and stability of the RNA preparation, was utilised for cDNA library preparation (93, 94).

Notably, intra-participant variability appeared a more significant concern for the pNK transcript data however, as PCA analysis suggests a significant degree of heterogeneity. To help ascertain data reproducibility, serial replicates would have been performed. However due to the low RNA concentrations obtained and cost this was not possible. The pNK and uNKs however paired, which permitted direct comparative analysis of the two subsets. To help identify transcript targets with low expression we employed a PE read technique, which is more accurate than single end sequencing, (364).

For the data analysis quality check-points were included through the data acquisition process, including raw read checks, pre- and post-alignment checks, normalisation and coverage quantification (364). The read alignment was good with the uniformity exon read coverage consistent with reassuring GC content, thereby suggesting no major PCR biases had arisen.

As quantification based upon raw read counts alone is not sufficient to compare sample expression, as these values are affected by factors such as transcript length, total reads, and sequencing biases, a normalisation step was introduced. This employs an expectation-maximization approach to estimate transcript abundance taking into account biases such as the non-uniform read distribution along the gene length. As demonstrated, post-normalisation box-plots were highly consistent (364).

Regarding transcript identification, as all NK samples were mapped to the latest reference transcriptome, hg38_RefSeq, the discovery of new, unannotated transcripts was precluded. Since our principal objective was comparative quantification analysis, this was not an issue. However, the RNA-seq data obtained did reveal a significant fraction of the transcriptome lacked protein-coding potential, for example short non-coding RNAs. Whether these represent key vitamin D targets is not known (366).

Albeit useful for identifying genes that may have roles in a given NK phenotype with mechanistic insights into the underlying biology of vitamin D obtained, there is also the potential for functional

over-interpretation of RNA-seq data. To aid interpretation, the analysis was simplified by grouping related transcripts into ontological groups according to their cited biological function. However, as a number of genes remain unannotated, with many existing annotations often low quality, RNA-seq interpretation may be inaccurate. Follow up studies are thus still required to validate the biological impact of specific $1,25(\text{OH})_2\text{D}_3$ -target genes in both pNK and uNK subsets.

The interpretation of RNA-seq data may also often be facilitated by integrating the results with other types of genome-wide data. Here this was not possible as to our knowledge no previous studies have assessed the effects of vitamin D upon uNK and pNK subsets utilising a non-targeted approach. A previous comparative microarray analysis of unstimulated uNK and pNK has been performed, however as for this pNKs were isolated into 2 distinct CD56^{bright} and CD56^{dim} subsets, this was not directly comparable (277).

6 Vitamin D and monocyte - macrophages in pregnancy

6.1 Introduction

6.1.1 Mononuclear phagocyte system

Elie Metchnikoff first established the phagocyte system as a critical component of human innate host defence in 1882. Soon after this was re-classified as the ‘mononuclear phagocyte system’ (MPS), and originally encompassed both monocyte and macrophage subsets. The DC was subsequently coined a key component, with these three subsets distinguished based upon their morphology, function and origin.

Traditionally, monocytes were thought to represent a linear precursor of both DC and macrophages, and differentiate following tissue migration from the blood following signal activation by pathogen-associated pattern recognition receptors and the inflammatory milieu. However, with advancing technology the developmental origins of these 3 major subsets has become increasingly complex, particularly given many of the original proposed unique subset markers are now found to be shared. It is also now understood both macrophages and DCs also develop independently of monocytes(367). Consequently, much debate regarding which subsets represent distinct cell types and which are simply modified versions of the same cell type has arisen. Inflammation complicates this further, as this induces phenotypical changes (368). As such, these subsets also display a high degree of functional overlap and plasticity, with roles in homeostasis, immune defence, and tissue repair and clearance of cellular debris reported. It is suggested a system based upon ontogeny with consideration to the location, function and phenotype of mononuclear cells may provide a more robust approach to their classification(367). The following sections broadly consider the functions of the monocyte and macrophage subsets. DCs are not considered here as in the decidua macrophages are the most important professional APCs in the decidua, with DCs otherwise appearing relatively sparse(369).

6.1.2 Monocytes

Monocytes represent a diverse population of cells primarily located in the circulation, bone marrow and spleen. Circulating monocytes, comprise 5–10% of peripheral blood leukocytes, and traditionally are defined upon the basis of morphology and cytochemistry, demonstrating significant variability in

size, granularity and nuclear morphology. More recently flow cytometry has been utilised, with monocytes sub-classified based upon expression patterns of the lipopolysaccharide receptor (CD14) and the Fc γ -III receptor (CD16). Three distinct human subsets have subsequently been identified: classical (CD14⁺⁺CD16⁻), intermediate (CD14⁺⁺CD16⁺), and non-classical (CD14⁺CD16⁺⁺) (370).

Peripherally, 'classical monocytes' are highly predominant (90%), with 'non-classical' monocytes representing the main alternative fraction (10%). Most functional studies have focussed upon these two subsets, with classical monocytes recognised as key mediators of the direct innate effector immune response, phagocytosis and tissue remodelling, releasing a range of inflammatory effector CKs in a TLR-dependent manner following pro-inflammatory LPS stimulation. Classical monocytes initiate innate immune responses by internalization, phagocytosis, and killing of pathogens and concurrently produce a wide range of costimulatory molecules, inflammatory CKs and chemokines. As a result, the activation of the adaptive immune response by soluble immune mediators, co-stimulatory molecules, and antigens presented by MHC I or II on APCs subsequently arises (371). Furthermore, in response to inflammation, classical monocytes extravasate to these sites and secrete acute pro-inflammatory CK such as IL-6, nitrous oxide (NO), and TNF- α .

The 'intermediate' subsets, which are found at very low frequencies, have gained increased attention as they too display unique features with increased inflammatory capacity, characterised by increased MHC II and TNF- α (372). Albeit not well understood, a potential highly diverse role for these intermediate monocytes is suggested, with CD14⁺⁺CD16⁺ monocytes linked to Ag processing and presentation, inflammation, monocyte activation, and angiogenesis (373).

Non-classical monocytes present later during inflammation (374). Functionally, these subsets appear less phagocytic, with roles in tissue patrolling to remove virally infected or injured cells, antigen presentation and innate surveillance anticipated. There is a suggestion that non-classical monocytes, as opposed to intermediate monocytes, are prepared to move out of the circulation due to their enhanced expression of genes relevant to adhesion and trans-endothelial migration (375, 376).

In vitro experiments have also shown that CD16+ monocytes are more mobile than CD16- cells, albeit their recruitment kinetics, function and differentiation capacity still remain less clear (375). It

It has been suggested these 3 monocyte subsets represent sequential maturation stages in the differentiation of peripheral monocytes; namely, classical monocytes originate from the bone marrow and mature into non-classical monocytes via intermediate monocytes (370). Whether intermediate subsets are more similar to their classical or non-classical counterparts is not entirely clear (374, 377). As summarised in Figure 6.0, both non-classical and intermediate subsets are postulated to replenish tissue resident macrophages and DCs, particularly within the context of inflammation(378).

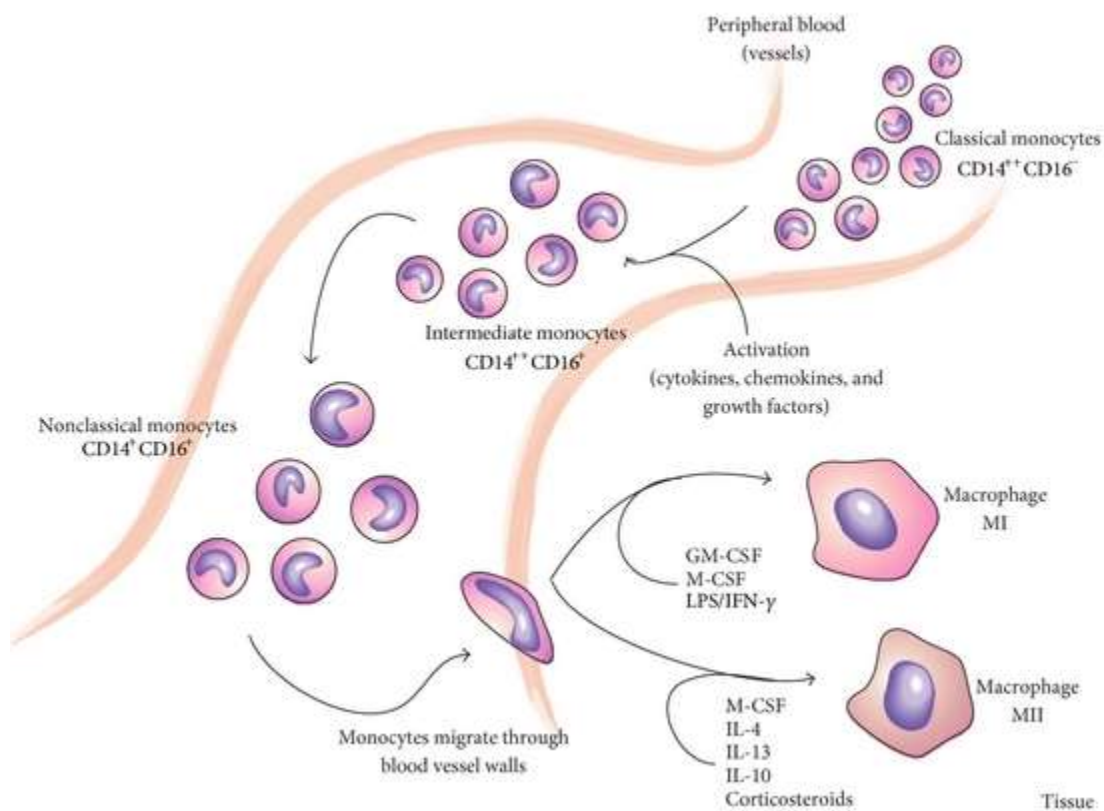


Figure 6.0 Differentiation of monocytes to tissue macrophages. This includes sub-classification of the three distinct human monocyte subsets in peripheral blood: classical (CD14+CD16-), intermediate (CD14++CD16+), and non-classical (CD14+CD16+). Following migration through the blood vessel walls into tissue, macrophage differentiation occurs with two distinct macrophage subsets defined here (MI and MII). Their polarisation is dependent upon the local cytokine milieu present. Revised from A Eljaszewicz *et al* (379).

6.1.3 Macrophages

Macrophages are large vacuolar cells, which reside in most tissues throughout the body. Classically they are recognised for their key roles in phagocytosis; protecting the host from pathogens and mediating clearance of apoptotic cells, cellular debris and pathogens. As key effectors for both the innate and adaptive immune system, macrophages represent important inflammatory mediators (380). However crucially they also demonstrate anti-inflammatory properties, with roles in the resolution of the inflammation and tissue homeostasis demonstrated (381).

Macrophages are extremely heterogeneous, which reflects their high sensitivity to the local environmental milieu. Traditionally, they were broadly categorised into two main subsets; classically activated 'M1' and alternatively activated 'M2' macrophages based upon their phenotype and functional characteristics. M1 macrophages are elicited through pro-inflammatory stimulation with IFN- γ , select CK such as TNF- α , and microbial products such as LPS via CD14. They are traditionally considered microbicidal and pro-inflammatory with a high capacity for antigen presentation and elevated production of reactive oxygen intermediates and NO (382).

M2 subsets demonstrate a much broader range of activities, and may be induced by a range of stimuli including IL-4, IL-10, IL-13, IL-33, TGF- β , and G-CSF. Principally they are anti-inflammatory with enhanced pro-regulatory properties. They are also implicated in angiogenesis, resolution of inflammation and tissue repair.

The robustness of this dichotomous M1/ M2 classification has received increased scrutiny; recent technological advances have provided a more detailed immunological insight into the complex mononuclear phagocyte system. Genome-scale data and meta-analysis of macrophage/DC datasets, including those polarized with different stimuli, failed to identify any set of genes equivalent to the proposed markers of the M1 or M2 activation. Further sub-categorisation definitions have since been proposed (383), however due to their increased complexity, the overall utility is questioned, particularly given differentiation appears driven by the local cellular milieu. It may be more informative to consider these subsets from a tissue specific perspective given their functional

variance. Furthermore, macrophages transition between states, rather than remaining committed to a single activation state, driven by the local tissue micro-environment.

6.1.4 Monocytes in pregnancy

Our understanding of circulating monocytes in normal human pregnancy remains limited. An important functional role is anticipated, as with advanced GA an increased number of circulating monocytes is identified. These display phenotypic activation, measured by significant upregulation of both CD11b and CD14. Despite previous assumptions that the syncytiotrophoblast forms an impenetrable barrier preventing access of maternal cells to fetal antigens, this is not true. The placental anatomic arrangement in reality introduces multiple possibilities for monocyte exposure and activation by fetal trophoblast and their respective antigens. Continual shedding of apoptotic syncytial nuclear aggregates and underlying trophoblast into the systemic maternal circulation is clearly demonstrated, with several grams expelled daily by the third trimester (224).

There is reasonable evidence to suggest these circulating subsets infiltrate the decidua at the onset of pregnancy and differentiate to tissue macrophages. Whether these cells represent classical, non-classical or intermediate subsets is uncertain. Both non-classical and intermediate monocytes have been implicated in pregnancy, with the combined percentage of these cells increased compared to non-pregnant controls. However recent reports of an increased preponderance of classical monocytes now oppose this (384).

Monocyte function is also anticipated to be altered within the context of human pregnancy; in particular the phagocytic function of monocytes appears decreased, with a greater preponderance to CK secretion and antigen presentation reported (376). Consistent with this, pregnant women are more susceptible to infections, which are often more severe (385). LPS stimulated monocytes obtained from pregnant women also demonstrate reduced CK production, becoming tolerant to activation. Conversely, co-stimulation with LPS and IFN- γ leads to increased CK production, including IL-1 β , TNF- α , IL-6 and IL-12. It appears IFN- γ , abrogates LPS tolerance, which may suggest monocyte activation and CK production are enhanced in pregnancy (386).

6.1.5 Macrophages in pregnancy

Macrophages comprise around 20% of the total CD45+ immune cell population within the decidua, and approximately 10% of total decidua cells. Unlike uNKs they remain relatively constant across gestation residing in close proximity to uNKs, T-cells, stromal cells, EVT and maternal spiral arteries. A key role in all stages of pregnancy, throughout fetal development, parturition, and postpartum uterine involution is subsequently anticipated.

Although circulating monocytes are considered likely precursors, once within the decidua macrophages develop a unique pattern of gene expression comparative to their peripheral counterparts. CK, chemokines and pregnancy hormones appear significant for mediating their recruitment and regulation (387, 388). In ovariectomised mice, migration appears significantly decreased with administration of estrogen shown to restore normal recruitment (389).

Exposure to the local tissue microenvironment subsequently drives monocyte differentiation to tissue-specific macrophage subsets, which as pregnancy progresses become increasingly heterogeneous. Defining the phenotype of these tissue resident cells remains a significant challenge despite detailed analysis using transcriptome and methylation profiling, flow cytometry, and immunohistochemistry (383). This reflects both their poor uniformity with either an M2 or an M1 signature, and the potential co-presence of several small sub-populations (390).

A range of functional activities for decidual macrophages have been identified (391). In the non-pregnant endometrium key roles in menstruation are cited. In pregnancy, macrophages appear concerned with implantation, placentation, fetal development, and parturition (392, 393). They also demonstrate immuno-regulatory properties against invasive fetal EVT, promoting fetal trophoblast tolerance and anti-inflammatory CK production. They do also produce an abundance of pro-inflammatory CK, indicating they are not simply concerned with immune regulation.

Utilising detailed microarray analysis, Houser *et al* identified two highly distinct first trimester decidua subsets based upon their relative expression of CD11c (390). The CD11c^{HI} were predominant, expressing less phagocytic receptors, CD209 and CD206, compared to those CD11c^{LO}. The CD11c^{HI}

macrophages expressed genes involved in invasion, mobility, inflammatory processes including lipid metabolism, and anti-apoptotic effects, whereas CD11c^{LO} macrophages expressed genes concerned with growth regulation and development, and cell signalling. Interestingly, the subsets did not differ in phagocytic capacity; albeit CD11c^{HI} appear the major APCs (390).

6.1.6 Monocytes, macrophages and disorders of malplacentation

Monocytes and decidual macrophages have also been implicated within the context of malplacentation, albeit the data remains limited. The reported changes in monocytes support the notion pregnancy is a pro-inflammatory condition, which is more prominent in PET (393). Monocyte activation appears more prominent, as characterised by increased CD11b, CD14, and CD64 expression (235). This has been linked with increased free radicals and pro-inflammatory CK production, marked upregulation of TLR-4, and LPS hyper-responsivity (384). However, studies investigating whether total monocyte frequencies are increased have been inconsistent, with both up and downregulation reported (376).

Within the context of PET, similarly an increased number of 'M1-like' subsets is reported, which reside around the spiral arteries within the decidua. These too appear aberrantly activated, characterised by increased production of pro-inflammatory CK, including IFN- γ , TNF- α , and NO. Importantly, these factors have been shown to disturb trophoblast invasion and increase their apoptotic sensitivity (387, 394). Spontaneous abortion has also been associated with an increased influx of macrophages into the decidual stroma, with an increased rate of trophoblast apoptosis (395). A similar shift towards M1 polarisation was shown to enhance abortion in CBA \times DBA/2 mouse mating's when treated with LPS(396).

6.1.7 Vitamin D and monocyte and macrophage function

The spectrum of vitamin D-mediated non-classical immune responses followed seminal observations of extra-renal 1 α -hydroxylase over-activity in patients with sarcoidosis, characterised by elevated circulating 1,25(OH)₂D₃ and associated hypercalcemia(39). Within the context of tuberculosis infection, vitamin D treatment significantly decreased *M. Tb* growth, and this was

enhanced in the presence of IFN- γ stimulation. Later this was found to arise in a TLR-dependent manner, with concomitant upregulation of CYP27B1 and VDR (44). TLR-activation induced cathelicidin antimicrobial peptide expression, which is crucial for macrophage-mediated defence.

Importantly, intracrine activation of vitamin D promotes antibacterial responses beyond simple induction of cathelicidin and other antibacterial proteins such as β -defensins (397). These include the induction of autophagy(398) and possible effects on intracellular iron concentrations via the iron export modulator hepcidin (399). Antimicrobial activity induction by vitamin D is not simply restricted to TLR-mediated signalling however and can involve other pathogen recognition receptors and antibacterial proteins (45, 400). The efficacy of subsequent antibacterial activity dependent upon the availability of 25(OH)D3 for intracrine conversion to 1,25(OH)₂D3, with vitamin D status appearing a key determinant. As such, low serum 25(OH)D3 restricts monocyte antibacterial activity, with an increased risk of infection evidenced (401).

In human blood monocytes pre-treatment with physiological concentrations of 25(OH)D3 or 1,25(OH)₂D3 inhibits LPS-induced p38 phosphorylation in a dose-dependent manner, with a significant decrease in IL-6 and TNF- α transcripts measured (402). Vitamin D may also actively regulate immune activation, as 1,25(OH)₂D3 is shown to potently downregulate expression of monocyte TLR-2 and TLR-4, thereby suppressing potential downstream pro-inflammatory responses (403). Vitamin D may also serve to control immune activation and prevent over-reactivity.

Vitamin D also modulates innate immune responses by affecting macrophage antigen presentation. Specifically, 1,25(OH)₂D3 promotes the differentiation of monocytes into macrophages, but inhibits the maturation of DCs by attenuating antigen presentation, thereby suppressing their capacity to present antigen to effector T-cells(330).

Whether vitamin D-mediated monocyte effects are enhanced following LPS stimulation has not yet been explored. An immuno-regulatory role may be anticipated, as in murine IFN- γ activated macrophages, 1,25(OH)₂D3 selectively suppressed key innate and inflammatory effector functions, including microbicidal activity, superoxide anion production, CCL5, CXCL10, CXCL9, and TLR-

2(404). However, it appears macrophages at different sites demonstrate differential responsiveness to 25(OH)D₃. Pulmonary alveolar macrophages convert 25(OH)D₃ to 1,25(OH)₂D₃ in the presence of IFN- γ stimulation. Unstimulated bone marrow subsets were capable of producing 1,25(OH)₂D₃, but this was enhanced 3-5 fold with stimulation (405).

Demonstration of a vitamin D-dependent response in monocytes and macrophages raises the possibility that similar innate immune responses will be present in decidua resident subsets (406). Purification of decidual cells into non-adherent stromal cells and adherent cells, which includes decidual macrophages, indicates adherent cells demonstrate a greater capacity for 1,25(OH)₂D₃ production(305). It seems likely macrophages will play a significant role in the localised generation of 1,25(OH)₂D₃ within the decidua.

The mechanisms regulating local synthesis of 1,25(OH)₂D₃ vary considerably and are not yet fully understood. Within the placental trophoblast, induction of cathelicidin and subsequent bacterial killing by 25(OH)D₃ appears to arise via constitutive expression of 1 α -hydroxylase, which is not enhanced further by TLR activation. Conversely, in keratinocytes, 1 α -hydroxylase expression is enhanced following TGF- β stimulation, with upregulation of TLR-2 and TLR-4 observed.

As yet, it is not clear whether similar pathogens and the associated antimicrobial responses will be evident in the decidua. Indeed, it is possible that decidual vitamin D will support alternative antimicrobial responses including potential antiviral activity(407). Decidual monocytes and macrophages may promote the same antibacterial responses observed for equivalent cells from the peripheral blood to combat infection by pathogens such as *Listeria monocytogenes* and Group B *Streptococcus*. Studies using un-purified first-trimester decidual cells have shown 25(OH)D₃- and 1,25(OH)₂D₃-mediated induction of cathelicidin (306). However, beyond their established innate antimicrobial activity, macrophages also play a pivotal role in tissue inflammation and antigen presentation, and both of these facets of immunity are crucial to normal decidual function.

6.2 Results

6.2.1 Distribution of decidua immune cells: comparative analysis with matched peripheral maternal blood and fetal cord blood – third trimester

Having demonstrated that within the decidua a unique immune cell population resides in the first trimester, third trimester analysis was performed. Distinctly, this included paired fetal cord blood obtained at the time of delivery alongside maternal peripheral blood. The relative proportion of major innate and adaptive immune cell subsets was subsequently assessed in matched decidua, maternal blood and cord blood from ‘low-risk’ pregnant women (n=4) at the time of elective caesarean section (ELCS)(>37w).

A similar gating strategy to that utilised in Chapter 5 was applied, with decidua, maternal and cord frequencies of APCs, NKs, CD4+ T cells, CD8+ T cells and B cells summarised in Figure 6.1. In the decidua, NKs were no longer predominant representing 27.9% (\pm SD12.9) of the CD45+ immune cell cohort, with APCs representing 4.1 % (\pm 1.7). T cells were the major immune subset (38.0% \pm 8.1), of which 14.4% (\pm 9.6) were CD4+ and 12.8% (\pm 9.5) CD8+. In the maternal blood, 15.4% (\pm 12.4) of CD45+ cells were of NK origin, with 3.0% (\pm 3.3) APCs. Consistent with our first trimester findings, CD3+ T cells were predominant representing 57.5% (\pm 12.7) of CD45+ cells. Here 17.4% (\pm 4.9) were CD4+, and 20.1% (\pm 6.9) CD8+. Similarly, in the cord blood NKs represented 13.0% (\pm 5.1) of the CD45+ population, with 4.7% (\pm 4.1) APCs. Similarly, CD3+ T cells were predominant, representing 45.2% (\pm 10.6) of CD45+ cells; 8.8% (\pm 9.0) were CD4+ and 10.8% (\pm 7.1) CD8+.

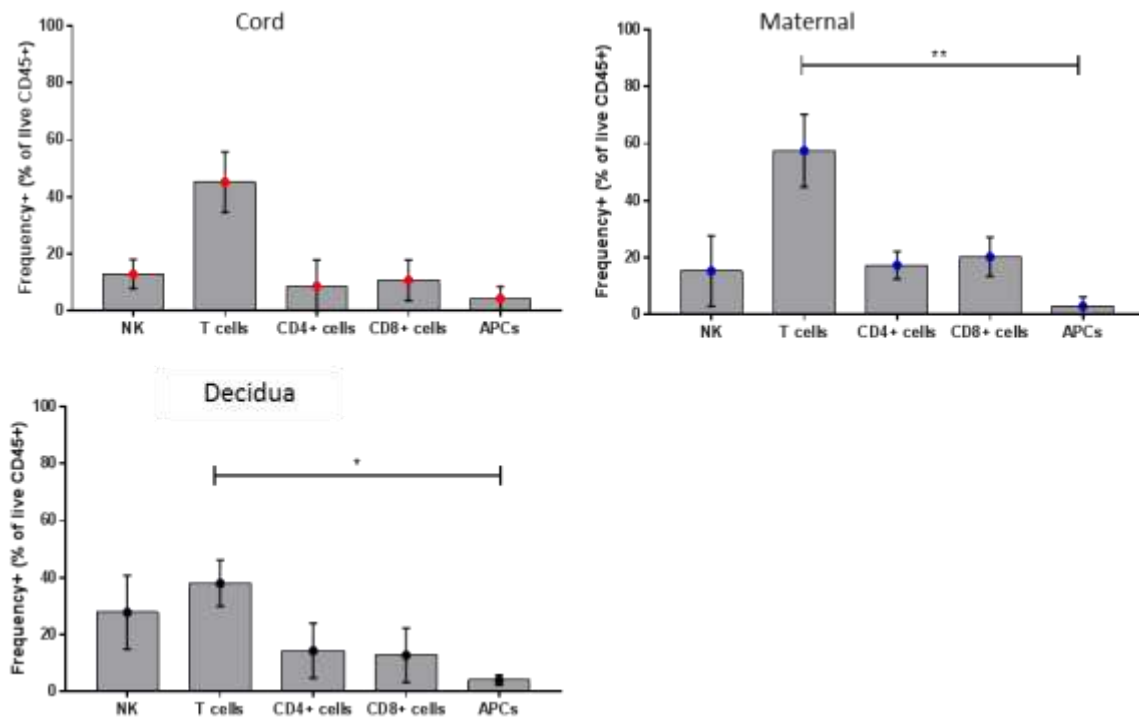


Figure 6.1 Comparative analysis of the relative proportion of CD45+ immune cell subsets in paired third trimester umbilical cord (vein) blood, maternal blood and decidua tissue samples. Mean values with bars denoting standard deviation are illustrated. Non-parametric Friedman test was performed. Statistically significant variations are indicated, * $p < 0.05$, ** $p < 0.01$. A comparative analysis of paired cord (red), maternal blood (blue) and decidua (black) CD45+ immune cell subsets, using flow cytometry, is shown. Relative frequencies (%) are summarised in their respective bar chart ($n=4$), including natural killer cells (NK), T cells, CD4+ T cells, CD8+ T cells and antigen presenting cells (APCs).

6.2.2 Comparative analysis of monocyte and macrophage subsets in decidua and maternal blood – first trimester analysis

Consistent with our findings in Chapter 5, no significant difference in the frequency of CD14+ cells as a percentage of total CD45+ cells was measured in first trimester paired maternal blood (9.4%; IQR 5.1-11.9) and decidua (13.3%; 7.1-18.7).

GA (w)	Decidua (%)	Maternal blood (%)
8+2w	5.39	7.06
9+3	12.6	18.7
10+2w	4.72	7.87
10+2 w	9.41	2.26
12+2w	11.2	4.35

Table 6.0 First trimester CD14+ cell analysis in paired decidua and maternal blood. The gestational age (GA) (weeks; w) and relative frequency of first trimester CD14+ cells in paired decidua and maternal blood, as a percentage (%) of the total CD45+ cell population, is summarised.

The proportions of non-classical (CD14+CD16++), intermediate (CD14++CD16+) and classical (CD14++CD16-) subsets were subsequently measured. This was assessed without an initial ficoll purification step, as this has previously been reported to decrease relative CD14++CD16- classical monocyte expression, with a concomitant expansion of CD14+ CD16++ non-classical monocytes (408).

Whole lymphocyte populations were gated as live CD45+ cells, negative for CD3, CD66b, CD56 and CD20, with those identified cells sub-categorised according to relative CD14 and CD16 expression. An example of the gating strategy utilised is summarised in Figure 6.2.

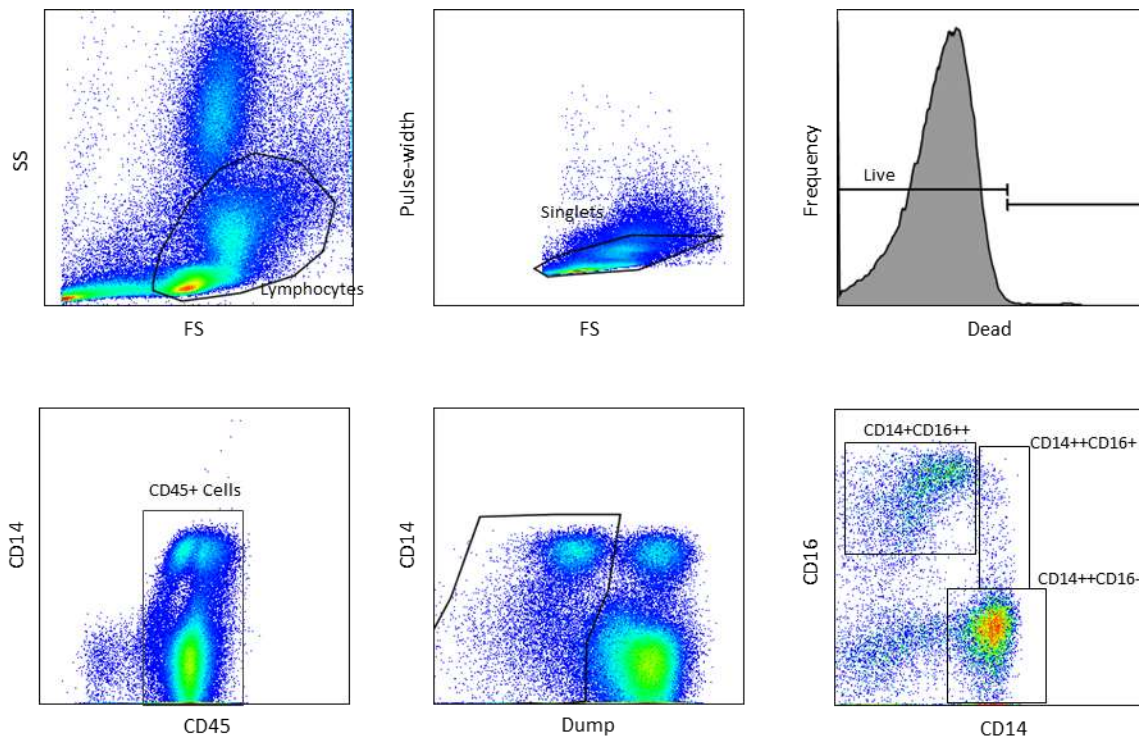


Figure 6.2 Summary of the flow cytometry gating strategy utilised to classify maternal and decidua derived whole lymphocyte subsets according to their expression of recognised mononuclear cell markers. The gating strategy was utilised to identify live CD45+ which were negative for CD66b, CD3, CD20 and CD56 ‘dump’. The negative population was subsequently subclassified according to CD14 and CD16 surface marker expression to identify CD14+CD16- (classical), CD14++CD16+ (intermediate) and CD14+CD16++ (non-classical) subsets.

As summarised in Table 6.1, this was assessed across a range of gestations (w), with the relative frequency (%) reported as a proportion of total CD14+ cells.

GA (w)	Decidua CD14++CD16+	Decidua CD14++CD16-	Decidua CD14+CD16++	Maternal CD14++CD16+	Maternal CD14+CD16-	Maternal CD14+CD16++
8+2	15.5	70.3	13.4	4	76.4	17
9+3	22.7	62.6	8.58	0.94	85.5	13.3
10+2	8.45	79.4	10.1	4.33	66.3	26.3
10+2	54.1	30.1	3.57	5.1	49.8	44
12+2	37.5	49.3	8.18	5.95	56.8	34.9
25% C	11.98	39.7	5.875	2.47	53.3	15.15
Median	22.7	62.6	8.58	4.33	66.3	26.3
75% C	45.8	74.85	11.75	5.525	80.95	39.45

Table 6.1 Summary of the relative frequencies of first trimester decidua and paired maternal blood subsets according to CD14 and CD16 expression. The relative frequencies of decidua and maternal subsets, as a percentage of total CD14+ cells, are shown. This includes CD14+CD16- classical, CD14++CD16+ intermediate and CD14+CD16++ non-classical subsets. The gestational ages (GA) (weeks; w) of each participant is shown. To summarise the data, the median and interquartile range (25th – 75th percentile [C]) have been utilised.

Overall, the median frequency of classical CD14++CD16- subsets was similar with 62.6% (39.7 – 74.8) in decidua and 66.3% (53.3 – 81.0) in maternal blood. Conversely, non-classical CD14+CD16++ subsets represented 8.58% (5.9- 11.8) of decidual CD14+ cells and 26.3% (15.2 – 39.5) in maternal blood. The intermediate CD14++CD16+ subsets represented 22.7% (12.0 – 45.8) of CD14+ cells in decidua, but only 4.3% (2.5 – 5.5) in maternal blood. No significant difference in each subset was measured between the two sites.

6.2.3 Comparative analysis of monocyte and macrophage subsets in decidua, maternal and cord blood – third trimester analysis

As summarised in Table 6.2, the frequency of CD14+ cells was assessed in paired third trimester (>37w) maternal blood, cord blood and decidua samples utilising flow cytometry (n=4).

Decidua	Maternal blood	Cord blood
11.2	7.18	11.2
15.4	8.32	8.24
13.8	12.1	16.5
19.2	4.26	7.84

Table 6.2 Relative frequencies of third trimester CD14+ cells in the decidua, maternal blood and cord blood. The relative frequency of third trimester CD14+ cells in paired decidua, maternal blood and cord blood, as a percentage (%) of the total CD45+ cell population, is summarised.

No significant difference in the median frequency of CD14+ cells was measured, with 7.8% (5.0-11.2), 9.7% (7.9-15.2) and 14.6% (11.9 –18.3) in maternal blood, cord blood and decidua respectively. The proportion of non-classical (CD14+CD16++), intermediate (CD14++CD16+) and classical (CD14++CD16-) subsets were similarly measured utilising the same gating strategy (Figure 6.2). As summarised in Table 6.3, the relative frequency (%) is reported as a proportion of the total CD14+ population. For the decidua, no CD14+CD16++ non-classical subset was consistently measured.

Overall, the median frequency expression of classical CD14++CD16- subsets was 14.9% (4.9-19.6), 75.0% (62.5-90.1) and 73.8% (52.8-87.9) in decidua, maternal blood and cord blood respectively. Conversely, intermediate CD14++CD16+ subsets represented 83.7% (78.3-94.5), 7.2% (4.8-8.9) and 2.5% (2.2- 4.2) of CD14+ cells in the decidua, maternal blood and cord blood. In maternal and cord blood, non-classical monocytes represented 16.4% (3.0-16.4) and 17.6% (6.5-41.1). Only a significant difference in the intermediate decidua and cord (p=0.03) subsets was measured.

	Decidua			Maternal			Cord	
	CD14++	CD14++	CD14++	CD14++	CD14+	CD14++	CD14++	CD14+
	CD16+	CD16-	CD16+	CD16-	CD16++	CD16+	CD16-	CD16++
	77.4	20.2	7.12	85	6.97	4.73	73.6	13.5
	97.2	2.52	7.26	64.9	25.9	2.76	74	21.6
	86.5	12.1	9.49	61.7	27.6	2.12	45.8	47.6
	80.8	17.7	3.96	91.8	1.74	2.35	92.5	4.12
25% C	78.25	4.915	4.75	62.5	3.048	2.178	52.75	6.465
Median	83.65	14.9	7.19	74.95	16.44	2.555	73.8	17.55
75% C	94.53	19.58	8.933	90.1	27.18	4.238	87.88	41.1

Table 6.3 Summary of the relative frequencies of third trimester paired decidua, maternal blood and cord blood subsets according to CD14 and CD16 expression. The relative frequencies of

paired third trimester decidua, maternal blood (maternal) and cord blood (cord) subsets (n=4), as a percentage of total CD14+ cells, are shown. This includes CD14+CD16- classical, CD14++CD16+ intermediate and CD14+CD16++ non-classical subsets (maternal and cord blood only). To summarise the data, the median and interquartile range (25th – 75th percentile [% C]) have been utilised.

Considering the effects of GA, in the decidua, the proportion of CD14++CD16+ subsets increased (22.7% to 83.7%), whereas the population of classical CD14++CD16- subsets appeared less prominent (62.6% to 14.9%) (Figure 6.3). The frequency of ‘non-classical’ subsets remained low at all GA. In paired maternal peripheral blood, monocyte phenotype remained relatively consistent.

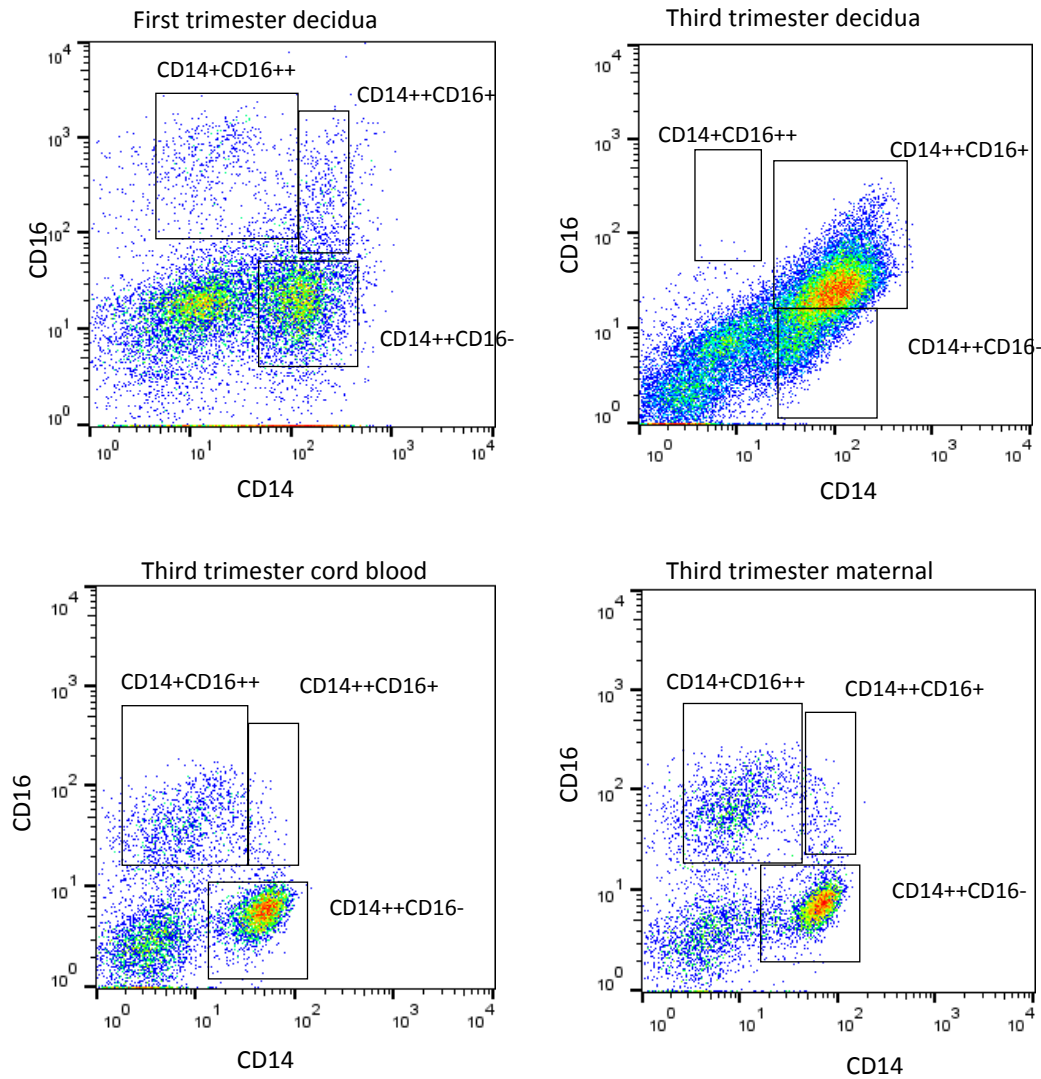


Figure 6.3 Flow cytometry plots of first and third trimester decidua, and third trimester cord and maternal monocyte / macrophage subsets classified according to CD14 and CD16 surface expression. Flow cytometry was utilised to identify CD14+CD16- classical, CD14++CD16+ intermediate and CD14+CD16++ non-classical subsets (maternal and cord blood only), with the same gating strategy utilised as summarised in Figure 6.2. Comparative analysis of first and third trimester decidua subsets is shown in the top row. The bottom row illustrates an example of the third trimester cord and maternal blood subset analysis.

6.2.4 Characterisation of first trimester monocyte and macrophage subsets in decidua and maternal blood

Having characterised the prominent monocyte and macrophage subsets within paired first trimester maternal blood and decidua, more detailed characterisation and comparative analysis of individual subsets was performed. Flow cytometry was utilised to measure the expression of a range of recognised monocyte and macrophage markers to help aid their functional classification, as summarised in Table 6.4. Total frequency (%) was measured, with subtraction of the isotype control to account for variability in the baseline fluorescence of blood and tissue resident subsets (Table 6.5). Classical maternal blood and decidua, and CD14⁺⁺CD16⁺ intermediate decidua subsets were compared since these appeared most prominent. Furthermore, the observed gestational shift (Figure 6.3) in decidua-derived classical and intermediate subsets meant both were of interest.

Marker	Functional Properties
CD209	C-type lectin signalling dendritic cell and macrophage marker – M2 marker - pathogen recognition
HLA-DR	MHC class II cell surface receptor encoded by the human leukocyte antigen complex - expression appears downregulated within the context of inflammatory disease such as sepsis(409)
CD163	Member of the scavenger receptor family – inflammatory mediator and tissue resident marker – expressed exclusively on monocytes and macrophages - M2 marker
CD80	Co-stimulatory signal necessary for T cell activation and survival
CD86	Co-stimulatory signal necessary for T cell activation and survival
TLR-2	Activation receptor - M1 polarisation mediator
TLR-4	Activation receptor – M1 polarisation mediator
Dectin	Lectin-like innate immune receptor. High expression in M2a macrophages, while M2b express low levels – pathogen recognition

Table 6.4 Functional summary of the surface protein markers utilised to characterise monocyte / macrophage subsets. The surface marker of interest and its associated functional properties are briefly outlined as detailed.

Marker	Maternal	Decidua	
	freq (%) (IQR)	freq (%) (IQR)	
	CD14++CD16-	CD14++CD16-	CD14++ CD16+
CD209	16.6 (16.1-34.9)	15.8 (12.1-24.6)	45.4 (37-47.4)
TLR-2	98.4 (97.0-98.9)	75.7 (63.5-85.6)	83.2 (72.1-90.5)
Dectin	94.2 (63.7-97.5)	13.9 (2.2-21.2)	39.6 (29.5-62.0)
CD80	33.9 (18.0-41.3)	17.9 (15.8-38.5)	46.8 (37.2-77.0)
CD86	95.0 (77.1-96.8)	30.2 (24.3-40.0)	38.9 (26.6 - 64.9)
HLA-DR	97.5 (57.9-98.7)	60.3 (56.5-88.5)	91.8 (87.1-99.0)
CD163	93.8 (79.5-97.3)	60.4 (24.7-66.0)	90.2 (88.1-93.4)
CD68	6.1 (0-18.9)	43.5 (24.5-44.7)	69.2 (66.4-69.3)
TLR-4	61.1 (25.7-95.0)	0.7 (0.2- 1.4)	5.5 (3.5-14.4)

Table 6.5 First trimester maternal and decidua subset expression of recognised monocyte and macrophage markers. Summary of the flow cytometric analysis of a range of recognised monocyte and macrophage markers in paired maternal blood and decidua CD14+ subsets; CD14+CD16- classical (maternal and decidua), and CD14++CD16+ intermediate (decidua only). The median frequency (Freq) (%) and interquartile range (IQR) are illustrated for each marker (n=3-5).

Figure 6.4 is included to facilitate interpretation of those with significant differences in expression. HLA-DR expression did not differ in the maternal or decidua subsets with expression relatively consistent. A significant difference in CD209 between the decidua CD14++CD16- and decidua CD14++CD16+ subsets was measured (p=0.01), with higher surface expression in the intermediate (45.4%) relative to classical CD14++CD16- subsets (15.8%). CD209 was also low in classical maternal CD14++CD16- cells (16.6%), but did not reach significance. Conversely, dectin another classical M2 marker was significantly lower in classical decidua C subsets (13.9%) comparative to their maternal blood counterparts (94.2%). Expression in the CD14++CD16+ decidua population (39.6%) was higher than the classical decidua subsets, but again lower than maternal blood.

Conversely, CD163, traditionally an M1 marker, demonstrated highest expression in the classical maternal (93.8%) and decidua intermediate (90.2%) populations. Expression was lower in the

classical decidua subsets (60.4%), albeit this was not significant. Consistent with this, CD80 expression was similar in classical maternal subsets (33.9%) and intermediate decidua subsets (46.8%), whereas classical decidua expression appeared lower (17.9%). However, CD86 expression was notably higher in maternal blood (95.0%) comparative to both classical (30.2%) ($p<0.05$) and intermediate (38.9%) decidua populations.

Considering TLR-4 and TLR-2, recognised M1 markers, both were highly expressed in maternal CD14⁺⁺CD16⁻ subsets, with 61.1% and 98.4% median expression respectively. TLR-4 was notably reduced in both decidua intermediate (5.5%) and classical (0.7%) subsets ($p<0.05$). TLR-2, expression was positive but lower in decidua CD14⁺⁺CD16⁺ (75.7%) ($p>0.05$) and CD14⁺⁺CD16⁻ subsets (72.1%) ($p<0.05$).

Finally, intracellular CD68, a glycoprotein used as a monocyte/macrophage marker was measured. In the decidua CD68 was higher in CD14⁺⁺CD16⁺ cells (69.2%; 66.4-69.2%), relative to those CD14⁺⁺CD16⁻ (43.5%; 24.5-43.5%). In the maternal blood the frequency of CD68 was significantly low (6.05%; 0-18.9%) comparative to paired CD14⁺⁺CD16⁺ from decidua ($p<0.05$).

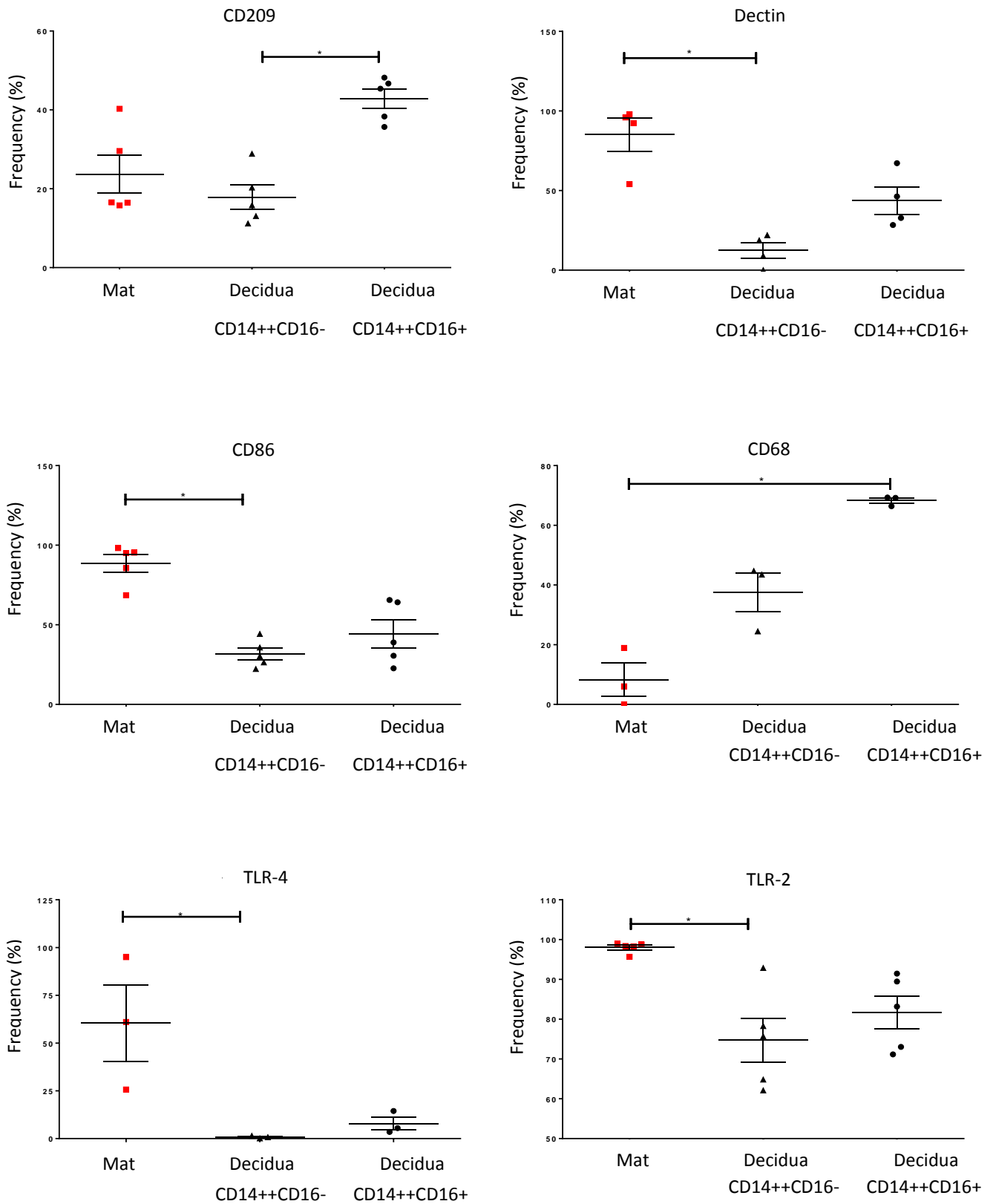


Figure 6.4 Summary of maternal (mat; red) classical CD14++CD16-, and decidua (black) classical CD14++CD16- and intermediate CD14++CD16+ subset expression of monocyte and

macrophage markers; CD209, dectin, CD86, CD68, TLR-4 and TLR-2. Median frequency (%) and interquartile range are shown, with statistically significant variations indicated * p<0.05.

6.2.5 Characterisation of third trimester monocyte and macrophage subsets in paired decidua, maternal and cord blood

	Cord	Maternal	Decidua	
	freq (%) (IQR)	freq (%) (IQR)	freq (%) (IQR)	
	CD14++CD16-	CD14++CD16-	CD14++CD16-	CD14++CD16+
CD209	1.3 (0.02 - 6.99)	3.8 (0.2 - 10.8)	3.1 (1.7-5.5)	26.9 (18.9-40.6)
TLR-2	98.3 (94.9-99.4)	98.2 (94.0 - 98.9)	68.0 (62.0- 75.8)	68.6 (19.1-76.0)
Dectin	85.6 (59.2-97.4)	86.8 (79.2-91.1)	6.2 (0.7-59.9)	41.0 (21.9-70.8)
CD80	6.3 (2.1-9.1)	6.3 (1.7-10.6)	12.2 (6.1-18.3)	63.0 (42.6-69.8)
CD86	43.9 (12.9-69.0)	68.2 (21.0-84.9)	4.9 (1.8-16.1)	32.6 (18.6-70.2)
HLA-DR	56.0 (7.5-87.1)	71.5 (15.0-94.1)	16.1 (5.4-43.9)	60.0 (39.9-91.5)
CD163	39.7 (35.6-42.6)	61.8 (18.1-73.5)	14.2 (4.9-27.8)	73.1 (41.3-88.7)
CD68	0 (0-15.7)	0 (0-36.6)	19.4 (12.8-26.0)	68.1 (61.1-75.0)

Table 6.6 Paired third trimester cord blood, maternal blood and decidua analysis of recognised monocyte and macrophage markers. Summary of the flow cytometric analysis of a range of recognised monocyte and macrophage markers in paired cord blood, maternal blood and decidua CD14+ subsets; CD14+CD16- classical (cord blood, maternal blood and decidua), and CD14++CD16+ intermediate (decidua only). The median frequency (freq) (%) and interquartile range (IQR) are illustrated for each marker (n=3-5).

As for the first trimester analyses, the median frequency of a range of recognised monocyte and macrophage markers (Table 6.4) was assessed. As summarised, HLA-DR expression did not significantly differ between the CD14++CD16- classical cord (56.0%) or maternal (71.5%) subsets or the decidua CD14++CD16+ intermediate (60.0%) subsets. Classical decidua CD14++CD16- HLA-DR expression appeared lower (16.1%) but also variable (5.4-43.9%), and this was not significant. Consistent with the first trimester, CD209 expression appeared higher in the CD14++CD16+ decidua subsets (26.9%) comparative to those classical CD14++CD16- from decidua (3.1%), maternal (3.8 %)

and cord blood (1.3%). Dectin another classical M2 marker was markedly lower in classical decidua CD14⁺⁺CD16⁻ (6.2%) comparative to those in peripheral maternal (86.8%) and cord blood (85.6%). Consistent with the first trimester (39.6%), expression in the intermediate decidua (41.0%) CD14⁺⁺CD16⁺ subsets, albeit higher than the classical decidua subsets, was also lower than those peripherally.

Conversely, CD163 demonstrated higher expression in the decidua CD14⁺⁺CD16⁺ intermediate (73.1%) and maternal CD14⁺⁺CD16⁻ classical (61.8%) subsets. Interestingly, expression appeared lower in the classical cord (39.7%) and decidua (14.2%) subsets. In the third trimester, CD80 expression overall appeared low, in particular for the 2 peripheral classical subsets; 6.3% cord, 6.3% maternal. Expression modestly increased in the decidua in both the classical (33.9%) and intermediate (46.8%) subsets. Consistent with the first trimester data, CD86 expression was higher in maternal blood (68.2 %) comparative to both the classical (4.9 %) ($p < 0.05$) and intermediate (32.6%) ($p > 0.05$) decidua subsets. Cord CD86 expression was moderate; 43.9% median frequency.

TLR-2 was highly expressed in maternal and cord CD14⁺⁺CD16⁻ classical subsets, with 98.2% and 98.3 % median expression respectively. In the decidua expression was moderate for both CD14⁺⁺CD16⁺ intermediate (68.6%)($p > 0.05$) and CD14⁺⁺CD16⁻ classical subsets (68.0 %). A significant difference was measured between the classical cord and classical decidua subsets ($p = 0.04$).

Finally, intracellular CD68, a glycoprotein used as a monocyte/macrophage marker. In the decidua, the median frequency of CD68 was higher in the CD14⁺⁺CD16⁺ intermediate subsets (68.1%), relative to the classical CD14⁺⁺CD16⁻ (19.4%) cells. Conversely, the frequency of CD68 was negligible in both the CD14⁺⁺CD16⁻ classical maternal (0%) and cord (0%) subsets.

6.2.6 Transcript analysis of the Vitamin D metabolic system in third trimester CD14⁺ monocyte and macrophage subsets

House-keeping gene optimisation

Due to the high RNase content in term placental tissue, the reliability of the house-keeping gene employed was assessed. This was particularly important for third trimester LPS-culture assays, since

pro-inflammatory, and hypoxic stimuli have also previously been reported to significantly alter the stability of expression(365). Comparative analysis of cytochrome- c-1 (CYC-1) and 18S, with all samples in triplicate, was performed. CYC-1 in particular has demonstrated good stability in placental tissue obtained from complicated and non-complicated pregnancies at an advanced GA previously (410).

Table 6.7 summarises the expression of both housekeeping genes in third trimester decidua monocyte/ macrophage subsets isolated from decidua, maternal and cord blood following culture for 24h in the presence and absence of LPS. Differential expression of both 18S rRNA and CYC-1 was consistently lower for the decidua-derived subsets comparative to those from cord and maternal blood. Albeit 18s demonstrated higher expression, overall heterogeneity appeared greater comparative to CYC-1. Moving forward CYC-1 was utilised for further transcript analysis.

CD14+ Origin	Treatment	CYC-1	18S
Cord	US	26.16372	17.85442
	US	26.04429	14.05769
	US	26.02066	17.1499
	LPS	26.26224	13.30304
	LPS	26.17989	11.57689
	LPS	26.27441	12.01914
	Maternal	US	24.95721
US		24.94769	11.63523
US		24.83023	12.63691
LPS		27.65986	13.0281
LPS		28.05831	13.07373
LPS		27.83424	14.24646
Decidua	US	30.32088	17.31346
	US	30.60384	16.50863
	US	30.32483	17.34443
	LPS	30.84199	20.0991
	LPS	30.73973	19.38229
	LPS	30.24451	22.2215

Table 6.7 House-keeping gene comparative analysis in third trimester paired cord blood, maternal blood and decidua. Comparative quantitative analysis of the expression of *CYC-1* and *18S* rRNA expression in third trimester decidua, maternal and cord blood CD14+ subsets (performed in triplicate) following 24h culture in the presence and absence (US) of LPS stimulation.

Purity of CD14+ cell isolation

Cord	Maternal	Decidua
(%)	(%)	(%)
93.1	86.7	77.3
76.7	76.6	77.6
87.1	67.9	85.0
74.4	76.5	71.6

Table 6.8 Third trimester CD14+ purity analysis; summary of the purity of matched CD14+ cells as a percentage (%) of the live total CD45+ population, as measured using flow cytometry in cord blood, maternal blood and decidua (n=4).

The median purity for CD14+ isolation in cord blood, maternal blood and decidua samples was 81.9% (75.0-91.6), 77.0% (77.0-84.2) and 77.5% (73.0-83.2) respectively (n=4).

Transcript analysis of the vitamin D metabolic apparatus in CD14+ cells

To ascertain whether isolated CD14+ monocyte / macrophage subsets express the metabolic apparatus required to mediate local 1,25(OH)₂D₃ production and function, qRT-PCR was used to measure *CYP27B1*, *CYP24A1* and *VDR* transcript expression (Figure 6.5). Relative expression to US maternal CD14+ cells was calculated for each transcript to permit comparison.

Expression of *CYP27B1*, the principal catalyst for 1,25(OH)₂D₃, was comparable in the paired US cord (1.4; 1.0-1.8) and US maternal subsets. In response to LPS-stimulation, expression increased in both the cord (4.8; 1.5-29.3) and maternal (9.3; 3.0-17.6) derived subsets. However, in the decidua higher baseline *CYP27B1* expression was measured in US subsets (4.3; 1.4-17.9) with no concomitant increase post LPS-stimulation (2.5; 0.3-22.1). No significant effect of 1,25(OH)₂D₃ upon *CYP27B1* was measured in all three subsets (n=4), thus 1 α -hydroxylase activity does not appear driven by vitamin D status.

Relative to US maternal CD14+ subsets, US cord (1.7; 0.6-2.2) and decidua (1.5; 1.4-2.5) *VDR* transcript expression was again similar at baseline. Consistent with *CYP27B1*, *VDR* expression

increased in response to LPS in both the cord (6.9; 4.1-20.3) and maternal (5.4; 4.2-7.0) cells, albeit not reaching statistical significance. No significant effect of 1,25(OH)₂D₃ upon *VDR* was measured in decidua. Interestingly a similar upregulation of *VDR* in response to LPS was not evident in the decidua (0.7; 0-1.7), with low expression measured across all four culture conditions.

Considering *CYP24A1*, relative expression appeared low in US cord (0.04; 0-2.0) and maternal (1.2; 1.0-1.1) subsets comparative to US decidua CD14⁺ cells (12.0; 1.9-541.9). As postulated, 1,25(OH)₂D₃ significantly induced expression of the catabolic enzyme in US cord (3573; 1103-8626), maternal (1988; 401-10040) (p=0.02) and decidua (738.1; 101.4-1493) (p=0.02) subsets. In the co-presence of LPS, *CYP24A1* expression notably increased in the cord (10354; 1783-39158) (p=0.003) and maternal (3707; 218.3-28110) (p=0.02) subsets, whereas in decidua lower relative expression was measured (122; 32.3-369.0) despite higher baseline levels.

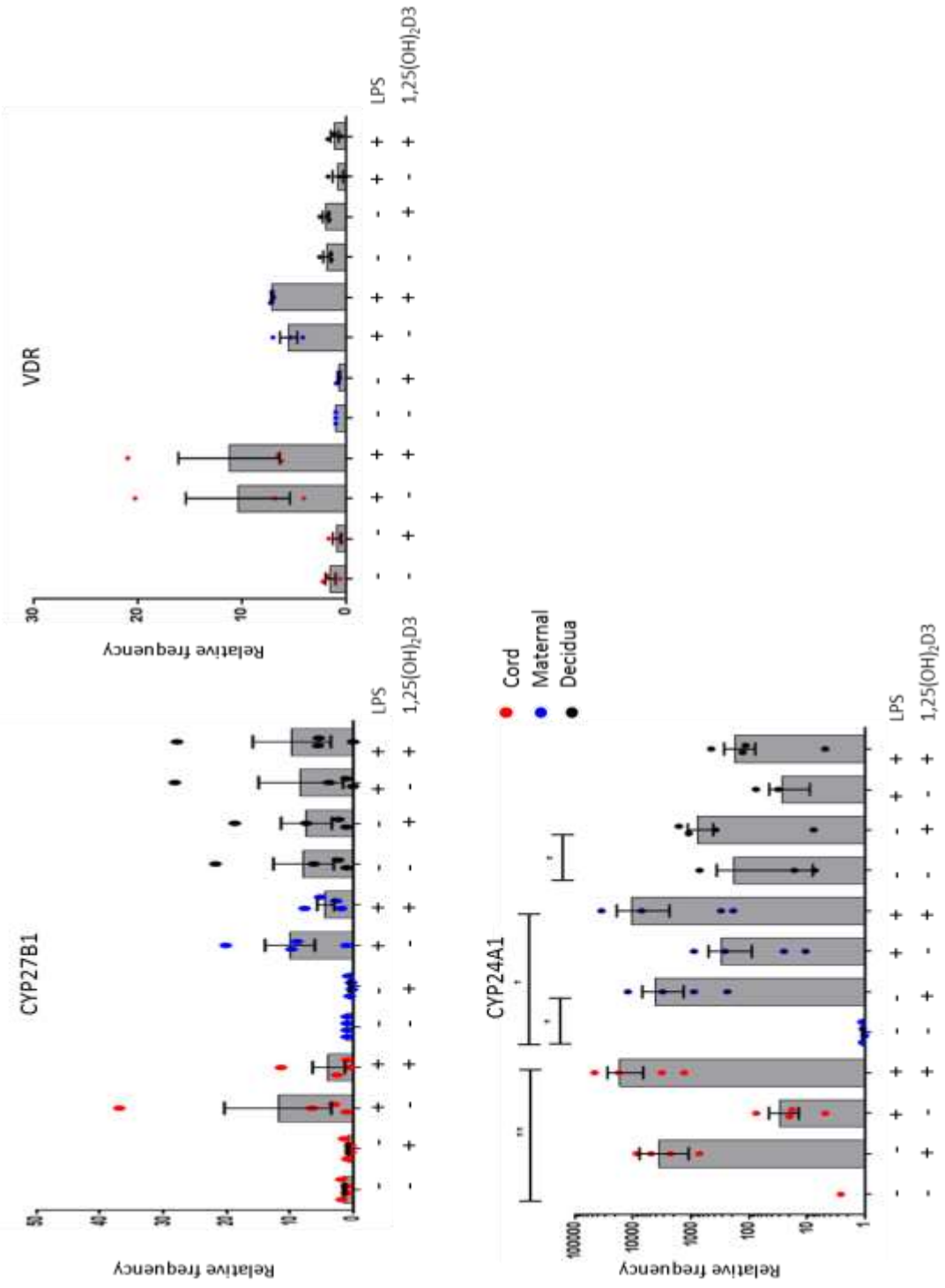


Figure 6.5 Transcript analysis of the vitamin D metabolic system in cord blood, maternal blood and decidua-derived CD14+ cells. Transcript expression analysis of *CYP27B1*, *VDR*, and *CYP24A1* in isolated unstimulated (-) and LPS stimulated (+) CD14+ cord (red), maternal (blue) and decidua (black) subsets in the presence (+) and absence (-) of 1,25(OH)₂D3. Relative expression comparative to US maternal CD14+ subsets. Mean values with standard error of the mean are illustrated.

Functional transcript analysis of paired cord, maternal and decidua CD14+ Cells

To delineate the potential functional role of vitamin D in pregnancy-derived CD14+ subsets, a range of recognised vitamin D responsive (*cathelicidin*) and LPS- responsive (*TNF- α* , *IFN- γ* and *IL-6*) transcripts were assessed. Cathelicidin, a recognised anti-microbial peptide target for vitamin D, was upregulated in response to 1,25(OH)₂D₃ in both the cord (78.7; 42.8-79.3) and maternal (50.7; 46.5-51.0) –derived subsets. In the decidua, this response was not evident (7.1; 3.9-20.4), with minimal induction comparative to US decidua subsets (3.9; 2.2-7.0) (Figure 6.6).

IFN- γ expression was consistently low in all maternal and cord subsets in the presence and absence of LPS and 1,25(OH)₂D₃. Conversely, decidua CD14+ group demonstrated relatively high *IFN- γ* transcript expression as baseline (174.2; 86.9-213.3), with marked induction (242.9; 209.9-476.7) in response to LPS. In the presence of 1,25(OH)₂D₃, expression was less marked in both US (21.6; 0 – 60.0) and LPS-stimulated (49.7; 48.3-92.6) groups, albeit not significant (Figure 6.6).

IL-6, a recognised innate immune marker in peripheral monocytes (411), was markedly upregulated in both cord (12821; 1927-35276) and maternal (3317; 923.2- 34676) CD14+ subsets in response to LPS. Notably, albeit the decidua-derived subsets demonstrated constitutively higher expression at baseline (2978; 241.2-18781), no LPS-induced upregulation was observed. In response to 1,25(OH)₂D₃ and LPS co-treatment, expression decreased in the cord (3166; 1088-10915), maternal (1438; 825.7-14293) and decidua (926.6; 227.6-2306) subsets respectively (Figure 6.6).

Finally, at baseline *TNF- α* expression in US cord (1.4; 0.9 – 2.1) was similar to maternal US subsets. In response to LPS stimulation this increased in both the cord (15.1; 10.3-34.5)($p=0.01$) and maternal CD14+ cells (14.9; 7.0-18.7) following LPS, albeit not significant ($p= 0.08$). No difference in those US subsets co-treated with 1,25(OH)₂D₃ was measured, whilst in the co-presence of LPS, *TNF- α* expression was lower in cord (6.2; 4.3-13.6) and maternal (5.7; 3.3-10.0) subsets. In the decidua *TNF- α* expression was constitutively higher at baseline (12.7; 6.1-23.1), with no significant change in expression in response to LPS (15.1; 10.4-60.0). Vitamin D had no effect upon *TNF- α* expression in US decidua subsets (10.6; 7.9 – 13.3), whilst in the presence of LPS a partial downregulation (6.4; 5.8-10.0) was observed, albeit not significant Figure 6.6.

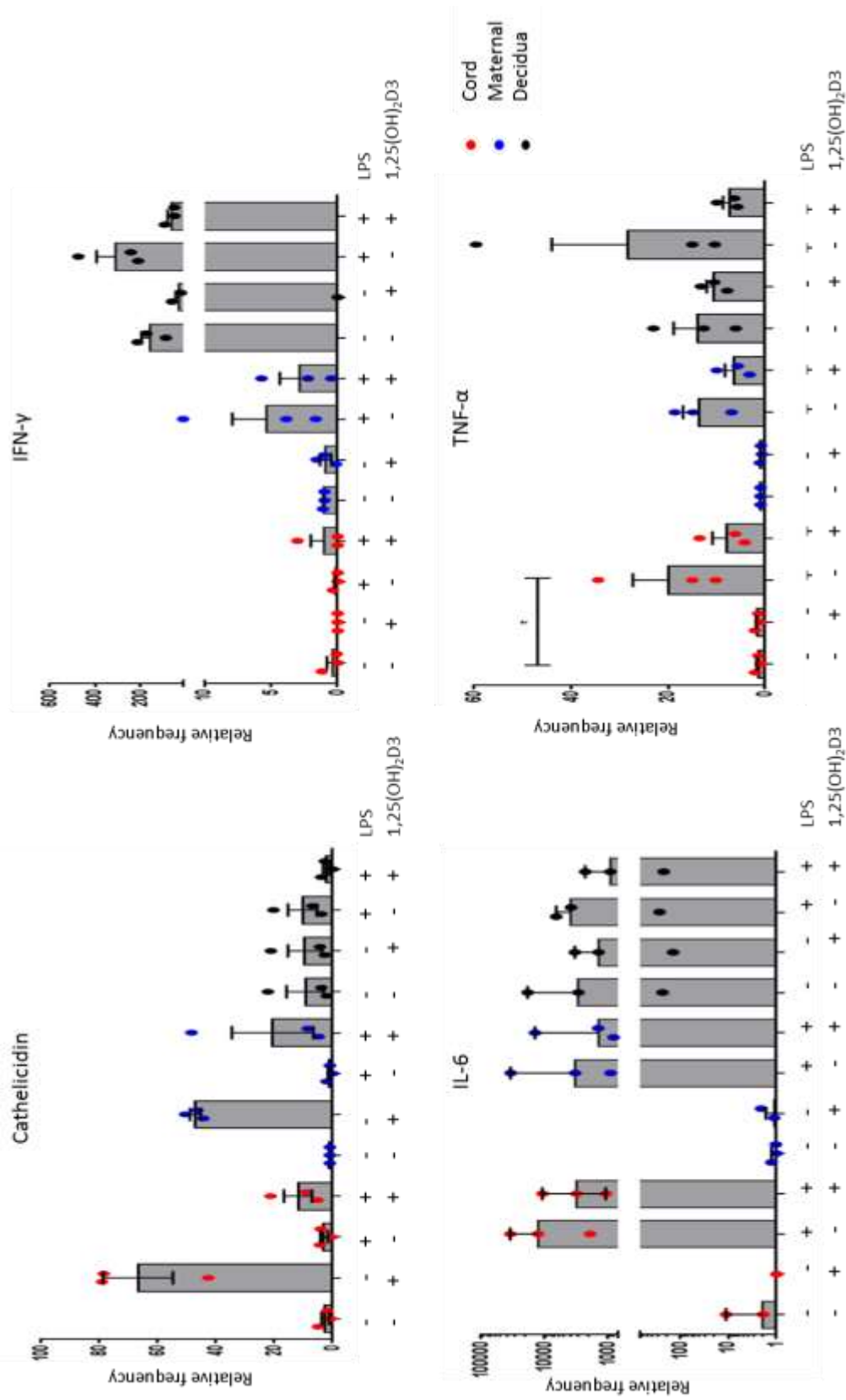


Figure 6.6 Transcript analysis of *cathelicidin*, *IFN- γ* , *IL-6* and *TNF- α* in cord blood, maternal blood and decidua-derived CD14+ cells. Transcript expression analysis of *cathelicidin*, *IFN- γ* , *IL-6* and *TNF- α* in isolated unstimulated (US) (-) and LPS stimulated (+) CD14+ cord (red), maternal (blue) and decidua (black) subsets in the presence (+) and absence (-) of 1,25(OH) $_2$ D3. Relative expression comparative to US maternal CD14+ subsets was calculated. Mean values with bars denoting standard error of the mean are illustrated.

6.2.7 Demographic summary of those participants with samples utilised for RNA-seq analysis

To more accurately elucidate the impact of 1,25(OH)₂D₃ upon third trimester monocyte/macrophages subsets at a transcript level we conducted a genome-wide RNA-seq analysis of matched third trimester subsets isolated from decidua, maternal and cord blood. Consistent with the NK studies performed in Chapter 5.0, this was performed within the context of LPS- stimulation as previous data indicate a greater role for 1,25(OH)₂D₃ within the context of immune challenge(402), certainly for those derived from maternal and cord blood. Participant demographics (n=4) are summarised in Table 6.9, with all women undergoing ELCS.

ID	Age	BMI	Ethnicity	GA at delivery (w)	Smoking	Alcohol	G/ P	Live	Stillbirth	Miscarriage	TOP	Vitamin D (iu)
669	37	22	White European	39+3	No	No	G1P0	0	0	0	0	400
672	29	31	White British	38+1	No	No	G3P2	2	0	0	0	400
676	37	31	White British	39+1	No	No	G2P1	1	0	0	0	400
687	30	22	White European	39+3	No	No	G1P0	0	0	0	0	400

Table 6.9 Demographic summary of third trimester maternal participant's recruited for RNA-seq analysis. Data show: Identification number (ID), age, body mass index (BMI), ethnicity, gestational age at delivery (weeks; w), smoking status, alcohol intake, gravida and parity (G/P), obstetric history; living, stillbirth, miscarriage, termination of pregnancy (TOP), and vitamin D supplementation (units; iu) for the n=4 3rd trimester maternal participants with samples utilised.

6.2.8 Purity of CD14+ FACS-sorted subsets

In total, n=4 participants were included, with matched FACS sorted monocyte/ macrophage subsets cultured with LPS ± 1,25(OH)₂D3 for 24h (n=24 samples for RNA -seq) assessed. FACS sorting was utilised to ascertain purity, with paired live CD45+ CD14+ HLA-DR+ (CD3- CD56-, CD66-, CD19-) cells isolated (n=4) with purity for maternal subsets 97.3% (93.9 – 98.6%), cord 94.7% (85.5 – 96.1%) and decidua 84.0% (82.0 -91.9%) respectively (Table 6.10). As summarised in Table 6.6, surface HLA-DR expression does not appear significantly different in the maternal, cord or decidua subsets (p >0.05).

Study ID	Maternal (%)	Cord (%)	Decidua (%)
669	98.8	94.3	91.9
672	96.7	96.4	83.1
676	93.9	82.6	81.6
687	97.8	95.1	84.7

Table 6.10 Purity analysis of CD14+ subsets from maternal blood, cord blood and decidua.

Summary of the purity of the CD14+ isolation for RNA-seq using FACS. Percentage frequencies (%) are reported as the proportion of live CD45+ CD14+ HLA-DR+ (CD3- CD56-, CD66-, CD19-) cells isolated, as measured by flow cytometry.

6.2.9 Principal component analysis

PCA was performed to the log₂ fold change on the whole dataset (Figure 6.7). Overall this revealed high variance in the transcriptional patterns of purified cord, maternal and decidua-derived subsets, PC1 23.1%, PC2 17.9%, PC3 8.5%, in relation to origin. The maternal and cord-derived subsets consistently clustered more tightly than their decidua-derived counterparts. In all 3 groups, those co-treated with 1,25(OH)₂D3 demonstrated relatively low variance in their whole transcript profiles comparative to those treated with LPS alone.

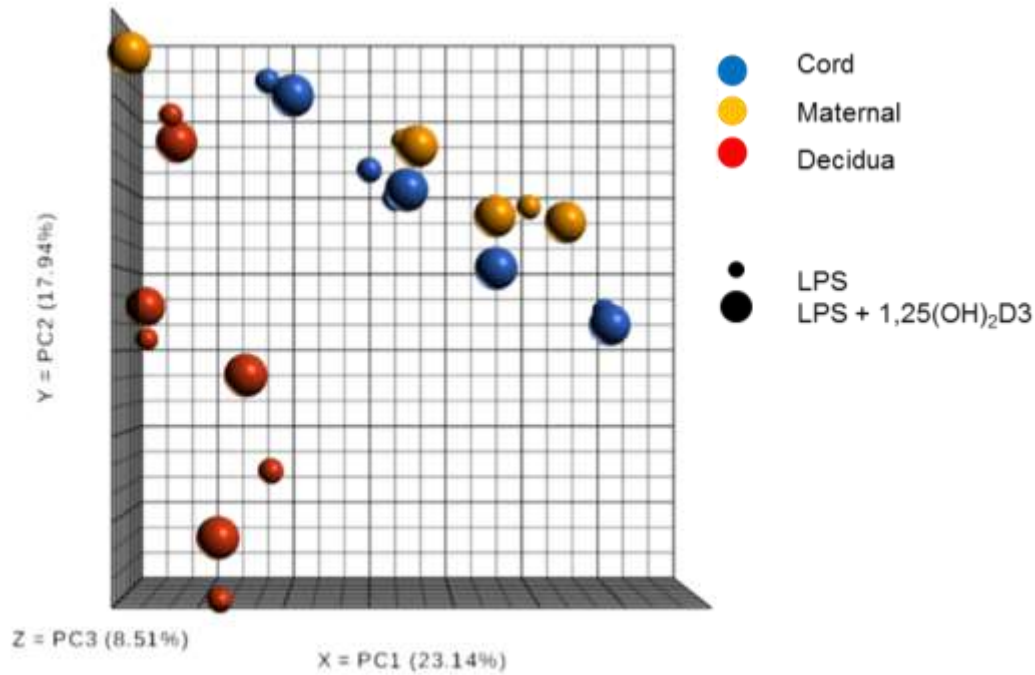


Figure 6.7 PCA analysis of LPS stimulated monocyte and macrophage subsets in the presence and absence of 1,25(OH)₂D₃. The 3D dot-plot summarises the main sources of variance measured across the whole data set by principal components; PC1 23.1%, PC2 17.9%, PC3 8.5% (x-, y-, z- axes respectively) is illustrated for cord blood- (blue), maternal blood- (yellow) and decidua- (red) derived monocyte / macrophage subsets in the presence (large dot) and absence (small dot) of 1,25(OH)₂D₃ co-treatment.

6.2.10 Comparative analysis of LPS treated cord, maternal and decidua monocyte/macrophage subsets.

Prior to treatment with 1,25(OH)₂D₃, comparative analysis of the LPS treated cord, maternal and decidua derived subsets was performed. First, comparing LPS treated peripheral maternal subsets, of the 7735 genes measured, 113 (1.5%) transcripts were significantly upregulated (fold-change >1.5, p<0.05) and 105 (1.4%) downregulated (fold-change <-1.5, p< 0.05) in the cord comparative to the maternal blood (Figure 6.8). Conversely, 846 (10.9%) transcripts were downregulated, and 1616 (20.9%) upregulated in the cord comparative to decidua. Comparative analysis of LPS-decidua versus LPS-maternal blood subsets identified 832 (10.8%) transcripts to be upregulated, and 1515 (19.6%)

downregulated. As summarised in the 2D volcano scatter plots (Figure 6.7), within the context of LPS monocyte transcript expression was highly akin for the cord, and maternal blood subsets, whilst those from the decidua appear highly distinct. As summarised in Figure 6.8, of those transcripts significantly upregulated in the cord comparative to decidua, 1211 (63.0%) were also upregulated in the maternal versus decidua comparative analysis group. Of those transcripts significantly downregulated in the cord comparative to decidua, 591 (54.5%) were similarly downregulated in the maternal versus decidua comparative analysis group.

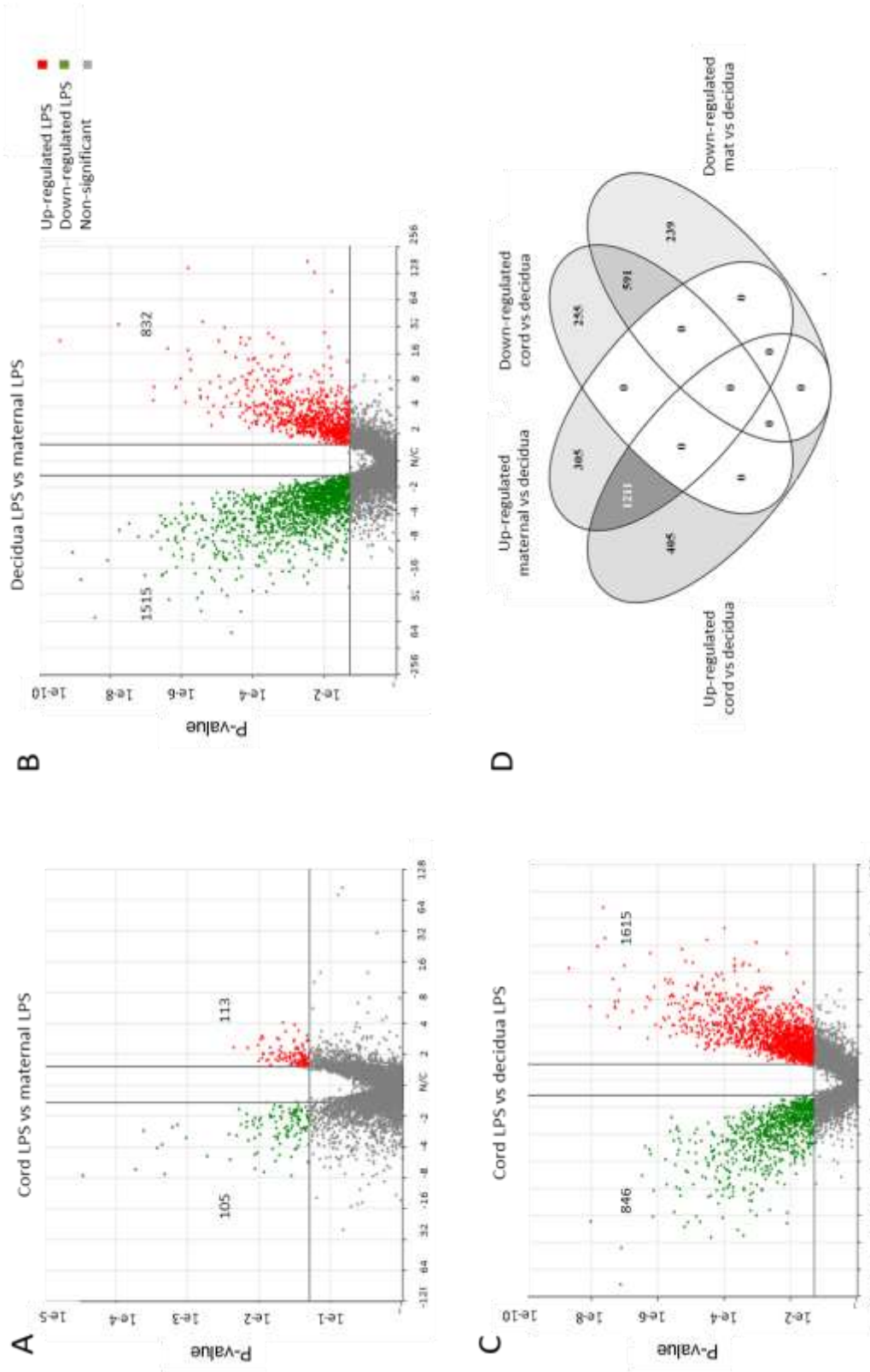


Figure 6.8 Comparative analysis of transcript expression in cord, maternal and decidua monocyte / macrophage subsets . The volcano plots

summarise those significantly differentially expressed gene transcripts ($p \leq 0.05$, fold change ≤ -1.5 or $\geq +1.5$) in paired (A) LPS treated cord vs. LPS maternal, (B) decidua LPS vs. maternal LPS, (C) cord LPS vs. decidua LPS ($n=4$ per site). Significantly upregulated genes are red, downregulated genes green, with those not significantly different in grey. (D) Summary of significant transcript overlaps between maternal LPS vs decidua LPS, and cord LPS vs decidua LPS comparative analyses.

6.2.11 Pathway analysis

To help delineate the differences in transcript expression complementary pathway analysis was performed to assess differences in both cord and maternal LPS monocytes compared to decidua LPS macrophages. Across both the WP (Figure 6.9 and 6.11) and Reactome (Figure 6.10 and 6.12) databases, a broad spectrum of enriched canonical pathways (2.0 fold-change) were identified with those significant ($p < 0.05$) ranked from a high to low Z-score. Overall, in cord 21 WP and 45 Reactome pathways were significantly enriched ($Z\text{-score} > 1.96$) in LPS cord monocytes relative to decidua LPS macrophages.

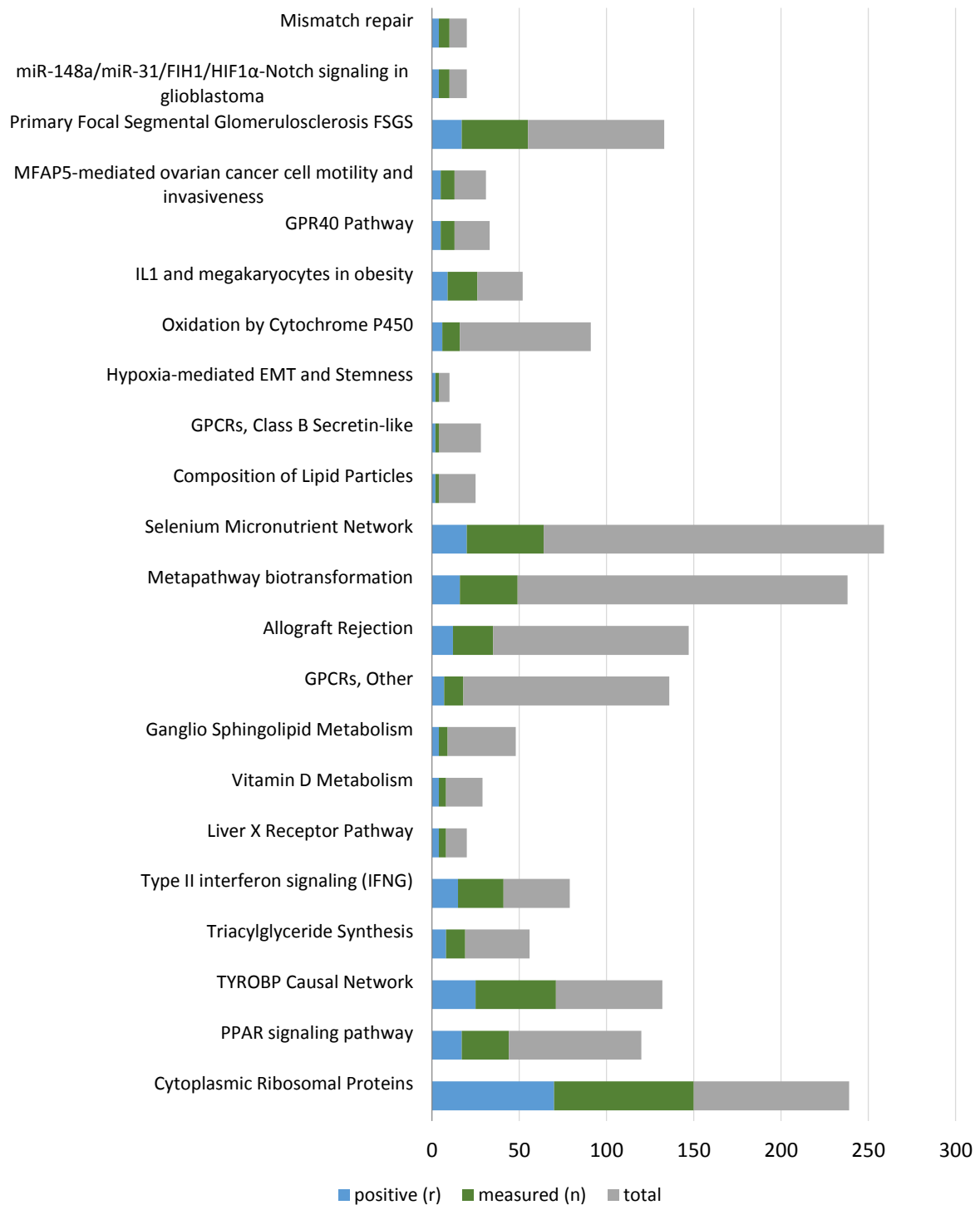


Figure 6.9 Summary of WikiPathway database comparative analysis for LPS treated cord and decidua subsets. Bars represent pathways significantly enriched ($p < 0.05$, Z-Score > 1.96), with the frequency of differentially expressed genes (blue) and total genes measured (green) as a proportion of the total frequency of pathway genes (grey). Bars are ranked from a high to low Z-score.

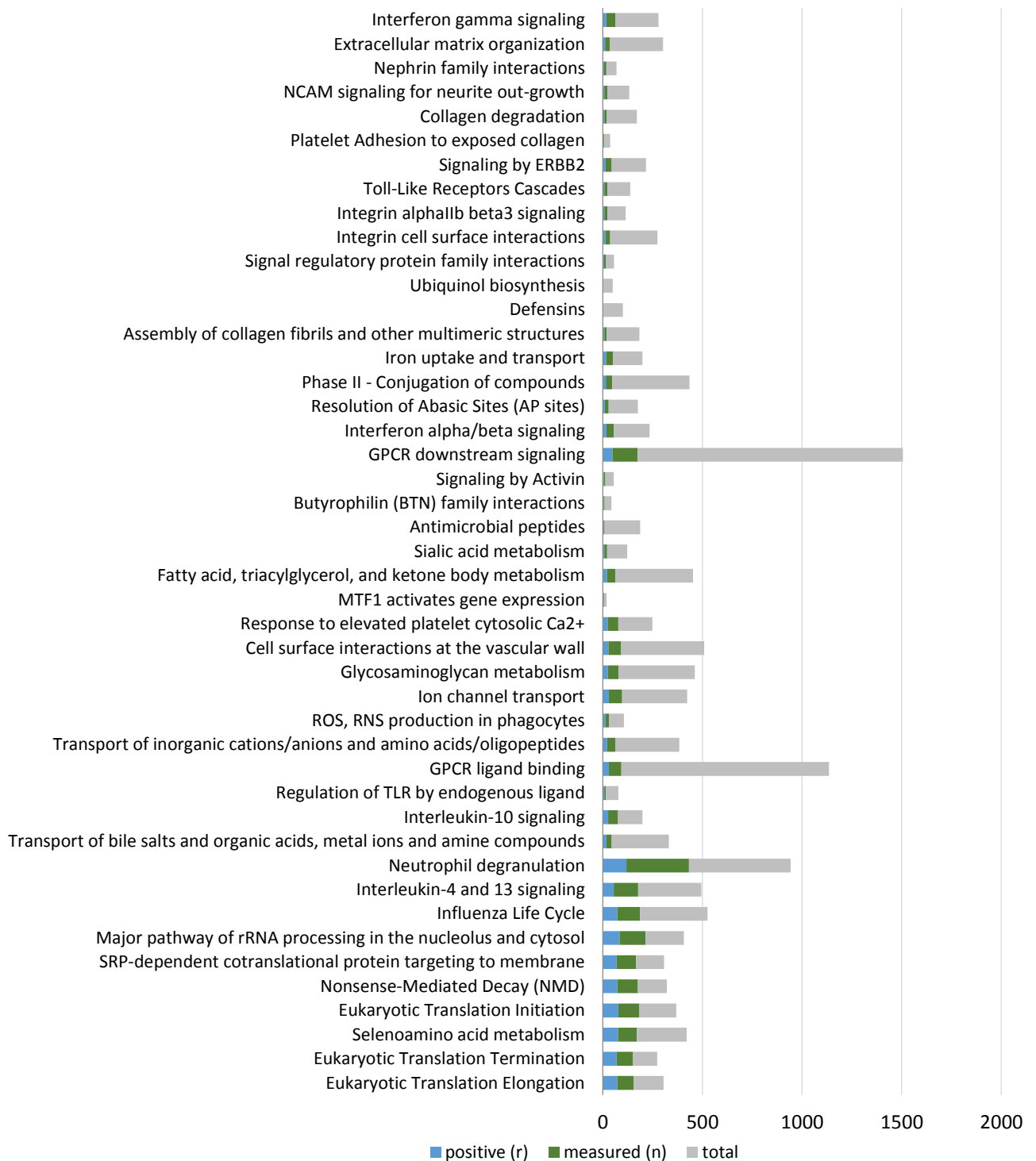


Figure 6.10 Summary of Reactome database comparative analysis for LPS treated cord and decidua subsets. Bars represent pathways significantly enriched ($p < 0.05$, $Z\text{-Score} > 1.96$), with the frequency of differentially expressed genes (blue) and total genes measured (green) as a proportion of the total frequency of pathway genes (grey). Bars are ranked from a high to low Z -score.

In LPS maternal monocytes relative to decidua LPS macrophages 23 WP and only 19 Reactome pathways were significantly enriched (Z-score >1.96). Notably in both these included pathways related primarily innate immune cell function, lipid and glucose metabolism. The WP database analysis pathways for cord included vitamin D metabolism (3.05), type II IFN signalling (3.08), triacylglyceride synthesis (3.09) and peroxisome proliferator-activated receptor (PPAR) signalling (3.74). Similar findings were also observed for maternal subsets, with vitamin D metabolism (3.23), triacylglyceride synthesis, PPAR signalling pathway (2.81) and also the inflammatory response pathway (2.81) over-represented. Utilising the Reactome database analysis, cord monocyte enriched pathways included reactive oxygen species (ROS), reactive nitrogen production (RNS) in phagocytes (3.23), IL-10 signalling (3.85), integrin α II β β 3 signalling (2.22), TLR- like receptor cascades (2.22), antimicrobial peptides (2.61) and IFN- γ signalling (1.96). In the maternal subsets inflammatory response (2.13), vitamin D metabolism (2.82) and PPAR signalling (2.86) Reactome pathways were enriched.

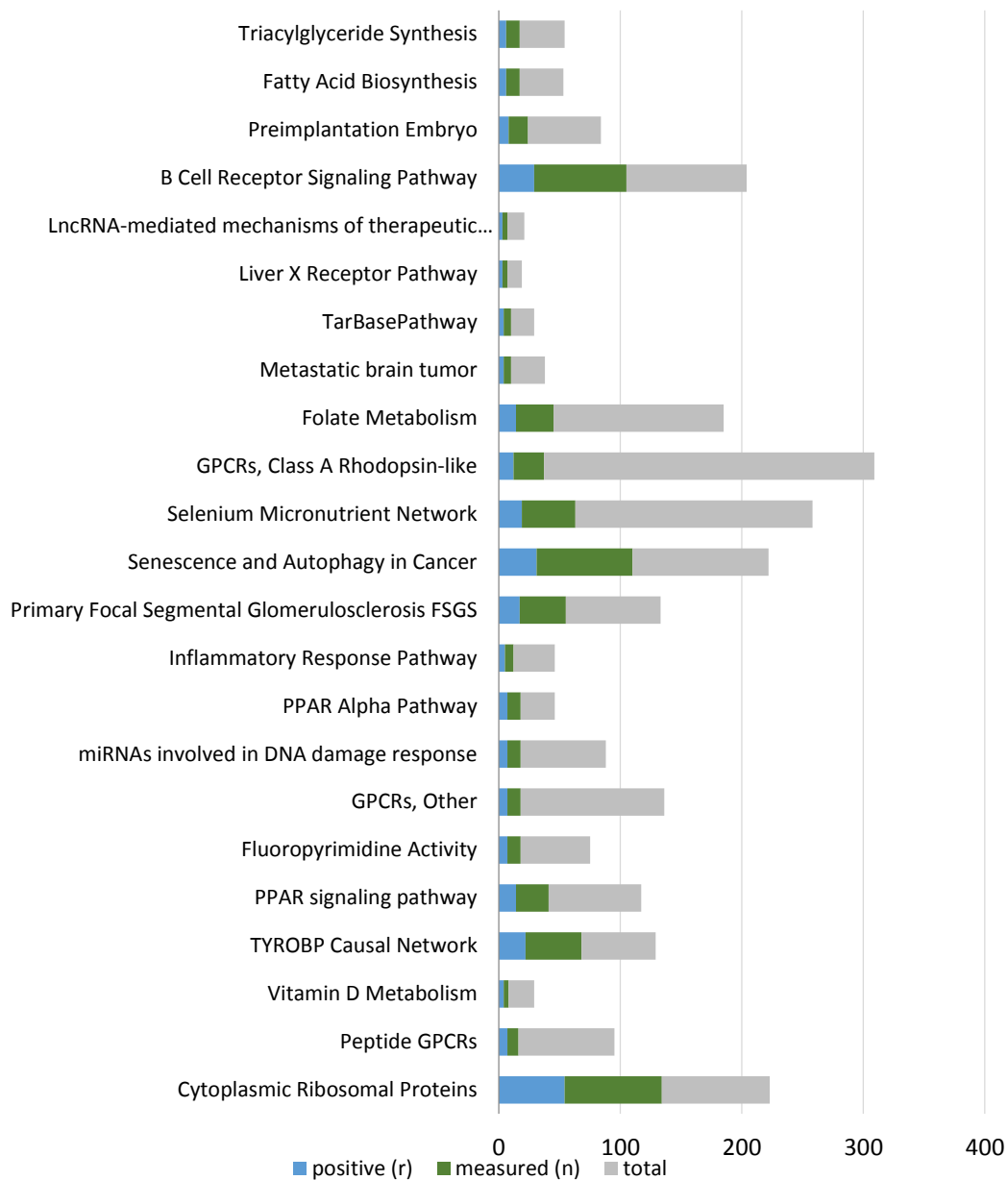


Figure 6.11 Summary of WikiPathway database comparative analysis for LPS maternal and decidua subsets. Bars represent those pathways significantly enriched ($p < 0.05$, Z-Score > 1.96), with the frequency of differentially expressed genes (blue) and total genes measured (green) as a proportion of the total frequency of pathway genes (grey). Bars are ranked from a high to low Z-score.

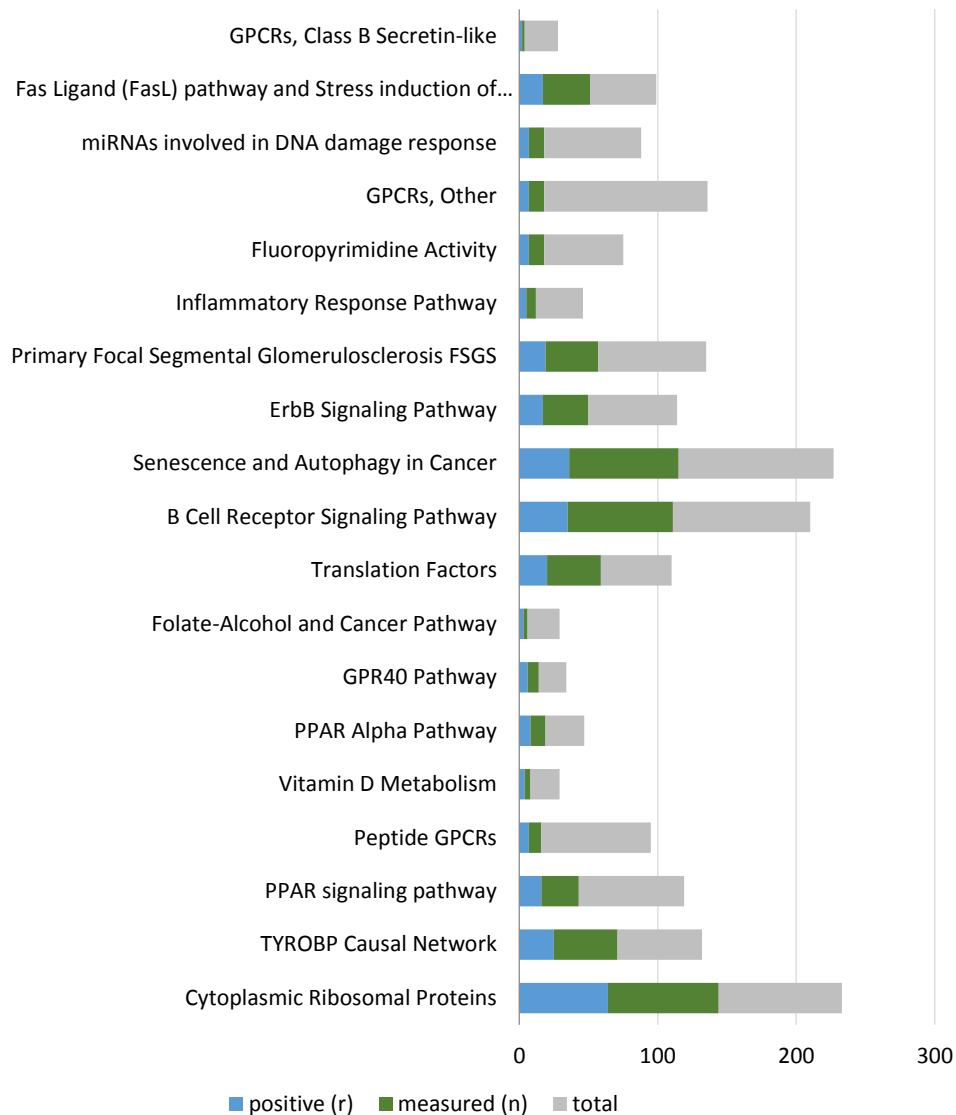


Figure 6.12 Summary of Reactome database comparative analysis for LPS maternal and decidua subsets. Bars represent those pathways significantly enriched ($p < 0.05$, $Z\text{-Score} > 1.96$), with the frequency of differentially expressed genes (blue) and total genes measured (green) as a proportion of the total frequency of pathway genes (grey). Bars are ranked from a high to low Z -score.

6.2.12 Vitamin D targets in maternal, cord and decidua subsets

Overall, only 2 differentially expressed genes, *CA* and *EFL1*, were shared between the three distinct decidua, maternal and cord group analyses, being upregulated by LPS+ 1,25(OH)₂D₃ comparative to LPS alone as summarised in Figure 6.13. In the blood, 16 (14.8%) significant differentially expressed

genes were shared in both cord and maternal LPS vs LPS and 1,25(OH)₂D₃ group analyses, being significantly upregulated relative to LPS-treatment in both.

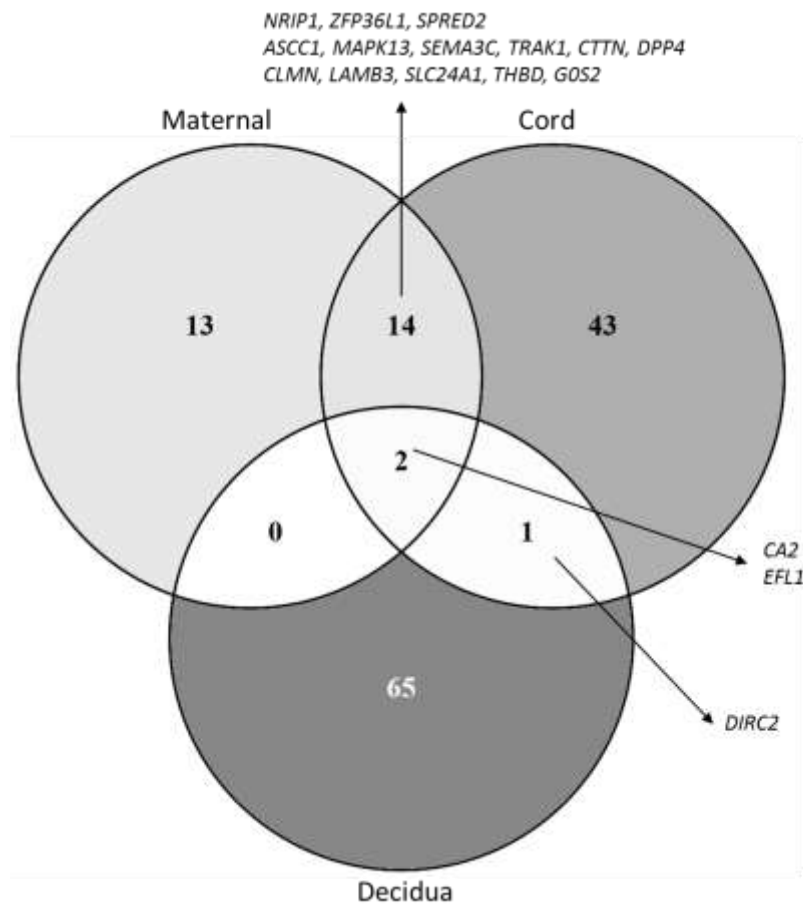


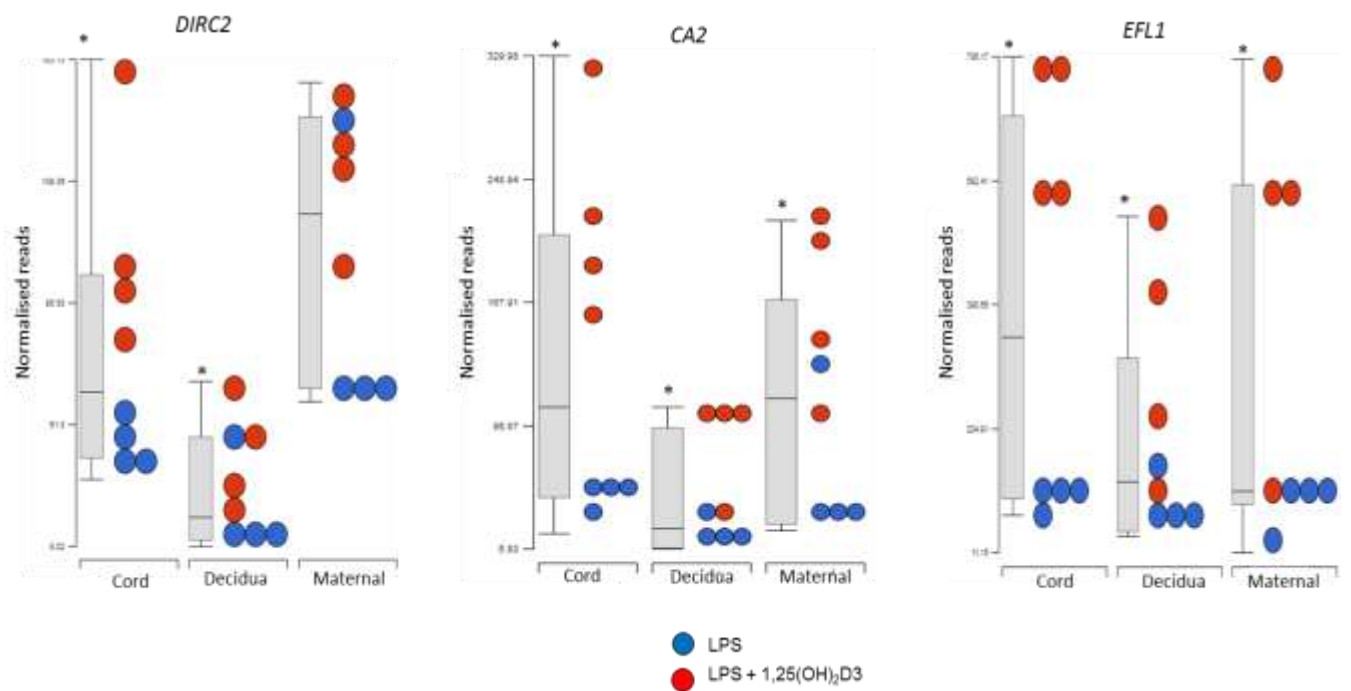
Figure 6.13 Summary of those transcripts significantly upregulated in cord blood, maternal blood and decidua derived LPS stimulated monocyte/ macrophage subsets in response to vitamin D. The venn diagram summarises the frequency of genes significantly ($p < 0.05$) upregulated (fold change > 1.5) in cord, maternal and decidua monocyte/ macrophage subsets in response to vitamin D, comparative to LPS alone. All shared upregulated genes between the 3 sites are annotated.

The function of these transcripts is summarised in Table 6.11, which indicates a number were concerned with cell processing, including cell proliferation, trafficking, migration and adhesion, such as *TRAK1*, *LAMB3*, *CLMN*, *CTTN*. Genetic processing and transcription modulation also appeared significant with genes including *NRIP1*, *ASCC1*, *MAPK13* and *ZFP36L1* all upregulated.

Transcript	Fold-change (p<0.05)		Function
	Cord	Maternal	
<i>NRIP1</i>	2.27	1.73	Nuclear Receptor Interacting Protein 1 which specifically interacts with the hormone-dependent activation domain AF2 of nuclear receptors and modulates transcriptional activity of the estrogen receptor.
<i>ASCC1</i>	1.81	1.83	Activating Signal Cointegrator 1 Complex Subunit 1 - a transcriptional coactivator
<i>CLMN</i>	12.6	3.46	Calmin - Negative regulation of cell proliferation
<i>ZFP36L1</i>	2.33	1.79	ZFP36 Ring Finger Protein Like 1 - destabilizes mRNA transcripts to attenuate protein synthesis
<i>SPRED2</i>	1.8	1.79	Sprouty Related EVH1 Domain Containing 2 - Regulates growth factor-induced activation of the MAP kinase cascade
<i>MAPK13</i>	2.46	1.91	Mitogen-Activated Protein Kinase 13 - Involved in a wide variety of cellular processes including proliferation, differentiation, transcription regulation and development.
<i>SEMA3C</i>	4.57	2.06	Semaphorin 3C - Binds to plexin family members and plays an important role in the regulation of developmental processes. Increased gene expression correlates with increased cancer cell invasion and adhesion
<i>TRAK1</i>	3.16	2.71	Trafficking Kinesin Protein 1 - Involved in the regulation of endosome-to-lysosome trafficking
<i>CTTN</i>	4.22	2.78	Cortactin - Regulates interactions between components of adherens-type junctions and organizes the cytoskeleton and cell adhesion structures of epithelia and carcinoma cells.
<i>DPP4</i>	6.07	3.19	Dipeptidyl Peptidase 4 - Classically recognised for its enzymatic ability to inactivate incretin hormones. Positive regulator of T-cell coactivation, with pro-regulatory functions.
<i>LAMB3</i>	6.72	3.62	Laminin Subunit Beta 3 - mediates the attachment, migration and organization of cells into tissues during embryonic development
<i>SLC24A1</i>	3.2	3.76	Solute Carrier Family 24 Member 1 - encodes a member of the potassium-dependent sodium/calcium exchanger protein family
<i>THBD</i>	3.32	3.8	Thrombomodulin - endothelial-specific type I membrane receptor that binds thrombin, which results in the activation of protein C, which degrades clotting factors Va and VIIIa and reduces thrombin generation.
<i>GOS2</i>	6.95	5.64	GO/G1 Switch 2 - Promotes apoptosis by binding to BCL2

Table 6.11 Summary of the shared transcripts measured in cord and maternal monocytes significantly upregulated in response to co-treatment with LPS and 1,25(OH)₂D₃. Those transcripts significantly upregulated (p<0.05) by 1,25(OH)₂D₃ are summarised in the table, with the fold-change and function summarised for cord (red) and maternal (blue) subsets.

In the cord and decidua, 3 shared transcripts were significantly upregulated by 1,25(OH)₂D₃, *DIRC2*, *CA2* and *EFL1*, comparative to LPS-treatment alone. Finally, comparing the maternal and decidua subsets, only 2 shared transcripts *CA2* and *EFL1* were identified. Albeit *DIRC2* was not significantly differentially expressed in maternal subsets, a similar response to 1,25(OH)₂D₃ co-treatment was measured (fold-change 1.64; p>0.05) (Figure 6.14).



	Fold-change (p<0.05)		
	<i>DIRC2</i>	<i>CA2</i>	<i>EFL1</i>
Cord	2.92	6.68	7.54
Decidua	1.97	8.57	4.71
Maternal	ns	3.66	6.32

Figure 6.14 Comparative analysis of cord, maternal and decidua monocyte/ macrophage transcript expression of *DIRC2*, *CA2* and *EFL1*. Transcript expression of *DIRC2*, *CA2* and *EFL1* in LPS treated (blue) and LPS + 1,25(OH)₂D₃ (red) CD14+ monocyte / macrophage subsets (n=4). All 3 subsets significantly (p<0.05) upregulated (fold change >1.5) expression (*) in response to 1,25(OH)₂D₃ comparative to LPS alone.

Of the 23 genes downregulated in the cord, 12 in maternal blood, and 82 in decidua, no transcripts were shared.

6.2.13 Vitamin D effects upon maternal monocytes

Of the 7735 genes identified, 41 (0.53%) transcripts were differentially expressed in the LPS and LPS + 1,25(OH)₂D₃ treated maternal subsets comparatively. Of these, 12 (29.2%) were significantly downregulated and 29 (70.7%) upregulated following co-treatment with vitamin D ($p \leq 0.05$, fold-change < -1.5 and > 1.5). This is summarised using hierarchical dendrogram clustering analysis, which using Euclidean dissimilarity for rows and columns, arranged similar transcript targets into homogeneous 'clusters' as illustrated in Figure 6.15. Importantly, those differentially expressed transcripts appeared consistently differentially expressed in the LPS comparative to LPS + 1,25(OH)₂D₃ sample subgroups, with clear patterns of transcript upregulation (blue) and downregulation (yellow) visualised.

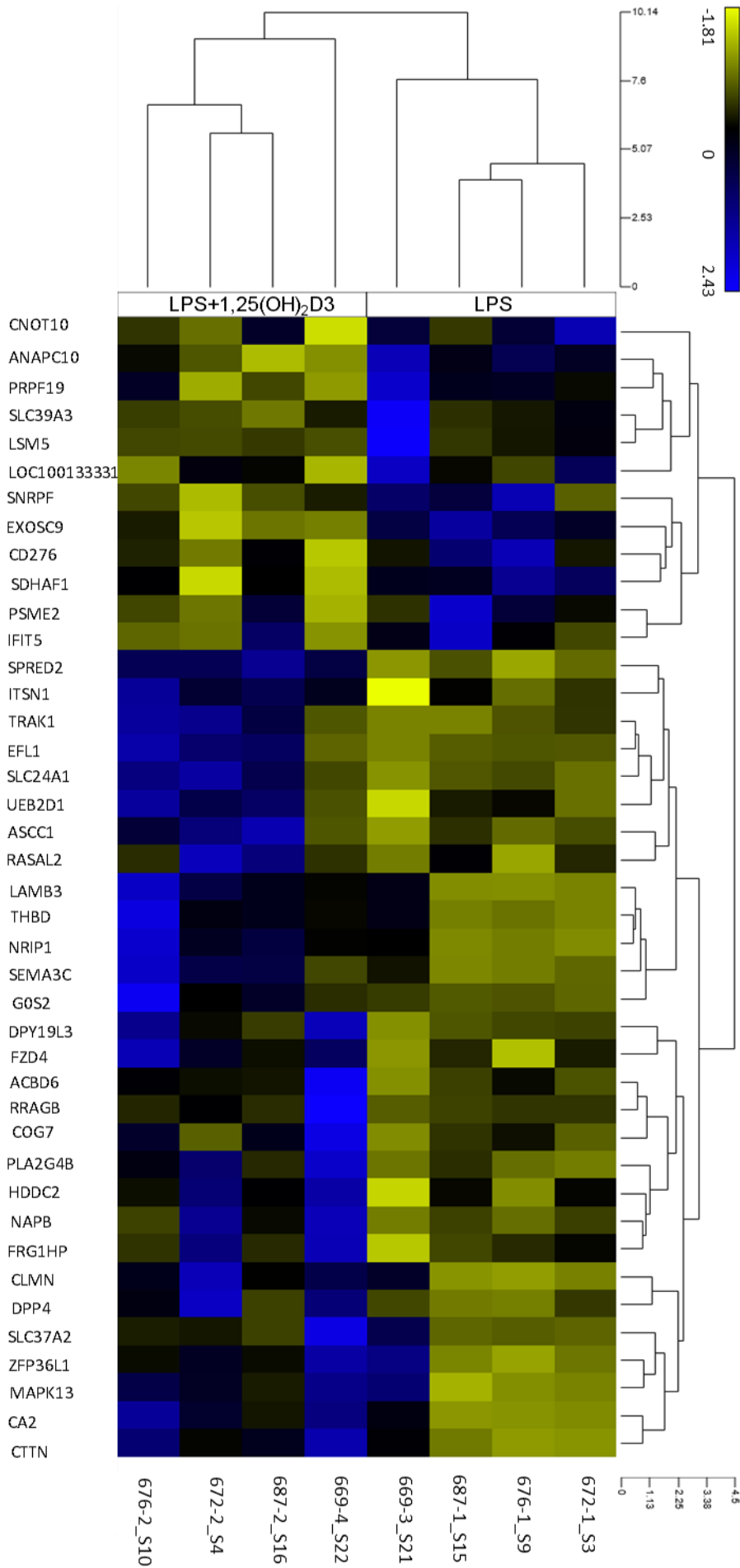


Figure 6.15 Hierarchical cluster dendrogram analysis of maternal LPS versus maternal LPS+1,25(OH)₂D3 subsets. Samples are on rows and transcripts on columns, with clustering according to LPS treatment alone (LPS) and co-treatment with 1,25(OH)₂D3 (LPS+1,25(OH)₂D3). The colours are based on standardised expression values, with yellow indicating low (-1.81 standard deviation) to blue high (2.43 standard deviation) levels. The y-axis and x-axis branch distance reflects the closeness of either the individual data sets or clusters.

As summarised in Table 6.12, treatment with 1,25(OH)₂D₃ appeared to primarily target genes associated with cellular function (n=13; 31.7%). All differentially expressed transcripts associated with cell processing were significantly upregulated and principally related to cell migration, adhesion, apoptosis and intracellular trafficking; *LAMB3* (fold-change 3.62), *TRAK1* (fold-change 2.71), *GOS2* (fold-change 5.64), *MAPK13* (fold-change 1.91). Importantly 9 (69.2%) of these were also significantly upregulated in the cord group, for which 40 (48.2%) of the total 83 transcripts significantly differentially expressed in the vitamin D group related to cell processing, in particular regulation of monocyte apoptosis, trafficking, adhesion and proliferation. A number of other differentially expressed transcripts were involved in genomic processing (10; 24.4%). There were also 7 (17.0%) related to glucose energy and cell metabolism, 3 (7.3%) immune function, 3 (7.3%) ion transport, 2 (4.9%) unknown function and 2 anti-sense (4.9%). Significant transcripts of interest primarily related to mRNA splicing and cell cycle regulation.

Functional classification	Total	Down-regulation by 1,25(OH) ₂ D ₃	Up-regulation by 1,25(OH) ₂ D ₃
Cell structure	1		<i>COG7</i>
Cell survival, proliferation, invasion, adhesion, angiogenesis, trafficking	13		<i>UBE2D1, SPRED2, MAPK13, ITSN1, SEMA3C, FZD4, NAPB, TRAK1, CTTN, CLMN, LAMB3, GOS2, THBD</i>
Immune function	3	<i>CD276, IFIT5, PSME2</i>	
Glucose energy and cell metabolism & lipogenesis	7	<i>SDHAF1</i>	<i>RASAL2, ACBD6, CA2, RRAGB, PLA2G4B, DPP4</i>
Genetic	10	<i>LSM5, EXOSC9, ANAPC10, SNRPF, PRPF19, CNOT10</i>	<i>NRIP1, ZFP36L1, ASCC1, EFL1</i>
Ion transport	3	<i>SLC39A3</i>	<i>SLC37A2, SLC24A1</i>
Unknown function	2		<i>HDDC2, DPY19L3</i>
Anti-sense, non-coding, snoRNAs	2	<i>LOC100133331</i>	<i>FRG1HP</i>

Table 6.12 Effect of 1,25(OH)₂D₃ upon gene expression in LPS maternal monocytes. Summary of total genes (n=41) differentially induced (red) (n= 29) or suppressed (green) (n=12) by 1,25(OH)₂D₃ (fold change < -1.5 or > +1.5, p ≤ 0.05), with sub-categorisation according to transcript function.

6.2.14 Vitamin D effects upon cord monocytes

Of the 7735 genes identified, 83 (1.07%) transcripts were differentially expressed in the LPS and LPS + 1,25(OH)₂D₃ treated cord subsets. Of these, 23 (27.7%) were downregulated and 60 (72.3%) upregulated following co-treatment with vitamin D. Hierarchical dendogram clustering analysis was similarly performed, and as illustrated in Figure 6.16, transcripts were consistently differentially expressed in the LPS comparative to LPS + 1,25(OH)₂D₃ groups, with patterns of transcript upregulation (blue) prominent in the LPS+1,25(OH)₂D₃ group.

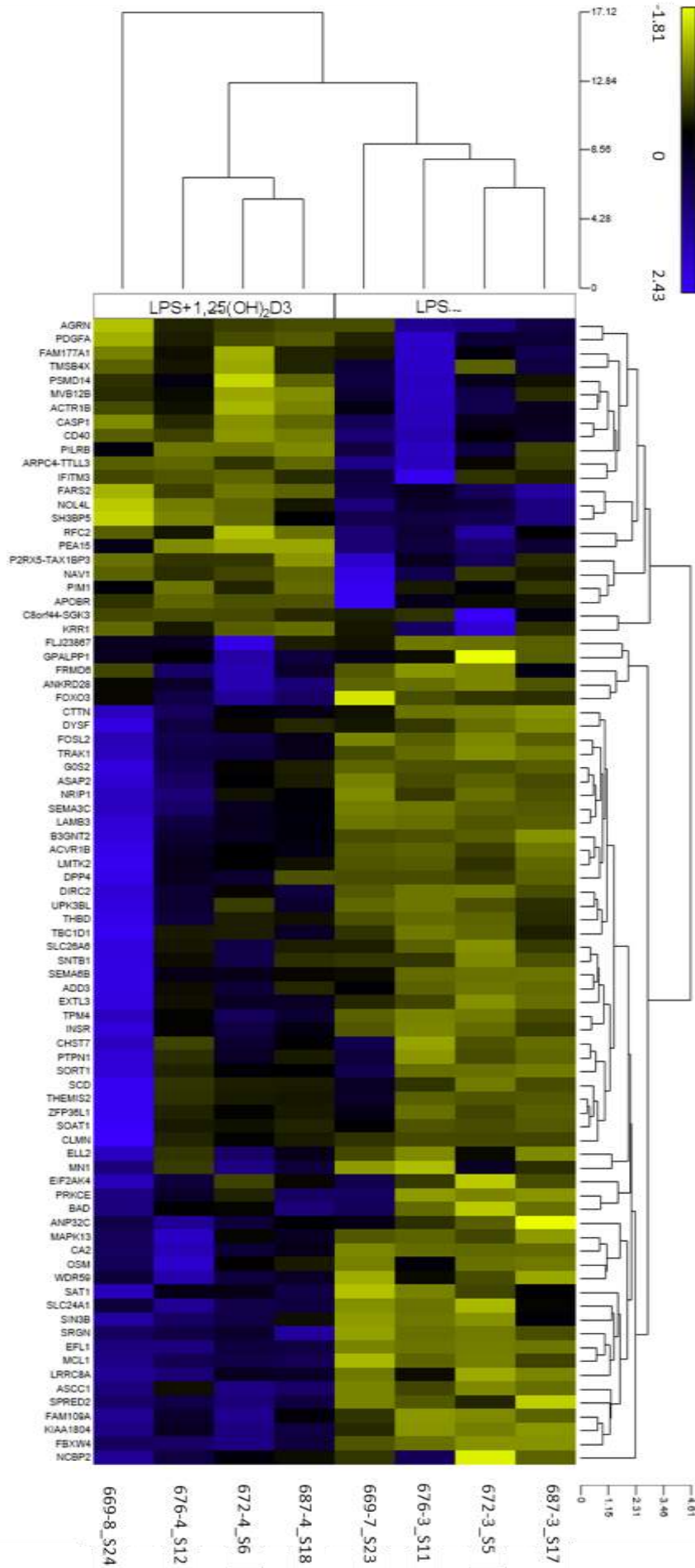


Figure 6.16 Hierarchical cluster dendrogram analysis of cord LPS versus cord LPS + 1,25(OH)₂D3 subsets. Samples are on rows and transcripts on columns, with clustering according to LPS treatment alone (LPS) and co-treatment with 1,25(OH)₂D3 (LPS+1,25(OH)₂D3). The colours are based on standardised expression values, with yellow indicating low (-1.81 standard deviation) to blue high (2.43 standard deviation) levels. The y-axis and x-axis branch distance reflects the closeness of either the individual data sets or clusters.

Consistent with the maternal blood derived subset analysis, most prominent were those transcripts related to cell survival, proliferation, invasion, adhesion, angiogenesis, trafficking (40; 48.2%), genetic processing (14; 16.9%), and glucose energy and cell metabolism (10; 12.0%). Overall, there were 7 (8.4%) concerned with immune function, and 2 (7.3%) ion transport, with 2 (10.8%) of unknown function and 2 anti-sense (2.4%). Those significant transcripts of particular interest are summarised in Table 6.13, relating primarily to lymphocyte homing and migration.

Functional classification	Total	Down-regulation by 1,25(OH) ₂ D ₃	Up-regulation by 1,25(OH) ₂ D ₃
Cell structure	0		
Cell survival, proliferation, invasion, adhesion, angiogenesis, trafficking	40	<i>C8orf44-SGK3, ARPC4-TLL3, PDGFA, CASP1, MVB12B, ACTR1B, TMSB4X, PIM1, PEA15</i>	<i>TBC1D1, PTPN1, SPRED2, FBXW4, MCL1, LRRC8A, BAD, ANP32C, WDR59, PRKCE, SRGN, SORT1, LMTK2, TPM4, MAPK13, NKRD28, DYSF, FRMD6, SNTB1, DIRC2, ACVR1B, TRAK1, ADD3, ASAP2, SEMA6B, CTTN, SEMA3C, LAMB3, GOS2, CLMN, THBD</i>
Immune function	7	<i>PILRB, IFITM3, CD40, SH3BP5</i>	<i>THEMIS2, OSM, KIAA1804</i>
Glucose energy and cell metabolism & lipogenesis	10	<i>APOBR</i>	<i>SAT1, CHST7, EXTL3, B3GNT2, SCD, SOAT1, INSR, DPP4, CA2</i>
Genetic	14	<i>RFC2, FARS2, PSMD14</i>	<i>ELL2, NCBP2, MN1, FOXO3, EIF2AK4, FOSL2, SIN3B, ASCC1, NRIP1, ZFP36L1, EFL1</i>
Ion transport	2		<i>SLC24A1, SLC26A6</i>
Unknown function	9	<i>NAV1, NOL4L, AGRN, KRR1, FAM177A1</i>	<i>GPALPP1, FAM109A, FLJ23867, UPK3BL</i>
Anti-sense, non-coding, snoRNAs	2	<i>P2RX5-TAX1BP3</i>	

Table 6.13 Effect of 1,25(OH)₂D₃ upon gene expression in LPS cord monocytes. Summary of the total genes (n=83) differentially induced (red) (n=60) and suppressed (green) (n=23) by 1,25(OH)₂D₃ (fold change <-1.5 or >+1.5, p ≤ 0.05), with sub-categorisation according to transcript function.

6.2.15 Vitamin D effects upon decidua macrophages

Of the 7735 genes identified, 150 (1.9%) transcripts were differentially expressed in the LPS- and LPS + 1,25(OH)₂D₃ treated decidua subsets. Of these, 82 (54.7%) were downregulated and 68 (45.3%) upregulated following co-treatment with vitamin D. Hierarchical dendrogram clustering analysis was similarly performed, with transcripts consistently differentially expressed in the LPS comparative to LPS + 1,25(OH)₂D₃ sample subgroups. Unlike cord and maternal subsets, transcript upregulation (blue) and downregulation was similarly prominent in the LPS+1,25(OH)₂D₃ groups (Figure 6.17).

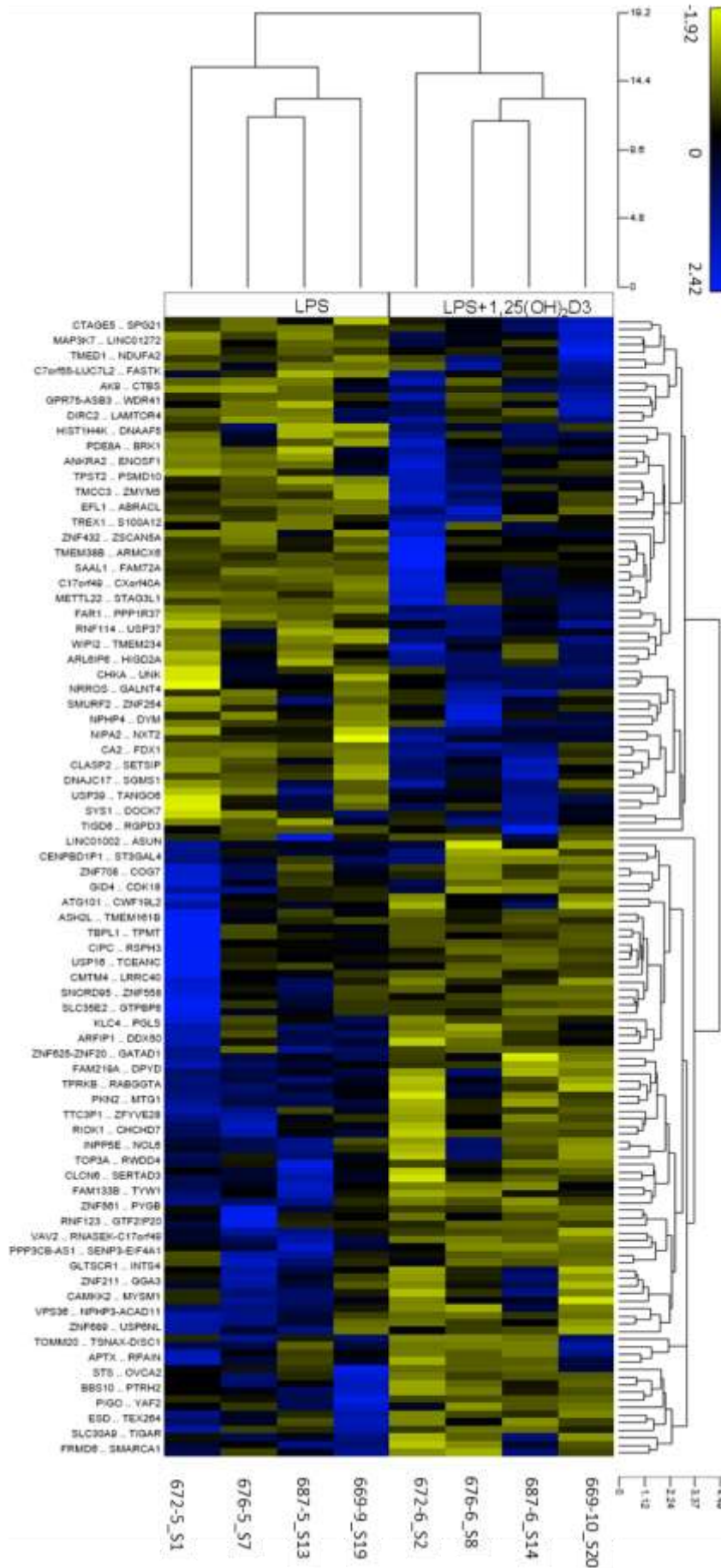


Figure 6.17 Hierarchical cluster dendrogram analysis of decidua LPS versus decidua LPS + 1,25(OH)₂D₃ subsets. Samples are on rows and transcripts on columns, with clustering according to LPS treatment alone (LPS) and co-treatment with 1,25(OH)₂D₃ (LPS+1,25(OH)₂D₃). The colours are based on standardised expression values, with yellow indicating low (-1.81 standard deviation) to blue high (2.43 standard deviation) levels. The y-axis and x-axis branch distance reflects the closeness of either the individual data sets or clusters.

Of those genes differentially expressed, unlike the maternal and cord analyses, those relating to genomic processing were most prominent (49; 32.7%). Genes related to cell survival, proliferation, invasion, adhesion, angiogenesis, trafficking were also highly prominent (40; 28.0%). There were 16 (10.7%) genes related to glucose energy and cell metabolism. Overall, there were 4 (2.7%) concerned with immune function, and 4 (2.7%) ion transport, with 15 (10.0%) of unknown function and 15 (10.0%) anti-sense. Those significant transcripts of particular interest are summarised in Table 6.14, relating primarily to transcription, RNA binding and RNA transport, and histone modification.

Functional classification	Total	Down-regulation by 1,25(OH) ₂ D3	Up-regulation by 1,25(OH) ₂ D3
Cell structure	0		
Cell survival, proliferation, invasion, adhesion, angiogenesis, trafficking	42	<i>RSPH3, OVCA2, PTRH2, CMTM4, CDK18, ARFIP1, FRMD6, VPS36, USP6NL, VAV2, RABGGTA, ZFYVE28, ZFYVE28, ATG101, PKN2, INPP5E, TOMM20, GGA3, CAMKK2</i>	<i>SGMS1, WIPI2, SYS1, DOCK7, BRK1, NXT2, PDE8A, SMURF2, CTAGE5, CLASP2, LAMTOR4, MAP3K7, TPST2, TANGO6, FASTK, DIRC2, NPHP4, DYM, PSMD10, S100A12, TMED1, GALNT4, FAM72A</i>
Immune function	4		<i>RNF114, NRROS, SPG21, SAAL1</i>
Glucose energy and cell metabolism & lipogenesis	16	<i>TPMT, STS, ESD, ST3GAL4, PGLS, PYGB, CHCHD7, TIGAR</i>	<i>FAR1, HIGD2A, CHKA, CTBS, ENOSF1, NDUFA2, FDX1, CA2</i>
Genetic	49	<i>TBPL1, TMEM161B, FAM133B, TCEANC, CIPC., ZNF708, ZNF558, SLC30A9, TYW1, MTG1, TPRKB, ZNF689, ASH2L, GLTSCR1, RNF123, GID4, SMARCA1, SERTAD3, NOL6, GATAD1, RPAIN, TOP3A, APTX, DPYD, DDX50, YAF2, ZNF211, ASUN, INTS4, USP16, MYSM1</i>	<i>USP39, UNK, USP37, METTL22, TREX1, HIST1H4K, ANKRA2, ZNF432, SETSIP, ZSCAN5A, ZNF254, TIGD6, AK9, DNAJC17, RGPLD3, C7orf55-LUC7L2, C17orf49, EFL1,</i>
Ion transport	4	<i>SLC35E2, CLCN6</i>	<i>NIPA2, TMEM38B</i>
Unknown function	15	<i>RWDD4, LRRC40, GTPBP8, TEX264, FAM219A, RIOK1, CWF19L2, CENPBD1P1</i>	<i>ZMYM5, ARL6IP6, WDR41, DNAAF5, TMEM234, ABRACL, GPR75-ASB3</i>
Anti-sense, non-coding, snoRNAs	15	<i>SNORD95, NPHP3-ACAD11, ZNF625-ZNF20, SENP3-EIF4A1, RNASEK-C17orf49, PPP3CB-AS1, GTF2IP20, TTC3P1, LINC01002, TSNAX-DISC1</i>	<i>Cxorf40A, TMCC3, LINC01272, ARM CX6, STAG3L1</i>

Table 6.14 Effect of 1,25(OH)₂D3 upon gene expression in LPS decidual macrophages. Summary of the total genes (n=150) differentially induced (red) (n=68) and suppressed (green) (n=82) by 1,25(OH)₂D3 (fold change < -1.5 or > +1.5, p ≤ 0.05), with sub-categorisation according to transcript function.

6.3 Discussion

Both monocytes and tissue macrophages provide both immediate defence against foreign agents and assist during the activation and development of the adaptive immune response. Within the context of human pregnancy a key role for both is anticipated, with critical roles in implantation, placentation, fetal development, and parturition anticipated (393). In the decidua, macrophages are postulated to participate in both the progression of inflammation, and to promote fetal–maternal immune tolerance, tissue remodelling and scavenging of apoptotic cells (15)(16). Furthermore, changes in the immunophenotype, metabolic characteristics, and distribution of peripheral monocytes and decidual macrophages have been implicated in the pathogenesis of pregnancy disorders including PET and preterm birth (235, 412, 413).

The potent effects of vitamin D upon innate monocytes and macrophages are well recognised outside of pregnancy, in particular their enhanced antimicrobial defence against pathogens such as *Mycobacterium tuberculosis*(414). What remains less clear is whether similar responses will be evident in the decidua, or whether alternative tissue effects such as tissue remodelling, angiogenesis, or immune-suppression may be identified. The potential impact of maternal vitamin D status upon fetal cord-derived monocyte phenotype and function is also potentially important, given the recognised association between maternal vitamin D deficiency and adverse neonatal outcomes, including bone health, respiratory disease and sepsis (415, 416).

6.3.1 A distinct immune cell population persists in third trimester decidua comparative to cord and maternal blood

The present study provides a detailed analysis of vitamin D and its effects upon matched monocyte and macrophage subsets present in ‘healthy’ maternal blood, cord blood and third trimester decidual tissues. Albeit T cells were prominent in both, relative total CD3 frequencies were increased in maternal blood (59.4%) compared to cord (45.8%), with lower CD4 and CD8 relative frequencies. No difference in NK or APC subsets was measured. Previous larger cohort studies have similarly reported lower T cell, B cell and NKT frequencies in neonatal cord blood, with higher monocytes and Treg cells measured (417).

In the decidua, initial third trimester analysis indicates a notable shift in the relative proportion of leukocyte subsets resident within decidua. Principally, a marked decrease in the preponderance of uNKs was observed, representing ~20-30% of total leukocytes comparative to ~50-60% in first trimester. This is consistent with previous reports (418), and likely reflects a principal role for uNKs in early spiral artery remodelling and trophoblast invasion (419). Albeit at term uNKs are still highly prominent compared to maternal blood, their function remains more poorly defined. With adaptive T cells representing the major immune subset, a more prominent role for the adaptive immune system is recognised with advancing gestation (317, 420). Here, the relative proportion of both CD4+ and CD8+ cells increased at term. Albeit not characterised here in further detail, it is important to recognise certain T cell subset protect the fetus from immune rejection and facilitate development, whilst others may contribute to pregnancy pathologies such as PET. Previous reports have identified significantly higher percentages of CD4+CD25^{bright} and CD8+CD28⁻ T-cells in third trimester decidua compared to peripheral blood, suggesting an important role for Treg subsets locally (421). This may reflect the observed increased T cell prominence in term decidua measured here.

Conversely the relative prevalence of APCs appeared lower with advanced GA, representing <10% at term. In mice, the number of uterine macrophages at 15d (4d pre-delivery) is reportedly significantly higher compared to non-pregnant controls. In this study concentrations returned to non-pregnant levels 1d prior to birth (317, 422). However there is conflicting evidence which supports enhanced macrophage recruitment at term, with increased myometrial CCL-2 monocyte/macrophage chemoattractant expression measured at d18 relative to earlier gestational time-points (423). In human decidua decreased CD14+ frequencies measured at term in 3rd trimester healthy samples compared to those obtained from both first and second trimester pregnancies (317). The reason for these discrepancies is uncertain.

6.3.2 Detailed monocyte and macrophage subset analysis reveals stark differences in third trimester decidua

Here we report a detailed analysis of monocyte and macrophage subsets comparatively in cord, maternal blood and decidua. This was performed in the first and third trimester utilising recognised

markers for subset differentiation; CD14, CD16 and intracellular CD68 markers. For the peripheral monocyte subsets, the proportion of non-classical (CD14⁺CD16⁺⁺), intermediate (CD14⁺⁺CD16⁺) and classical (CD14⁺⁺CD16⁻) subsets was assessed (370, 424).

In maternal blood, classical subsets were most prominent in both trimesters representing ~66% and 75% respectively. Consistent with this, classical subsets were predominant (74%) in third trimester cord blood. In both, a smaller population of non-classical subsets was measured, whilst the relative frequency of intermediate subsets was low in both. In the non-pregnant state, classical subsets are often more prevalent, representing at least 80-90% of the total monocyte population (374, 408). Here a more detailed gating strategy was utilised to ensure exclusion of potential contaminants prior to analysis, including T cells, neutrophils, NK cells and B cells, which may explain the difference in subset relative proportions. Consistent with our data, the percentage of combined non-classical/intermediate monocytes has previously been reported to be higher from the first trimester in humans as compared to non-pregnant controls(376). The proportion of non-classical subsets was also higher than intermediate subsets for both.

Understanding the functional differences between monocyte subsets remains a challenge. Outside of pregnancy, classical monocytes are recognised as key mediators of the direct innate effector immune response and phagocytosis and tissue remodelling, releasing a range of inflammatory effector CK in a TLR-dependent manner following pro-inflammatory LPS stimulation. Within the context of pregnancy, functional changes in monocytes from pregnant women are now demonstrated, including increased production of oxygen free radicals(235) and decreased phagocytosis(385). The shift in peripheral monocyte subsets observed here appears consistent with the theory that pregnancy is a pro-inflammatory condition, as increased numbers of combined non-classical/intermediate monocytes have been associated with several inflammatory diseases and malignancy (378).

Conversely, non-classical monocytes appear poorly phagocytic and do not generate reactive oxygen species. They do display 'inflammatory' characteristics upon activation, and properties for antigen presentation (408), demonstrating infiltration into resting and inflamed tissue where they may initiate the inflammatory response (424). Intermediate monocytes display both phagocytic and inflammatory

function, with higher levels of MHC II for antigen presentation, and receptors relevant to angiogenesis(374).

Here we consider decidual tissue macrophages utilising the same gating strategy as monocytes to compare CD14 and CD16 surface expression, and intracellular CD68. In the first trimester a CD14⁺⁺CD16⁻ subset (~63%) analogous in appearance to the classical monocytes was most prevalent, with only 8.6% CD14⁺CD16⁺⁺ and 23% CD14⁺⁺CD16⁺ frequencies measured. Circulating monocytes are considered tissue macrophage precursors which extravasate from the blood and develop into resident macrophages(393). Our findings indicate this arises from the first trimester. However, since pre-pregnancy endometrial macrophages are also shown to be important in breakdown, repair, and regeneration of endometrium during the menstrual cycle (425), the extent to which first trimester subsets reflect classical monocyte recruitment remains unclear, with further follow up studies required.

In the third trimester a stark shift was observed, with ~84% of cells CD14⁺⁺CD16⁺ and more akin to an intermediate monocyte phenotype. The observed increase in CD16 and lower CD14 expression is commonly defined when comparing macrophages to peripheral monocyte subsets (426). Inflammation is present at the materno-fetal interface and results in resident macrophage activation, which increases the production of CK, chemokines, and other inflammatory mediators, as well as monocyte recruitment. A gestational shift has also previously been observed, when comparing second and third trimester decidua subsets (427).

Consistent with the first trimester, intracellular CD68 expression in the decidua CD14⁺⁺CD16⁺ subsets was higher than for the CD14⁺⁺CD16⁻ subsets. As a recognised macrophage marker, CD68 was not expressed in the classical CD14⁺⁺CD16⁻ monocyte subsets in either the maternal or cord blood. Importantly, CD68, which binds to tissue- specific lectins or selectins, is highly expressed by tissue macrophages. It is also a member of the scavenger receptor family, which classically function to clear cellular debris, promote phagocytosis, and mediate the recruitment and activation of macrophages. Since CD68 immuno-reactivity has been detected in other cell types, including DCs,

NK cell and endothelial cells, a strict exclusion gating strategy was applied to define our monocyte / macrophage population (428).

6.3.3 Decidual macrophages positively express a range of recognised ‘M1’ and ‘M2’ markers

To elucidate the potential role of circulating monocyte and tissue macrophage subsets in pregnancy, protein expression of a range of recognised markers was assessed. This was performed using whole blood and decidua to avoid surface protein alterations, which may arise as a result of the CD14+ bead isolation procedure. Although important to note that DCs are CD14+CD16-, these cells represent only 1-2% of all CD45+ cells within the decidua, thus were not considered significant contaminants (369).

To date, studies exploring the characteristics and functional responses of cord monocytes have been relatively limited. Overall, cord and maternal classical subset surface expression appeared relatively analogous between the two sites, with no significant differences measured. This is consistent with Sohlberg *et al*, who assessed CD153, HLA-DR, CD80 and CD86 using a similar classification (429). However, it is recognised that the haemopoietic and immune function of activated cord blood leukocytes comparative to maternal leukocytes appears developmentally immature with reduced effector functions (430). This may account for the lower expression of HLA-DR, CD163 and CD86 measured, albeit not significant. Overall, both maternal and cord CD14++CD16- subsets positively expressed a range of recognised classical markers, including TLR-2, CD86, and HLA-DR.

Considering the tissue resident macrophage population, the same markers were applied. Our findings confirm decidua macrophages do not conform to the simple bipolar classification, with positive expression of a range of M1 and M2-associated genes. Comparison of first trimester CD14++CD16- decidua and maternal subsets revealed significantly lower TLR-4, TLR-2 and CD86 expression in those from decidua. This appears consistent with a dampened pro-inflammatory phenotype at the materno-fetal interface (431). Gustafsson *et al* identified in first trimester macrophages that few upregulated decidua genes were signature of classically activated M1 macrophage phenotype, whilst several corresponded to markers of alternatively activated

macrophages, such as CD209 (431). Another previous microarray analysis comparing decidua macrophages and maternal monocytes failed to categorise subsets according to traditional ‘M1’ and ‘M2’ classification system however, with first trimester decidual macrophages producing both inflammatory and anti-inflammatory CKs including TNF- α , IL-10 and TGF- β (390). Here, CD209, HLA-DR and CD163 were strongly expressed in decidua subsets, whilst CD86, TLR-4, and dectin were low. Overall, this is consistent with previous reports, in which CD14⁺ decidual macrophages expressed high CD209, HLA-DR, and CD68, with low CD80, CD83 and CD86 (431). Traditionally CD209 and CD163 are considered M2 markers, generally associated with an alternative macrophage activation profile. Upregulation of CD209 in decidua has previously been characterised, and appears an early pregnancy event potentially induced by the invading trophoblast / pregnancy specific factors since this is not expressed by cells in the endometrium (432). CD163, a member of the scavenger receptor family and recognised tissue resident marker has been reported to exert an anti-inflammatory function (433). Consistent with these findings, mixed leukocyte reaction studies have been used to demonstrate a suppression of mitogen-induced proliferation of decidual macrophages comparative to their peripheral blood counterparts, indicating a functional suppressive phenotype is favourable for maintenance of the semi-allogeneic fetus (434). During the peri-implantation period, decidual macrophages appear skewed towards an M1 phenotype after which they transition in response to EVT invasion of the uterine stroma (435). Overall, M2 macrophages then appear predominant, with typical M2-associated markers, including CD206, and CD209, low co-stimulatory CD86, and high IL-10 reported previously (390). This balance may explain how tissue macrophages exert such heterogenic roles, including host defence, immune regulation, tissue development, angiogenesis, and tissue remodelling and repair (393, 431).

6.3.4 Decidual macrophages demonstrate differential transcript expression and responsivity of the vitamin D metabolic system

To our knowledge, this is the first time the vitamin D metabolic system has been characterised in purified CD14⁺ decidua-derived subsets and compared to paired cord and maternal blood subsets. As

anticipated, maternal and cord blood CD14⁺ subsets demonstrate the capacity to detect and control 1,25(OH)₂D₃ via regulation of CYP24A1. Specifically, when there is sufficient local 1,25(OH)₂D₃, *CYP24A1* expression is enhanced. In response to LPS stimulation a marked shift towards 1,25(OH)₂D₃ production and maintenance was evident. Consistent with this, both cord and maternal monocytes express *VDR*, and upregulate its expression in response to LPS. Pinzone *et al*, who used monocytes from healthy volunteers, found LPS (100ng/mL) significantly upregulated *CYP27B1*. As shown here, LPS had no effect on *CYP24A1*, but decreased *VDR* expression in the first 24h (436); the reason for this discrepancy is unclear. Within the context of *M. Tb*, TLR activation similarly induced *VDR* expression in human monocytes and macrophages (437). Overall, our findings appear consistent with previous reports.

Albeit decidua-derived macrophages also express the vitamin D metabolic apparatus, a unique responsiveness to both 1,25(OH)₂D₃ and LPS was clearly evident. Within the decidua, macrophages express constitutively higher *CYP27B1* and *CYP24A1* than those circulating peripherally. However, neither LPS nor 1,25(OH)₂D₃ affected expression. In healthy human alveolar macrophages *CYP27B1* expression appears highly dependent upon prior stimulation, such as by LPS. However, alveolar macrophages obtained from patients with sarcoidosis demonstrate 1,25(OH)₂D₃ synthesis without prior stimulation (405). High constitutive *CYP27B1* expression in the decidua may similarly reflect prior macrophage priming within the pro-inflammatory CK milieu at the materno-fetal interface. *CYP24A1* expression was similarly constitutively higher at baseline, with only modest upregulation measured in response to 1,25(OH)₂D₃. Previously we have shown that within the decidua 1,25(OH)₂D₃ concentrations are markedly higher than the fetal placenta (104). High exposure to 1,25(OH)₂D₃ concentrations in the decidua may have already induced increased CYP24A1 expression at baseline, with no further negative feedback therefore evident. However, whether this represents an alternative splice variant of CYP24 which encodes a dominant negative-acting protein which is catalytically inactive and permits accumulation of decidua 1,25(OH)₂D₃ was not ascertained (438).

VDR expression remained low across the 4 culture assays compared to maternal and cord subsets, with no effect of 1,25(OH)₂D₃ or LPS measured. This may reflect a paracrine role for locally-generated 1,25(OH)₂D₃ upon neighbouring *VDR*-expressing cells, such as T cells. Previous reports within the context of T cells have shown addition of inactive 25(OH)D₃ is only sufficient to alter T cell responses in the co-presence of bystander APCs(330). Mechanistically, *CYP27B1* is induced in DCs upon maturation with LPS or T cell contact resulting in the generation and release of 1,25(OH)₂D₃, which subsequently affects T cell responses. It is also possible the decidua resident subsets are more mature. For many years, the key action of vitamin D upon macrophages was considered its ability to stimulate differentiation of precursor monocytes to mature phagocytic macrophages, as supported by the differential expression of *VDR* and *CYP27B1* at different stages of differentiation (439).

The recognised vitamin D target *cathelicidin* antimicrobial peptide transcript was upregulated in both cord and maternal subsets following treatment with 1,25(OH)₂D₃ (41). Conversely, upregulation of *cathelicidin* in response to 1,25(OH)₂D₃ or LPS was not evident in CD14⁺ decidua subsets, with relative expression lower comparative to both peripheral CD14⁺ subsets. Within the decidua a differential role for vitamin D is apparent, which may be less concerned with innate immunity (440). Within the placental trophoblast and decidua, *cathelicidin* expression has been measured previously (441, 442). Here Lim *et al* found treatment of fetal membranes and myometrium with cathelicidin's active component LL-37 significantly induced pro-inflammatory cytokines IL-6 and TNF- α , and chemokines IL-8 and MCP-1, and induced pro-labour mediators (442). As our samples were from pregnant women undergoing ELCS (not in labour) delivery, lower *cathelicidin* expression may reflect a pro-tolerogenic materno-fetal environment.

IFN- γ expression was relatively low in maternal and cord CD14⁺ subsets, whilst decidua CD14⁺ expression was high at baseline, with only modest receptivity to LPS. In murine models, IFN- γ is vital for normal placentation. Specifically, IFN- γ null mice exhibit inappropriate decidualisation and spiral artery modifications, and significant fetal loss (333). Treatment with IFN- γ restores normal

decidual and arterial morphology(333). The marked induction of *IFN- γ* in the decidua subsets may suggest an important role in the third trimester also.

In contrast to the cord, maternal monocytes demonstrated ~5-fold greater upregulation of *IFN- γ* in response to LPS. We anticipate this may simply reflect the relative immaturity of cord subsets, with this enhanced maternal response to LPS reflecting more efficient generation of a pro-inflammatory M1 phenotype. Interestingly, both maternal and decidua CD14+ subsets showed partial *IFN- γ* suppression in the co-presence of 1,25(OH)₂D₃, however as this was not significant the validity of this response is not yet certain. Traditionally, both monocyte and macrophages are considered targets rather than producers of *IFN- γ* (443). However, more recent studies have suggested macrophages secrete *IFN- γ* in response to various stimuli with roles in the early phase of host response against infectious agents(444). Within the placenta, a role for VDR-dependent 1,25(OH)₂D₃ mediated inhibition of pro-inflammatory CKs, including *IFN- γ* , *IL-6* and *TNF- α* has been reported (332).

IL-6 and *TNF- α* , both recognised innate immune markers in peripheral monocytes (411), were markedly upregulated in both cord and maternal CD14+ subsets in response to LPS-stimulation. Notably, the decidua-derived CD14+ subsets demonstrated constitutively higher expression. In response to LPS+1,25(OH)₂D₃ co-treatment, expression decreased at all 3 sites, albeit not significant. Previous reports have in range of cell types (445, 446), including monocytes (402, 436, 447) reported 1,25(OH)₂D₃-mediated *IL-6* downregulation. However, the influence of 1,25(OH)₂D₃ upon monocytes/macrophages appears dependent upon the degree of maturation, and stimulus employed (448). This is anticipated an immunomodulatory mechanism to control expression of innate pro-inflammatory mediators (448). Within first trimester decidua, *IL-6* is postulated to be involved in tissue remodelling and placentation, whilst in the third trimester its function appears relatively unclear. Significantly higher decidual concentrations have been measured within the context of clinical chorioamnionitis and PET (449, 450).

1,25(OH)₂D₃ has also recently been shown to suppress LPS-induced *TNF- α* in THP-1 cells and human primary monocytes (451). In human peritoneal macrophages, incubation with 1,25(OH)₂D₃ prior to stimulation with LPS inhibited *TNF- α* expression at both an mRNA and protein level (452).

Peripherally this may similarly be anticipated to support an immuno-modulatory role. TNF- α has previously been shown to be constitutively produced in the decidua and its secretion by decidual cell suspensions has been shown to be enhanced by LPS. There is also some evidence that third trimester macrophages increase production of TNF- α in response to infection, thereby contributing to an intrauterine inflammatory reaction and risk of preterm labour(453).

6.3.5 Whole transcriptome analysis of third trimester paired cord, maternal and decidua monocyte and macrophage subsets

Our principal objective was to compare vitamin D effects upon peripheral materno-fetal blood monocytes and decidua-derived macrophage populations utilising a non-biased whole transcriptomic approach. To optimise monocyte / macrophage purity, FACS technology was utilised, with a method adapted from Mukherjee *et al* (408) which sequentially excluded neutrophils, NK cells, B cells and T cells from analysis prior to FACS. Given the lack of evidence as to how 1,25(OH)₂D₃ may function within the decidua, detailed analysis of the whole CD14⁺ monocyte/ macrophage population was decided most informative, particularly given the stark differences in the relative subset frequencies measured between decidua and peripheral blood.

Pro-inflammatory LPS was utilised, as a well-recognised monocyte and macrophage activator (454). Based upon our initial studies we anticipated activation with LPS would enhance the potential transcriptomic comparisons between the three groups. Previous studies using DNA microarrays have revealed greater transcript differentially expressed following LPS activation in cord monocytes, with significant transcriptomic variations compared to adult peripheral blood monocyte subsets (371). Albeit our analysis suggested some evidence of differential responsivity to LPS in maternal and cord monocytes, with 219 (2.8%) transcripts differentially expressed, this was not explored further here.

Notably decidua subsets appear highly distinct from matched peripheral fetal and maternal subsets. This is clearly highlighted by PCA analysis, in which LPS treated decidua-derived macrophages were consistently the major source of variance compared to both LPS-treated maternal and cord monocytes. Overall 31.8% and 30.3% of cord and maternal transcripts respectively were differentially expressed

comparative to the decidua following LPS stimulation. In both, approximately twice as many transcripts were downregulated in the decidua. Comparing these genes, a significant degree of overlap was observed with 63% and 54% differentially expressed transcripts shared between the maternal LPS vs. decidua LPS and cord LPS vs decidua LPS groups respectively. Consistent with this, whole transcriptomic analysis of monocyte to macrophage differentiation and polarised activation recently demonstrated monocyte maturation to be associated with significant global transcriptome modifications (455). Specifically, monocyte-to-macrophage differentiation involved modulation of genes involved in cell cycle activation, metabolic activities, lipid metabolism, and G protein-coupled receptor and chemokine signalling(455). Previous microarray analysis of CD14+ blood and endometrial monocyte and macrophage subsets in pregnant cows suggested a common mononuclear lineage, but with highly diverse functions. Overall, 13,422 genes expressed in both cell types, with 450 genes exclusively expressed by endometrial CD14+ cells and 1,386 genes expressed exclusively by blood CD14+. A preponderance of genes implicated in cell signalling, migration and cell motility in the blood monocytes was measured, whilst genes with key roles in immune regulation, tissue remodelling, angiogenesis, and apoptosis were measured in the endometrial macrophages (456). Previous microarray-based comparison of paired unstimulated CD14+ maternal, cord and placental fetal trophoblast-derived Höfbauer cells reported a close resemblance in the molecular signature of monocytes from maternal blood and the placenta. Overall, 73% transcriptome homology was identified, with quantitative rather than qualitative differences measured. Consistent with our data, cord and maternal transcript expression was comparatively highly analogous. The placental CD14+ cells were consistent with a tissue resident subset reflecting clusters of both classic-M1 and adaptive-M2 subtypes, with over-representation of chemokines, pro inflammatory CK and pro-regulatory CK. By contrast the maternal monocytes strongly expressed genes related to leucocyte adhesion and chemotaxis, antigen presentation and pathogen recognition and response (457). These findings support our primary hypothesis, that within the decidua a unique immune cell population exists, which is disparate to circulating peripheral maternal and those of fetal origin (i.e. fetal cord blood and placental trophoblast)(457).

6.3.6 Differential regulation of third trimester maternal blood, cord blood and decidua monocyte and macrophage subsets by 1,25(OH)₂D₃

Previous studies delineating the non-classical effects of vitamin D upon immune cell function have demonstrated a greater functional responsivity of both innate and adaptive subsets within the context of immune cell activation (56, 330). This is mediated in part by increased expression of VDR in activated immune cells(353), which was here measured in both the cord and maternal subsets. The high number of differentially expressed 1,25(OH)₂D₃ targets measured in the decidua macrophages was perhaps not anticipated given the relatively lower VDR expression measured. However it is recently understood that the VDR transcriptome demonstrates significant diversity, being both cell type and time dependent(458). Classically 1,25(OH)₂D₃ mediated transcript activation and suppression of target genes arises via VDR binding, dimerization with RXR and subsequent complex formation with VDRE in the promotor regions of select target genes, such as *CYP24A1*, *BGLAP61* and *CA2*. ChIP-sequencing has uncovered many of the molecular processes governing vitamin D-mediated transcription, leading to the identification of novel regions within the genome to which vitamin D-induced VDR/RXR binds. Co-repressors and coactivators are then recruited to promote gene expression (458). However, only a limited number of genes contain VDREs in their promoter regions and are under the direct transcriptional control of 1,25(OH)₂D₃. Indirect modulation of signalling cascades or unknown non-genomic mechanisms also appear at play. This may account for the broad spectrum of functional transcript targets for vitamin D identified (459). Present models of vitamin D signalling indicate that 1,25(OH)₂D₃-mediated primary target gene activation via VDR binding to its genomic sites occurs within 2–3h. The majority of non-genomic secondary target genes demonstrate a significant transcriptional response 4h post 1,25(OH)₂D₃ exposure. By selecting a 24h time-point both primary and secondary vitamin D target genes should have been detected in our study. Albeit not possible to discern between these early and late targets, both the primary and secondary effects of vitamin D were of interest (199, 460).

Overall, only 2 shared transcripts, *CA2* and *EFL1*, were upregulated by vitamin D in all 3 subsets. The finding that 1,25(OH)₂D₃ upregulated *CA2* is consistent with previous reports in mononuclear

bone marrow cells, in which vitamin D promoted differentiation towards an osteoclast phenotype and subsequent bone resorption activity (461, 462). Monocytes and macrophages also express CA2, albeit at low levels comparative to the osteoclast lineage (461). CA2 encodes carbonic anhydrase, which is involved in the reversible hydration of carbon dioxide and is widely distributed across human tissue sites, with important roles in gas transport, acid/base regulation and key biosynthetic reactions including gluconeogenesis, lipogenesis, and tumorigenesis (463). Importantly, the uterine endometrium also expresses *CA2*, with its enzymatic activity doubling during the luteal phase of the menstrual cycle. Furthermore, in women suffering from recurrent pregnancy loss, higher frequencies of serum CA2 auto-antibodies have been measured (464). The underlying significance of this and the role of 1,25(OH)₂D₃-mediated *CA2* up regulation in cord, maternal and decidua subsets is not yet clear, but warrants future investigation.

Considering *EFL1*, which encodes elongation factor 1 this is involved in the biogenesis of the 60S ribosomal subunit and translational activation of ribosomes. More recent ribosome studies also suggest a key role in tRNA and mRNA translocation (465). Importantly, defective late maturation of the 60S ribosomal subunit may impair translational control, with subsequent tumour progression. To our knowledge no previous studies delineating the effects of 1,25(OH)₂D₃ upon *EFL1* are reported. How this upregulation may influence monocyte and macrophage function is not clear, but it is plausible this serves as a control during cell development and function in the context of immune stimulation.

In the cord and maternal subsets, 16 shared transcripts were identified. These were highly heterogenic, with roles in regulating genomic processing and cell processing, including cell proliferation, migration and apoptosis most prominent. As only a small number of transcripts were identified overall as significant for the maternal and cord subsets, the degree of overlap was marked. Conversely, for the decidua, other than *CA2* and *EFL1*, only *DIRC2* was shared with 1,25(OH)₂D₃-treated cord subsets, with a similar trend also measured in the maternal subsets (fold-change 1.64, p>0.05).

In the maternal blood, treatment with 1,25(OH)₂D₃ significantly altered 41 (0.53%) transcripts compared to LPS alone, primarily upregulating genes associated with cellular function (n=13; 31.7%), relating to cell migration, adhesion, apoptosis and intracellular trafficking; Importantly 9 (69.2%) of these were also significantly upregulated in the cord group, for which 40 (48.2%) of the total 83 transcripts significantly differentially expressed in the vitamin D group related to cell processing, in particular regulation of monocyte apoptosis, trafficking, adhesion and proliferation.

Genomic processing was also a prominent vitamin D regulated group for both cord and maternal subsets, with 14 (16.9%) and 10 (24.3%) measured respectively. Of these, 4 were shared; *NRIP1*, *ZFP36L1*, *ASCC1* and *EFL1*, all of which are implicated in mediating gene translation, transcription and ribosomal processing (465, 466). In both a number of transcripts were also concerned with mRNA splicing and processing, and cell cycle regulation, including maternal *LSM5*, *PRPF19*, *SNRPF*, *ANAPC10* and cord *NCBP2*, *SIN3B* transcripts. Together these results indicate that vitamin D, like other nuclear steroids, exerts important genomic actions upon monocyte subsets. A common anti-proliferative VDR function is associated with arrest at G₀/G₁ of the cell cycle, coupled with upregulation of a number of cell cycle inhibitors (467). This is highly relevant as chromatin modification, transcription, translation, RNA processing and post-translational modification provide the major checkpoints for a cell to regulate overall gene expression. These vitamin D mediated epigenomic changes may represent an initial step in the modulation of the monocyte transcriptome. Consistent with this, in THP-1 cells it has been shown using formaldehyde-assisted isolation of regulatory elements sequencing that the chromatin accessibility of approximately 9000 loci was significantly altered by 1,25(OH)₂D₃. Maximal chromatin opening was observed after 24h. These findings suggest that a large number of 1,25(OH)₂D₃-triggered epigenome-wide events precede and accompany the transcriptional activation of target genes (468, 469).

A number of transcripts were also involved in energy metabolism in both 1,25(OH)₂D₃-treated maternal (7; 17.0%) and cord blood (10; 12.0%) monocytes. Regulation of a number of markers of both lipid and glucose metabolism, including maternal *ACBD6*, *SDHAF1*, *DPP4*, *CA2* and cord *APOBR*, *SAT1*, *B3GNT2*, *SCD*, *DPP4*, *CA2* and *INSR*, were regulated by vitamin D in both. *DPP4*,

which was upregulated by vitamin D in both is best known for its enzymatic ability to inactivate the incretin hormones. Within the context of type-2 diabetes, DPP4 inhibitors improve glucose metabolism via prolonged insulin release and trophic beta cell effects(459). However, beyond this a much broader functional role is now recognised. In epithelial cell lines, transfection with DPP4 decreases cell migration and increases apoptosis. Similarly, in a range of cancer cell lines DPP4 overexpression resulted in pronounced anti-tumorigenic effects, including inhibition of in vitro cell migration, growth, and increased apoptosis (459). Consistent with our data, DPP4 is upregulated in breast cancer tumour cells (alongside CA2) post exposure to 1,25(OH)₂D₃ (470). Upregulation in artery smooth muscle cells exposed to 1,25(OH)₂D₃ is also reported, with enhanced apoptosis prominent (471). It appears that the actions of vitamin D upon DPP4 are cell-type specific, as in type-2 diabetes, downregulation is instead reported (472). Within the context of immune function, DPP4 is expressed on a range of innate and adaptive subsets, including monocytes. For T cells, a co-stimulatory role with Th1 activation and proliferation is characterised (459), however a pro-regulatory role is also evident; within the context of antigen-induced arthritis DPP4-deficient mice demonstrate increased disease severity with evidence of dysregulated pro-inflammatory chemokine release (473). The effects of vitamin D upon *DPP4* expression in immune cell subsets is to our knowledge yet to be characterised, but shall likely be pregnancy and monocyte specific.

Albeit only a small number of immune transcripts were regulated by vitamin D in the maternal and cord monocytes (3 maternal and 7 cord), overall our data indicates an immuno-regulatory role for vitamin D within the context of pregnancy. In the maternal subsets, CD276 was significantly downregulated in those treated with LPS and vitamin D comparative to LPS alone. This co-stimulatory molecule participates in the regulation of T-cell mediated immune response, with expression markedly induced on monocytes by inflammatory CK (474). Importantly, this costimulatory molecule co-stimulates proliferation of CD4⁺ and CD8⁺ T cells, thereby enhancing the induction of cytotoxic T cells and selectively stimulating IFN- γ production in the presence of T cell receptor signaling. Consistent with this, IFN-induced protein with tetratricopeptide repeats (*IFITs-5*), which is involved in innate immune defense was also significantly downregulated by vitamin D (475).

In the cord, *THEMIS2* and *KIAA1804*, which are both negative regulators of TLR-4 mediated signaling were upregulated by vitamin D, which may suggest an overall suppression of this inflammatory pathway. In monocytes, 1,25(OH)₂D₃-mediated induction of hypo-responsiveness to pathogen-associated molecular pattern (PAMPs) by downregulating expression of TLR-2 and TLR-4 on monocytes has previously been shown, which may limit inflammatory T cell responses (403). Oncostatin M, a CK and growth regulator that inhibits the proliferation of a number of tumour cell lines and regulates the production of pro-inflammatory CK, such as IL-6, was also upregulated by vitamin D. Furthermore, CD40, a well-documented receptor on APCs which is critical for mediating a broad variety of immune and inflammatory responses was significantly downregulated(476). Finally, *IFITIM3*, an IFN-induced antiviral protein, which inhibits the entry of viruses to the host cell cytoplasm(477), was again downregulated by vitamin D. Inconsistent with our data, within the context of normal healthy adults and cancer, monocytes/ macrophages have been shown to be enhance cellular cytotoxicity and phagocytosis following exposure to 1,25(OH)₂D₃(478, 479). This includes 1,25(OH)₂D₃-mediated antibacterial defense, with induction of phagocytosis and antimicrobial peptides evident. This may have been anticipated here given our previous finding that vitamin D markedly induced *cathelicidin* mRNA expression in unstimulated CD14⁺ monocytes. However, interestingly this was not observed in the co-presence of LPS stimulation. The reason for this is not certain, but may be pregnancy specific, and warrants further study.

Previous reports of immune effects upon vitamin D upon peripheral monocytes have otherwise been relatively heterogenic with a range of pro-regulatory anti-inflammatory actions also described (480, 481). Rigby *et al*, using healthy adult monocytic cells found vitamin D to decrease monocyte function as an APC. Specifically, vitamin D pre-treatment induced a defect in accessory T cell function and proliferation. However, these effects were only significantly altered by 1,25(OH)₂D₃ at >24h, with decreased T cell proliferation observed only at 40h (482). Previous microarray analysis of 1,25(OH)₂D₃-regulated gene expression in THP-1 cells showed that 46 genes were differentially expressed after 2.5h, 288 at 4h and 1204 at 24h. Furthermore, combined 1,25(OH)₂D₃ (100nM) and glucocorticoid treatment of PBMCs at different time points (8 and 24h) similarly revealed time-

dependent variations in transcriptional responses to $1,25(\text{OH})_2\text{D}_3$, with enrichment of genes associated with immunomodulation and immune defense occurring only after 24h (341).

Given the range of metabolic and pro-regulatory immune targets identified, it is interesting to consider their combined role in relation to monocyte function 'immuno-metabolism'. It has long been known that macrophage function and metabolism are connected. For instance, glutamine and L-arginine metabolism has been recognised to be involved in macrophage functions like nitric oxide production, microbicidal activity, and phagocytosis(483). For example, circulating fatty acids activate TLR-4 signalling in adipocytes and macrophages. Moreover, mice lacking TLR-4 are protected from the ability of systemic lipid infusion to (a) suppress insulin signaling in muscle and (b) reduce insulin-mediated changes in systemic glucose metabolism. These data suggest the innate immune system participates in the regulation of energy balance and insulin resistance in response to changes in the nutritional environment. Here we show LPS mediated transcript expression is altered by vitamin D, with a number of metabolic markers related to glucose metabolism differentially expressed (484).

Unlike the cord and maternal subsets for which most transcripts were upregulated by $1,25(\text{OH})_2\text{D}_3$, in the decidua both up (45.3%) and downregulation (54.7%) of transcripts was evident. Notably, despite relatively lower VDR expression, the number of differentially expressed targets was increased comparative to both peripheral monocyte subsets. To our knowledge, this is the first study comparing the relative responsivity of paired monocyte and macrophages subsets to vitamin D. Whether increased VDR sensitivity is a common feature of tissue resident or decidua specific macrophage subsets is not known. There is evidence to suggest VDR activity is highly cell-specific with significant variability in its downstream signalling effects, with possible explanations including differing tissue specific N-terminal VDR variant expression, post transcriptional epigenetic modifications to VDR, or alternative chromatin modifications (467).

Considering those decidual macrophage targets identified, vitamin D primarily targeted genes related to genomic processing. A predominance of transcripts positively implicated in protein synthesis was measured, in particular those related to transcription activation, RNA transport, histone modification and cell-cycle progression, including *SETSIP*, *RGPD3*, *ZNF432*, *HIST1H4K* and *PKN2*.

It has been suggested that signals propagated in the utero-placental environment may contribute to amplification of inflammation at the maternal-fetal interface through activation and reprogramming of maternal monocytes(457). Albeit not ascertainable from our data alone, we anticipate these genomic modifications may in part reflect monocyte-to-macrophage differentiation given vitamin D is already implicated in this process outside the decidua (104). This process evokes significant transcriptome changes, including alteration of cell cycle genes, metabolic activities, lipid metabolism, and chemokine signalling (455). Previous reports similarly describe significant alterations in genomic targets during macrophage differentiation, including over-representation of cell cycle and cell *division*-associated proteins (455).

A high preponderance of transcripts relating to cell processing, in particular vesicle mediated transport (*KLC4*, *USP6NL*, *INPP5E*, *SYS1*, *CTAGE5* and *TMED1*), intracellular trafficking (*BBS10*, *ARFIP1*, *SYS1*, *BRK1*, *DIRC2*, *VPS36*, *NXT2*, *TOMM20*, *GGA3* and *TANGO6*), migration and adhesion (*SI00A12*, *DOCK1*, *CDK18*, *PKN2* and *VAV2*), cell growth / proliferation (*OVCA2*, *PSMD10*, *FRMD6*, *ZFYVE28*, *LAMTOR4*, *PSMD10*, *PPP1R37*, and *FAM72A*) and apoptosis (*OVCA2*, *SGMS1*, *MAP3K7*, *PPP1R37*, *PTRH2*, *RABGGTA*, *FRMD6*, *ATG101*, *CAMKK2* and *WIPI2*) regulation were identified for the decidua macrophages. Given the heterogenic effects upon transcript expression, how vitamin D may influence overall function is difficult to ascertain without further validation studies.

Our data indicates vitamin D promotes autophagy, which contributes to anti-aging, antimicrobial defence, and tumour suppression, playing a key role in overall tissue homeostasis(485). Macrophages have previously been implicated in phagocytosis and apoptotic cell and trophoblast cell debris clearance, via the secretion of extracellular matrix proteins and CK. This supports cross-gestation effects upon decidualisation and tissue remodelling, with regulation of placental cell invasion, and angiogenesis reported. It is also suggested this apoptotic cell clearance induces an immunosuppressive, anti-inflammatory macrophage phenotype (486). This is consistent with a pro-apoptotic role for vitamin D as described in breast-derived mammary cells, in which 1,25(OH)₂D₃ modulated autophagy in a VDR-dependent manner. Interestingly, this autophagy-related gene

expression signature, was absent in those cells with cancer (487). Autophagy can be induced by a range of factors, including cellular stress and hypoxia, and represents a key host defence strategy to remove the harmful stimuli via lysosomal degradation. Importantly, in our data-set *WIPI2* transcript was upregulated in response to vitamin D. This encodes an early component of the autophagy machinery, which is involved in formation of mature degradative phagosomes. Autophagy Related 101, which conversely stabilises *ATG13* thereby protecting it from proteasomal degradation and autophagy initiation was downregulated by vitamin D(485).

As eluded to, vitamin D mediated modulation of genes involved in cellular metabolism was a prominent feature of the decidua macrophages. This included targets relating to glycogen storage, the mitochondrial respiratory electron chain, fatty acid breakdown, and phospholipid biosynthesis. This included upregulation of *FDXI*, a recognised vitamin D target which is an electron mediator involved in multiple physiological processes, including electron donation to cytochrome P450 enzymes, thereby driving vitamin D metabolism (488). Macrophage metabolism is connected to their phenotype and function, and that metabolism is controlled by cues derived from tissue microenvironment(483). As illustrated in Figure 6.18, increased expression of genes relating to glucose metabolism, lipid, cholesterol and fatty acid metabolism, and triglycerides synthesis mark macrophage differentiation and activation (457). Further delineation of these processes is certainly important, as dysregulated macrophage metabolism is associated with metabolic disease. In mice, deletion of macrophage VDR is shown to induce insulin resistance by promoting M2 macrophage accumulation in the liver as well as increasing CK secretion and hepatic glucose production. Reversal with bone marrow transplant of VDR-expressing cells improved insulin sensitivity, suppressed atherosclerosis, and decreased foam cell formation (489). It is of certain interest whether dysregulated monocyte / macrophage function is implicated in the underlying pathogenesis of gestational diabetes(490). Furthermore, as hyperglycaemia manifests as placental-mediated disorder, which is associated with inflammation and oxidative stress, aberrant macrophage metabolism and function may help drive this process(491).

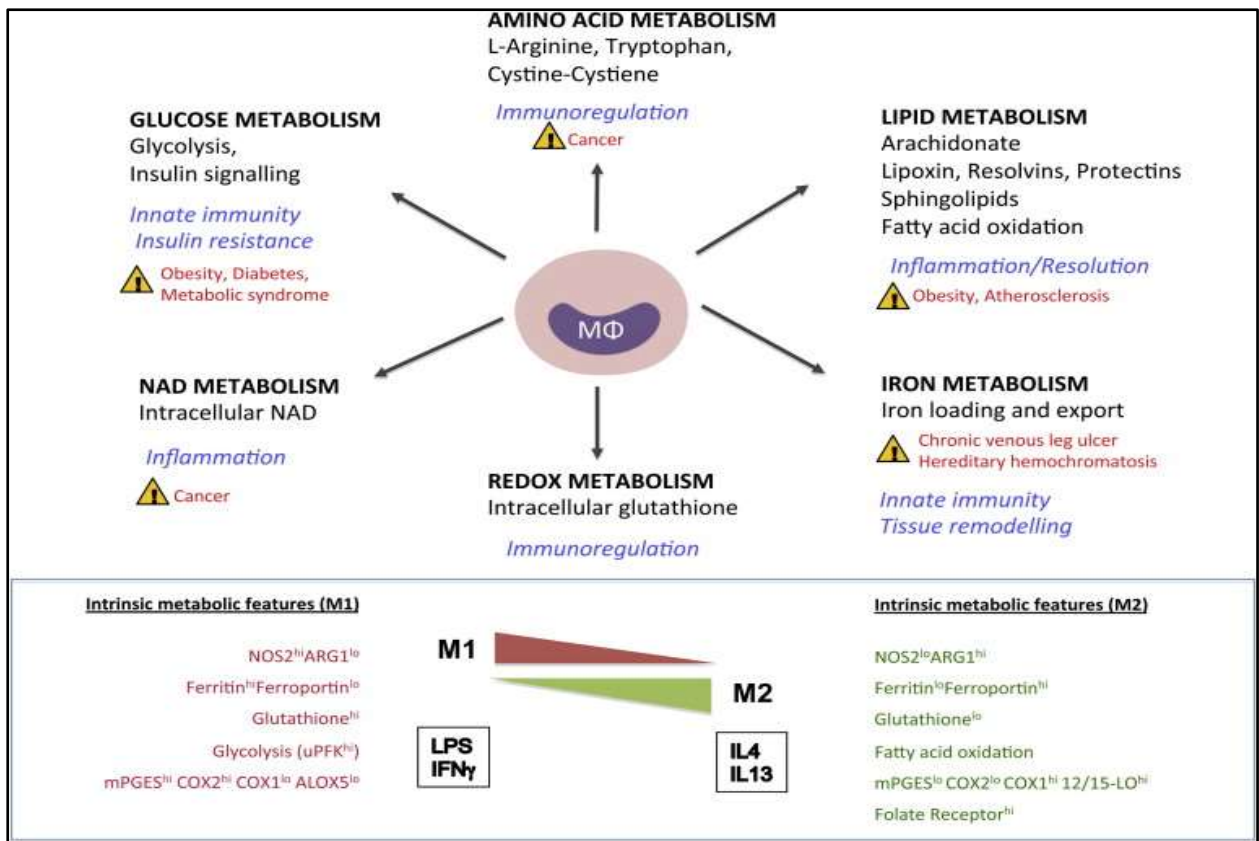


Figure 6.18 Orchestration of Metabolism by Macrophages. Italicized words indicate macrophage-mediated functions related to metabolic activities. Red; associated diseases, blue; associated biological processes, and the inset; selected metabolic features of polarised M1 and M2 macrophages. Elsevier permission approved. (483).

Finally, consistent with the cord and maternal monocytes, several immune transcripts were altered by vitamin D at 24h in decidual macrophages. Overall, these were consistent with a potential immuno-regulatory role for vitamin D. In particular, *NRROS*, which plays a critical role in desensitizing TLR signaling through inhibition of TLR-mediated NF-kappa-B activation and CK production(492) was upregulated by vitamin D. This arises via inhibition of reactive oxygen species production by phagocytes during inflammatory response. *SPG21*, which is implicated in suppression of T cell activation(493), was also significantly upregulated. Recent reports determining the functional role of mid-term and term macrophages found neither could stimulate allogeneic umbilical cord blood T cells to express the activation marker CD69. In addition, lymphocyte proliferation was impaired in both, indicating decidual macrophages have an impaired capacity to induce T cell

activation and proliferation during pregnancy (427). Moving forward, experiments assessing how vitamin D affects decidual macrophage-mediated effects upon T cells are of certain interest. We postulate altered antigen presentation, with enhanced T regulatory cell induction may be observed.

Data from the current study show for the first time that decidual macrophage subsets are an important target for $1,25(\text{OH})_2\text{D}_3$, with effects distinct to those measured in cord and maternal blood monocyte subsets. Overall it appeared decidual macrophages are more responsive to vitamin D despite their lower VDR expression, with roles in cell processing, metabolism, RNA processing and immune function identified. The implications of vitamin D deficiency during pregnancy may have an important impact upon macrophage function in the third trimester. Further studies are required to better understand the functional implications of this.

6.3.7 Study limitations

Through the above studies the potential effects of vitamin D upon third trimester monocyte and macrophage subsets have been assessed. It is important to highlight all women recruited underwent ELCS, and as such were not in active labour. This is important as in women spontaneously delivering at term an increased macrophage tissue density is reported comparative to those delivered at term who did not labour. Furthermore, with the initiation of parturition, decidua expression of anti-inflammatory mediators decreases with a concomitant upregulation of surge in pro-inflammatory mediators. Given the recognised plasticity of decidua macrophages, it is likely the phenotype, and potential functional responsivity to vitamin D may differ between our cohort and those obtained from women with spontaneous labour. As such, the conclusions drawn here do not relate to the process of parturition (422). This warrants future study however, as decidua macrophages are closely implicated in this process(494).

As alluded to in Section 6.2.6, the purity of the CD14⁺ subsets obtained using a positive is enrichment methodology in which monocytes are labelled with antibodies for CD14 receptors ranged from 71.6% to 93.1%. At all three sites, CD3-positive T cells were the main contaminant. This is particularly important when assessing the qRT-PCR data, certainly with regards to the CD14⁺

decidua subsets, for which transcript analysis of the vitamin D metabolic system has not been previously reported.

Although some studies of cell populations were performed on whole blood, thus avoiding the need for potentially cell-activating isolation procedures, for most of the studies performed, isolation of a pure population of cells was essential. The potential effects of different isolation procedures upon both monocyte and macrophage phenotype and function are now recognised. A systematic comparative analysis of four monocyte isolation/ enrichment procedures: positive selection, negative selection, adherence, and RosetteSep techniques reported variable monocyte purities of 98.5%, 97.0%, 67.3%, and 64.2% respectively. Importantly, positive selection yielded the highest results for monocyte isolation. Furthermore, following positive-selection procedures, abundant CD14 expression was still detected, indicating the functional condition of these cells remained intact including their phagocytic properties (495).

For the RNA-seq analyses, FACS was utilised due to its superior accuracy in cell isolation. In preparation for this, detailed knowledge of surface receptor expression on each of the 3 subsets was required. To limit any potential confounding factors which may alter cell surface expression this was assessed using whole PBMC populations. From this a specific monocyte/ macrophage multi-antibody panel was designed, which effectively excluded all other major innate and adaptive CD45+ immune cell subsets. As reported here, the purity utilising this method was greatly enhanced, as unlike the MACS enrichment procedure, flow sorting permitted detailed analysis of each individual cell.

FACS as a method does however pose certain limitations that require recognition. Firstly, during the FACS process, cells undergo a number of traumatic effects which may induce apoptosis, including the field pulse applied to deflect cells interest, expulsion of the cells into collection tubes and prolonged sorting times(496). To optimise cell viability, samples were processed immediately following collection, with tissue handling limited to a minimum requirement. At the point of FACS, a PI dead discrimination dye was utilised to accurately identify and exclude all non-viable cells from the purified cell population. Following collection, cells were immediately transferred to complete culture medium, to limit potential cell death post the sorting procedure. What remains unclear however is the

frequency of cells that became pre-apoptotic or senescent during the cell preparation protocol (496), and to what extent their phenotype and function may have been altered.

Another important limiting factor of the FACS method for both blood and tissue samples was total target cell recovery. This negatively dictated the total assays and culture conditions which could be performed simultaneously. One solution may have been to pool donor samples; however this would have certainly been deleterious for the final RNA-seq output data and analysis given the intra-participant variability observed in the PCA.

While RNA-seq is a powerful tool for defining global changes in gene expression for specific cell types and treatments, there is the potential for functional over-interpretation. The general limitations of this method have been discussed already in Chapter 5, Section 5.3.7. For this data, the total post-alignment coverage was reduced relative to the first trimester project, with the mean total reads per sample ~ 12155275 . This may in part account for the lower number of differentially expressed genes than was anticipated based upon the current literature for monocyte THP-1 cells and vitamin D (340). Determining the required coverage for an RNA-Seq experiment is a complex task as different transcripts are expressed at different levels, meaning that more reads will be captured from highly expressed genes while fewer reads will be captured by genes expressed at low levels. Furthermore, albeit the cost of sequencing continues to fall, the feasibility of RNA-seq remains partly dictated by costs. For example, to detect a rare transcript or variant, considerable depth is required.

Clearly further follow up studies are required to validate the biological impact of specific $1,25(\text{OH})_2\text{D}_3$ -target genes in both monocyte and macrophage subsets in pregnancy.

7 Final Discussion

Vitamin D deficiency is highly prevalent in pregnant women, and is associated with a range of non-classical adverse pregnancy outcomes, including PET (116). Based upon current definitions, our study confirms the prevalence of low serum vitamin D in pregnancy, with overall 78.4% of pregnant women 'deficient' and 94.3% 'insufficient' in this West Midlands cohort (109). The definition of normal 'vitamin D status' has generated much debate, with what constitutes optimal or adequate vitamin D status remaining the subject of intense discussion. Utilising a novel LC MS-MS protocol we provide the most comprehensive analysis to date of vitamin D in pregnant women, with the data presented strongly supporting a change in how we assess vitamin D status in normal pregnancy. Measurement of 25(OH)D₃ alone appears to be too simplistic as a marker of pregnancy health outcomes - no significant alteration in serum 25(OH)D₃ concentrations were observed, including analysis of free and bioavailable 25(OH)D₃.

Uniquely, we performed a comprehensive metabolite analysis utilising paired maternal serum, placental, decidua tissue and urine samples, establishing the relationship between circulating and tissue-specific levels of vitamin D metabolites in both normal pregnancy and PET. We demonstrate that normal human pregnancy is associated with significant changes in vitamin D physiology; with a marked increase in the generation of circulating active 1,25(OH)₂D₃ and catabolic 24,25(OH)₂D₃ most prominent. Furthermore, in contrast to previous reports describing decreased serum 25(OH)D₃ in PET (116, 159), vitamin D-deficiency was observed for most of the women in the current study, despite this being a predominantly white Caucasian cohort. We show that in PET dysregulation of vitamin D metabolism is clearly evident, with significant alterations in circulating serum and placental metabolites measured. Significant alterations in circulating 1,25(OH)₂D₃, 3-epi-25(OH)D₃ and 24,25(OH)₂D₃ in different pregnancy settings strongly suggests that alternative vitamin D metabolic pathways are an important feature of pregnancy. We anticipate this may be more pronounced in non-Caucasian groups, and certainly warrants further consideration alongside future functional studies determining the physiological activity of these metabolites.

In normal pregnancy, increased placental accumulation of 25(OH)D₃ occurs with advancing gestational age, despite no apparent change in serum DBP (104). This raises important questions concerning the transport of vitamin D metabolites from mother to fetus. Importantly, in PET, placental accumulation of 25(OH)D₃ appears impaired at the materno-fetal interface. This may reflect aberrant spiral artery development and placental blood flow, both of which are associated with malplacentation (497) and may alter uptake of 25(OH)D₃, either in its free/unbound form or when bound to its carrier protein DBP. Data from the current study also clearly suggest dysregulation of placental 25(OH)D₃ metabolism ensues, as placental concentrations of 24,25(OH)₂D₃ and 3-epi-25(OH)D₃ were higher in PET tissue, indicating that the pregnancy disorder was associated with enhanced catabolism of 25(OH)D₃. Future work delineating whether aberrant vitamin D placental uptake and metabolism is also reflected in the fetus is required since this was not assessed.

What remains unclear from the above studies is whether dysregulation of vitamin D metabolism precedes PET onset and whether metabolite analysis beyond serum 25(OH)D₃ offers a potential predictive biomarker for PET and other adverse events in pregnancy. Utilising a sub-cohort of the Ireland SCOPE study, we successfully quantified a range of vitamin D metabolites in early second trimester pregnant women's serum and urine, prior to development of PET and directly compared the resulting data to matched data for normotensive pregnant women and non-pregnant controls. Importantly, serum analysis alone did not reveal a significant alteration in vitamin D metabolite concentrations. Marked alterations in the association between 25(OH)D₃ with 3-epi-25(OH)D₃ and 24,25(OH)₂D₃ was however clearly evident in the PET group, suggesting aberrant metabolism may arise early in the pathogenesis of PET. Dysregulated metabolism of vitamin D was also evident in these PET samples, with a trend towards 1,25(OH)₂D₃ production again prominent in the sub-clinical disease stage. Moving forward, a prospective study significantly powered to establish whether the degree of dysregulation is associated with disease severity and/ or adverse materno-fetal outcomes is now warranted.

Development of a novel LC MS-MS methodology to measure urinary vitamin D metabolites also enabled comparison with circulating serum levels of vitamin D metabolites. This strategy provided,

for the first time, insight into possible reference ranges for urinary vitamin D metabolites in pregnancy. In particular, lower urinary 25(OH)D₃ and 24,25(OH)₂D₃ excretion was identified as a potential early indicator for a predisposition towards developing PET. Further studies are now warranted to validate these findings given the potential clinical applications of this study for the assessment of vitamin D metabolism in conditions related to vitamin D deficiency. Since urinalysis is routinely performed in the UK antenatally as a screening test for the detection of PET and proteinuria (498), the value of urinary vitamin D analysis is of certain interest.

The principal aim of this PhD was to delineate the potential extra-skeletal effects of vitamin D in pregnancy. Initial data by our group highlighted tissue accumulation of 25(OH)D₃ and 1,25(OH)₂D₃ in decidua early in pregnancy to be significant, albeit the determinants of these levels remained unclear. Furthermore, there is much current interest in the potent immunomodulatory effects of vitamin D and the potential impact this may have on pregnancy, with previous studies suggesting a local decidual intracrine vitamin D system specifically in certain immune cell subsets (207). Specifically, these studies suggested localised 1,25(OH)₂D₃ production as a mechanism for maintaining antibacterial activity, with decidual macrophages considered a likely target, promoting antibacterial responses in a cathelicidin-mediated manner (306). To our knowledge this is the first study delineating the effects of vitamin D upon individual decidua-derived immune cell subsets. Here, we provides novel evidence that isolated 1st trimester decidua uNK cells and 3rd trimester macrophages represent key targets for vitamin D with highly receptive vitamin D metabolic systems, particularly within the context of immune challenge. Furthermore, our data clearly indicate both decidua-derived uNK and macrophages are highly distinct from their peripheral blood counterparts with regards to their functional responsivity to vitamin D, with non-classical actions extending far beyond simply immuno-regulation at the materno-fetal interface. This may be anticipated given both decidual cell types demonstrate a highly unique tissue phenotype compared to their paired peripheral counterparts, including fetal cord blood-derived monocyte subsets, as supported by subsequent detailed pathway analysis. Importantly, we recommend peripheral immune cells are an inappropriate model for analysis of their tissue-resident counterparts, including both decidual NK and macrophages.

To delineate the effects of vitamin D directly at the decidua interface, tissue-derived immune cell based studies are crucial.

Given both the broad range of extra-skeletal vitamin D actions reported and the novel nature of this study, a non-targeted RNA-seq analysis was performed to assess whole transcriptome effects of vitamin D upon both activated NK and monocyte/ macrophage subsets in an unbiased fashion. Our data provides the first cellular and molecular evidence of the ability of 1,25(OH)₂D₃ to target decidual uNK and macrophages with actions targeting whole decidual immune cell function.

Crucially, both first trimester uNK and pNKs express a functional vitamin D metabolic signaling system, and convert inactive 25(OH)D₃ to active 1,25(OH)₂D₃. This is mediated in part by increased VDR expression in activated immune cells (353), with this response more pronounced in uNK. Considering the role of vitamin D, in uNK a significant enrichment of genes involved in cell metabolism, migration, adhesion and apoptosis was measured, with ~40% associated with cell survival, proliferation, invasion, adhesion, angiogenesis, and trafficking. Furthermore, in uNK 1,25(OH)₂D₃ treatment caused significant up-regulation of several key genes with recognised roles in placentation, tissue invasion and angiogenesis. Follow up studies are now warranted to confirm the biological impact of specific 1,25(OH)₂D₃-target genes in uNK given their essential role in fetal implantation, placentation and vascular remodeling (267, 268, 499). We anticipate dysregulation of vitamin D metabolism within the context of PET may have a significant impact upon decidual uNK function during early implantation. Validation of this would more reliably inform future vitamin D supplementation trials. Based upon the data presented in Chapters 4 and 5, we strongly suggest these studies should evaluate the effect of pre-conceptual vitamin D supplementation in pregnancy, as opposed to antenatal treatment, to be truly informative.

For decidual macrophages, despite demonstrating lower expression of *VDR*, expression of metabolic enzymes *CYP27B1* and *CYP24A1* was constitutively higher relative to other circulating populations. This may in part be conducive to paracrine effects upon proximal bystander cells, such as fetal trophoblast or maternal stromal cells. RNA-seq also revealed an increased responsiveness of isolated LPS-stimulated decidual macrophages to 1,25(OH)₂D₃ despite their relatively lower *VDR*. Consistent

with uNK, a broad range of vitamin D –mediated effects upon transcript expression were identified, in particular relating to genomic processing, metabolism, lipogenesis and cell processing. It appears the effects of vitamin D upon decidual macrophages extend far beyond previously reported effects on cathelicidin-mediated anti-microbial function. Outside the decidua this also appears evident; within the context of diabetes, deletion of macrophage VDR in mice is shown to induce insulin resistance and promote atherosclerosis formation (500). Furthermore, in type 2 diabetic patients 1,25(OH)₂D₃ is found to suppress macrophage migration, reversing atherogenic cholesterol metabolism (501). Considering the range of macrophage-related functions recognised, including antigen presentation, phagocytosis and secretion of cytokines, chemokines, angiogenic growth factors and proteases, we anticipate the potential scope of vitamin D functions to be far-reaching in human decidua (393, 502).

Our understanding of this is however reliant upon ongoing studies delineating the exact functional role of third trimester decidua macrophages in normal and pathological pregnancy, as at present this remains unclear (393). Alongside this, further studies investigating how vitamin D alters LPS-mediated monocyte and macrophage function will be important, particularly given the association between aberrant LPS exposure and adverse fetal outcome, including PET, SGA and preterm birth (503, 504). Given this and the significant dysregulation of placental vitamin D metabolism evidenced in Chapter 4, we speculate altered immune cell function may be highly relevant within the context of malplacentation. Future studies exploring how isolated uNKs and macrophages from pregnancies complicated by PET differ in phenotype and their responsiveness to vitamin D are now justified.

8 References

1. Tambllyn JA, Lissauer DM, Powell R, Cox P, Kilby MD. The immunological basis of villitis of unknown etiology - Review. *Placenta*. 2013.
2. Cheng JB, Motola DL, Mangelsdorf DJ, Russell DW. De-orphanization of cytochrome P450 2R1: a microsomal vitamin D 25-hydroxylase. *The Journal of biological chemistry*. 2003;278(39):38084-93.
3. Cheng JB, Levine MA, Bell NH, Mangelsdorf DJ, Russell DW. Genetic evidence that the human CYP2R1 enzyme is a key vitamin D 25-hydroxylase. *Proceedings of the National Academy of Sciences of the United States of America*. 2004;101(20):7711-5.
4. Lips P. Relative value of 25(OH)D and 1,25(OH)₂D measurements. *Journal of bone and mineral research : the official journal of the American Society for Bone and Mineral Research*. 2007;22(11):1668-71.
5. Adams JS, Chen H, Chun R, Gacad MA, Encinas C, Ren S, et al. Response element binding proteins and intracellular vitamin D binding proteins: novel regulators of vitamin D trafficking, action and metabolism. *The Journal of steroid biochemistry and molecular biology*. 2004;89-90(1-5):461-5.
6. Bikle DD. Vitamin D metabolism, mechanism of action, and clinical applications. *Chemistry & biology*. 2014;21(3):319-29.
7. Masuda S, Kaufmann M, Byford V, Gao M, St-Arnaud R, Arabian A, et al. Insights into Vitamin D metabolism using cyp24 over-expression and knockout systems in conjunction with liquid chromatography/mass spectrometry (LC/MS). *The Journal of steroid biochemistry and molecular biology*. 2004;89-90(1-5):149-53.
8. Masuda S, Byford V, Arabian A, Sakai Y, Demay MB, St-Arnaud R, et al. Altered pharmacokinetics of 1 α ,25-dihydroxyvitamin D₃ and 25-hydroxyvitamin D₃ in the blood and tissues of the 25-hydroxyvitamin D-24-hydroxylase (Cyp24a1) null mouse. *Endocrinology*. 2005;146(2):825-34.
9. Liu S, Gupta A, Quarles LD. Emerging role of fibroblast growth factor 23 in a bone-kidney axis regulating systemic phosphate homeostasis and extracellular matrix mineralization. *Current opinion in nephrology and hypertension*. 2007;16(4):329-35.
10. Fu GK, Lin D, Zhang MY, Bikle DD, Shackleton CH, Miller WL, et al. Cloning of human 25-hydroxyvitamin D-1 α -hydroxylase and mutations causing vitamin D-dependent rickets type 1. *Mol Endocrinol*. 1997;11(13):1961-70.
11. Sakaki T, Sawada N, Komai K, Shiozawa S, Yamada S, Yamamoto K, et al. Dual metabolic pathway of 25-hydroxyvitamin D₃ catalyzed by human CYP24. *European Journal of Biochemistry*. 2000;267(20):6158-65.
12. Evans RM, Mangelsdorf DJ. Nuclear Receptors, RXR, and the Big Bang. *Cell*. 2014;157(1):255-66.
13. Goltzman D, Hendy GN, Karaplis AC, Kremer R, Miao D. Chapter 36 - Understanding Vitamin D From Mouse Knockout Models A2 - Feldman, David. *Vitamin D (Fourth Edition)*: Academic Press; 2018. p. 613-31.
14. Malloy PJ, Pike JW, Feldman D. The vitamin D receptor and the syndrome of hereditary 1,25-dihydroxyvitamin D-resistant rickets. *Endocr Rev*. 1999;20(2):156-88.
15. St-Arnaud R, Arabian A, Travers R, Barletta F, Raval-Pandya M, Chapin K, et al. Deficient Mineralization of Intramembranous Bone in Vitamin D-24-Hydroxylase-Ablated Mice Is Due to Elevated 1,25-Dihydroxyvitamin D and Not to the Absence of 24,25-Dihydroxyvitamin D*. *Endocrinology*. 2000;141(7):2658-66.
16. Safadi FF, Thornton P, Magiera H, Hollis BW, Gentile M, Haddad JG, et al. Osteopathy and resistance to vitamin D toxicity in mice null for vitamin D binding protein. *The Journal of clinical investigation*. 1999;103(2):239-51.

17. Glendenning P, Chew GT, Inderjeeth CA, Taranto M, Fraser WD. Calculated free and bioavailable vitamin D metabolite concentrations in vitamin D-deficient hip fracture patients after supplementation with cholecalciferol and ergocalciferol. *Bone*. 2013;56(2):271-5.
18. Nykjaer A, Dragun D, Walther D, Vorum H, Jacobsen C, Herz J, et al. An endocytic pathway essential for renal uptake and activation of the steroid 25-(OH) vitamin D₃. *Cell*. 1999;96(4):507-15.
19. Zella LA, Shevde NK, Hollis BW, Cooke NE, Pike JW. Vitamin D Binding Protein Influences Total Circulating Levels of 1,25-Dihydroxyvitamin D₃ but Does Not Directly Modulate the Bioactive Levels of the Hormone in Vivo. *Endocrinology*. 2008.
20. Rowling MJ, Kemmis CM, Taffany DA, Welsh J. Megalin-mediated endocytosis of vitamin D binding protein correlates with 25-hydroxycholecalciferol actions in human mammary cells. *The Journal of nutrition*. 2006;136(11):2754-9.
21. Powe C, Evans, MK, Wenger, J, Zonderman, AB, Berg, A, Nalls, M, Tamez, H, Bhan, I, Karumanchi, SA, Powe, NR, Thadhani, R. Vitamin D Binding Protein and Vitamin D Status of Black and White Americans. *New England Journal of Medicine*. 2013.
22. Chun RF. New perspectives on the vitamin D binding protein. *Cell Biochem Funct*. 2012.
23. Chun RF, Peercy BE, Orwoll ES, Nielson CM, Adams JS, Hewison M. Vitamin D and DBP: The free hormone hypothesis revisited. *The Journal of steroid biochemistry and molecular biology*. 2013.
24. Nielson CM, Jones KS, Chun RF, Jacobs J, Wang Y, Hewison M, et al. Role of Assay Type in Determining Free 25-Hydroxyvitamin D Levels in Diverse Populations. *New England Journal of Medicine*. 2016;374(17):1695-6.
25. Cashman KD, Kinsella M, Walton J, Flynn A, Hayes A, Lucey AJ, et al. The 3 epimer of 25-hydroxycholecalciferol is present in the circulation of the majority of adults in a nationally representative sample and has endogenous origins. *The Journal of nutrition*. 2014;144(7):1050-7.
26. Ooms N, van Daal H, Beijers AM, Gerrits GP, Semmekrot BA, van den Ouweland JM. Time-course analysis of 3-epi-25-hydroxyvitamin D₃ shows markedly elevated levels in early life, particularly from vitamin D supplementation in preterm infants. *Pediatric research*. 2016;79(4):647-53.
27. Bailey D, Veljkovic K, Yazdanpanah M, Adeli K. Analytical measurement and clinical relevance of vitamin D₃ C₃-epimer. *Clinical Biochemistry*. 2013;46(3):190-6.
28. Kamao M, Tatematsu S, Hatakeyama S, Sakaki T, Sawada N, Inouye K, et al. C-3 epimerization of vitamin D₃ metabolites and further metabolism of C-3 epimers: 25-hydroxyvitamin D₃ is metabolized to 3-epi-25-hydroxyvitamin D₃ and subsequently metabolized through C-1 α or C-24 hydroxylation. *The Journal of biological chemistry*. 2004;279(16):15897-907.
29. Kamao M, Hatakeyama S, Sakaki T, Sawada N, Inouye K, Kubodera N, et al. Measurement and characterization of C-3 epimerization activity toward vitamin D₃. *Archives of biochemistry and biophysics*. 2005;436(1):196-205.
30. Kadiyala S, Nagaba S, Takeuchi K, Yukihiro S, Qiu W, Eyes ST, et al. Metabolites and analogs of 1 α ,25-dihydroxyvitamin D(3): evaluation of actions in bone. *Steroids*. 2001;66(3-5):347-55.
31. Brown AJ, Ritter CS, Weiskopf AS, Vouros P, Sasso GJ, Uskokovic MR, et al. Isolation and identification of 1 α -hydroxy-3-epi-vitamin D₃, a potent suppressor of parathyroid hormone secretion. *Journal of cellular biochemistry*. 2005;96(3):569-78.
32. Lutsey PL, Eckfeldt JH, Ogagarue ER, Folsom AR, Michos ED, Gross M. The 25-hydroxyvitamin D₃ C-3 epimer: distribution, correlates, and reclassification of 25-hydroxyvitamin D status in the population-based Atherosclerosis Risk in Communities Study (ARIC). *Clinica chimica acta; international journal of clinical chemistry*. 2015;442:75-81.
33. Haussler MR, Haussler CA, Bartik L, Whitfield GK, Hsieh JC, Slater S, et al. Vitamin D receptor: molecular signaling and actions of nutritional ligands in disease prevention. *Nutr Rev*. 2008;66(10 Suppl 2):S98-112.
34. Bikle D. Nonclassic Actions of Vitamin D. *The Journal of Clinical Endocrinology & Metabolism*. 2009;94(1):26-34.

35. Hewison M, Burke F, Evans KN, Lammas DA, Sansom DM, Liu P, et al. Extra-renal 25-hydroxyvitamin D3-1 α -hydroxylase in human health and disease. *J Steroid Biochem Mol Biol.* 2007;103(3-5):316-21.
36. Morris HA, Anderson PH. Autocrine and Paracrine Actions of Vitamin D. *The Clinical Biochemist Reviews.* 2010;31(4):129-38.
37. Olmos-Ortiz A, Avila E, Durand-Carbajal M, Díaz L. Regulation of Calcitriol Biosynthesis and Activity: Focus on Gestational Vitamin D Deficiency and Adverse Pregnancy Outcomes. *Nutrients.* 2015;7(1):443-80.
38. Overbergh L, Decallonne B, Valckx D, Verstuyf A, Depovere J, Laureys J, et al. Identification and immune regulation of 25-hydroxyvitamin D-1- α -hydroxylase in murine macrophages. *Clinical and Experimental Immunology.* 2000;120(1):139-46.
39. Bell NH, Stern PH, Pantzer E, Sinha TK, DeLuca HF. Evidence that increased circulating 1 α , 25-dihydroxyvitamin D is the probable cause for abnormal calcium metabolism in sarcoidosis. *The Journal of clinical investigation.* 1979;64(1):218-25.
40. Bikle DD. Vitamin D and the immune system: role in protection against bacterial infection. *Curr Opin Nephrol Hypertens.* 2008;17(4):348-52.
41. Hewison M. Vitamin D and the immune system: new perspectives on an old theme. *Endocrinol Metab Clin North Am.* 2010;39(2):365-79, table of contents.
42. Lin R. Crosstalk between Vitamin D Metabolism, VDR Signalling, and Innate Immunity. *BioMed Research International.* 2016;2016:1375858.
43. Hewison M. Vitamin D and the intracrinology of innate immunity. *Molecular and cellular endocrinology.* 2010;321(2):103-11.
44. Rook GA, Steele J, Fraher L, Barker S, Karmali R, O'Riordan J, et al. Vitamin D3, gamma interferon, and control of proliferation of Mycobacterium tuberculosis by human monocytes. *Immunology.* 1986;57(1):159-63.
45. Edfeldt K, Liu PT, Chun R, Fabri M, Schenk M, Wheelwright M, et al. T-cell cytokines differentially control human monocyte antimicrobial responses by regulating vitamin D metabolism. *Proceedings of the National Academy of Sciences of the United States of America.* 2010;107(52):22593-8.
46. Nunn JD, Katz DR, Barker S, Fraher LJ, Hewison M, Hendy GN, et al. Regulation of human tonsillar T-cell proliferation by the active metabolite of vitamin D3. *Immunology.* 1986;59(4):479-84.
47. Provvedini DM, Manolagas SC. 1 α ,25-dihydroxyvitamin D3 receptor distribution and effects in subpopulations of normal human T lymphocytes. *J Clin Endocrinol Metab.* 1989;68(4):774-9.
48. Boonstra A, Barrat FJ, Crain C, Heath VL, Savelkoul HF, O'Garra A. 1 α ,25-Dihydroxyvitamin d3 has a direct effect on naive CD4(+) T cells to enhance the development of Th2 cells. *Journal of immunology.* 2001;167(9):4974-80.
49. Overbergh L, Decallonne B, Waer M, Rutgeerts O, Valckx D, Casteels KM, et al. 1 α ,25-dihydroxyvitamin D3 induces an autoantigen-specific T-helper 1/T-helper 2 immune shift in NOD mice immunized with GAD65 (p524-543). *Diabetes.* 2000;49(8):1301-7.
50. O'Kelly J, Hisatake J, Hisatake Y, Bishop J, Norman A, Koeffler HP. Normal myelopoiesis but abnormal T lymphocyte responses in vitamin D receptor knockout mice. *The Journal of clinical investigation.* 2002;109(8):1091-9.
51. Gorman S, Kuritzky LA, Judge MA, Dixon KM, McGlade JP, Mason RS, et al. Topically applied 1,25-dihydroxyvitamin D3 enhances the suppressive activity of CD4+CD25+ cells in the draining lymph nodes. *Journal of immunology.* 2007;179(9):6273-83.
52. Bettelli E, Korn T, Kuchroo VK. Th17: the third member of the effector T cell trilogy. *Curr Opin Immunol.* 2007;19(6):652-7.
53. Colin EM, Asmawidjaja PS, van Hamburg JP, Mus AM, van Driel M, Hazes JM, et al. 1,25-dihydroxyvitamin D3 modulates Th17 polarization and interleukin-22 expression by memory T cells from patients with early rheumatoid arthritis. *Arthritis Rheum.* 2010;62(1):132-42.

54. Palmer MT, Lee YK, Maynard CL, Oliver JR, Bikle DD, Jetten AM, et al. Lineage-specific effects of 1,25-dihydroxyvitamin D(3) on the development of effector CD4 T cells. *The Journal of biological chemistry*. 2010;286(2):997-1004.
55. Daniel C, Sartory NA, Zahn N, Radeke HH, Stein JM. Immune modulatory treatment of trinitrobenzene sulfonic acid colitis with calcitriol is associated with a change of a T helper (Th) 1/Th17 to a Th2 and regulatory T cell profile. *J Pharmacol Exp Ther*. 2008;324(1):23-33.
56. Jeffery LE, Burke F, Mura M, Zheng Y, Qureshi OS, Hewison M, et al. 1,25-Dihydroxyvitamin D(3) and IL-2 combine to inhibit T cell production of inflammatory cytokines and promote development of regulatory T cells expressing CTLA-4 and FoxP3. *Journal of immunology*. 2009;183(9):5458-67.
57. Gregori S, Casorati M, Amuchastegui S, Smiroldo S, Davalli AM, Adorini L. Regulatory T cells induced by 1 alpha,25-dihydroxyvitamin D3 and mycophenolate mofetil treatment mediate transplantation tolerance. *Journal of immunology*. 2001;167(4):1945-53.
58. Dong X, Bachman LA, Kumar R, Griffin MD. Generation of antigen-specific, interleukin-10-producing T-cells using dendritic cell stimulation and steroid hormone conditioning. *Transpl Immunol*. 2003;11(3-4):323-33.
59. Adorini L, Giarratana N, Penna G. Pharmacological induction of tolerogenic dendritic cells and regulatory T cells. *Semin Immunol*. 2004;16(2):127-34.
60. Hewison M. Vitamin D and innate and adaptive immunity. *Vitam Horm*. 2011;86:23-62.
61. Medicine Tlo. Report on dietary reference intakes for vitamin D and calcium. Washington DC: The National Academies Press; 2011.
62. Nutrition SACo. Vitamin D and health. London: The Stationary Office: 2016.
63. Munns CF, Shaw N, Kiely M, Specker BL, Thacher TD, Ozono K, et al. Global Consensus Recommendations on Prevention and Management of Nutritional Rickets. *J Clin Endocrinol Metab*. 2016;101(2):394-415.
64. Henry HL, Bouillon R, Norman AW, Gallagher JC, Lips P, Heaney RP, et al. 14th Vitamin D Workshop consensus on vitamin D nutritional guidelines. *The Journal of steroid biochemistry and molecular biology*. 2010;121(1-2):4-6.
65. Hypponen E, Laara E, Reunanen A, Jarvelin MR, Virtanen SM. Intake of vitamin D and risk of type 1 diabetes: a birth-cohort study. *Lancet*. 2001;358(9292):1500-3.
66. Cannell JJ, Vieth R, Umhau JC, Holick MF, Grant WB, Madronich S, et al. Epidemic influenza and vitamin D. *Epidemiol Infect*. 2006;134(6):1129-40.
67. Munger KL, Levin LI, Hollis BW, Howard NS, Ascherio A. Serum 25-hydroxyvitamin D levels and risk of multiple sclerosis. *Jama*. 2006;296(23):2832-8.
68. Grant WB, Mohr SB. Ecological Studies Of Ultraviolet B, Vitamin D And Cancer Since 2000. *Ann Epidemiol*. 2009.
69. Brehm JM, Schuemann B, Fuhlbrigge AL, Hollis BW, Strunk RC, Zeiger RS, et al. Serum vitamin D levels and severe asthma exacerbations in the Childhood Asthma Management Program study. *J Allergy Clin Immunol*. 2010;126(1):52-8 e5.
70. Zittermann A. Vitamin D and disease prevention with special reference to cardiovascular disease. *Prog Biophys Mol Biol*. 2006;92(1):39-48.
71. Tamblyn J, Hewison M, Wagner C, Bulmer J, Kilby M. Immunological role of vitamin D at the maternal–fetal interface. *Journal of Endocrinology*. 2015;224(3):R107-R21.
72. Gaksch M, Jorde R, Grimnes G, Joakimsen R, Schirmer H, Wilsgaard T, et al. Vitamin D and mortality: Individual participant data meta-analysis of standardized 25-hydroxyvitamin D in 26916 individuals from a European consortium. *PloS one*. 2017;12(2):e0170791.
73. Stokes CS, Lammert F. Vitamin D supplementation: less controversy, more guidance needed. *F1000Research*. 2016;5:F1000 Faculty Rev-2017.
74. El-Khoury JM, Reineks EZ, Wang S. Progress of liquid chromatography-mass spectrometry in measurement of vitamin D metabolites and analogues. *Clinical Biochemistry*. 2011;44(1):66-76.

75. Turner C, Dalton N, Inaoui R, Fogelman I, Fraser WD, Hampson G. Effect of a 300 000-IU loading dose of ergocalciferol (Vitamin D₂) on circulating 1,25(OH)₂-vitamin D and fibroblast growth factor-23 (FGF-23) in vitamin D insufficiency. *J Clin Endocrinol Metab.* 2013;98(2):550-6.
76. Jenkinson C, Taylor AE, Hassan-Smith ZK, Adams JS, Stewart PM, Hewison M, et al. High throughput LC–MS/MS method for the simultaneous analysis of multiple vitamin D analytes in serum. *Journal of Chromatography B.* 2016;1014:56-63.
77. Keevil BG. Novel liquid chromatography tandem mass spectrometry (LC-MS/MS) methods for measuring steroids. *Best practice & research Clinical endocrinology & metabolism.* 2013;27(5):663-74.
78. Tranquilli AL, Brown MA, Zeeman GG, Dekker G, Sibai BM. The definition of severe and early-onset preeclampsia. Statements from the International Society for the Study of Hypertension in Pregnancy (ISSHP). *Pregnancy Hypertens.* 2013;3(1):44-7.
79. Kenny LC, Black MA, Poston L, Taylor R, Myers JE, Baker PN, et al. Early pregnancy prediction of preeclampsia in nulliparous women, combining clinical risk and biomarkers: the Screening for Pregnancy Endpoints (SCOPE) international cohort study. *Hypertension.* 2014;64(3):644-52.
80. Kiely ME, Zhang JY, Kinsella M, Khashan AS, Kenny LC. Vitamin D status is associated with uteroplacental dysfunction indicated by pre-eclampsia and small-for-gestational-age birth in a large prospective pregnancy cohort in Ireland with low vitamin D status. *Am J Clin Nutr.* 2016;104(2):354-61.
81. Ogawa S, Ooki S, Shinoda K, Higashi T. Analysis of urinary vitamin D(3) metabolites by liquid chromatography/tandem mass spectrometry with ESI-enhancing and stable isotope-coded derivatization. *Analytical and bioanalytical chemistry.* 2014;406(26):6647-54.
82. Chun RF, Lauridsen AL, Suon L, Zella LA, Pike JW, Modlin RL, et al. Vitamin D-Binding Protein Directs Monocyte Responses to 25-Hydroxy- and 1,25-Dihydroxyvitamin D. *J Clin Endocrinol Metab.*
83. Chun RF, Peercy BE, Adams JS, Hewison M. Vitamin D binding protein and monocyte response to 25-hydroxyvitamin D and 1,25-dihydroxyvitamin D: analysis by mathematical modeling. *PloS one.* 2012;7:e30773.
84. Peake M, Whiting M. Measurement of serum creatinine--current status and future goals. *The Clinical biochemist Reviews.* 2006;27(4):173-84.
85. Henney CS, Kuribayashi K, Kern DE, Gillis S. Interleukin-2 augments natural killer cell activity. *Nature.* 1981;291(5813):335-8.
86. Nguyen KB, Salazar-Mather TP, Dalod MY, Van Deusen JB, Wei XQ, Liew FY, et al. Coordinated and distinct roles for IFN-alpha beta, IL-12, and IL-15 regulation of NK cell responses to viral infection. *Journal of immunology.* 2002;169(8):4279-87.
87. Tripp CS, Wolf SF, Unanue ER. Interleukin 12 and tumor necrosis factor alpha are costimulators of interferon gamma production by natural killer cells in severe combined immunodeficiency mice with listeriosis, and interleukin 10 is a physiologic antagonist. *Proceedings of the National Academy of Sciences of the United States of America.* 1993;90(8):3725-9.
88. Barteneva NS, Ketman K, Fasler-Kan E, Potashnikova D, Vorobjev IA. Cell sorting in cancer research—Diminishing degree of cell heterogeneity. *Biochimica et Biophysica Acta (BBA) - Reviews on Cancer.* 2013;1836(1):105-22.
89. Bendix M, Dige A, Deleuran B, Dahlerup JF, Peter Jorgensen S, Bartels LE, et al. Flow cytometry detection of vitamin D receptor changes during vitamin D treatment in Crohn's disease. *Clin Exp Immunol.* 2015.
90. Alter G, Malenfant JM, Altfeld M. CD107a as a functional marker for the identification of natural killer cell activity. *Journal of immunological methods.* 2004;294(1):15-22.
91. Lisovsky I, Isitman G, Bruneau J, Bernard NF. Functional analysis of NK cell subsets activated by 721.221 and K562 HLA-null cells. *Journal of leukocyte biology.* 2015;97(4):761-7.
92. Strand C, Enell J, Hedenfalk I, Fernö M. RNA quality in frozen breast cancer samples and the influence on gene expression analysis – a comparison of three evaluation methods using microcapillary electrophoresis traces. *BMC Molecular Biology.* 2007;8(1):38.

93. Fajardy I, Moitrot E, Vambergue A, Vandersippe-Millot M, Deruelle P, Rousseaux J. Time course analysis of RNA stability in human placenta. *BMC Molecular Biology*. 2009;10:21-.
94. Ramskold D, Luo S, Wang YC, Li R, Deng Q, Faridani OR, et al. Full-length mRNA-Seq from single-cell levels of RNA and individual circulating tumor cells. *Nature biotechnology*. 2012;30(8):777-82.
95. Picelli S, Bjorklund AK, Faridani OR, Sagasser S, Winberg G, Sandberg R. Smart-seq2 for sensitive full-length transcriptome profiling in single cells. *Nature methods*. 2013;10(11):1096-8.
96. Picelli S, Bjorklund AK, Faridani OR, Sagasser S, Winberg G, Sandberg R. Smart-seq2 for sensitive full-length transcriptome profiling in single cells. *Nat Meth*. 2013;10(11):1096-8.
97. Malhotra D, Fletcher AL, Astarita J, Lukacs-Kornek V, Tayalia P, Gonzalez SF, et al. Transcriptional profiling of stroma from inflamed and resting lymph nodes defines immunological hallmarks. *Nature immunology*. 2012;13(5):499-510.
98. Dobin A, Davis CA, Schlesinger F, Drenkow J, Zaleski C, Jha S, et al. STAR: ultrafast universal RNA-seq aligner. *Bioinformatics (Oxford, England)*. 2013;29(1):15-21.
99. Trapnell C, Williams BA, Pertea G, Mortazavi A, Kwan G, van Baren MJ, et al. Transcript assembly and quantification by RNA-Seq reveals unannotated transcripts and isoform switching during cell differentiation. *Nat Biotech*. 2010;28(5):511-5.
100. Maglott D, Ostell J, Pruitt KD, Tatusova T. Entrez Gene: gene-centered information at NCBI. *Nucleic acids research*. 2005;33(Database issue):D54-8.
101. Povey S, Lovering R, Bruford E, Wright M, Lush M, Wain H. The HUGO Gene Nomenclature Committee (HGNC). *Hum Genet*. 2001;109(6):678-80.
102. Kutmon M, Riutta A, Nunes N, Hanspers K, Willighagen EL, Bohler A, et al. WikiPathways: capturing the full diversity of pathway knowledge. *Nucleic acids research*. 2016;44(D1):D488-94.
103. Bohler A, Wu G, Kutmon M, Pradhana LA, Coort SL, Hanspers K, et al. Reactome from a WikiPathways Perspective. *PLoS Comput Biol*. 2016;12(5):e1004941.
104. Tamblyn JA, Susarla R, Jenkinson C, Jeffery LE, Ohizua O, Chun RF, et al. Dysregulation of maternal and placental vitamin D metabolism in preeclampsia. *Placenta*. 2017;50:70-7.
105. Tamblyn J, Jenkinson C, Lerner D, Hewison M, Kilby M. Serum and urine vitamin D metabolite analysis in early preeclampsia. *Endocrine connections*. 2017.
106. Saraf R, Morton SM, Camargo CA, Jr., Grant CC. Global summary of maternal and newborn vitamin D status - a systematic review. *Matern Child Nutr*. 2016;12(4):647-68.
107. Saneei P, Salehi-Abargouei A, Esmailzadeh A. Serum 25-hydroxy vitamin D levels in relation to body mass index: a systematic review and meta-analysis. *Obesity reviews : an official journal of the International Association for the Study of Obesity*. 2013;14(5):393-404.
108. Nassar N, Halligan GH, Roberts CL, Morris JM, Ashton AW. Systematic review of first-trimester vitamin D normative levels and outcomes of pregnancy. *American journal of obstetrics and gynecology*. 2011;205(3):208.e1-.e7.
109. Holick MF, Binkley NC, Bischoff-Ferrari HA, Gordon CM, Hanley DA, Heaney RP, et al. Evaluation, treatment, and prevention of vitamin D deficiency: an Endocrine Society clinical practice guideline. *J Clin Endocrinol Metab*. 2011;96(7):1911-30.
110. Gale CR, Robinson SM, Harvey NC, Javaid MK, Jiang B, Martyn CN, et al. Maternal vitamin D status during pregnancy and child outcomes. *European journal of clinical nutrition*. 2008;62(1):68-77.
111. Bodnar LM, Simhan HN, Powers RW, Frank MP, Cooperstein E, Roberts JM. High prevalence of vitamin D insufficiency in black and white pregnant women residing in the northern United States and their neonates. *The Journal of nutrition*. 2007;137(2):447-52.
112. Holick MF. Vitamin D deficiency. *N Engl J Med*. 2007;357(3):266-81.
113. Holick MF. Vitamin D Status: Measurement, Interpretation, and Clinical Application. *Ann Epidemiol*. 2008.

114. Javaid MK, Crozier SR, Harvey NC, Gale CR, Dennison EM, Boucher BJ, et al. Maternal vitamin D status during pregnancy and childhood bone mass at age 9 years: a longitudinal study. *Lancet*. 2006;367(9504):36-43.
115. Lerchbaum E, Obermayer-Pietsch B. MECHANISMS IN ENDOCRINOLOGY: Vitamin D and fertility: a systematic review. *European journal of endocrinology*. 2012;166(5):765-78.
116. Bodnar LM, Catov JM, Simhan HN, Holick MF, Powers RW, Roberts JM. Maternal vitamin D deficiency increases the risk of preeclampsia. *J Clin Endocrinol Metab*. 2007.
117. Bodnar LM, Krohn MA, Simhan HN. Maternal Vitamin D Deficiency Is Associated with Bacterial Vaginosis in the First Trimester of Pregnancy. *The Journal of nutrition*. 2009.
118. Bodnar LM, Catov JM, Zmuda JM, Cooper ME, Parrott MS, Roberts JM, et al. Maternal serum 25-hydroxyvitamin D concentrations are associated with small-for-gestational age births in white women. *The Journal of nutrition*.140(5):999-1006.
119. Zhang C, Qiu C, Hu FB, David RM, van Dam RM, Bralley A, et al. Maternal plasma 25-hydroxyvitamin D concentrations and the risk for gestational diabetes mellitus. *PLoS one*. 2008;3(11):e3753.
120. Leffelaar ER, Vrijkotte TG, van Eijsden M. Maternal early pregnancy vitamin D status in relation to fetal and neonatal growth: results of the multi-ethnic Amsterdam Born Children and their Development cohort. *The British journal of nutrition*.104(1):108-17.
121. Camargo CA, Jr., Ingham T, Wickens K, Thadhani R, Silvers KM, Epton MJ, et al. Cord-blood 25-hydroxyvitamin D levels and risk of respiratory infection, wheezing, and asthma. *Pediatrics*. 2011;127(1):e180-7.
122. Harvey NC, Holroyd C, Ntani G, Javaid K, Cooper P, Moon R, et al. Vitamin D supplementation in pregnancy: a systematic review. *Health technology assessment*. 2014;18(45):1-190.
123. Bivins R. "The English Disease" or "Asian Rickets"? : Medical Responses to Postcolonial Immigration. *Bulletin of the History of Medicine*. 2007;81(3):533-68.
124. Hollis BW, Johnson D, Hulsey TC, Ebeling M, Wagner CL. Vitamin D supplementation during pregnancy: Double-blind, randomized clinical trial of safety and effectiveness. *Journal of bone and mineral research : the official journal of the American Society for Bone and Mineral Research*. 2011;26(10):2341-57.
125. Kiely M, Hemmingway A, O'Callaghan KM. Vitamin D in pregnancy: current perspectives and future directions. *Therapeutic Advances in Musculoskeletal Disease*. 2017;9(6):145-54.
126. England PH. SACN vitamin D and health report. . London: The Stationary Office: 2016.
127. Cooper C, Harvey NC, Bishop NJ, Kennedy S, Papageorgiou AT, Schoenmakers I, et al. Maternal gestational vitamin D supplementation and offspring bone health (MAVIDOS): A multicentre, double-blind, randomised placebo-controlled trial. *The Lancet Diabetes and Endocrinology*. 2016;4(5):393-402.
128. De-Regil LM, Palacios C, Ansary A, Kulier R, Pena-Rosas JP. Vitamin D supplementation for women during pregnancy. *Cochrane Database Syst Rev*. 2012;2:CD008873.
129. Wei SQ, Qi HP, Luo ZC, Fraser WD. Maternal vitamin D status and adverse pregnancy outcomes: a systematic review and meta-analysis. *J Matern Fetal Neonatal Med*. 2013;26(9):889-99.
130. Kumar R, Cohen WR, Silva P, Epstein FH. Elevated 1,25-dihydroxyvitamin D plasma levels in normal human pregnancy and lactation. *The Journal of clinical investigation*. 1979;63(2):342-4.
131. Delvin EE, Gilbert M, Pere MC, Garel JM. In vivo metabolism of calcitriol in the pregnant rabbit doe. *Journal of developmental physiology*. 1988;10(5):451-9.
132. Jones KS, Assar S, Prentice A, Schoenmakers I. Vitamin D expenditure is not altered in pregnancy and lactation despite changes in vitamin D metabolite concentrations. *Scientific Reports*. 2016;6:26795.
133. Gray TK, Lester GE, Lorenc RS. Evidence for extra-renal 1 alpha-hydroxylation of 25-hydroxyvitamin D3 in pregnancy. *Science*. 1979;204(4399):1311-3.

134. Weisman Y, Vargas A, Duckett G, Reiter E, Root AW. Synthesis of 1,25-dihydroxyvitamin D in the nephrectomized pregnant rat. *Endocrinology*. 1978;103(6):1992-6.
135. Ginde AA, Sullivan AF, Mansbach JM, Camargo CA, Jr. Vitamin D insufficiency in pregnant and nonpregnant women of childbearing age in the United States. *American journal of obstetrics and gynecology*. 202(5):436 e1-8.
136. Bikle DD, Gee E, Halloran B, Haddad JG. Free 1,25-dihydroxyvitamin D levels in serum from normal subjects, pregnant subjects, and subjects with liver disease. *The Journal of clinical investigation*. 1984;74(6):1966-71.
137. Gude NM, Roberts CT, Kalionis B, King RG. Growth and function of the normal human placenta. *Thrombosis research*. 2004;114(5-6):397-407.
138. Vinketova K, Mourdjeva M, Oreshkova T. Human Decidual Stromal Cells as a Component of the Implantation Niche and a Modulator of Maternal Immunity. *Journal of Pregnancy*. 2016;2016:8689436.
139. Weisblum Y, Panet A, Zakay-Rones Z, Kochman R, Goldman-Wohl D, Ariel I, et al. Modeling of Human Cytomegalovirus Maternal-Fetal Transmission in a Novel Decidual Organ Culture 2011. 13204-13 p.
140. Gellersen B, Brosens IA, Brosens JJ. Decidualization of the human endometrium: mechanisms, functions, and clinical perspectives. *Semin Reprod Med*. 2007;25(6):445-53.
141. Salamonsen LA, Hannan NJ, Dimitriadis E. Cytokines and chemokines during human embryo implantation: roles in implantation and early placentation. *Semin Reprod Med*. 2007;25(6):437-44.
142. Oreshkova T, Dimitrov R, Mourdjeva M. A cross-talk of decidual stromal cells, trophoblast, and immune cells: a prerequisite for the success of pregnancy. *American journal of reproductive immunology*. 2012;68(5):366-73.
143. Weisman Y, Harell A, Edelstein S, David M, Spierer Z, Golander A. 1 alpha, 25-Dihydroxyvitamin D3 and 24,25-dihydroxyvitamin D3 in vitro synthesis by human decidua and placenta. *Nature*. 1979;281(5729):317-9.
144. Zehnder D, Evans KN, Kilby MD, Bulmer JN, Innes BA, Stewart PM, et al. The ontogeny of 25-hydroxyvitamin D(3) 1alpha-hydroxylase expression in human placenta and decidua. *The American journal of pathology*. 2002;161(1):105-14.
145. Novakovic B, Sibson M, Ng HK, Manuelpillai U, Rakyan V, Down T, et al. Placenta-specific methylation of the vitamin D 24-hydroxylase gene: implications for feedback autoregulation of active vitamin D levels at the fetomaternal interface. *The Journal of biological chemistry*. 2009;284(22):14838-48.
146. Willnow TE, Hilpert J, Armstrong SA, Rohlmann A, Hammer RE, Burns DK, et al. Defective forebrain development in mice lacking gp330/megalin. *Proceedings of the National Academy of Sciences of the United States of America*. 1996;93(16):8460-4.
147. Panda DK, Miao D, Tremblay ML, Sirois J, Farookhi R, Hendy GN, et al. Targeted ablation of the 25-hydroxyvitamin D 1alpha -hydroxylase enzyme: evidence for skeletal, reproductive, and immune dysfunction. *Proceedings of the National Academy of Sciences of the United States of America*. 2001;98(13):7498-503.
148. Yoshizawa T, Handa Y, Uematsu Y, Takeda S, Sekine K, Yoshihara Y, et al. Mice lacking the vitamin D receptor exhibit impaired bone formation, uterine hypoplasia and growth retardation after weaning. *Nature genetics*. 1997;16(4):391-6.
149. Ghulmiyyah L, Sibai B. Maternal mortality from preeclampsia/eclampsia. *Seminars in perinatology*. 2012;36(1):56-9.
150. Mol BWJ, Roberts CT, Thangaratnam S, Magee LA, de Groot CJM, Hofmeyr GJ. Pre-eclampsia. *The Lancet*. 387(10022):999-1011.
151. Fisher SJ. Why is placentation abnormal in preeclampsia? *American journal of obstetrics and gynecology*. 2015;213(4 Suppl):S115-22.
152. Redman CWG, Sargent IL. REVIEW ARTICLE: Immunology of Pre-Eclampsia. *American journal of reproductive immunology*. 2010;63(6):534-43.

153. Rădulescu C, Bacărea A, Huțanu A, Gabor R, Dobreanu M. Placental Growth Factor, Soluble fms-Like Tyrosine Kinase 1, Soluble Endoglin, IL-6, and IL-16 as Biomarkers in Preeclampsia. *Mediators of Inflammation*. 2016;2016:3027363.
154. Petla LT, Chikkala R, Ratnakar KS, Kodati V, Sritharan V. Biomarkers for the management of pre-eclampsia in pregnant women. *The Indian Journal of Medical Research*. 2013;138(1):60-7.
155. Jadli A, Sharma N, Damania K, Satoskar P, Bansal V, Ghosh K, et al. Promising prognostic markers of preeclampsia: new avenues in waiting. *Thrombosis research*. 2015;136(2):189-95.
156. Lafayette RA, Druzin M, Sibley R, Derby G, Malik T, Huie P, et al. Nature of glomerular dysfunction in pre-eclampsia. *Kidney international*. 1998;54(4):1240-9.
157. Garovic VD. The Role of the Podocyte in Preeclampsia. *Clinical Journal of the American Society of Nephrology*. 2014;9(8):1337-40.
158. Kolialexi A, Mavreli D, Tounta G, Mavrou A, Papantoniou N. Urine proteomic studies in preeclampsia. *PROTEOMICS – Clinical Applications*. 2015;9(5-6):501-6.
159. Djekic-Ivankovic M, Weiler H, Jones G, Kaufmann M, Kaludjerovic J, Aleksic-Velickovic V, et al. Vitamin D status in mothers with pre-eclampsia and their infants: a case-control study from Serbia, a country without a vitamin D fortification policy. *Public Health Nutr*. 2016:1-11.
160. Burris HH, Rifas-Shiman SL, Kleinman K, Litonjua AA, Huh SY, Rich-Edwards JW, et al. Vitamin D deficiency in pregnancy and gestational diabetes mellitus. *American journal of obstetrics and gynecology*. 2012;207(3):182 e1-8.
161. Wagner CL, Baggerly C, McDonnell S, Baggerly KA, French CB, Baggerly L, et al. Post-hoc analysis of vitamin D status and reduced risk of preterm birth in two vitamin D pregnancy cohorts compared with South Carolina March of Dimes 2009-2011 rates. *The Journal of steroid biochemistry and molecular biology*. 2016;155(Pt B):245-51.
162. Aghajafari F, Nagulesapillai T, Ronksley PE, Tough SC, O'Beirne M, Rabi DM. Association between maternal serum 25-hydroxyvitamin D level and pregnancy and neonatal outcomes: systematic review and meta-analysis of observational studies. *BMJ (Clinical research ed)*. 2013;346:f1169.
163. Hypponen E, Cavadino A, Williams D, Fraser A, Vereczeky A, Fraser WD, et al. Vitamin D and pre-eclampsia: original data, systematic review and meta-analysis. *Ann Nutr Metab*. 2013;63(4):331-40.
164. Powe CE, Seely EW, Rana S, Bhan I, Ecker J, Karumanchi SA, et al. First trimester vitamin D, vitamin D binding protein, and subsequent preeclampsia. *Hypertension*. 56(4):758-63.
165. Thota C, Menon R, Fortunato SJ, Brou L, Lee JE, Al-Hendy A. 1,25-Dihydroxyvitamin D deficiency is associated with preterm birth in African American and Caucasian women. *Reprod Sci*. 2014;21(2):244-50.
166. Bennett SE, Casey C, McPeake J, McCance DR, Manderson JG, McGinty A. 3-Epi-25 hydroxyvitamin D in pregnancy. *Pregnancy Hypertens*. 2014;4(3):236.
167. Chun RF, Peercy BE, Orwoll ES, Nielson CM, Adams JS, Hewison M. Vitamin D and DBP: The free hormone hypothesis revisited. *The Journal of steroid biochemistry and molecular biology*. 2014;144, Part A:132-7.
168. Zehnder D, Bland R, Williams MC, McNinch RW, Howie AJ, Stewart PM, et al. Extrarenal expression of 25-hydroxyvitamin d(3)-1 alpha-hydroxylase. *J Clin Endocrinol Metab*. 2001;86(2):888-94.
169. DeLuca HF. Metabolism of vitamin D: current status. *Am J Clin Nutr*. 1976;29(11):1258-70.
170. Takemoto F, Shinki T, Yokoyama K, Inokami T, Hara S, Yamada A, et al. Gene expression of vitamin D hydroxylase and megalin in the remnant kidney of nephrectomized rats. *Kidney international*. 2003;64(2):414-20.
171. Revelle W. 2014. *Psych: Procedures for psychological, psychometric, and personality research*, Northwestern University, Evanston, Illinois, <https://cran.r-project.org/web/packages/psych/index.html>.

172. Shah AD, Hsiao EC, O'Donnell B, Salmeen K, Nussbaum R, Krebs M, et al. Maternal Hypercalcemia Due to Failure of 1,25-Dihydroxyvitamin-D3 Catabolism in a Patient With CYP24A1 Mutations. *The Journal of clinical endocrinology and metabolism*. 2015;100(8):2832-6.
173. Marwaha RK, Tandon N, Chopra S, Agarwal N, Garg MK, Sharma B, et al. Vitamin D status in pregnant Indian women across trimesters and different seasons and its correlation with neonatal serum 25-hydroxyvitamin D levels. *The British journal of nutrition*. 2011;106(9):1383-9.
174. Lechtermann C, Hauffa BP, Herrmann R, Schundeln MM, Gellhaus A, Schmidt M, et al. Maternal vitamin D status in preeclampsia: seasonal changes are not influenced by placental gene expression of vitamin D metabolizing enzymes. *PloS one*. 2014;9(8):e105558.
175. Bodnar LM, Catov JM, Simhan HN, Holick MF, Powers RW, Roberts JM. Maternal vitamin D deficiency increases the risk of preeclampsia. *J Clin Endocrinol Metab*. 2007;92(9):3517-22.
176. Turner M, Barre PE, Benjamin A, Goltzman D, Gascon-Barre M. Does the maternal kidney contribute to the increased circulating 1,25-dihydroxyvitamin D concentrations during pregnancy? *Miner Electrolyte Metab*. 1988;14(4):246-52.
177. Bowden SJ, Emly JF, Hughes SV, Powell G, Ahmed A, Whittle MJ, et al. Parathyroid hormone-related protein in human term placenta and membranes. *J Endocrinol*. 1994;142(2):217-24.
178. Liu NQ, Hewison M. Vitamin D, the placenta and pregnancy. *Archives of biochemistry and biophysics*. 2011.
179. Halhali A, Diaz L, Avila E, Ariza AC, Garabedian M, Larrea F. Decreased fractional urinary calcium excretion and serum 1,25-dihydroxyvitamin D and IGF-I levels in preeclampsia. *The Journal of steroid biochemistry and molecular biology*. 2007;103(3-5):803-6.
180. Diaz L, Arranz C, Avila E, Halhali A, Vilchis F, Larrea F. Expression and activity of 25-hydroxyvitamin D-1 alpha-hydroxylase are restricted in cultures of human syncytiotrophoblast cells from preeclamptic pregnancies. *J Clin Endocrinol Metab*. 2002;87(8):3876-82.
181. Ma R, Gu Y, Zhao S, Sun J, Groome LJ, Wang Y. Expressions of vitamin D metabolic components VDBP, CYP2R1, CYP27B1, CYP24A1, and VDR in placentas from normal and preeclamptic pregnancies. *American journal of physiology Endocrinology and metabolism*. 2012;303(7):E928-35.
182. Messerlian S, Gao X, St-Arnaud R. The 3-epi- and 24-oxo-derivatives of 1alpha,25 dihydroxyvitamin D(3) stimulate transcription through the vitamin D receptor. *The Journal of steroid biochemistry and molecular biology*. 2000;72(1-2):29-34.
183. Fleet JC, Bradley J, Reddy GS, Ray R, Wood RJ. 1 alpha,25-(OH)₂-vitamin D₃ analogs with minimal in vivo calcemic activity can stimulate significant transepithelial calcium transport and mRNA expression in vitro. *Archives of biochemistry and biophysics*. 1996;329(2):228-34.
184. Singh RJ, Taylor RL, Reddy GS, Grebe SK. C-3 epimers can account for a significant proportion of total circulating 25-hydroxyvitamin D in infants, complicating accurate measurement and interpretation of vitamin D status. *J Clin Endocrinol Metab*. 2006;91(8):3055-61.
185. Karras S, Kotsa K, Angeloudi E, Zebekakis P, Naughton D. The Road Not So Travelled: Should Measurement of Vitamin D Epimers during Pregnancy Affect Our Clinical Decisions? *Nutrients*. 2017;9(2):90.
186. Horne CH, Howie PW, Goudie RB. Serum-alpha₂-macroglobulin, transferrin, albumin, and IgG levels in preeclampsia. *Journal of clinical pathology*. 1970;23(6):514-6.
187. Bulmer JN, Pace D, Ritson A. Immunoregulatory cells in human decidua: morphology, immunohistochemistry and function. *Reprod Nutr Dev*. 1988;28(6B):1599-613.
188. Blum M, Dolnikowski G, Seyoum E, Harris SS, Booth SL, Peterson J, et al. Vitamin D₃ in fat tissue. *Endocrine*. 2008;33(1):90-4.
189. WAGNER D, DIAS AG, SCHNABL K, VAN DER KWAST T, VIETH R. Determination of 1,25-dihydroxyvitamin D Concentrations in Human Colon Tissues and Matched Serum Samples. *Anticancer Research*. 2012;32(1):259-63.
190. Rubin LP, Yeung B, Vouros P, Vilner LM, Reddy GS. Evidence for human placental synthesis of 24,25-dihydroxyvitamin D₃ and 23,25-dihydroxyvitamin D₃. *Pediatric research*. 1993;34(1):98-104.

191. Park H, Wood MR, Malysheva OV, Jones S, Mehta S, Brannon PM, et al. Placental vitamin D metabolism and its associations with circulating vitamin D metabolites in pregnant women. *Am J Clin Nutr.* 2017;106(6):1439-48.
192. Karras SN, Shah I, Petroczi A, Goulis DG, Bili H, Papadopoulou F, et al. An observational study reveals that neonatal vitamin D is primarily determined by maternal contributions: implications of a new assay on the roles of vitamin D forms. *Nutr J.* 2013;12:77.
193. Bouillon R, Van Assche FA, Van Baelen H, Heyns W, De Moor P. Influence of the vitamin D-binding protein on the serum concentration of 1,25-dihydroxyvitamin D₃. Significance of the free 1,25-dihydroxyvitamin D₃ concentration. *The Journal of clinical investigation.* 1981;67(3):589-96.
194. Delvin EE, Glorieux FH, Salle BL, David L, Varenne JP. Control of vitamin D metabolism in preterm infants: feto-maternal relationships. *Archives of Disease in Childhood.* 1982;57(10):754-7.
195. Marx SJ, Swart EG, Jr., Hamstra AJ, DeLuca HF. Normal intrauterine development of the fetus of a woman receiving extraordinarily high doses of 1,25-dihydroxyvitamin D₃. *J Clin Endocrinol Metab.* 1980;51(5):1138-42.
196. Lundgren S, Carling T, Hjalms G, Juhlin C, Rastad J, Pihlgren U, et al. Tissue distribution of human gp330/megalin, a putative Ca(2+)-sensing protein. *The journal of histochemistry and cytochemistry : official journal of the Histochemistry Society.* 1997;45(3):383-92.
197. Liu NQ, Ouyang Y, Bulut Y, Lagishetty V, Chan SY, Hollis BW, et al. Dietary Vitamin D Restriction in Pregnant Female Mice Is Associated With Maternal Hypertension and Altered Placental and Fetal Development. *Endocrinology.* 2013.
198. Chan SY, Susarla R, Canovas D, Vasilopoulou E, Ohizua O, McCabe CJ, et al. Vitamin D promotes human extravillous trophoblast invasion in vitro. *Placenta.* 2015;36(4):403-9.
199. Excellence. NifHaC. Antenatal care. NICE clinical guideline 62. Manchester: 2008.
200. O'Reilly-Marshall A ICoGP. Antenatal Care. Nutrition in pregnancy. https://www.icgp.ie/assets/21/7FB21F16-19B9-E185-83915661D103354F_document/DL23-28.pdf: 2010 Contract No.: 156.
201. Kenny LC, Broadhurst DI, Dunn W, Brown M, North RA, McCowan L, et al. Robust Early Pregnancy Prediction of Later Preeclampsia Using Metabolomic Biomarkers. *Hypertension.* 2010;56(4):741-9.
202. Powe CE, Seely EW, Rana S, Bhan I, Ecker J, Karumanchi SA, et al. First trimester vitamin D, vitamin D binding protein, and subsequent preeclampsia. *Hypertension.* 2010;56(4):758-63.
203. Soma-Pillay P, Catherine N-P, Tolppanen H, Mebazaa A, Tolppanen H, Mebazaa A. Physiological changes in pregnancy. *Cardiovascular Journal of Africa.* 2016;27(2):89-94.
204. Swanson CM, Nielson CM, Shrestha S, Lee CG, Barrett-Connor E, Jans I, et al. Higher 25(OH)D(2) Is Associated With Lower 25(OH)D(3) and 1,25(OH)(2)D(3). *The Journal of Clinical Endocrinology and Metabolism.* 2014;99(8):2736-44.
205. Demetriou ET, Travison TG, Holick MF. Treatment with 50,000 IU vitamin D(2) every other week and effect on serum 25-hydroxyvitamin D(2), 25-hydroxyvitamin D(3), and total 25-hydroxyvitamin D in a clinical setting. *Endocrine practice : official journal of the American College of Endocrinology and the American Association of Clinical Endocrinologists.* 2012;18(3):399-402.
206. Jones KS, Assar S, Harnpanich D, Bouillon R, Lambrechts D, Prentice A, et al. 25(OH)D(2) Half-Life Is Shorter Than 25(OH)D(3) Half-Life and Is Influenced by DBP Concentration and Genotype. *The Journal of Clinical Endocrinology and Metabolism.* 2014;99(9):3373-81.
207. Evans KN, Bulmer JN, Kilby MD, Hewison M. Vitamin D and placental-decidual function. *Journal of the Society for Gynecologic Investigation.* 2004;11(5):263-71.
208. Nicolaidou P, Hatzistamatiou Z, Papadopoulou A, Kaleyias J, Floropoulou E, Lagona E, et al. Low vitamin D status in mother-newborn pairs in Greece. *Calcified tissue international.* 2006;78(6):337-42.
209. Salle BL, Delvin EE, Lapillonne A, Bishop NJ, Glorieux FH. Perinatal metabolism of vitamin D. *Am J Clin Nutr.* 2000;71(5 Suppl):1317s-24s.

210. Kanagal DV, Rajesh A, Rao K, Devi UH, Shetty H, Kumari S, et al. Levels of Serum Calcium and Magnesium in Pre-eclamptic and Normal Pregnancy: A Study from Coastal India. *Journal of Clinical and Diagnostic Research* : JCDR. 2014;8(7):OC01-OC4.
211. Ephraim RKD, Osakunor DNM, Denkyira SW, Eshun H, Amoah S, Anto EO. Serum calcium and magnesium levels in women presenting with pre-eclampsia and pregnancy-induced hypertension: a case-control study in the Cape Coast metropolis, Ghana. *BMC Pregnancy and Childbirth*. 2014;14:390.
212. Szmidi-Adjide V, Vendittelli F, David S, Bredent-Bangou J, Janky E. Calciuria and preeclampsia: a case-control study. *European journal of obstetrics, gynecology, and reproductive biology*. 2006;125(2):193-8.
213. Ozcan T, Kaleli B, Ozeren M, Turan C, Zorlu G. Urinary calcium to creatinine ratio for predicting preeclampsia. *American journal of perinatology*. 1995;12(5):349-51.
214. Organization WH. Guideline: calcium supplementation in pregnant women: World Health Organization; 2013.
215. Buppasiri P, Lumbiganon P, Thinkhamrop J, Ngamjarus C, Laopaiboon M, Medley N. Calcium supplementation (other than for preventing or treating hypertension) for improving pregnancy and infant outcomes. *Cochrane Database of Systematic Reviews*. 2015(2).
216. Fraser WD, Milan AM. Vitamin D assays: past and present debates, difficulties, and developments. *Calcified tissue international*. 2013;92(2):118-27.
217. Carter GD, Berry JL, Gunter E, Jones G, Jones JC, Makin HL, et al. Proficiency testing of 25-hydroxyvitamin D (25-OHD) assays. *The Journal of steroid biochemistry and molecular biology*. 2010;121(1-2):176-9.
218. Moon HW, Cho JH, Hur M, Song J, Oh GY, Park CM, et al. Comparison of four current 25-hydroxyvitamin D assays. *Clin Biochem*. 2012;45(4-5):326-30.
219. Taylor AE, Keevil B, Huhtaniemi IT. Mass spectrometry and immunoassay: how to measure steroid hormones today and tomorrow. *European journal of endocrinology*. 2015;173(2):D1-12.
220. Cheung KL, Lafayette RA. Renal Physiology of Pregnancy. *Advances in chronic kidney disease*. 2013;20(3):209-14.
221. Rivera-Núñez Z, Meliker JR, Linder AM, Nriagu JO. Reliability of spot urine samples in assessing arsenic exposure. *International Journal of Hygiene and Environmental Health*. 2010;213(4):259-64.
222. Middleton DRS, Watts MJ, Hamilton EM, Ander EL, Close RM, Exley KS, Crabbe H, Leonardi GS, Fletcher T and Polya D.A. 2016. Urinary arsenic profiles reveal substantial exposures to inorganic arsenic from private drinking water supplies in Cornwall, UK, *Sci Rep*, DOI: SREP25656.
223. Adams KM, Yan Z, Stevens AM, Nelson JL. The changing maternal "self" hypothesis: a mechanism for maternal tolerance of the fetus. *Placenta*. 2007;28(5-6):378-82.
224. Abumaree MH, Chamley LW, Badri M, El-Muzaini MF. Trophoblast debris modulates the expression of immune proteins in macrophages: a key to maternal tolerance of the fetal allograft? *Journal of reproductive immunology*. 2012;94(2):131-41.
225. Bulmer JN, Sunderland CA. Immunohistological characterization of lymphoid cell populations in the early human placental bed. *Immunology*. 1984;52(2):349-57.
226. Tilburgs T, Schonkeren D, Eikmans M, Nagtzaam NM, Datema G, Swings GM, et al. Human decidua contains differentiated CD8+ effector-memory T cells with unique properties. *Journal of immunology*. 2010;185(7):4470-7.
227. Petroff MG. Immune interactions at the maternal-fetal interface. *Journal of reproductive immunology*. 2005;68(1-2):1-13.
228. Taglauer ES, Adams Waldorf KM, Petroff MG. The hidden maternal-fetal interface: events involving the lymphoid organs in maternal-fetal tolerance. *The International journal of developmental biology*. 2010;54(2-3):421-30.
229. Hunt JS. Stranger in a strange land. *Immunological Reviews*. 2006;213(1):36-47.

230. Ferreira LMR, Meissner TB, Tilburgs T, Strominger JL. HLA-G: At the Interface of Maternal-Fetal Tolerance. *Trends in immunology*. 2017;38(4):272-86.
231. Moldenhauer LM, Hayball JD, Robertson SA. Utilising T cell receptor transgenic mice to define mechanisms of maternal T cell tolerance in pregnancy. *Journal of reproductive immunology*. 2010;87(1-2):1-13.
232. Erlebacher A, Vencato D, Price KA, Zhang D, Glimcher LH. Constraints in antigen presentation severely restrict T cell recognition of the allogeneic fetus. *Journal of Clinical Investigation*. 2007;117(5):1399-411.
233. Tilburgs T, Roelen DL, van der Mast BJ, de Groot-Swings GM, Kleijburg C, Scherjon SA, et al. Evidence for a selective migration of fetus-specific CD4+CD25bright regulatory T cells from the peripheral blood to the decidua in human pregnancy. *Journal of immunology*. 2008;180(8):5737-45.
234. Powell RM, Lissauer D, Tamblyn J, Beggs A, Cox P, Moss P, et al. Decidual T Cells Exhibit a Highly Differentiated Phenotype and Demonstrate Potential Fetal Specificity and a Strong Transcriptional Response to IFN. *Journal of immunology*. 2017;199(10):3406-17.
235. Sacks GP, Studena K, Sargent K, Redman CW. Normal pregnancy and preeclampsia both produce inflammatory changes in peripheral blood leukocytes akin to those of sepsis. *American journal of obstetrics and gynecology*. 1998;179(1):80-6.
236. Sargent IL, Borzychowski AM, Redman CWG. NK cells and human pregnancy – an inflammatory view. *Trends in immunology*. 2006;27(9):399-404.
237. Colucci F, Kieckbusch J. Maternal uterine natural killer cells nurture fetal growth: in medio stat virtus. *Trends in molecular medicine*. 2015;21(2):60-7.
238. Moffett A, Colucci F. Uterine NK cells: active regulators at the maternal-fetal interface. *The Journal of clinical investigation*. 2014;124(5):1872-9.
239. Cooper MA, Fehniger TA, Caligiuri MA. The biology of human natural killer-cell subsets. *Trends in immunology*. 2001;22(11):633-40.
240. Schmitt C, Ghazi B, Bensussan A. NK cells and surveillance in humans. *Reproductive biomedicine online*. 2008;16(2):192-201.
241. Karre K. Natural killer cell recognition of missing self. *Nat Immunol*. 2008;9(5):477-80.
242. Bryceson YT, March ME, Ljunggren HG, Long EO. Activation, coactivation, and costimulation of resting human natural killer cells. *Immunol Rev*. 2006;214:73-91.
243. Ferlazzo G, Thomas D, Lin SL, Goodman K, Morandi B, Muller WA, et al. The abundant NK cells in human secondary lymphoid tissues require activation to express killer cell Ig-like receptors and become cytolytic. *Journal of immunology*. 2004;172(3):1455-62.
244. Loza MJ, Perussia B. The IL-12 signature: NK cell terminal CD56+high stage and effector functions. *Journal of immunology*. 2004;172(1):88-96.
245. de Rham C, Ferrari-Lacraz S, Jendly S, Schneiter G, Dayer J-M, Villard J. The proinflammatory cytokines IL-2, IL-15 and IL-21 modulate the repertoire of mature human natural killer cell receptors. *Arthritis Research & Therapy*. 2007;9(6):R125-R.
246. Orange JS. Human natural killer cell deficiencies. *Current opinion in allergy and clinical immunology*. 2006;6(6):399-409.
247. Topham NJ, Hewitt EW. Natural killer cell cytotoxicity: how do they pull the trigger? *Immunology*. 2009;128(1):7-15.
248. Pallmer K, Oxenius A. Recognition and Regulation of T Cells by NK Cells. *Frontiers in immunology*. 2016;7:251.
249. Chan A, Hong DL, Atzberger A, Kollnberger S, Filer AD, Buckley CD, et al. CD56bright human NK cells differentiate into CD56dim cells: role of contact with peripheral fibroblasts. *Journal of immunology*. 2007;179(1):89-94.
250. Jacobs R, Hintzen G, Kemper A, Beul K, Kempf S, Behrens G, et al. CD56bright cells differ in their KIR repertoire and cytotoxic features from CD56dim NK cells. *European journal of immunology*. 2001;31(10):3121-7.
251. Caligiuri MA. Human natural killer cells. *Blood*. 2008;112(3):461-9.

252. Berahovich RD, Lai NL, Wei Z, Lanier LL, Schall TJ. Evidence for NK cell subsets based on chemokine receptor expression. *Journal of immunology*. 2006;177(11):7833-40.
253. Gregoire C, Chasson L, Luci C, Tomasello E, Geissmann F, Vivier E, et al. The trafficking of natural killer cells. *Immunol Rev*. 2007;220:169-82.
254. Guillerey C, Huntington ND, Smyth MJ. Targeting natural killer cells in cancer immunotherapy. *Nat Immunol*. 2016;17(9):1025-36.
255. Peng H, Wisse E, Tian Z. Liver natural killer cells: subsets and roles in liver immunity. *Cellular and Molecular Immunology*. 2016;13(3):328-36.
256. Lassen MG, Lukens JR, Dolina JS, Brown MG, Hahn YS. Intrahepatic IL-10 Maintains NKG2A⁺Ly49⁻ Liver NK Cells in a Functionally Hyporesponsive State. *The Journal of Immunology*. 2010;184(5):2693-701.
257. Sun H, Sun C, Tian Z, Xiao W. NK cells in immunotolerant organs. *Cell Mol Immunol*. 2013;10(3):202-12.
258. Lee JY, Lee M, Lee SK. Role of endometrial immune cells in implantation. *Clinical and Experimental Reproductive Medicine*. 2011;38(3):119-25.
259. Bulmer JN, Williams PJ, Lash GE. Immune cells in the placental bed. *Int J Dev Biol*. 2010;54(2-3):281-94.
260. Chantakru S, Miller C, Roach LE, Kuziel WA, Maeda N, Wang WC, et al. Contributions from self-renewal and trafficking to the uterine NK cell population of early pregnancy. *Journal of immunology (Baltimore, Md : 1950)*. 2002;168(1):22-8.
261. Hanna J, Wald O, Goldman-Wohl D, Prus D, Markel G, Gazit R, et al. CXCL12 expression by invasive trophoblasts induces the specific migration of CD16⁺ human natural killer cells. *Blood*. 2003;102(5):1569-77.
262. Vacca P, Vitale C, Montaldo E, Conte R, Cantoni C, Fulcheri E, et al. CD34⁺ hematopoietic precursors are present in human decidua and differentiate into natural killer cells upon interaction with stromal cells. *Proceedings of the National Academy of Sciences of the United States of America*. 2011;108(6):2402-7.
263. Gendron RL, Baines MG. Infiltrating decidual natural killer cells are associated with spontaneous abortion in mice. *Cell Immunol*. 1988;113(2):261-7.
264. Guimond MJ, Wang B, Croy BA. Engraftment of bone marrow from severe combined immunodeficient (SCID) mice reverses the reproductive deficits in natural killer cell-deficient tg epsilon 26 mice. *J Exp Med*. 1998;187(2):217-23.
265. Chaouat G, Tranchot Diallo J, Volumenie JL, Menu E, Gras G, Delage G, et al. Immune suppression and Th1/Th2 balance in pregnancy revisited: a (very) personal tribute to Tom Wegmann. *American journal of reproductive immunology*. 1997;37(6):427-34.
266. Bulmer JN, Lash GE. Human uterine natural killer cells: a reappraisal. *Mol Immunol*. 2005;42(4):511-21.
267. Hanna J, Goldman-Wohl D, Hamani Y, Avraham I, Greenfield C, Natanson-Yaron S, et al. Decidual NK cells regulate key developmental processes at the human fetal-maternal interface. *Nature medicine*. 2006;12(9):1065-74.
268. Lash GE, Otun HA, Innes BA, Percival K, Searle RF, Robson SC, et al. Regulation of extravillous trophoblast invasion by uterine natural killer cells is dependent on gestational age. *Human reproduction*. 2010;25(5):1137-45.
269. Hunkapiller NM, Fisher SJ. Placental remodeling of the uterine vasculature. *Methods in enzymology*. 2008;445:281-302.
270. Bulmer JN, Morrison L, Longfellow M, Ritson A, Pace D. Granulated lymphocytes in human endometrium: histochemical and immunohistochemical studies. *Human reproduction*. 1991;6(6):791-8.
271. Kalkunte SS, Mselle TF, Norris WE, Wira CR, Sentman CL, Sharma S. Vascular endothelial growth factor C facilitates immune tolerance and endovascular activity of human uterine NK cells at the maternal-fetal interface. *Journal of immunology*. 2009;182(7):4085-92.

272. Greenwood JD, Minhas K, di Santo JP, Makita M, Kiso Y, Croy BA. Ultrastructural studies of implantation sites from mice deficient in uterine natural killer cells. *Placenta*. 2000;21(7):693-702.
273. Rajagopalan S, Long EO. Cellular senescence induced by CD158d reprograms natural killer cells to promote vascular remodeling. *Proceedings of the National Academy of Sciences of the United States of America*. 2012;109(50):20596-601.
274. El Costa H, Casemayou A, Aguerre-Girr M, Rabot M, Berrebi A, Parant O, et al. Critical and differential roles of NKp46- and NKp30-activating receptors expressed by uterine NK cells in early pregnancy. *Journal of immunology*. 2008;181(5):3009-17.
275. Koka R, Burkett PR, Chien M, Chai S, Chan F, Lodolce JP, et al. Interleukin (IL)-15R α -deficient Natural Killer Cells Survive in Normal but Not IL-15R α -deficient Mice. *The Journal of Experimental Medicine*. 2003;197(8):977-84.
276. Koka R, Burkett P, Chien M, Chai S, Boone DL, Ma A. Cutting edge: murine dendritic cells require IL-15R alpha to prime NK cells. *Journal of immunology*. 2004;173(6):3594-8.
277. Koopman LA, Kopcow HD, Rybalov B, Boyson JE, Orange JS, Schatz F, et al. Human decidual natural killer cells are a unique NK cell subset with immunomodulatory potential. *The Journal of experimental medicine*. 2003;198(8):1201-12.
278. Male V, Sharkey A, Masters L, Kennedy PR, Farrell LE, Moffett A. The effect of pregnancy on the uterine NK cell KIR repertoire. *European journal of immunology*. 2011;41(10):3017-27.
279. Hanna J, Mandelboim O. When killers become helpers. *Trends in immunology*. 2007;28(5):201-6.
280. Saito S, Nakashima A, Myojo-Higuma S, Shiozaki A. The balance between cytotoxic NK cells and regulatory NK cells in human pregnancy. *Journal of reproductive immunology*. 2008;77(1):14-22.
281. Fu B, Li X, Sun R, Tong X, Ling B, Tian Z, et al. Natural killer cells promote immune tolerance by regulating inflammatory TH17 cells at the human maternal-fetal interface. *Proceedings of the National Academy of Sciences*. 2013;110(3):E231-E40.
282. Sargent IL, Borzychowski AM, Redman CW. NK cells and pre-eclampsia. *Journal of reproductive immunology*. 2007;76(1-2):40-4.
283. Parham P. NK cells and trophoblasts: partners in pregnancy. *The Journal of experimental medicine*. 2004;200(8):951-5.
284. Kim YM, Bujold E, Chaiworapongsa T, Gomez R, Yoon BH, Thaler HT, et al. Failure of physiologic transformation of the spiral arteries in patients with preterm labor and intact membranes. *American journal of obstetrics and gynecology*. 2003;189(4):1063-9.
285. Dosiou C, Giudice LC. Natural killer cells in pregnancy and recurrent pregnancy loss: endocrine and immunologic perspectives. *Endocr Rev*. 2005;26(1):44-62.
286. Ashkar AA, Di Santo JP, Croy BA. Interferon γ contributes to initiation of uterine vascular modification, decidual integrity, and uterine natural killer cell maturation during normal murine pregnancy. *The Journal of experimental medicine*. 2000;192(2):259-70.
287. Ashkar AA, Croy BA. Interferon-gamma contributes to the normalcy of murine pregnancy. *Biology of reproduction*. 1999;61(2):493-502.
288. Fu B, Zhou Y, Ni X, Tong X, Xu X, Dong Z, et al. Natural Killer Cells Promote Fetal Development through the Secretion of Growth-Promoting Factors. *Immunity*. 2017;47(6):1100-13.e6.
289. Sacks G, Yang Y, Gowen E, Smith S, Fay L, Chapman M. Detailed analysis of peripheral blood natural killer cells in women with repeated IVF failure. *American journal of reproductive immunology*. 2012;67(5):434-42.
290. Seshadri S, Sunkara SK. Natural killer cells in female infertility and recurrent miscarriage: a systematic review and meta-analysis. *Human reproduction update*. 2014;20(3):429-38.
291. Polgar K, Hill JA. Identification of the white blood cell populations responsible for Th1 immunity to trophoblast and the timing of the response in women with recurrent pregnancy loss. *Gynecologic and obstetric investigation*. 2002;53(1):59-64.

292. Dudley DJ, Hunter C, Mitchell MD, Varner MW, Gately M. Elevations of serum interleukin-12 concentrations in women with severe pre-eclampsia and HELLP syndrome. *Journal of reproductive immunology*. 1996;31(1-2):97-107.
293. Dudley DJ. Pre-term labor: an intra-uterine inflammatory response syndrome? *Journal of reproductive immunology*. 1997;36(1-2):93-109.
294. Hu W, Wang H, Wang Z, Huang H, Dong M. Elevated serum levels of interleukin-15 and interleukin-16 in preeclampsia. *Journal of reproductive immunology*. 2007;73(2):166-71.
295. Hiby SE, Walker JJ, O'Shaughnessy KM, Redman CW, Carrington M, Trowsdale J, et al. Combinations of maternal KIR and fetal HLA-C genes influence the risk of preeclampsia and reproductive success. *The Journal of experimental medicine*. 2004;200(8):957-65.
296. Fraser R, Whitley GS, Thilaganathan B, Cartwright JE. Decidual natural killer cells regulate vessel stability: implications for impaired spiral artery remodelling. *Journal of reproductive immunology*. 2015;110:54-60.
297. Wallace AE, Fraser R, Gurung S, Goulwara SS, Whitley GS, Johnstone AP, et al. Increased angiogenic factor secretion by decidual natural killer cells from pregnancies with high uterine artery resistance alters trophoblast function. *Human reproduction*. 2014;29(4):652-60.
298. Tang AW, Alfirevic Z, Quenby S. Natural killer cells and pregnancy outcomes in women with recurrent miscarriage and infertility: a systematic review. *Human reproduction (Oxford, England)*. 2011;26(8):1971-80.
299. Merino F, Alvarez-Mon M, de la Hera A, Ales JE, Bonilla F, Durantez A. Regulation of natural killer cytotoxicity by 1,25-dihydroxyvitamin D₃. *Cell Immunol*. 1989;118(2):328-36.
300. Moran-Auth Y, Penna-Martinez M, Shoghi F, Ramos-Lopez E, Badenhoop K. Vitamin D status and gene transcription in immune cells. *The Journal of steroid biochemistry and molecular biology*. 2013;136:83-5.
301. Ravid A, Koren R, Maron L, Liberman UA. 1,25(OH)₂D₃ increases cytotoxicity and exocytosis in lymphokine-activated killer cells. *Molecular and cellular endocrinology*. 1993;96(1-2):133-9.
302. Weeres MA, Robien K, Ahn Y-O, Neulen M-L, Bergerson R, Miller JS, et al. The effects of 1, 25-dihydroxyvitamin D₃ on in vitro human NK cell development from hematopoietic stem cells. *The Journal of Immunology*. 2014;193(7):3456-62.
303. Ota K, Dambaeva S, Han AR, Beaman K, Gilman-Sachs A, Kwak-Kim J. Vitamin D deficiency may be a risk factor for recurrent pregnancy losses by increasing cellular immunity and autoimmunity. *Human reproduction*. 2014;29(2):208-19.
304. Chan S, Susarla R, Canovas D, Vasilopoulou E, Ohizua O, McCabe C, et al. Vitamin D promotes human extravillous trophoblast invasion in vitro. *Placenta*. 2015.
305. Kachkache M, Rebut-Bonneton C, Demignon J, Cynober E, Garabedian M. Uterine cells other than stromal decidual cells are required for 1,25-dihydroxyvitamin D₃ production during early human pregnancy. *FEBS letters*. 1993;333(1-2):83-8.
306. Evans KN, Nguyen L, Chan J, Innes BA, Bulmer JN, Kilby MD, et al. Effects of 25-Hydroxyvitamin D₃ and 1,25-Dihydroxyvitamin D₃ on Cytokine Production by Human Decidual Cells. *Biology of reproduction*. 2006.
307. Grundmann M, Haidar M, Placzko S, Niendorf R, Darashchonak N, Hubel CA, et al. Vitamin D improves the angiogenic properties of endothelial progenitor cells. *American journal of physiology Cell physiology*. 2012;303(9):C954-62.
308. Bernardi RJ, Johnson CS, Modzelewski RA, Trump DL. Antiproliferative Effects of 1 α ,25-Dihydroxyvitamin D₃ and Vitamin D Analogs on Tumor-Derived Endothelial Cells. *Endocrinology*. 2002;143(7):2508-14.
309. King A, Birkby C, Loke YW. Early human decidual cells exhibit NK activity against the K562 cell line but not against first trimester trophoblast. *Cell Immunol*. 1989;118(2):337-44.
310. Shabrish S, Gupta M, Madkaikar M. A Modified NK Cell Degranulation Assay Applicable for Routine Evaluation of NK Cell Function. *Journal of Immunology Research*. 2016;2016:3769590.

311. Clausen J, Vergeiner B, Enk M, Petzer AL, Gastl G, Gunsilius E. Functional significance of the activation-associated receptors CD25 and CD69 on human NK-cells and NK-like T-cells. *Immunobiology*. 2003;207(2):85-93.
312. Jeffery LE, Qureshi OS, Gardner D, Hou TZ, Briggs Z, Soskic B, et al. Vitamin D Antagonises the Suppressive Effect of Inflammatory Cytokines on CTLA-4 Expression and Regulatory Function. *PLoS one*. 2015;10(7):e0131539.
313. Shaw P. *Introductory Multivariate Statistics for the Environmental Science*: John Wiley and Sons Ltd, Wiley-Blackwell; 2003.
314. Poli A, Michel T, Thérésine M, Andrès E, Hentges F, Zimmer J. CD56(bright) natural killer (NK) cells: an important NK cell subset. *Immunology*. 2009;126(4):458-65.
315. Lash GE, Robson SC, Bulmer JN. Review: Functional role of uterine natural killer (uNK) cells in human early pregnancy decidua. *Placenta*. 2010;31 Suppl:S87-92.
316. Lachapelle MH, Miron P, Hemmings R, Roy DC. Endometrial T, B, and NK cells in patients with recurrent spontaneous abortion. Altered profile and pregnancy outcome. *Journal of immunology*. 1996;156(10):4027-34.
317. Williams PJ, Searle RF, Robson SC, Innes BA, Bulmer JN. Decidual leucocyte populations in early to late gestation normal human pregnancy. *Journal of reproductive immunology*. 2009;82(1):24-31.
318. Lynch L, Golden-Mason L, Eogan M, O'Herlihy C, O'Farrelly C. Cells with haematopoietic stem cell phenotype in adult human endometrium: relevance to infertility? *Human reproduction*. 2007;22(4):919-26.
319. Vacca P, Moretta L, Moretta A, Mingari MC. Origin, phenotype and function of human natural killer cells in pregnancy. *Trends in immunology*. 2011;32(11):517-23.
320. Hudspeth K, Pontarini E, Tentorio P, Cimino M, Donadon M, Torzilli G, et al. The role of natural killer cells in autoimmune liver disease: a comprehensive review. *J Autoimmun*. 2013;46:55-65.
321. Hanna J, Goldman-Wohl D, Hamani Y, Avraham I, Greenfield C, Natanson-Yaron S, et al. Decidual NK cells regulate key developmental processes at the human fetal-maternal interface. *Nature medicine*. 2006;12(9):1065-74.
322. Murphy SP, Fast LD, Hanna NN, Sharma S. Uterine NK cells mediate inflammation-induced fetal demise in IL-10-null mice. *Journal of immunology*. 2005;175(6):4084-90.
323. Ferry BL, Starkey PM, Sargent IL, Watt GM, Jackson M, Redman CW. Cell populations in the human early pregnancy decidua: natural killer activity and response to interleukin-2 of CD56-positive large granular lymphocytes. *Immunology*. 1990;70(4):446-52.
324. De Maria A, Bozzano F, Cantoni C, Moretta L. Revisiting human natural killer cell subset function revealed cytolytic CD56(dim)CD16+ NK cells as rapid producers of abundant IFN-gamma on activation. *Proceedings of the National Academy of Sciences of the United States of America*. 2011;108(2):728-32.
325. Zourbas S, Dubanchet S, Martal J, Chaouat G. Localization of pro-inflammatory (IL-12, IL-15) and anti-inflammatory (IL-11, IL-13) cytokines at the foetomaternal interface during murine pregnancy. *Clin Exp Immunol*. 2001;126(3):519-28.
326. Kovacs E, Meichsner-Frauli M, Ludwig H. Interleukin-2 receptor positive cells in human decidua during the first trimester of pregnancy and their association with macrophages. *Archives of Gynecology and Obstetrics*. 1992;251(2):93-100.
327. Jokhi PP, King A, Sharkey AM, Smith SK, Loke YW. Screening for cytokine messenger ribonucleic acids in purified human decidual lymphocyte populations by the reverse-transcriptase polymerase chain reaction. *Journal of immunology*. 1994;153(10):4427-35.
328. Garzia E, Clauser R, Persani L, Borgato S, Bulfamante G, Avagliano L, et al. Prolactin and proinflammatory cytokine expression at the fetomaternal interface in first trimester miscarriage. *Fertil Steril*. 2013;100(1):108-15.e1-2.

329. Robinson CJ, Alanis MC, Wagner CL, Hollis BW, Johnson DD. Plasma 25-hydroxyvitamin D levels in early-onset severe preeclampsia. *American journal of obstetrics and gynecology*. 2010.
330. Jeffery LE, Wood AM, Qureshi OS, Hou TZ, Gardner D, Briggs Z, et al. Availability of 25-Hydroxyvitamin D3 to APCs Controls the Balance between Regulatory and Inflammatory T Cell Responses. *Journal of immunology*. 2012;189(11):5155-64.
331. Tuoresmäki P, Väisänen S, Neme A, Heikkinen S, Carlberg C. Patterns of Genome-Wide VDR Locations. *PloS one*. 2014;9(4):e96105.
332. Diaz L, Noyola-Martinez N, Barrera D, Hernandez G, Avila E, Halhali A, et al. Calcitriol inhibits TNF-alpha-induced inflammatory cytokines in human trophoblasts. *Journal of reproductive immunology*. 2009;81(1):17-24.
333. Ashkar AA, Di Santo JP, Croy BA. Interferon gamma contributes to initiation of uterine vascular modification, decidual integrity, and uterine natural killer cell maturation during normal murine pregnancy. *J Exp Med*. 2000;192(2):259-70.
334. Lee J, Choi BC, Cho C, Hill JA, Baek KH, Kim JW. Trophoblast apoptosis is increased in women with evidence of TH1 immunity. *Fertil Steril*. 2005;83(4):1047-9.
335. Ragab D, Soliman D, Samaha D, Yassin A. Vitamin D status and its modulatory effect on interferon gamma and interleukin-10 production by peripheral blood mononuclear cells in culture. *Cytokine*. 2016;85:5-10.
336. Fabri M, Stenger S, Shin DM, Yuk JM, Liu PT, Realegeno S, et al. Vitamin D is required for IFN-gamma-mediated antimicrobial activity of human macrophages. *Science translational medicine*. 2011;3(104):104ra2.
337. Kutmon M, van Iersel MP, Bohler A, Kelder T, Nunes N, Pico AR, et al. PathVisio 3: An Extendable Pathway Analysis Toolbox. *PLOS Computational Biology*. 2015;11(2):e1004085.
338. Wang F, Zhou Y, Fu B, Wu Y, Zhang R, Sun R, et al. Molecular signatures and transcriptional regulatory networks of human immature decidual NK and mature peripheral NK cells. *European journal of immunology*. 2014;44(9):2771-84.
339. Bosshart H, Heinzelmann M. THP-1 cells as a model for human monocytes. *Annals of Translational Medicine*. 2016;4(21):438.
340. Seuter S, Neme A, Carlberg C. Epigenome-wide effects of vitamin D and their impact on the transcriptome of human monocytes involve CTCF. *Nucleic acids research*. 2016;44(9):4090-104.
341. Kupfer SS, Maranville JC, Baxter SS, Huang Y, Rienzo AD. Comparison of Cellular and Transcriptional Responses to 1,25-Dihydroxyvitamin D3 and Glucocorticoids in Peripheral Blood Mononuclear Cells. *PloS one*. 2013;8(10):e76643.
342. Kimura F, Suzu S, Nakamura Y, Nakata Y, Yamada M, Kuwada N, et al. Cloning and Characterization of a Novel RING-B-box-Coiled-coil Protein with Apoptotic Function. *Journal of Biological Chemistry*. 2003;278(27):25046-54.
343. Chen Z, Wang Z, Guo W, Zhang Z, Zhao F, Zhao Y, et al. TRIM35 Interacts with pyruvate kinase isoform M2 to suppress the Warburg effect and tumorigenicity in hepatocellular carcinoma. *Oncogene*. 2015;34(30):3946-56.
344. Freerman AJ, Johnson AR, Sacks GN, Milner JJ, Kirk EL, Troester MA, et al. Metabolic reprogramming of macrophages: glucose transporter 1 (GLUT1)-mediated glucose metabolism drives a proinflammatory phenotype. *The Journal of biological chemistry*. 2014;289(11):7884-96.
345. Kariuki SN, Blischak JD, Nakagome S, Witonsky DB, Di Rienzo A. Patterns of Transcriptional Response to 1,25-Dihydroxyvitamin D3 and Bacterial Lipopolysaccharide in Primary Human Monocytes. *G3: Genes | Genomes | Genetics*. 2016;6(5):1345-55.
346. Zuo R-J, Gu X-W, Qi Q-R, Wang T-S, Zhao X-Y, Liu J-L, et al. Warburg-like Glycolysis and Lactate Shuttle in Mouse Decidua during Early Pregnancy. *The Journal of biological chemistry*. 2015;290(35):21280-91.
347. Kelly B, O'Neill LAJ. Metabolic reprogramming in macrophages and dendritic cells in innate immunity. *Cell Res*. 2015;25(7):771-84.

348. Iriyama T, Sun K, Parchim NF, Li J, Zhao C, Song A, et al. Elevated Placental Adenosine Signaling Contributes to the Pathogenesis of Preeclampsia. *Circulation*. 2015;131(8):730-41.
349. Mador ES, Pam IC, Isichei CO. Uric acid: A hypothetical cause of preeclampsia-eclampsia. *Nigerian Medical Journal : Journal of the Nigeria Medical Association*. 2013;54(5):362-4.
350. Díaz-Gimeno P, Horcajadas JA, Martínez-Conejero JA, Esteban FJ, Alamá P, Pellicer A, et al. A genomic diagnostic tool for human endometrial receptivity based on the transcriptomic signature. *Fertility and Sterility*. 2011;95(1):50-60.e15.
351. Brar AK, Kessler CA, Meyer AJ, Cedars MI, Jikihara H. Retinoic acid suppresses in-vitro decidualization of human endometrial stromal cells. *Molecular human reproduction*. 1996;2(3):185-93.
352. Schrader M, Bendik I, Becker-Andre M, Carlberg C. Interaction between retinoic acid and vitamin D signaling pathways. *The Journal of biological chemistry*. 1993;268(24):17830-6.
353. Adams JS, Hewison M. Unexpected actions of vitamin D: new perspectives on the regulation of innate and adaptive immunity. *Nat Clin Pract Endocrinol Metab*. 2008;4(2):80-90.
354. Blois SM, Conrad ML, Freitag N, Barrientos G. Galectins in angiogenesis: consequences for gestation. *Journal of reproductive immunology*. 2015;108:33-41.
355. Heusschen R, Freitag N, Tirado-González I, Barrientos G, Moschansky P, Muñoz-Fernández R, et al. Profiling Lgals9 Splice Variant Expression at the Fetal-Maternal Interface: Implications in Normal and Pathological Human Pregnancy. *Biology of reproduction*. 2013;88(1):22, 1-10-22, 1-10.
356. Heusschen R, Freitag N, Tirado-Gonzalez I, Barrientos G, Moschansky P, Munoz-Fernandez R, et al. Profiling Lgals9 splice variant expression at the fetal-maternal interface: implications in normal and pathological human pregnancy. *Biology of reproduction*. 2013;88(1):22.
357. Wang L, Li Q, Wu L, Liu S, Zhang Y, Yang X, et al. Identification of SERPINB1 As a Physiological Inhibitor of Human Granzyme H. *The Journal of Immunology*. 2012.
358. Sica GL, Zhu G, Tamada K, Liu D, Ni J, Chen L. RELT, a new member of the tumor necrosis factor receptor superfamily, is selectively expressed in hematopoietic tissues and activates transcription factor NF-kappaB. *Blood*. 2001;97(9):2702-7.
359. Chin KC, Cresswell P. Viperin (cig5), an IFN-inducible antiviral protein directly induced by human cytomegalovirus. *Proceedings of the National Academy of Sciences of the United States of America*. 2001;98(26):15125-30.
360. Waggoner SN, Reighard SD, Gyurova IE, Cranert SA, Mahl SE, Karnele EP, et al. Roles of natural killer cells in antiviral immunity. *Curr Opin Virol*. 2016;16:15-23.
361. Liang Y, Jansen M, Aronow B, Geiger H, Van Zant G. The quantitative trait gene latexin influences the size of the hematopoietic stem cell population in mice. *Nat Genet*. 2007;39(2):178-88.
362. Oldridge EE, Walker HF, Stower MJ, Simms MS, Mann VM, Collins AT, et al. Retinoic acid represses invasion and stem cell phenotype by induction of the metastasis suppressors RARRES1 and LXN. *Oncogenesis*. 2013;2:e45.
363. Waldhauer I, Steinle A. NK cells and cancer immunosurveillance. *Oncogene*. 2008;27(45):5932-43.
364. Conesa A, Madrigal P, Tarazona S, Gomez-Cabrero D, Cervera A, McPherson A, et al. A survey of best practices for RNA-seq data analysis. *Genome Biology*. 2016;17:13.
365. Arenas-Hernandez M, Vega-Sanchez R. Housekeeping gene expression stability in reproductive tissues after mitogen stimulation. *BMC Research Notes*. 2013;6(1):285.
366. Wang ET, Sandberg R, Luo S, Khrebtkova I, Zhang L, Mayr C, et al. Alternative isoform regulation in human tissue transcriptomes. *Nature*. 2008;456(7221):470-6.
367. Guilliams M, Ginhoux F, Jakubzick C, Naik SH, Onai N, Schraml BU, et al. Dendritic cells, monocytes and macrophages: a unified nomenclature based on ontogeny. *Nature reviews Immunology*. 2014;14(8):571-8.

368. Yona S, Kim KW, Wolf Y, Mildner A, Varol D, Breker M, et al. Fate mapping reveals origins and dynamics of monocytes and tissue macrophages under homeostasis. *Immunity*. 2013;38(1):79-91.
369. Gardner L, Moffett A. Dendritic cells in the human decidua. *Biology of reproduction*. 2003;69(4):1438-46.
370. Ziegler-Heitbrock L, Ancuta P, Crowe S, Dalod M, Grau V, Hart DN, et al. Nomenclature of monocytes and dendritic cells in blood. *Blood*. 2010;116(16):e74-80.
371. Jiang H, Van De Ven C, Satwani P, Baxi LV, Cairo MS. Differential gene expression patterns by oligonucleotide microarray of basal versus lipopolysaccharide-activated monocytes from cord blood versus adult peripheral blood. *Journal of immunology*. 2004;172(10):5870-9.
372. Rossol M, Kraus S, Pierer M, Baerwald C, Wagner U. The CD14(bright) CD16+ monocyte subset is expanded in rheumatoid arthritis and promotes expansion of the Th17 cell population. *Arthritis and rheumatism*. 2012;64(3):671-7.
373. Zawada AM, Rogacev KS, Rotter B, Winter P, Marell RR, Fliser D, et al. SuperSAGE evidence for CD14++CD16+ monocytes as a third monocyte subset. *Blood*. 2011;118(12):e50-61.
374. Wong KL, Tai JJ, Wong WC, Han H, Sem X, Yeap WH, et al. Gene expression profiling reveals the defining features of the classical, intermediate, and nonclassical human monocyte subsets. *Blood*. 2011;118(5):e16-31.
375. Idzkowska E, Eljaszewicz A, Miklasz P, Musial WJ, Tycinska AM, Moniuszko M. The Role of Different Monocyte Subsets in the Pathogenesis of Atherosclerosis and Acute Coronary Syndromes. *Scandinavian journal of immunology*. 2015;82(3):163-73.
376. Melgert BN, Spaans F, Borghuis T, Klok PA, Groen B, Bolt A, et al. Pregnancy and Preeclampsia Affect Monocyte Subsets in Humans and Rats. *PloS one*. 2012;7(9):e45229.
377. Cros J, Cagnard N, Woollard K, Patey N, Zhang S-Y, Senechal B, et al. Human CD14dim Monocytes Patrol and Sense Nucleic Acids and Viruses via TLR7 and TLR8 Receptors. *Immunity*. 2010;33(3):375-86.
378. Fingerle G, Pforte A, Passlick B, Blumenstein M, Strobel M, Ziegler-Heitbrock HW. The novel subset of CD14+/CD16+ blood monocytes is expanded in sepsis patients. *Blood*. 1993;82(10):3170-6.
379. Eljaszewicz A, Wiese M, #x142, gorzata, Helmin-Basa A, Jankowski M, et al. Collaborating with the Enemy: Function of Macrophages in the Development of Neoplastic Disease. *Mediators of Inflammation*. 2013;2013:11.
380. Ginhoux F, Jung S. Monocytes and macrophages: developmental pathways and tissue homeostasis. *Nature reviews Immunology*. 2014;14(6):392-404.
381. Aad G, Abajyan T, Abbott B, Abdallah J, Abdel Khalek S, Abdelalim AA, et al. Search for magnetic monopoles in sqrt[s]=7 TeV pp collisions with the ATLAS detector. *Phys Rev Lett*. 2012;109(26):261803.
382. Zhang YH, He M, Wang Y, Liao AH. Modulators of the Balance between M1 and M2 Macrophages during Pregnancy. *Frontiers in immunology*. 2017;8:120.
383. Mantovani A, Sica A, Sozzani S, Allavena P, Vecchi A, Locati M. The chemokine system in diverse forms of macrophage activation and polarization. *Trends in immunology*. 2004;25(12):677-86.
384. Al-ofi E, Coffelt SB, Anumba DO. Monocyte subpopulations from pre-eclamptic patients are abnormally skewed and exhibit exaggerated responses to Toll-like receptor ligands. *PloS one*. 2012;7(7):e42217.
385. Lampe R, Kover A, Szucs S, Pal L, Arnyas E, Adany R, et al. Phagocytic index of neutrophil granulocytes and monocytes in healthy and preeclamptic pregnancy. *Journal of reproductive immunology*. 2015;107:26-30.
386. Chen J, Ivashkiv LB. IFN-gamma abrogates endotoxin tolerance by facilitating Toll-like receptor-induced chromatin remodeling. *Proceedings of the National Academy of Sciences of the United States of America*. 2010;107(45):19438-43.

387. Faas MM, Spaans F, De Vos P. Monocytes and macrophages in pregnancy and pre-eclampsia. *Frontiers in immunology*. 2014;5:298.
388. Faas MM, de Vos P. Uterine NK cells and macrophages in pregnancy. *Placenta*. 2017;56(Supplement C):44-52.
389. Goldsmith LT, Weiss G, Palejwala S, Plant TM, Wojtczuk A, Lambert WC, et al. Relaxin regulation of endometrial structure and function in the rhesus monkey. *Proceedings of the National Academy of Sciences of the United States of America*. 2004;101(13):4685-9.
390. Houser BL, Tilburgs T, Hill J, Nicotra ML, Strominger JL. Two unique human decidual macrophage populations. *Journal of immunology*. 2011;186(4):2633-42.
391. Takeda K, Akira S. Toll-like receptors in innate immunity. *Int Immunol*. 2005;17(1):1-14.
392. Final report on the safety assessment of Glycyrrhetic Acid, Potassium Glycyrrhetinate, Disodium Succinoyl Glycyrrhetinate, Glyceryl Glycyrrhetinate, Glycyrrhetinyl Stearate, Stearyl Glycyrrhetinate, Glycyrrhizic Acid, Ammonium Glycyrrhizate, Dipotassium Glycyrrhizate, Disodium Glycyrrhizate, Trisodium Glycyrrhizate, Methyl Glycyrrhizate, and Potassium Glycyrrhizinate. *Int J Toxicol*. 2007;26 Suppl 2:79-112.
393. Ning F, Liu H, Lash GE. The Role of Decidual Macrophages During Normal and Pathological Pregnancy. *American journal of reproductive immunology*. 2016;75(3):298-309.
394. Prins JR, Faas MM, Melgert BN, Huitema S, Timmer A, Hylkema MN, et al. Altered expression of immune-associated genes in first-trimester human decidua of pregnancies later complicated with hypertension or foetal growth restriction. *Placenta*. 33(5):453-5.
395. Guenther S, Vrekoussis T, Heublein S, Bayer B, Anz D, Knabl J, et al. Decidual macrophages are significantly increased in spontaneous miscarriages and over-express FasL: a potential role for macrophages in trophoblast apoptosis. *International journal of molecular sciences*. 2012;13(7):9069-80.
396. Jaiswal MK, Gilman-Sachs A, Chaouat G, Beaman KD. Placental ATPase expression is a link between multiple causes of spontaneous abortion in mice. *Biology of reproduction*. 2011;85(3):626-34.
397. Liu N, Kaplan AT, Low J, Nguyen L, Liu GY, Equils O, et al. Vitamin D induces innate antibacterial responses in human trophoblasts via an intracrine pathway. *Biology of reproduction*. 2009;80(3):398-406.
398. Shin DM, Yuk JM, Lee HM, Lee SH, Son JW, Harding CV, et al. Mycobacterial Lipoprotein Activates Autophagy via TLR2/1/CD14 and a Functional Vitamin D Receptor Signaling. *Cell Microbiol*. 2011.
399. Bacchetta J ZJ, Sea JL, Chun RF, Lisse TS, Zavala K, Nayak A, Westerman M, Hollis BW, Salusky IB, Hewison M. Suppression of iron-regulatory hepcidin by vitamin D. *Journal of the American Society for Nephrology*. 2013;(submitted).
400. Hewison M. Vitamin D and innate and adaptive immunity. *Vitam Horm*. 86:23-62.
401. Adams JS, Ren S, Liu PT, Chun RF, Lagishetty V, Gombart AF, et al. Vitamin d-directed rheostatic regulation of monocyte antibacterial responses. *Journal of immunology*. 2009;182(7):4289-95.
402. Zhang Y, Leung DYM, Richers BN, Liu Y, Remigio LK, Riches DW, et al. Vitamin D Inhibits Monocyte/macrophage Pro-inflammatory Cytokine Production by Targeting Mitogen-Activated Protein Kinase Phosphatase 1. *Journal of Immunology (Baltimore, Md : 1950)*. 2012;188(5):2127-35.
403. Sadeghi K, Wessner B, Laggner U, Ploder M, Tamandl D, Friedl J, et al. Vitamin D3 down-regulates monocyte TLR expression and triggers hyporesponsiveness to pathogen-associated molecular patterns. *European journal of immunology*. 2006;36(2):361-70.
404. Helming L, Bose J, Ehrchen J, Schiebe S, Frahm T, Geffers R, et al. 1alpha,25-Dihydroxyvitamin D3 is a potent suppressor of interferon gamma-mediated macrophage activation. *Blood*. 2005;106(13):4351-8.

405. Reichel H, Koeffler HP, Barbers R, Norman AW. Regulation of 1,25-dihydroxyvitamin D₃ production by cultured alveolar macrophages from normal human donors and from patients with pulmonary sarcoidosis. *J Clin Endocrinol Metab.* 1987;65(6):1201-9.
406. Bacchetta J, Salusky IB, Hewison M. Beyond mineral metabolism, is there an interplay between FGF23 and vitamin D in innate immunity? *Pediatric nephrology (Berlin, Germany).* 2013;28(4):577-82.
407. Equils O, Hewison M. A role for vitamin D in placental immunology. *The Journal of infectious diseases.* 201(12):1950-1; author reply 1.
408. Mukherjee R, Kanti Barman P, Kumar Thatoi P, Tripathy R, Kumar Das B, Ravindran B. Non-Classical monocytes display inflammatory features: Validation in Sepsis and Systemic Lupus Erythematosus. 2015;5:13886.
409. Volk H-D, Reinke P, Krausch D, Zuckermann H, Asadullah K, Müller JM, et al. Monocyte deactivation-rationale for a new therapeutic strategy in sepsis. *Intensive Care Medicine.* 1996;22(4):S474-S81.
410. Cleal JK, Day P, Hanson MA, Lewis RM. Measurement of housekeeping genes in human placenta. *Placenta.* 2009;30.
411. Daigneault M, Preston JA, Marriott HM, Whyte MKB, Dockrell DH. The Identification of Markers of Macrophage Differentiation in PMA-Stimulated THP-1 Cells and Monocyte-Derived Macrophages. *PloS one.* 2010;5(1):e8668.
412. Schonkeren D, van der Hoorn ML, Khedoe P, Swings G, van Beelen E, Claas F, et al. Differential distribution and phenotype of decidual macrophages in preeclamptic versus control pregnancies. *The American journal of pathology.* 2011;178(2):709-17.
413. Kim JS, Romero R, Cushenberry E, Kim YM, Erez O, Nien JK, et al. Distribution of CD14+ and CD68+ macrophages in the placental bed and basal plate of women with preeclampsia and preterm labor. *Placenta.* 2007;28(5-6):571-6.
414. Adams JS, Liu P, Chun R, Modlin RL, Hewison M. Vitamin D in Defense of the Human Immune Response. *Annals of the New York Academy of Sciences.* 2007.
415. Lykkedegn S, Sorensen GL, Beck-Nielsen SS, Christesen HT. The impact of vitamin D on fetal and neonatal lung maturation. A systematic review. *American journal of physiology Lung cellular and molecular physiology.* 2015;308(7):L587-602.
416. Cooper C, Harvey NC, Bishop NJ, Kennedy S, Papageorghiou AT, Schoenmakers I, et al. Maternal gestational vitamin D supplementation and offspring bone health (MAVIDOS): a multicentre, double-blind, randomised placebo-controlled trial. *The Lancet Diabetes & Endocrinology.* 4(5):393-402.
417. Prabhu SB, Rathore DK, Nair D, Chaudhary A, Raza S, Kanodia P, et al. Comparison of Human Neonatal and Adult Blood Leukocyte Subset Composition Phenotypes. *PloS one.* 2016;11(9):e0162242.
418. Haller H, Radillo O, Rukavina D, Tedesco F, Candussi G, Petrovic O, et al. An immunohistochemical study of leucocytes in human endometrium, first and third trimester basal decidua. *Journal of reproductive immunology.* 1993;23(1):41-9.
419. Hanna J, Goldman-Wohl D, Hamani Y, Avraham I, Greenfield C, Natanson-Yaron S, et al. Decidual NK cells regulate key developmental processes at the human fetal-maternal interface. *Nature medicine.* 2006;12(9):1065-74.
420. Abadia-Molina AC, Ruiz C, Montes MJ, King A, Loke YW, Olivares EG. Immune phenotype and cytotoxic activity of lymphocytes from human term decidua against trophoblast. *Journal of reproductive immunology.* 1996;31(1):109-23.
421. Tilburgs T, Roelen DL, van der Mast BJ, van Schip JJ, Kleijburg C, de Groot-Swings GM, et al. Differential Distribution of CD4+CD25bright and CD8+CD28- T-cells in Decidua and Maternal Blood During Human Pregnancy. *Placenta.* 2006;27:47-53.
422. Mackler AM, Iezza G, Akin MR, McMillan P, Yellon SM. Macrophage trafficking in the uterus and cervix precedes parturition in the mouse. *Biology of reproduction.* 1999;61(4):879-83.

423. Shynlova O, Tsui P, Dorogin A, Lye SJ. Monocyte Chemoattractant Protein-1 (CCL-2) Integrates Mechanical and Endocrine Signals That Mediate Term and Preterm Labor. *The Journal of Immunology*. 2008;181(2):1470-9.
424. Gordon S, Taylor PR. Monocyte and macrophage heterogeneity. *Nat Rev Immunol*. 2005;5(12):953-64.
425. Jensen AL, Collins J, Shipman EP, Wira CR, Guyre PM, Pioli PA. A Subset of Human Uterine Endometrial Macrophages is Alternatively Activated. *American journal of reproductive immunology (New York, NY : 1989)*. 2012;68(5):374-86.
426. Ziegler-Heitbrock HW, Fingerle G, Strobel M, Schraut W, Stelter F, Schutt C, et al. The novel subset of CD14+/CD16+ blood monocytes exhibits features of tissue macrophages. *European journal of immunology*. 1993;23(9):2053-8.
427. Wang H, He M, Hou Y, Chen S, Zhang X, Zhang M, et al. Role of decidual CD14(+) macrophages in the homeostasis of maternal-fetal interface and the differentiation capacity of the cells during pregnancy and parturition. *Placenta*. 2016;38:76-83.
428. Fagerberg L, Hallstrom BM, Oksvold P, Kampf C, Djureinovic D, Odeberg J, et al. Analysis of the human tissue-specific expression by genome-wide integration of transcriptomics and antibody-based proteomics. *Molecular & cellular proteomics : MCP*. 2014;13(2):397-406.
429. Sohlberg E, Saghafian-Hedengren S, Bremme K, Sverre-remark-Ekström E. Cord blood monocyte subsets are similar to adult and show potent peptidoglycan-stimulated cytokine responses. *Immunology*. 2011;133(1):41-50.
430. Brichard B, Varis I, Latinne D, Deneys V, de Bruyere M, Leveugle P, et al. Intracellular cytokine profile of cord and adult blood monocytes. *Bone marrow transplantation*. 2001;27(10):1081-6.
431. Gustafsson C, Mjosberg J, Matussek A, Geffers R, Matthiesen L, Berg G, et al. Gene expression profiling of human decidual macrophages: evidence for immunosuppressive phenotype. *PloS one*. 2008;3(4):e2078.
432. Kammerer U, Eggert AO, Kapp M, McLellan AD, Geijtenbeek TB, Dietl J, et al. Unique appearance of proliferating antigen-presenting cells expressing DC-SIGN (CD209) in the decidua of early human pregnancy. *The American journal of pathology*. 2003;162(3):887-96.
433. Bockle BC, Solder E, Kind S, Romani N, Sepp NT. DC-sign+ CD163+ macrophages expressing hyaluronan receptor LYVE-1 are located within chorion villi of the placenta. *Placenta*. 2008;29(2):187-92.
434. Mizuno M, Aoki K, Kimbara T. Functions of macrophages in human decidual tissue in early pregnancy. *American journal of reproductive immunology*. 1994;31(4):180-8.
435. Jaiswal MK, Mallers TM, Larsen B, Kwak-Kim J, Chaouat G, Gilman-Sachs A, et al. V-ATPase upregulation during early pregnancy: a possible link to establishment of an inflammatory response during preimplantation period of pregnancy. *Reproduction*. 2012;143(5):713-25.
436. Pinzone MR, Di Rosa M, Celesia BM, Condorelli F, Malaguarnera M, Madeddu G, et al. LPS and HIV gp120 modulate monocyte/macrophage CYP27B1 and CYP24A1 expression leading to vitamin D consumption and hypovitaminosis D in HIV-infected individuals. *European review for medical and pharmacological sciences*. 2013;17(14):1938-50.
437. Liu PT, Stenger S, Li H, Wenzel L, Tan BH, Krutzik SR, et al. Toll-like receptor triggering of a vitamin D-mediated human antimicrobial response. *Science*. 2006;311(5768):1770-3.
438. Ren S, Nguyen L, Wu S, Encinas C, Adams JS, Hewison M. Alternative splicing of vitamin D-24-hydroxylase: a novel mechanism for the regulation of extrarenal 1,25-dihydroxyvitamin D synthesis. *The Journal of biological chemistry*. 2005;280(21):20604-11.
439. Kreutz M, Andreesen R, Krause SW, Szabo A, Ritz E, Reichel H. 1,25-dihydroxyvitamin D3 production and vitamin D3 receptor expression are developmentally regulated during differentiation of human monocytes into macrophages. *Blood*. 1993;82(4):1300-7.
440. Gombart AF, Borregaard N, Koeffler HP. Human cathelicidin antimicrobial peptide (CAMP) gene is a direct target of the vitamin D receptor and is strongly up-regulated in myeloid cells by 1,25-

- dihydroxyvitamin D3. *FASEB journal : official publication of the Federation of American Societies for Experimental Biology*. 2005;19(9):1067-77.
441. Olmos-Ortiz A, García-Quiroz J, López-Marure R, González-Curiel I, Rivas-Santiago B, Olivares A, et al. Evidence of sexual dimorphism in placental vitamin D metabolism: Testosterone inhibits calcitriol-dependent cathelicidin expression. *The Journal of steroid biochemistry and molecular biology*. 2016;163:173-82.
442. Lim R, Barker G, Lappas M. Human cathelicidin antimicrobial protein 18 (hCAP18/LL-37) is increased in foetal membranes and myometrium after spontaneous labour and delivery. *Journal of reproductive immunology*. 2015;107:31-42.
443. Hayes MP, Freeman SL, Donnelly RP. IFN-gamma priming of monocytes enhances LPS-induced TNF production by augmenting both transcription and mRNA stability. *Cytokine*. 1995;7(5):427-35.
444. Gessani S, Belardelli F. IFN-gamma expression in macrophages and its possible biological significance. *Cytokine & growth factor reviews*. 1998;9(2):117-23.
445. Nonn L, Peng L, Feldman D, Peehl DM. Inhibition of p38 by vitamin D reduces interleukin-6 production in normal prostate cells via mitogen-activated protein kinase phosphatase 5: implications for prostate cancer prevention by vitamin D. *Cancer Res*. 2006;66(8):4516-24.
446. Joshi S, Pantalena LC, Liu XK, Gaffen SL, Liu H, Rohowsky-Kochan C, et al. 1,25-dihydroxyvitamin D(3) ameliorates Th17 autoimmunity via transcriptional modulation of interleukin-17A. *Molecular and cellular biology*. 31(17):3653-69.
447. Muller K, Haahr PM, Diamant M, Rieneck K, Kharazmi A, Bendtzen K. 1,25-Dihydroxyvitamin D3 inhibits cytokine production by human blood monocytes at the post-transcriptional level. *Cytokine*. 1992;4(6):506-12.
448. Di Rosa M, Malaguarnera G, De Gregorio C, Palumbo M, Nunnari G, Malaguarnera L. Immuno-modulatory effects of vitamin D3 in human monocyte and macrophages. *Cell Immunol*. 2012;280(1):36-43.
449. Lockwood CJ, Murk WK, Kayisli UA, Buchwalder LF, Huang SJ, Arcuri F, et al. Regulation of Interleukin-6 Expression in Human Decidual Cells and Its Potential Role in Chorioamnionitis. *The American journal of pathology*. 2010;177(4):1755-64.
450. Lockwood CJ, Yen C-F, Basar M, Kayisli UA, Martel M, Buhimschi I, et al. Preeclampsia-Related Inflammatory Cytokines Regulate Interleukin-6 Expression in Human Decidual Cells. *The American journal of pathology*. 2008;172(6):1571-9.
451. Kuo YT, Kuo CH, Lam KP, Chu YT, Wang WL, Huang CH, et al. Effects of vitamin D3 on expression of tumor necrosis factor-alpha and chemokines by monocytes. *Journal of food science*. 2010;75(6):H200-4.
452. Cohen ML, Douvdevani A, Chaimovitz C, Shany S. Regulation of TNF- α by 1 α ,25-dihydroxyvitamin D3 in human macrophages from CAPD patients. *Kidney international*. 2001;59(1):69-75.
453. Singh U, Nicholson G, Urban BC, Sargent IL, Kishore U, Bernal AL. Immunological properties of human decidual macrophages--a possible role in intrauterine immunity. *Reproduction*. 2005;129(5):631-7.
454. Hambleton J, Weinstein SL, Lem L, DeFranco AL. Activation of c-Jun N-terminal kinase in bacterial lipopolysaccharide-stimulated macrophages. *Proceedings of the National Academy of Sciences of the United States of America*. 1996;93(7):2774-8.
455. Martinez FO, Gordon S, Locati M, Mantovani A. Transcriptional Profiling of the Human Monocyte-to-Macrophage Differentiation and Polarization: New Molecules and Patterns of Gene Expression. *The Journal of Immunology*. 2006;177(10):7303-11.
456. Oliveira LJ, McClellan S, Hansen PJ. Differentiation of the Endometrial Macrophage during Pregnancy in the Cow. *PloS one*. 2010;5(10):e13213.

457. Basu S, Leahy P, Challier JC, Minium J, Catalano PM, Hauguel-de Mouzon S. Molecular phenotype of monocytes at the maternal–fetal interface. *American journal of obstetrics and gynecology*. 2011;205(3):265.e1-.e8.
458. Haussler MR, Whitfield GK, Kaneko I, Haussler CA, Hsieh D, Hsieh JC, et al. Molecular mechanisms of vitamin d action. *Calcified tissue international*. 2013;92(2):77-98.
459. Deeb KK, Trump DL, Johnson CS. Vitamin D signalling pathways in cancer: potential for anticancer therapeutics. *Nat Rev Cancer*. 2007;7(9):684-700.
460. Neme A, Nurminen V, Seuter S, Carlberg C. The vitamin D-dependent transcriptome of human monocytes. *The Journal of steroid biochemistry and molecular biology*. 2016;164:180-7.
461. Hall GE, Kenny AD. Role of carbonic anhydrase in bone resorption induced by 1,25 dihydroxyvitamin D3 in vitro. *Calcified tissue international*. 1985;37(2):134-42.
462. Billecocq A, Emanuel JR, Levenson R, Baron R. 1 alpha,25-dihydroxyvitamin D3 regulates the expression of carbonic anhydrase II in nonerythroid avian bone marrow cells. *Proceedings of the National Academy of Sciences*. 1990;87(16):6470-4.
463. Pinard MA, Mahon B, McKenna R. Probing the Surface of Human Carbonic Anhydrase for Clues towards the Design of Isoform Specific Inhibitors. *BioMed Research International*. 2015;2015:453543.
464. Karahan SC, Guven S, Mentese A, Bacak A, Kopuz M, Ozeren M. Serum anti-carbonic anhydrase I and II antibodies and idiopathic recurrent pregnancy loss. *Reproductive biomedicine online*. 2009;19(6):859-63.
465. Weis F, Giudice E, Churcher M, Jin L, Hilcenko C, Wong CC, et al. Mechanism of eIF6 release from the nascent 60S ribosomal subunit. *Nature structural & molecular biology*. 2015;22(11):914-9.
466. Jung DJ, Sung HS, Goo YW, Lee HM, Park OK, Jung SY, et al. Novel transcription coactivator complex containing activating signal cointegrator 1. *Molecular and cellular biology*. 2002;22(14):5203-11.
467. Campbell MJ. Vitamin D and the RNA transcriptome: more than mRNA regulation. *Frontiers in Physiology*. 2014;5:181.
468. Carlberg C. Genome-wide (over)view on the actions of vitamin D. *Frontiers in Physiology*. 2014;5:167.
469. Carlberg C, Campbell MJ. Vitamin D receptor signaling mechanisms: Integrated actions of a well-defined transcription factor. *Steroids*. 2013;78(2):127-36.
470. Milani C, Katayama ML, de Lyra EC, Welsh J, Campos LT, Brentani MM, et al. Transcriptional effects of 1,25 dihydroxyvitamin D(3) physiological and supra-physiological concentrations in breast cancer organotypic culture. *BMC cancer*. 2013;13:119.
471. Shalhoub V, Shatzen EM, Ward SC, Young JI, Boedigheimer M, Twehues L, et al. Chondro/osteoblastic and cardiovascular gene modulation in human artery smooth muscle cells that calcify in the presence of phosphate and calcitriol or paricalcitol. *Journal of cellular biochemistry*. 2010;111(4):911-21.
472. Barchetta I, Cimini FA, Bloise D, Cavallo MG. Dipeptidyl peptidase-4 inhibitors and bone metabolism: is vitamin D the link? *Acta Diabetologica*. 2016;53(5):839-44.
473. Busso N, Wagtmann N, Herling C, Chobaz-Peclat V, Bischof-Delaloye A, So A, et al. Circulating CD26 is negatively associated with inflammation in human and experimental arthritis. *The American journal of pathology*. 2005;166(2):433-42.
474. Chapoval AI, Ni J, Lau JS, Wilcox RA, Flies DB, Liu D, et al. B7-H3: a costimulatory molecule for T cell activation and IFN-gamma production. *Nat Immunol*. 2001;2(3):269-74.
475. Zhou X, Michal JJ, Zhang L, Ding B, Lunney JK, Liu B, et al. Interferon Induced IFIT Family Genes in Host Antiviral Defense. *International Journal of Biological Sciences*. 2013;9(2):200-8.
476. Laman JD, Claassen E, Noelle RJ. Functions of CD40 and its ligand, gp39 (CD40L). *Critical reviews in immunology*. 1996;16(1):59-108.

477. Stacey MA, Clare S, Clement M, Marsden M, Abdul-Karim J, Kane L, et al. The antiviral restriction factor IFN-induced transmembrane protein 3 prevents cytokine-driven CMV pathogenesis. *The Journal of clinical investigation*. 2017;127(4):1463-74.
478. Goldman R. Induction of a high phagocytic capability in P388D1, a macrophage-like tumor cell line, by 1 alpha, 25-dihydroxyvitamin D3. *Cancer Res*. 1984;44(1):11-9.
479. Spittler A, Willheim M, Leutmezer F, Öhler R, Krugluger W, Reissner C, et al. Effects of 1 α ,25-dihydroxyvitamin D3 and cytokines on the expression of MHC antigens, complement receptors and other antigens on human blood monocytes and U937 cells: role in cell differentiation, activation and phagocytosis. *Immunology*. 1997;90(2):286-93.
480. Hansdottir S, Monick MM. Vitamin D effects on lung immunity and respiratory diseases. *Vitam Horm*. 2011;86:217-37.
481. Adams JS, Hewison M. Unexpected actions of vitamin D: new perspectives on the regulation of innate and adaptive immunity. *Nature Clinical Practice Endocrinology and Metabolism*. 2008.
482. Rigby WF, Waugh MG. Decreased accessory cell function and costimulatory activity by 1,25-dihydroxyvitamin D3-treated monocytes. *Arthritis and rheumatism*. 1992;35(1):110-9.
483. Biswas Subhra K, Mantovani A. Orchestration of Metabolism by Macrophages. *Cell Metabolism*. 2012;15(4):432-7.
484. Shi H, Kokoeva MV, Inouye K, Tzameli I, Yin H, Flier JS. TLR4 links innate immunity and fatty acid-induced insulin resistance. *Journal of Clinical Investigation*. 2006;116(11):3015-25.
485. Wu S, Sun J. Vitamin D, Vitamin D Receptor, and Macroautophagy in Inflammation and Infection. *Discovery Medicine*. 2011;11(59):325-35.
486. Abrahams VM, Kim YM, Straszewski SL, Romero R, Mor G. Macrophages and apoptotic cell clearance during pregnancy. *American journal of reproductive immunology*. 2004;51(4):275-82.
487. Tavera-Mendoza LE, Westerling T, Libby E, Marusyk A, Cato L, Cassani R, et al. Vitamin D receptor regulates autophagy in the normal mammary gland and in luminal breast cancer cells. *Proceedings of the National Academy of Sciences*. 2017;114(11):E2186-E94.
488. Cai K, Tonelli M, Frederick RO, Markley JL. Human Mitochondrial Ferredoxin 1 (FDX1) and Ferredoxin 2 (FDX2) Both Bind Cysteine Desulfurase and Donate Electrons for Iron-Sulfur Cluster Biosynthesis. *Biochemistry*. 2017;56(3):487-99.
489. Oh J, Riek AE, Darwech I, Funai K, Shao J, Chin K, et al. Deletion of macrophage Vitamin D receptor promotes insulin resistance and monocyte cholesterol transport to accelerate atherosclerosis in mice. *Cell reports*. 2015;10(11):1872-86.
490. Burris HH, Camargo CA. Vitamin D and Gestational Diabetes Mellitus. *Current diabetes reports*. 2014;14(1):451-.
491. Jarmuzek P, Wielgos M, Bomba-Opon D. Placental pathologic changes in gestational diabetes mellitus. *Neuro endocrinology letters*. 2015;36(2):101-5.
492. Kawai T, Akira S. The role of pattern-recognition receptors in innate immunity: update on Toll-like receptors. *Nat Immunol*. 11(5):373-84.
493. Zeitlmann L, Sirim P, Kremmer E, Kolanus W. Cloning of ACP33 as a Novel Intracellular Ligand of CD4. *Journal of Biological Chemistry*. 2001;276(12):9123-32.
494. Gomez-Lopez N, StLouis D, Lehr MA, Sanchez-Rodriguez EN, Arenas-Hernandez M. Immune cells in term and preterm labor. *Cell Mol Immunol*. 2014;11(6):571-81.
495. Zhou L, Somasundaram R, Nederhof RF, Dijkstra G, Faber KN, Peppelenbosch MP, et al. Impact of Human Granulocyte and Monocyte Isolation Procedures on Functional Studies. *Clinical and Vaccine Immunology*. 2012;19(7):1065-74.
496. Tomlinson MJ, Tomlinson S, Yang XB, Kirkham J. Cell separation: Terminology and practical considerations. *Journal of Tissue Engineering*. 2013;4:2041731412472690.
497. Fisher SJ. Why is placentation abnormal in preeclampsia? *American journal of obstetrics and gynecology*. 2015;213(4, Supplement):S115-S22.
498. NICE. Hypertension in pregnancy: diagnosis and management. *Clinical guideline [CG107]* 2010.

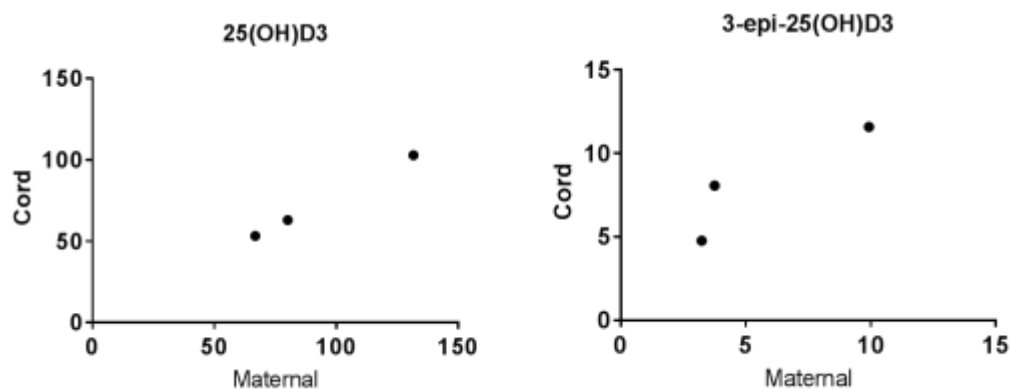
499. Lash GE, Naruse K, Innes BA, Robson SC, Searle RF, Bulmer JN. Secretion of angiogenic growth factors by villous cytotrophoblast and extravillous trophoblast in early human pregnancy. *Placenta*. 2010;31(6):545-8.
500. Oh J, Riek AE, Darwech I, Funai K, Shao J, Chin K, et al. Deletion of Macrophage Vitamin D Receptor Promotes Insulin Resistance and Monocyte Cholesterol Transport to Accelerate Atherosclerosis in Mice. *Cell reports*. 2015;10(11):1872-86.
501. Riek AE, Oh J, Bernal-Mizrachi C. 1,25(OH)₂ vitamin D suppresses macrophage migration and reverses atherogenic cholesterol metabolism in type 2 diabetic patients. *The Journal of steroid biochemistry and molecular biology*. 2013;136:309-12.
502. Epelman S, Lavine KJ, Randolph GJ. Origin and Functions of Tissue Macrophages. *Immunity*. 2014;41(1):21-35.
503. Liu X-J, Wang B-W, Zhao M, Zhang C, Chen Y-H, Hu C-Q, et al. Effects of Maternal LPS Exposure during Pregnancy on Metabolic Phenotypes in Female Offspring. *PloS one*. 2014;9(12):e114780.
504. Gong P, Liu M, Hong G, Li Y, Xue P, Zheng M, et al. Curcumin improves LPS-induced preeclampsia-like phenotype in rat by inhibiting the TLR4 signaling pathway. *Placenta*. 2016;41:45-52.
505. Liu NQ, Lerner DP, Yao Q, Chun RF, Ouyang Y, Zhou R, et al. Vitamin D-deficiency and sex-specific dysregulation of placental inflammation. *The Journal of steroid biochemistry and molecular biology*.

9 Appendices

9.1.1 SCOPE exclusion criteria

Predetermined high risk of PET; an SGA baby; or spontaneous preterm birth due to underlying medical conditions including chronic hypertension requiring antihypertensive drugs, diabetes, renal disease, systemic lupus erythematosus, antiphospholipid syndrome, sickle cell disease, HIV, previous cervical knife cone biopsy, ≥ 3 terminations of a pregnancy, ≥ 3 miscarriages, or current ruptured membranes; known major fetal anomaly or abnormal karyotype; or an intervention that could modify pregnancy outcome (such as aspirin use or cervical cerclage)(79).

9.1.2 Effect of maternal serum 25(OH)D3 and 3-epi-25(OH)D3 upon fetal cord concentrations at delivery



Appendix Figure 9.0 Correlation between maternal blood and cord blood 25(OH)D3 (nmol/L) and 3-epi-25(OH)D3 (nmol/L) (n=3).

10 Publications arising from this thesis

Tamblyn JA, Hewison M, Wagner CL, Bulmer JN, Kilby MD. Immunological role of vitamin D at the maternal-fetal interface. *J Endocrinol.* 2015; 224(3):R107-21(71).

Tamblyn JA, Susarla R, Jenkinson C, Jeffery L, Ohizua O, Chun R, Chan S, Kilby M, Hewison M. Dysregulation of Maternal and Placental Vitamin D Metabolism in Preeclampsia. *Placenta* 50, 70-77. 2016 (104).

Tamblyn J, Jenkinson C, Lerner D, Hewison M, Kilby M. Serum and urine vitamin D metabolite analysis in early preeclampsia. *Endocr Connect.* 2017; pii: EC-17-0308 (105).

Liu NQ, Lerner D, Yao Q, Chun R, Zhou R, **Tamblyn JA**, Wagner C, Hewison M. Vitamin D-deficiency and sex-specific dysregulation of placental inflammation. *Journal of Steroid Biochemistry and Molecular Biology* 2017; S0960-0760(17)30163-2(505).

Powell R, Lissauer D, **Tamblyn J**, Beggs A, Cox P, Moss P, Kilby M. Decidual T cells exhibit a highly differentiated phenotype and demonstrate potential fetal-specificity and a strong transcriptional response to interferon. *Journal of Immunology* 2017; 199(10):3406-3417 (234)